Mechanism(s) of hepatitis C virus induced liver injury.

by

Garrick Kenardo Wilson

A thesis submitted to The University of Birmingham for the degree of Doctor of Philosophy.

College of Medical and Dental Sciences

School of Immunity and Infection

University of Birmingham

Supervisors: Professors Jane McKeating and Stefan Hübscher

January 2012

Abstract

Hepatitis C virus (HCV) infects hepatocytes of the liver causing progressive liver disease including; fibrosis, cirrhosis and hepatocellular carcinoma. However, the precise mechanism(s) underlying HCV induced liver injury are poorly understood. Hepatocytes are highly polarized with distinct apical and basolateral membranes separated by tight junctions that maintain a normal liver physiology. We studied the role of HCV infection in driving hepatic injury. Our studies show that HCV infection induces hepatocellular reprogramming via hypoxia inducible factor-1α (HIF-1α) stabilization and increased glucocorticoid receptor (GR) signaling. HIF-1α stabilization promoted epithelial to mesenchymal transition accompanied by reduced polarity and cell adhesion. Whereas GR signaling increased cholesterol synthesis and altered HCV receptor expression. Alterations in hepatocellular biology induced a cellular state conducive for virus entry and replication.

Consequently, cells de-differentiate to acquire a malignant phenotype via HIF-1α target genes including vascular endothelial growth factor (VEGF) and transforming growth factor-beta (TGFβ). In addition, GR transcription induced by glucocorticoid treatment or HCV infection enhanced virus uptake, highlighting the caveat for glucocorticoid immunosuppression post liver transplantation. Importantly, HIF-1α inhibitors and GR antagonist reversed the effects of both transcription factors on virus infection and hepatocellular biology. These findings suggest that HCV potentiate liver injury via indirect mechanisms.

Dedication

I dedicate this thesis to my mother Claire Pennant, who stands in a league of her own; none can compare to the world's greatest mom. My grandmother Advira Elizabeth Pennant, as a child she reasoned with me saying "*the student who succeeds goes far above and beyond the required standard.*" She reminded me that;

The heights by great men, reached and kept

Were not attained by sudden flight

But they whilst their companions slept

Were toiling upward through the night

Henry Wadsworth Longfellow

For thoughtful encouragement, laughter and advice I'm grateful to George Beason, Yoneasha Beason, Gyannah Mitchell, Virginia Thomas and my best friend David Haughton.

The end of a road is never truly told, but it ends

Fulfillment of a dream is more than it seems

Will the sun shine, will the rain pass

Yet there is no pause until he accomplishes the cause

What a noble deed driven to succeed

But it's over now…

Excerpt from Marvin Winans (Over)

Because I obtained the data, analyzed it, wrote about and structured it, I dedicate this thesis to me too.

Acknowledgements

I thank Professors Jane McKeating and Stefan Hübscher for excellent supervision and guidance throughout my studies. I also thank members past and present of the Birmingham HCV Research Group for their technical support and intellectual discussions, in no particular order; Anne Schwarz, Amy Barnes, Christopher Davis, Christopher Mee, Claire Brimacombe, Colin Howard, Daniel Rodgers, Ditte Hedegaard, Helen Harris, Ian Rowe, Jennifer Timpe, Joe Grove, Ke Hu, Luke Meredith, Megan Roberts, Michelle Farquhar, Nicola Fletcher, Peter Balfe, Samantha Pollock, Samantha Tilakaratne, Sukhdeep Galsinh and Zania Stamataki. I am grateful to Christopher Mee for training me in the art of polarity and tight junction assays and for excellent teaching during the first year of my PhD. Michelle Farquhar provided excellent critical analysis and proofreading of thesis chapters for which I am grateful. Thanks to Gary Reynolds for liver tissue processing and training in immunohistochemistry and to Ricky Bhogal for help with reactive oxygen species assays and expert advice.

My work wouldn't have been possible without reagents from the following people; Margret Ashcroft (University College, London), Roy Bicknell (University of Birmingham), Takaji Wakita (National Institute of Infectious Diseases, Tokyo), Ragai Mitry (Kings College, London), Stuart Ray (John's Hopkins University, Maryland), Flossie Wong Staal (Itherx, California) and Charles Rice (Rockefellar University, New York).

My studentship was funded by the Medical Research Council and this work was supported by the Wellcome Trust.

Frequently used Abbreviations

EMT	Epithelial to Mesenchymal Transition
GR	Glucocorticoid receptor
HCC	Hepatocellular Carcinoma
HCV	Hepatitis C Virus
HCVcc	Cell culture proficient hepatitis C virus
HCVpp	Hepatitis C virus pseudoparticles
HIF-1α	Hypoxia inducible factor-1α
IRI	Ischemia reperfusion injury
J6/JFH-1	Japanese Fulminant Hepatitis-1 (viral isolate)
MRP-2	Multi Drug Resistant Protein 2
PHH	Primary Human Hepatocytes
SR-BI	Scavenger Receptor Class B member I
TGFβ	Transforming Growth Factor-beta
VEGF	Vascular Endothelial Growth Factor

Table of contents

List of Figures

List of Tables

1. INTRODUCTION

1.1 Introduction to viral hepatitis

World War II was a global conflict that began in 1939 and lasted for six years. Over 100 million allied troops were mobilized to subdue Nazi Germany conquering of continental Europe. On the surface there was a fight for freedom by brave men and women of the allied forces. Lurking below the surface was an elusive pathogen that caused hepatitis; a severe inflammation of the liver in a significant number of service personnel's who received blood transfusion. Research carried out in the 1940's identified two immunologically distinct viruses that were the putative agents of post transfusion hepatitis (159, 236, 300). The viral variants were named hepatitis A virus (HAV) and hepatitis B virus (HBV). HAV demonstrated a faecal-oral route of transmission, suggesting that HAV was not the agent of post transfusion hepatitis. In contrast, HBV transmitted via the blood; moreover, the discovery of the HBV surface antigen, also known as the Australia antigen (HBsAg) further strengthened an association between HBV and post transfusion hepatitis (203). By the early 1970's screening of blood from volunteer donors for HBsAg became standardised in the USA, resulting in a 90% reduction of post transfusion viral hepatitis (7).

In the late 1970's, Acquired Immuno Deficient Syndrome (AIDS) caused by the human immunodeficiency virus (HIV) was highly prevalent in the USA. In the backdrop of a looming HIV epidemic, a significant number of intravenous drug users and recipients of HBsAg negative blood transfusions developed hepatitis. Soon after, blood supplies across the

world became contaminated with a viral agent causing what was termed post-transfusion non-A, non-B hepatitis. Unlike HBV, the course of non-A, non-B hepatitis was characterised by a shorter incubation time with an increasing number of sufferers experiencing recurrent hepatitis (6, 160, 327, 348). For several years the cause of non-A, non-B hepatitis eluded identification due to difficulties in isolating and culturing the virus. In 1978 a report documented the successful transmission of non-A, non-B hepatitis from man to chimpanzee (390). Subsequent advances in recombinant DNA technology allowed Choo and colleagues (74) to generate a cDNA library from the plasma of an infected chimpanzee and to identify a single clone that was reactive with non-A, non-B patient sera. Sequencing of this clone revealed a positive sense single stranded RNA genome that showed resemblance to several members of the *Flaviviridae* family of viruses which include (yellow fever, dengue and west nile viruses). The culprit was designated hepatitis C virus (HCV) and was classified to a new genus (*Hepacivirus*) of the *Flaviviridae* family.

HCV particles range between 50-60nm in diameter; each particle is comprised of a lipid bilayer envelope bearing the E1E2 glycoprotein complex that facilitates particle and host cell interactions. The envelope surrounds a capsid that contains the positive sense single stranded RNA genome (Figure 1-1). The RNA genome is 9,600 nucleotides long, comprising of two untranslated regions at the 5’ and 3’ termini and a single open reading frame encoding a large polyprotein approximately 3000 amino acids in length. The internal ribosome entry site (IRES) located within the 5’ NCR initiates translation of the polyprotein which is modified by host and viral proteases into three structural proteins (Core, E1 and E2)

which are the capsid and envelope glycoproteins respectively, a small ion channel (p7) and six non-structural proteins (NS2, NS3,NS4B, NS5A and NS5B). The structural proteins comprise the building blocks for the new virion and the non-structural proteins replicates the viral RNA (400). HCV genome and replication will be described in more detail section 1.8.

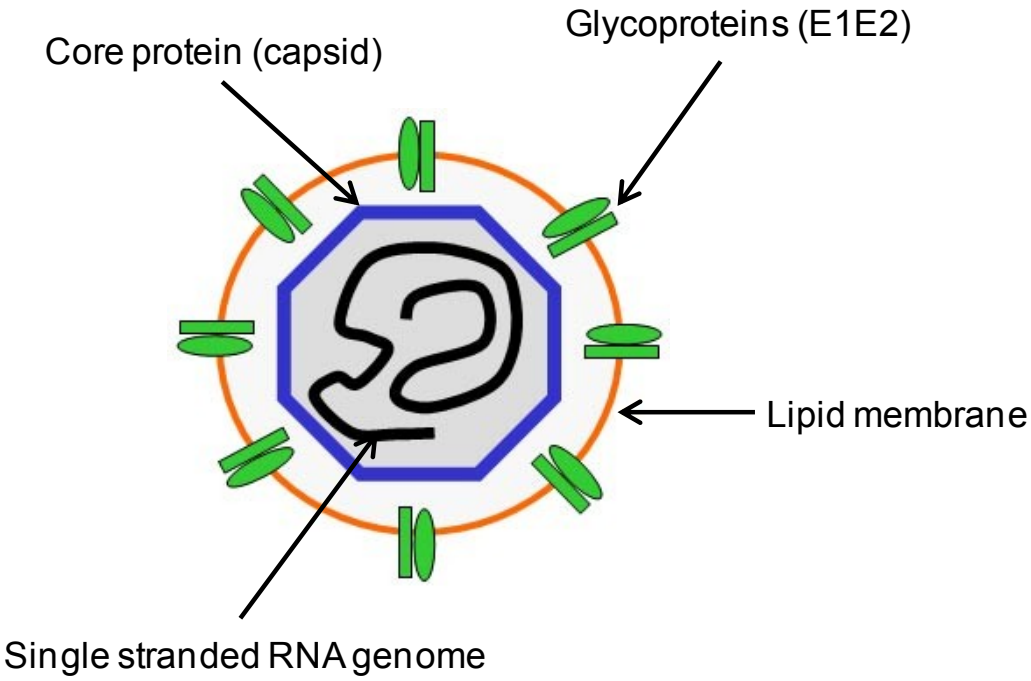

Figure 1-1. A cartoon of the HCV particle.

1.2 The hepatic microenvironment

The major reservoir for HCV replication are hepatocytes of the liver, this is achieved via the utilization of four receptor molecules; scavenger receptor BI (SR-BI), CD81, Claudin-1 and Occludin (108, 314, 316, 357), this process will be uncovered in section 1.6. The liver is the largest organ in the human body, weighing between 1.2 and 1.5kg with central roles in metabolic, endocrine and secretory pathways including the storage, transport and synthesis of lipids (393). It is located below the diaphragm to the right of the stomach and possesses a unique location between the peripheral lymphoid organs and the gastrointestinal tract. Anatomically, the liver is divided into two major lobes when observed from the anterior; a large right lobe and a smaller left lobe. Both lobes are separated by the falciform ligament anteriorly, by the fissure for the ligamentum venosum posteriorly and by the fissure for the ligamentum teres inferiorly. Two additional minor lobes exist between the left and right lobes. They are the caudate lobe located on the posterior surface and the quadrate lobe on the anterior surface (35, 92, 311, 404). The liver has a dual blood supply from the hepatic artery and the hepatic portal vein; the hepatic artery supplies oxygenated blood from the heart and the hepatic portal vein provides deoxygenated nutrient rich blood from the gastrointestinal tract. Arterial and venous bloods traverse the liver parenchyma via the sinusoids, generating a mixed supply which is collected in the central vein. Blood from the central vein travels via the hepatic vein to the inferior vena cava where it becomes re-oxygenated (207). Figure 1-2 shows an outline of the liver anatomy.

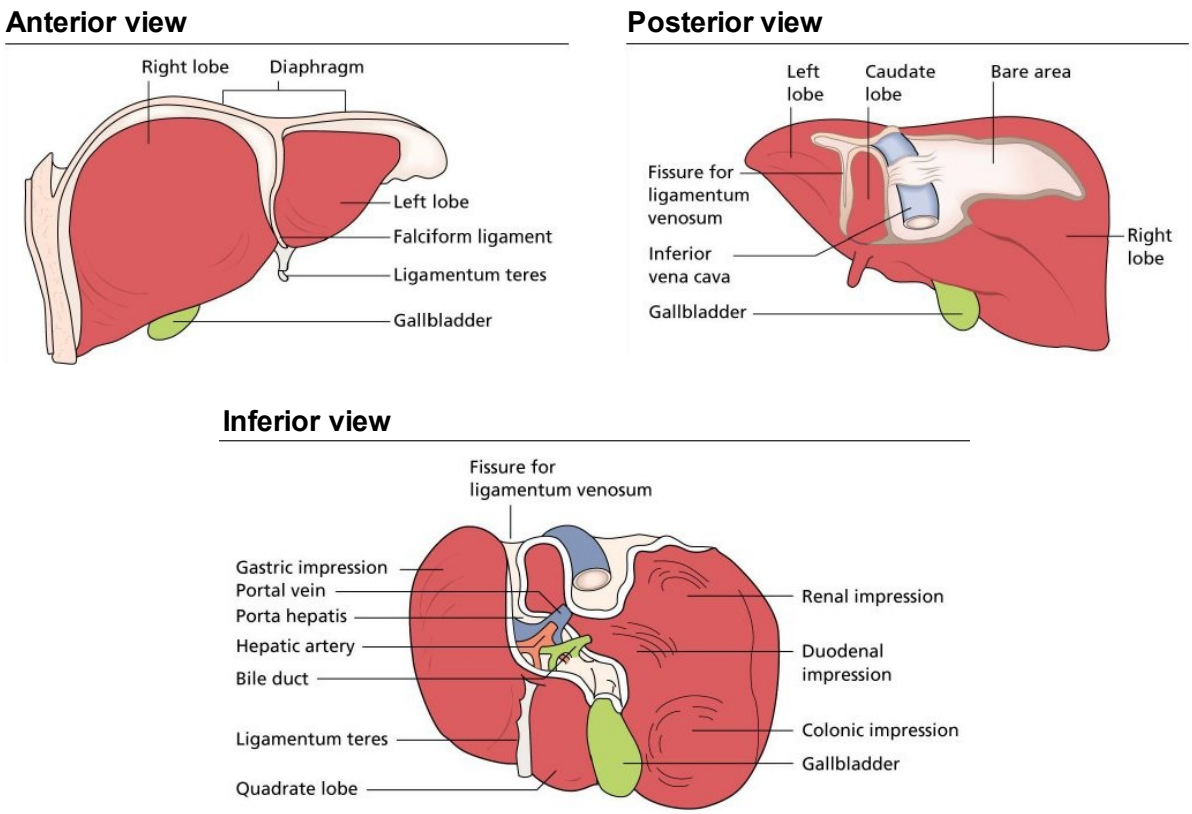

Figure 1-2. Anatomy of the liver.

The liver is shown anteriorly, posteriorly and inferiorly (95).

The main cell type of the liver that performs most of its functions is the hepatocyte. Hepatocytes are also referred to as liver parenchymal cells and comprise 80% of the entire liver mass. They are the major epithelial cells of the liver; and possess a unique polygonal architecture compared to other epithelial cells. Hepatocytes have three faces that enable them to be in contact with neighbouring hepatocytes, the sinusoids and the bile canaliculus simultaneously (88, 118, 305, 368). As such, hepatocytes form a complex polarity, in which adjacent plasma membranes are separated by tight junction proteins into sinusoidal (basolateral) and apical (canalicular) domains. Polarity is crucial for the correct physiological functioning of the liver with the tight junctions separating the secretory bile from the blood flow. In contrast epithelial cells such as those lining the gut demonstrate simple polarity due to a single face resulting in single apical and basolateral domains (63, 88, 373).

The remaining 20% of the liver mass consists of cells collectively termed non-parenchymal cells including; endothelial cells, kupffer cells, lymphocytes and stellate cells. Endothelial cells line the hepatic circulatory vessels known as sinusoids; the hepatocytes are in turn arranged into plates separated by sinusoids which provide a large surface area for nutrient absorption (46). The sinusoids possess a narrow lumen which is infiltrated by kupffer cells and lymphocytes. Kupffer cells are the resident macrophages of the liver, they are predominantly located in the peripheral region of the liver; this unique localization allows them to phagocytose invading pathogens or foreign particles that enter the liver via the portal blood flow (196, 378). Lymphocytes form part of the innate immune response that helps to protect the liver against infection. Between the

hepatocytes and the sinusoidal endothelium lies the Space of Disse which contains an extracellular matrix made up of fibronectin, collagen and hepatic stellate cells. These cells store vitamin A and are activated upon liver injury to become collagen synthesizing myofibroblasts that produce most of the factors that lead to hepatic fibrosis (393). In addition, the liver contains cholangiocytes also reffered to as biliary epithelial cells due to their unique localization in the biliary tracts. They are the first line of defence against pathogens invading the bile ducts due to the production of cytokines and chemokines (188). An outline of the liver architecture including cell types and their localization is shown in Figure 1-3.

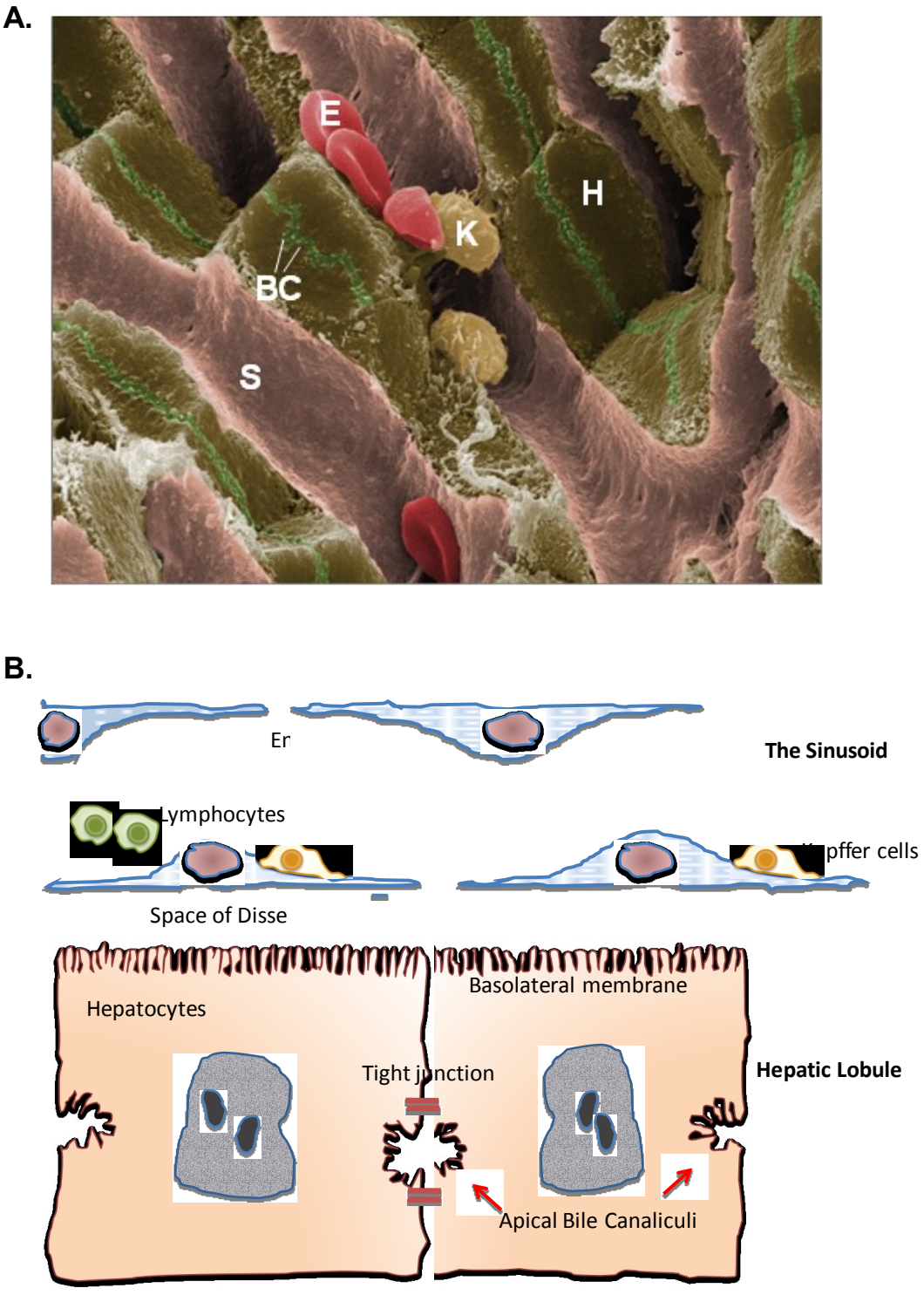

Figure 1-3. Architectural layout of the liver.

A. Scanning electron micrograph of the liver showing hepatocytes (H), Kupffer cells (K), sinusoids (S), bile canaliculi (BC) and erythrocytes (E). Courtesy of the Wellcome Trust Image Library. **B.** Cartoon depicting the localization of liver cells in proximity to hepatocytes.

1.3 HCV disease

Epidemiology and treatment

Globally, an estimated 180 million people are infected with HCV, equating to around ~3% of the world's population (370). It is difficult to obtain accurate estimates from different countries as acute HCV infection is often asymptomatic. However, HCV prevalence is divergent in different parts of the world with high incidence in India (3-5 million cases), North America (2-4 million cases), Europe (5-10 million) Asia (6-12 million cases) and Africa (10 million cases) (WHO epidemiological record, 2009). Up to 150, 000 new cases occur annually in Europe and North America, of these only 25% are symptomatic. More than 60% of infections will progress to chronic liver sequelae, 20% of whom will develop cirrhosis of the liver and 5-7% will develop end stage liver disease such as hepatocellular carcinoma (HCC) which becomes fatal (68, 365, 366). Intriguingly, 15-20% of infected individuals will spontaneously clear the virus following sero-conversion, a mechanism which is poorly understood (352).

Prior to 1992, the prevalence of HCV transmission was high amongst individuals who came into contact with contaminated blood; primary routes of transmission included the receipt of blood transfusion or organ transplantation, consequently HCV antibodies were detected in 80% of haemophilic patients (18). The establishment of robust clinical standards for blood screening significantly reduced the number of new HCV cases from blood transfusion or organ transplantation. Today, HCV is predominantly transmitted amongst intravenous drug users sharing contaminated needles. Other routes of transmission include perinatal and

sexual transmission which contributes moderately to the global HCV prevalence (54).

HCV pathogenesis can be monitored by the detection of viral RNA; however viral load does not necessarily correlate with disease severity (352). Several factors including age, gender, immunological status, alcohol consumption and co-infection with HIV have been reported to affect HCV pathogenesis (366). Indeed, it was reported that HCV pathogenicity is greater amongst individuals from ethnic minority backgrounds; in the USA 90-100% of new infections are detected in people of African origin, 70-80% in Hispanics and 60-70% in Caucasians (367), these findings are unlikely to be biological but may reflect social living conditions.

A classic feature of HCV replication is the generation of distinct variants with up to 35% nucleotide divergence, these variants are termed genotypes. There are six major HCV genotypes, many of which comprise related subtypes resulting in 11 distinct antigenic groups (377). More recently, a genotype 7 virus has been proposed (144). All genotypes share an identical set of genes similar in size. Even so, HCV genotypes show differences in their pathogenesis, sensitivity to antiviral therapies and geographical distribution. Genotypes 1, 2 and 3 have become widely distributed amongst intravenous drug users and are responsible for a significant proportion of infections in Europe, the Mediterranean and North America. Genotypes 4 and 5 are prevalent in developing countries such as South Africa and Egypt whilst genotype 6 is widespread in Asia (102, 183). Figure 1-4 shows the major HCV genotypes and their geographical distribution.

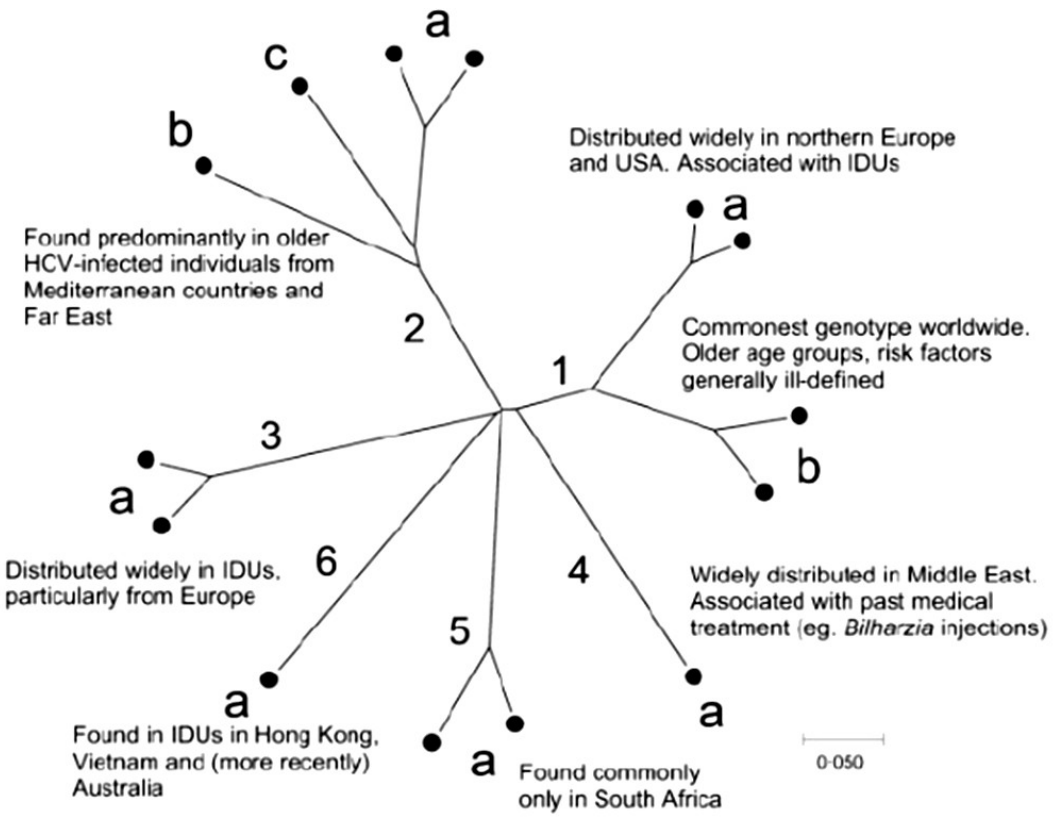

Figure 1-4. Phylogenetic analysis of HCV sequences from variant isolates showing the six major HCV genotypes, secondary groupings within some genotype and their geographical distribution (377).

To date there is no vaccine for HCV, antiviral therapy includes a combination of interferon-alpha (INFα) and ribavirin which is only partially effective and is dependent on early diagnosis of the disease; furthermore, the combination can be toxic and costly (161). The outcome of HCV infection is associated with the infecting genotype; individuals infected with HCV genotype 1 viruses are more likely to develop chronic hepatitis and HCC (249, 338). Furthermore, genotype 1 viruses are increasingly resistant to INFα and ribavirin with only a partial success rate of 50% (116, 442). Infection caused by genotypes 2 and 3 viruses are associated the hepatocellular steatosis and fibrosis with a successful treatment rate of up to 80% (116, 442). Patients with chronic liver disease have limited treatment options primarily because they respond poorly to INFα and ribavirin. Liver transplantation is the only viable option in most cases; however, circulating virus in the blood reinfects the new graft. Fatality rates 5 years post transplantation in HCV patients are around 70% due to reinfection and the progressive nature of the disease (358).

Recently, two protease inhibitors (Telaprevir and Boceprevir) that target the NS3/NS4A serine protease have been licensed. Telaprevir demonstrated potent inhibition of HCV infection with a 50% inhibitory concentration of 354nM and a 50% cytotoxicity concentration of 83μM (204). Preclinical studies showed that telaprevir had sufficient liver exposure in dogs and rats and is synergistic with interferon-α and additive with ribavirin against genotype 1 viruses (223). The majority of patients receiving telaprevir had sustained virological responses; 79% compared to patients in receipt of standard interferon and ribavirin therapy (46%) (Vertex Pharmaceuticals, 2011). Telaprevir is associated with mild side

effects such as fatigue and nausea; however, these symptoms are normally manageable.

Boceprevir is a serine protease inhibitor that binds reversibly to NS3 and is administered in combination with INFα and ribavirin. The combination treatment significantly increases the rate of sustained virological response in previously untreated individuals with chronic HCV genotype 1 infection (323).

Tropism and immunobiology

Although hepatocytes are the main reservoir for HCV replication, studies have shown extrahepatic manifestations associated with HCV infection. We and others have shown that neuroepithelioma cell lines are permissive for HCV infection suggesting that HCV may infect the central nervous system (52, 121). More recently, we have shown that HCV infects brain endothelial cells, highlighting the possibility that HCV perturbs the blood brain barrier in vivo resulting in neuropathology seen in many infected patients (Fletcher et al, 2011, in press). A minority of individuals infected with HCV developed the B-cell disorder cryoglobulinaemia (347) and peripheral blood mononuclear cells (PMBC) are also affected by HCV infection (210, 282). Together, these studies show that additional non-hepatic cellular reservoirs for HCV infection exist which implicates the virus in additional pathological disorders.

Little is known about the frequency of HCV infected hepatocytes in the liver, due to difficulties in staining liver tissue for viral antigens. A study by Liang et al, used two-photon microscopy techniques to visualize HCV infected hepatocytes in liver tissue. The authors showed NS3 positive cells

that were focally distributed and suggested that around 10-15% of hepatocytes in vivo are actively infected (221). However, virus production is thought to be high with genomic RNA burden in the order of 1×10^{12} RNA copies/day (284). HCV specific antibodies can be detected in patient sera as early as 8 weeks post infection (301). Nevertheless, the role of the humoral immune response is unclear as high antibody titres are often detected in patients with chronic infection suggesting limited neutralizing activity (232, 266). Studies have shown that a sustained T-cell response is crucial for viral clearance during acute infections. This response is associated with CD4+ and CD8+ T-cells (211, 375, 399). However, in persistent HCV infection CD4+ and CD8+ T-cells response is weak and are sometimes undetectable (83). It is not yet clear what factors governs a sustained immune response to virus infection, although a prolonged and specific immune response is likely to affect the outcome of HCV infection. Attempts to design HCV vaccines have largely focused on eliciting appropriate T cell response (45, 194, 383), however, inoculation of SCID uPA mice with patient immunoglobulin or anti-E2 antibodies resulted in immune protection against HCV to revitalise hopes for a B-cell vaccine (212, 407).

HCV transmits via a cell free and cell-cell routes of transmission; recent evidence from our laboratory has shown that the cell-cell route is the preferred mode of transmission. This route provides a means for virus evasion of the immune response (50, 401). HCV infection is associated with a robust interferon response, however this does not correlate with the outcome of virus infection (103, 131, 385). Several virus proteins including core and NS3-4A block interferon signalling by modulating the JAK-STAT

pathway and IFNβ production respectively (128, 218). Furthermore, HCV NS5A blocks protein kinase receptor (PKR) signalling allowing virus escape from type 1 interferon signalling (187). IFNα therapy is administered to substitute for the disrupted IFN secretion in infected cells and to stimulate the activation of natural killer cells and dendritic cell maturation (116). The interferon inducible protein IP-10, a ligand for the chemokine receptor CXCR3 is upregulated in hepatocytes surrounded by lymphocyte infiltrates and may promote CXCR3 expressing T-cells to sites of inflammation (372).

HCV associated carcinogenesis

Hepatocellular carcinoma (HCC) is a complex and heterogeneous tumour with limited treatment options and poor prognosis. It is the most common liver malignancy and rates fifth in incidence and third in mortality of cancers in the world (107). A rapid increase in HCC has been associated with HCV infections (25), HCV associated HCC accounted for 155,000 deaths in the USA in 2002, although this figure is likely to underestimate the number of deaths today (306). HCV replicates in the cytoplasm and does not integrate into the host genome indicating that HCC occurs via indirect effects of HCV infection including the inflammatory response and the perturbation of cellular pathways (27, 253, 291). It is not known whether cancer arises in the infected hepatocyte or whether a bystander effect induces carcinogenesis in surrounding cells. This is difficult to ascertain as the detection of HCV RNA in transformed hepatocytes is unreliable because HCV circulates the blood and likely to be present in the tissue parenchyma.

In vivo, hepatocytes do not divide; however, there is an increase in the frequency of hepatocytes expressing the proliferation marker Ki67 in HCV infected livers (198). Furthermore, individuals with increased Ki67 expression are more likely to develop HCC (104). It is not known whether proliferating hepatocytes are infected with HCV or whether surrounding uninfected cells are proliferating due to the loss of infected cells by virus induced apoptosis (253). This is difficult to ascertain due to difficulties in detecting infected hepatocytes in vivo (221).

Small animal model studies have shown that the liver is highly regenerative. Following a partial hepatotectomy over 90% of quiescent hepatic cells enter the cell cycle. The mechanism of liver repair is highly complex involving cooperative signals from cytokines and growth factors. Damaged hepatocytes activate growth factors and cytokines that induces a significant alteration of the liver architecture including, increased fibronectin production and changes in cellular junctions to initiate liver repair (268, 269). During liver regeneration (Figure 1-5), it is believed that vascular endothelial growth factor (VEGF); a potent angiogenic cytokine binds to its receptors expressed on sinusoidal endothelial cells to initiate the release of hepatocyte growth factor (HGF) precursor proHGF from stellate cells. proHGF is cleaved by urokinase-type plasminogen activators which liberates HGF to bind to its receptors on hepatocytes (53). HGF-hepatocyte interactions activate phosphatidylinositol 3-kinase (PI3K) and AKT signalling which in turn stimulate the expression of transforming growth factor alpha (TGFα), insulin growth factor binding protein-1 and various cellular kinases. These in turn induce cell cycle transition by increasing cyclins D and E expression (93, 216, 290). Subsequently,

several factors crucial for the innate immune response (lipopolysaccharides and complement molecules) activate kupffer cells resulting in increased tumour necrosis factor alpha (TNFα) synthesis. TNFα up-regulates interleukin 6 (IL-6) and together they activate neighbouring hepatocytes leading to the expression of various signalling molecules and inhibitory proteins including transforming growth factor beta (TGFβ) produced by stellate cells to terminate liver regeneration through repression of cyclins D and E. Subsequently, hepatocytes return to their normal quiescent state (246, 382). In this manner, a complex interplay between cytokines and growth factors is critical for liver repair, the role of cytokines and growth factors in liver repair is reviewed in (393). Figure 1-5 depicts growth factors and cytokines pathways during liver regeneration.

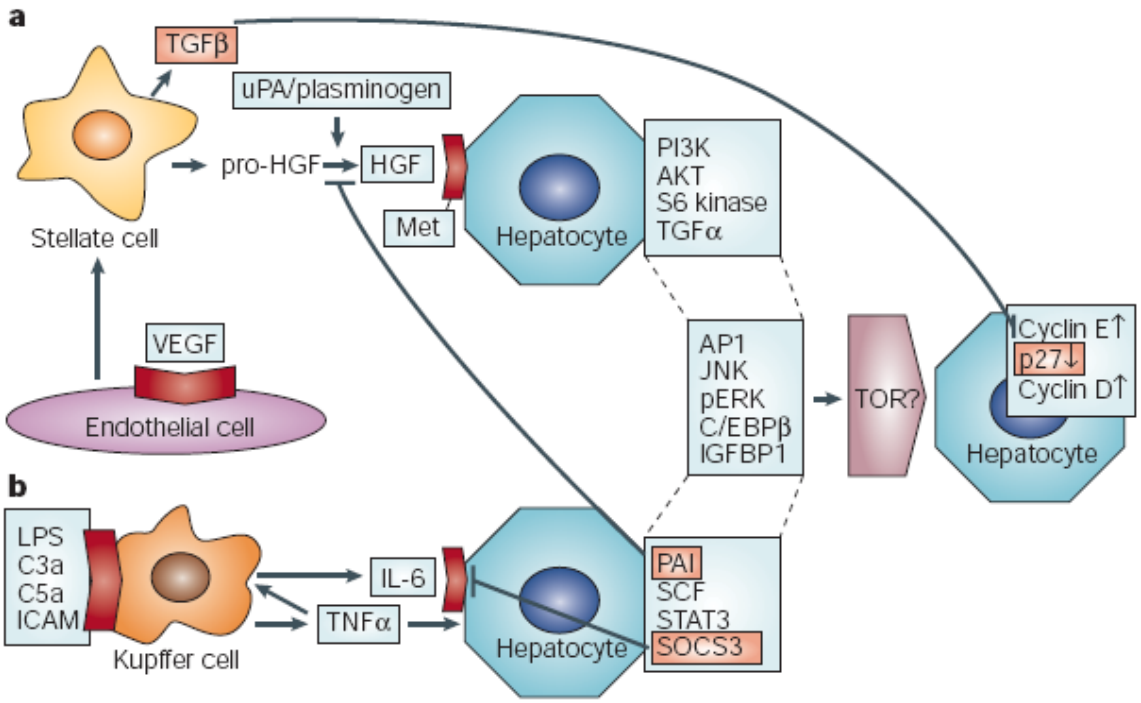

Figure 1-5. Growth factor and cytokine signaling during liver regeneration.

A. The growth factor mediated pathway. Vascular endothelial growth factor (VEGF) stimulates the release of hepatocyte growth factor (HFG) precursor pro-HGF which is cleaved by urokinase-type plasminogen activator (uPA) and plasminogen proteases that liberates HGF. HGF activates phosphatidylinositol 3-kinase (PI3K), and other downstream factors leading to cell cycle transition via cyclins D and E. **B.** The cytokine mediated pathway. Lipopolysaccharides (LPS) complement factors (C3/C5) and others activate kupffer cells which secretes tumour necrosis factor-alpha (TNFα). This leads to interleukin-6 (IL-6) production. TNFα/IL-6 activates neighbouring hepatocytes resulting in the activation of several molecules including stem cell factor (SCF). Additionally, TGFβ, plasminogen activator inhibitor (PAI) and cyclin inhibitors are activated to terminate cell division (393).

Liver regeneration results in significant histological changes to the parenchyma, including the deposition of a fibronectin matrix associated with fibrogenesis (86, 393). It is believed that the liver reverts to an early embryonic state associated with signalling pathways important for morphogenesis and regeneration including; sonic hedgehog (SHh) signalling and epithelial to mesnchymal transition (EMT) (72). Both pathways are crucial for embryogenesis, organogenesis and development; however, as we will discuss later these pathways are also implicated in tumourgenesis. SHh signalling and EMT induces a cellular de-differentiation state resulting in the expression mesenchymal markers associated with the loss of adhesion and tight junction molecules. This is followed by increased proliferation, which is necessary for tissue regeneration (287, 292, 398). However, this process is transient as subsequent inhibitory signals leads to a reversal course known as mesenchymal to epithelial transition (MET) whereby cells regain their hepatic/epithelia features. When EMT activity exceed MET, repair is mainly fibrotic resulting in severe scarring of the liver (72).

HCV infection has been linked to SHh signalling (71, 304) and EMT (28), suggesting the intriguing possibility that HCV exploits the regenerative events of the liver to promote its transmission. Figure 1-6 depicts EMT in polarized epithelial cells. We will continue this section by drawing upon experimental evidence demonstrating a role for cytokines and growth factors in regulating hepatocyte polarity, potentiating HCV infection and driving hepatic carcinogenesis.

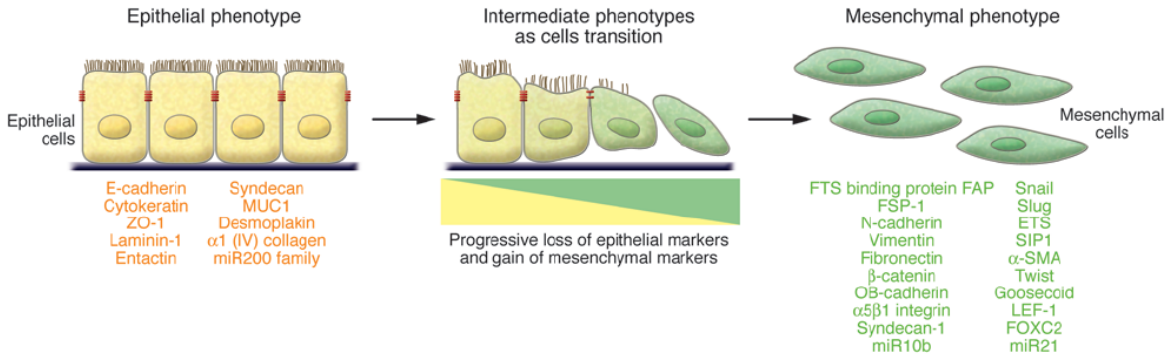

Figure 1-6. EMT in polarized epithelial cells.

EMT is associated with a gradual loss of epithelial properties resulting in a de-differentiation process whereby cells gain mesenchymal properties. Cartoon lists epithelial (orange) and mesenchymal (green) markers. Taken from (185).

HCV infection is associated with an inflammatory response that promotes fibrogenesis. The activation of stellate cells is most likely to drive this process although little is known about HCV-stellate cells activation. However, it is believed that detection of double stranded RNA produced during HCV replication by Toll-like receptor 3 (TRL3) and the induction of endoplasmic reticulum (ER) stress by HCV infection leads to the activation of NF-ќB and proinflammatory cytokines which in turn primes stellate cells to activate fibrogenesis (353, 419, 420).

There is a growing body of evidence demonstrating a role for proinflammatory cytokines in regulating tight junction dynamics in epithelia and enodthelia phenotypes (reviewed in, (57)). For example, TNFα and IFNγ modulation of tight junction proteins causes inflammatory bowel disease, a severe inflammation of the colon. Whilst the pathobiology of this disease is complex, one prominent feature is increased paracellular permeability resulting in exposure of tissue to luminal pathogens (120). Tight junctions regulate the transcellular movement of molecules between apical and basolateral membranes (fence function) and create a semi-permeable barrier between cells to restrict the flow of molecules through the paracellular space (barrier function), in doing so tight junctions establish cell polarity (373). The role of tight junctions in establishing hepatocyte polarity and HCV entry will be described in detail in section 1.6.

Studies have shown elevated TNFα in serum from HCV infected patients which is associated with enhanced fibrosis (119, 449). Furthermore, HCV NS3 protein increases TNFα production in HepG2 cells reinforcing a link between infection and inflammation (158). A recent study from our group

showed that treatment of HepG2 cells with TNFα and IFNγ perturbed tight junction permeability (260), together these studies suggest that that cytokines produced during HCV infection may potentiate barrier breakdown leading to liver injury. Indeed, alterations in tight junction structure and distribution promote the malignancy of various carcinomas including HCC (166, 293). We have previously reported aberrant tight junction protein distribution in HCV infected liver tissue, indicating that virus infection affects tight junction dynamics in vivo (341). More recently, several reports have shown that HCV infection is associated with the stabilization of hypoxia inducible factor-1 alpha (HIF-1α) a transcription factor that regulates a variety of genes implicated in invasion and metastasis, providing new insights into the role of HCV in HCC (157, 280, 344).

Solid tumours are characterized by low oxygen levels (hypoxia); the cellular response to hypoxia is mediated by HIF-1α and HIF-1β (HIFs). HIFs are heterodimeric transcription factors that are constitutively expressed in cells. During normoxia (high oxygen) HIF-1α transcription is regulated by hydroxylation of the alpha subunit at prolyl and asparagynyl residues followed by the binding of von Hippel-Lindau (VHL) E3 ligase that targets HIF-α for ubiquitination and degradation via the proteasome (179, 180). During hypoxia HIF-1α hydroxylation is inhibited resulting in its stabilization and translocation to the nucleus where it dimerizes with HIF-1β and binds to the HIF-1 responsive element in various genes involved in cell survival, proliferation and metabolism (369). Figure 1-7 depicts HIF-1α signalling in normoxia and hypoxia.

Proteomic analysis of HCV infected cells indicate a reprogramming of hepatocellular metabolism and biogenesis which favours virus replication and pathogenesis (37, 90, 425). It is believed that HIF-1α target genes play a major role in HCV induced changes in the hepatic environment. Importantly, several HIF-1α target genes are upregulated during HCV infection, of significance are VEGF and TGFβ. VEGF signalling plays a key role in driving angiogenesis; HCC is a hypervascular tumour requiring angiogenesis to promote tumour growth and metastasis. We and others have shown that HCV infection increases VEGF expression (157, 258, 280). Moreover, VEGF negatively regulates hepatocellular polarity by reorganizing Occludin distribution in polarized HepG2 cells to promote HCV entry. Anti-VEGF neutralizing antibodies and the receptor kinase inhibitor sorafenib restored polarity and reduced virus entry (258). Schmitt et al, reported that VEGF disrupts tight junctions in a protein kinase A dependent manner resulting in enhanced HCC spread into the normal liver parenchyma (362). Taken together, these data suggest that HCV promotion of VEGF expression may aid in HCC pathogenesis.

TGFβ is a pleiotropic cytokine that regulates diverse cell signalling pathways including proliferation, apoptosis and invasion (264). Several reports demonstrated increased TGFβ levels in patients with chronic liver diseases (70, 130, 240, 381). In HCC, TGFβ signalling exerts tumour suppressor functions during the early stages of tumourgenesis by mediating hepatocyte apoptosis. During the latter stages, TGFβ switches from tumour suppressor to tumour promoter (264, 345). Ectopic expression of HCV core proteins isolated from patients with HCC modulates TGFβ plasticity from tumour suppressor to tumour promoter via SMAD

phosphorylation (28). In addition, HCV proteins induce oxidative stress and the production of reactive oxygen species (ROS) in a TGFβ dependent manner (44). Moreover, a recent study by Presser and colleagues showed that HCV infection promotes TGFβ expression resulting in increased virus replication, suggesting a role for TGFβ in the virus lifecycle (326).

Several studies have shown the induction of EMT by TGFβ signalling (139, 184, 438). As previously discussed EMT is required for various developmental processes including liver regeneration (185). Nevertheless, there is a growing body of evidence implicating EMT in driving the invasive and metastatic potential of human cancers including HCC (1, 213, 248, 405, 431, 432). A balanced interplay between EMT and MET dictates the outcome of liver injury, in this regard, when EMT supersedes MET liver repair is mainly fibrotic leading to increased migration of hepatic cells (reviewed in, (72)). Battaglia and colleagues reported that HCV core protein induces EMT in a TGFβ dependent manner (28). Furthermore, Li et al; demonstrated that HCV core protein induces EMT via the lysyl oxidase-like 2 (LOXL2) pathway to drive cholangiocarcinoma; a malignant growth of the bile ducts, suggesting that HCV may also induce other hepatic malignancies (219). The LOXL2 pathway is regulated by TGFβ indicating a role for TGFβ in driving this process. Figure 1-8 depicts EMT in cancer progression.

These data indicate that HCV in not an oncogenic virus per se; however, virus infection results in an inflammatory response to initiate liver repair. HCV may in turn hijack the repair mechanism. Consequently, the hepatic environment is modified to favour virus replication and transmission. In

response to uncontrolled repair mechanisms, cells maintain a mesenchymal phenotype resulting in increased fibrosis, migration and invasion that promotes hepatic carcinogenesis.

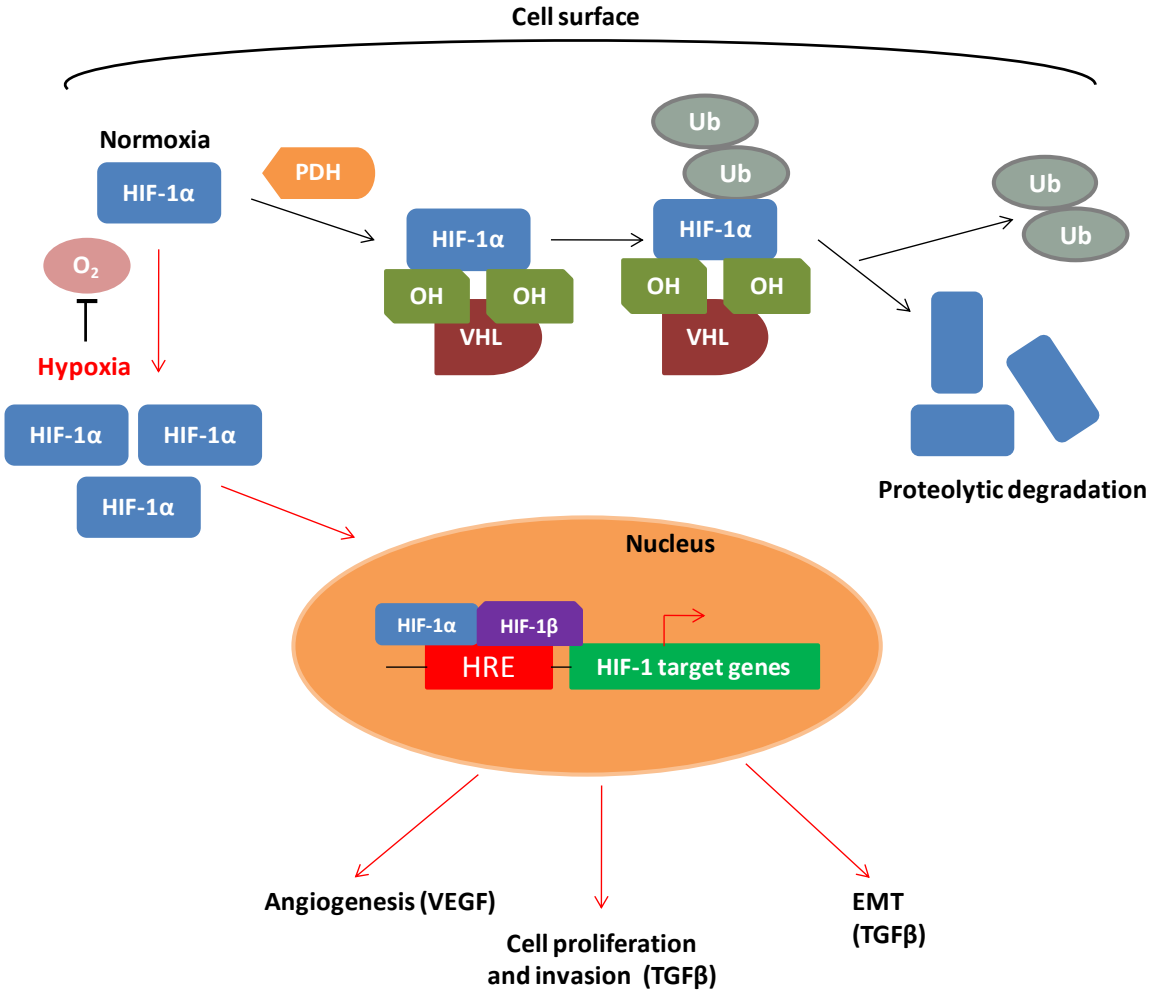

Figure 1-7. HIF-1 signaling in normoxia (black arrows) and hypoxia (red arrows).

In normoxia, HIF-1α is hydroxylated by proline hydroxylases (PHD). Hydroxylated HIF-1α (OH) is recognised by VHL (von Hippel–Lindau tumour suppressor gene) which, together with a ubiquitin (Ub) ligase complex, tags HIF-1α for proteasome degradation. In response to hypoxia, proline hydroxylation is inhibited and HIF-1α is stabilized resulting in HIF-1α accumulation and translocation to the nucleus. There, HIF-1α dimerizes with HIF-1β, binds to hypoxia-response element (HRE) within the promoter region of target genes to affect their transcriptional activity. A range of cell functions are regulated by HIF-1α target genes including VEGF and TGFβ as indicated.

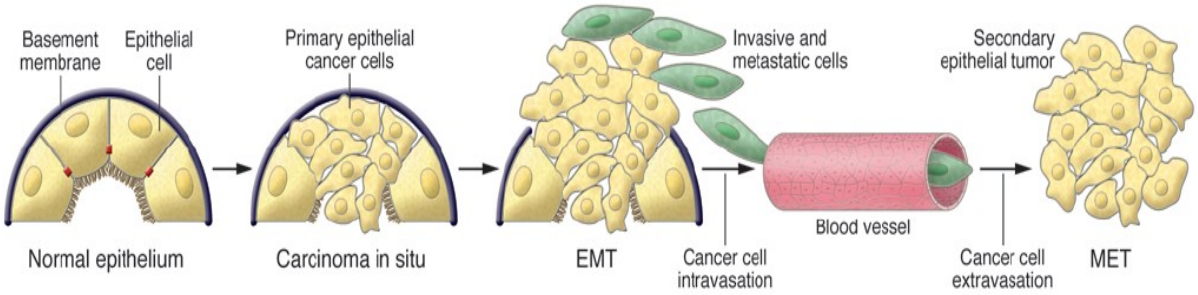

Figure 1-8. EMT during cancer progression.

During cancer progression cells lose their polarity and detach from the basement membrane. The basement membrane also changes via re-modeling of the extracellular matrix. The next stage of EMT involves an angiogenic factor that facilitates tumour growth through vascularisation leading to the detachment of de-differentiated epithelial cells that becomes invasive. Invasive cells enter the circulation and exit the blood stream at a distal site where they form a secondary tumour or reverse via MET to regain a normal phenotype (185).

1.4 Model systems to study the HCV lifecycle

The study of a new virus is made possible by the availability of model systems to study entry and replication. The liver is a highly specialized and complex organ and the development of in vitro systems that reflect the complexity of the liver has proven difficult. Consequently, studies of the HCV life-cycle were hindered for many years due to a lack of appropriate in vitro models. Indeed, host cell receptor molecules that potentiate HCV infection were identified over a decade after the virus was discovered. This section will outline breakthroughs made in the past two decades of HCV research that enables us to study the virus in vitro.

Primary hepatocytes and immortalized hepatocyte based models

Initial studies of the HCV lifecycle capitalized on the hypothesis that virus infection was dependent on host factors expressed in highly differentiated cells. As such, primary hepatocyte cultures from humans or chimpanzees chronically infected with HCV were used for infection studies. However, the use of primary cell cultures were inadequate for several reasons; 1) they supported low levels of HCV replication; 2) the infectivity of the sera did not correlate with the HCV RNA levels making experiments difficult to reproduce; 4) heterogeneous virus populations and HCV specific antibodies in the sera of infected patients impaired the levels of infection; 5) primary cells were difficult to obtain and isolation techniques varied in different laboratories (reviewed in (20, 141)). In addition to primary cell culture, several immortalized human hepatocyte cell lines were reported; PH5CH and HuS-E cells were generated by immortalizing primary human hepatocytes (PHHs) with the large T antigen of simian virus 40 and the

E6/E7 genes of human papiloma virus, respectively (8, 176). Both cell lines supported HCV replication; however, the production of virus particles were restricted and the levels of RNA replication were low making them non-viable for long term studies. Further studies utilised reverse transcriptase polymerase chain reaction (RT-PCR) to detect HCV RNA levels which was indicative of virus replication (356). This technique proved useful in detecting low levels of HCV RNA; however, it also presented new challenges including the potential for random priming by cellular nucleic acids, contamination of RNA samples and lack of strand specificity due to RNA self-priming (209, 391). As such additional criteria were introduced to validate HCV replication, these included treatment of infected cells with interferon-α (IFNα) to cure viral RNA and sequence analysis to demonstrate genome variability.

HCV replicons

The low levels of HCV replication in primary hepatocytes made it difficult to manipulate the viral genome to study its lifecycle in detail. In 1999, Lohmann and colleagues created bicistronic sub-genomic replicons from the liver RNA of a chronically infected patient (233). The regions encoding core to p7 genes were replaced with a neomycin selective marker and the IRES of the enchephalomyocarditis virus (EMCV) (233). Translation of the first cistron (neomycin gene) was directed by the HCV IRES and the second cistron (NS2 or NS3 to NS5B and the 3' UTR) by the EMCV IRES (Figure 1-9). Replicons are genetic elements that can replicate autonomously. The recombinant HCV construct was able to replicate autonomously when introduced into several hepatoma cell lines allowing for the identification of permissive cell types and adaptive mutations that promote HCV replication

in vitro. These mutations were at the N-terminus of NS3, in two positions of NS4B/NS5A and in the C-terminus of NS5B (39, 41, 201). Importantly, when introduced into full length HCV genomes, these adaptations allowed for the complete replication of the viral genome in vitro (40). In the following years, several groups successfully generated full length and sub-genomic replicons (177, 190, 313). HCV replicons made it possible to identity permissive hepatoma cell lines that support efficient HCV replication. Blight and colleagues transfected Huh-7 hepatoma cells with sub-genomic replicons and selected cells containing replicating RNA for prolonged INFα treatment to cure cells of the viral RNA. Sustained INFα treatment resulted in clonal populations that were tested for their ability to support HCV replication after re-transfection with HCV replicons (41). One clone in particular; denoted Huh-7.5, showed a significant enhancement in HCV replication compared to other clones. Efficient virus replication in these cells was partly attributed to a defective retinoic-acid-inducible gene-I (*RIG-I)* pathway which essential for an antiviral immune response (208, 384). The replicon system made it possible to study host and viral signalling necessary for virus replication and echoed a new dawn in HCV research. However, the process of viral entry and assembly could not be realised using this system. Figure 1-9 outlines the HCV replicon system.

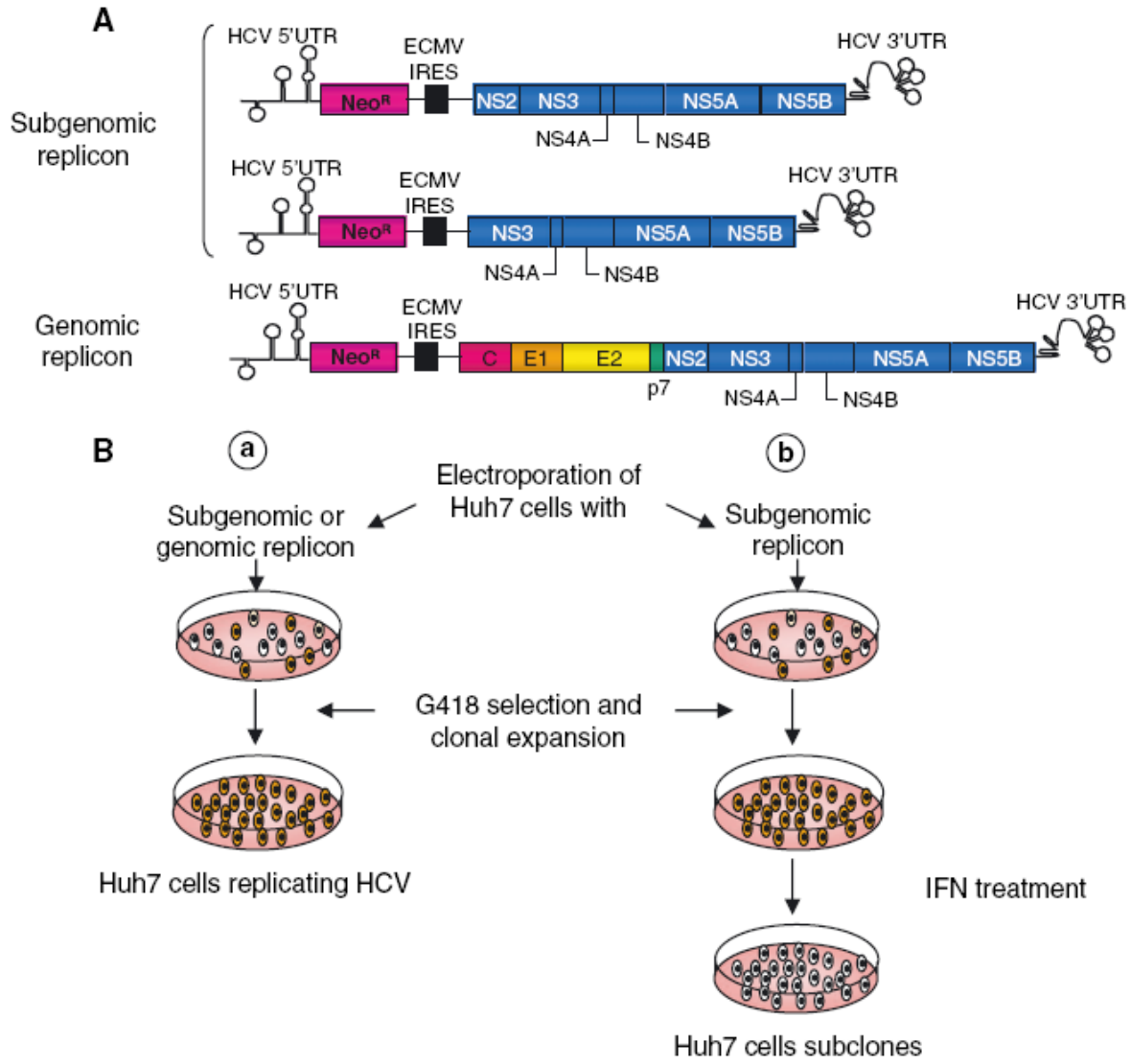

Figure 1-9. HCV replicon system.

A. Huh-7 cells are electroporated with replicon RNA. Cells efficiently replicating HCV replicons were selected by G418 treatment. (**Ba**). In parallel, Huh-7 sub-clones that are highly permissive for HCV replication can be obtained by G418 treatment of cells transfected with HCV replicons, followed by treatment with interferon-α (IFN) to eliminate the HCV replicon resulting in clones that are permissive for HCV replication (**Bb**). Taken from(336).

HCV pseudoparticles (HCVpp)

One approach employed by researchers to realise how HCV interacts with host cells was to express the viral encoded glycoproteins (E1E2) in isolation from other viral encoded proteins. However, high level expression of E1E2 resulted in misfolded aggregates which affected their transmembrane domains (80). To overcome these problems researchers expressed chimeric glycoproteins incorporating transmembrane regions of E1E2 known to be expressed at the plasma membrane or truncated glycoproteins lacking transmembrane domains (414). Deletion of the HCV E2 transmembrane domain resulted in the secretion of a soluble form of E2 (sE2) (267); sE2 was used to identify two putative HCV receptors (SR-BI and CD81) which will be described later in the context of HCV entry. The identification of two putative receptors using sE2 indicated that E2 is the major glycoprotein responsible for receptor binding. However, E1E2 exist as heterodimers suggesting that sE2 was unlikely to recapitulate functional HCV glycoproteins.

The development of infectious HCV pseudoparticles (HCVpp) enabled studies of the entry aspect of the virus lifecycle (171). Pseudoparticles take advantage of the ability of retroviruses to incorporate heterologous glycoproteins in their membrane during budding. HCVpp's were generated by co-transfecting three plasmids into human embryonic kidney (293T) cells; (1) the *gap-pol* gene of HIV or murine leukaemia virus (MLV), (2) a GFP or luciferase reporter gene which allows for the rapid assessment of viral entry and the HCV E1E2 glycoproteins. *Gag-pol* expression resulted in the formation of retroviral particles into which the provirus genome

encoding the reporter is packaged. During budding E1E2 is incorporated into the pseudo-envelope, because there are no retroviral glycoproteins in the system cell entry is determined solely by the HCV glycoproteins. Entry results in the delivery of the retroviral nucleocapsid protein into the cytoplasm followed by reverse transcription and incorporation of the viral genome into the host cell genome. The reporter gene is then expressed allowing for a read out of HCVpp entry into the cell (reviewed in, (336, 411, 414). A schematic representation of HCVpp generation is depicted in Figure 1-10. HCVpp infection of hepatoma cells was ablated by specific E1 and E2 neutralizing reagents to confirm that both E1 and E2 are indispensible for HCV entry (24, 171, 205) and provided the first functional assay to screen the effects of neutralizing antibodies on virus entry. HCVpp from diverse genotypes has allowed for the analysis of genotype specific neutralization and entry efficacy (24). HCVpp's were critical in the identification of HCV co-receptors Claudin-1 and Occludin, the identification of these receptors and their role in the HCV lifecycle will be described later. To date, HCVpp have allowed comprehensive studies of HCV binding, attachment and internalization.

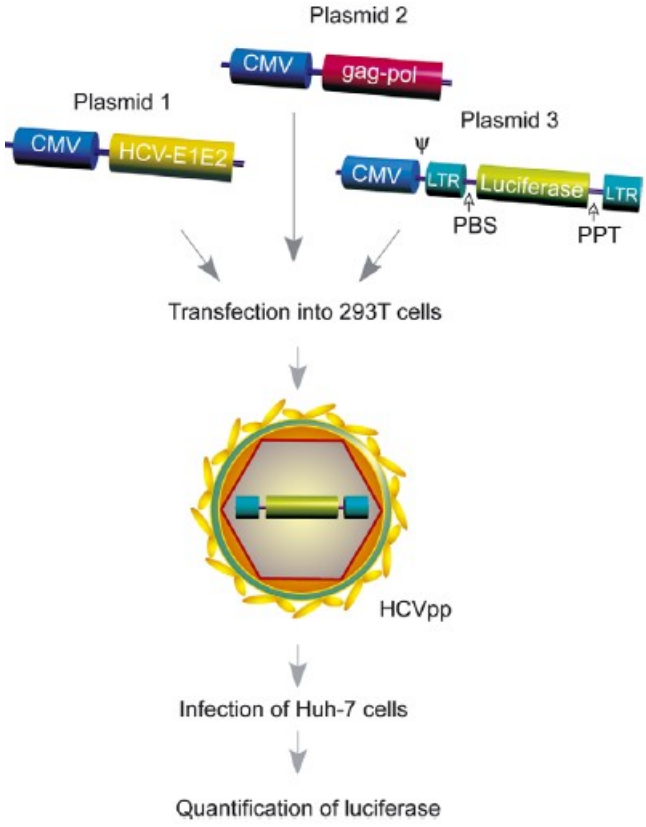

Figure 1-10. A cartoon depicting the generation of HCV pseudoparticles modified from (411).

Cell culture derived HCV (HCVcc)

2005 hallmarked a major breakthrough in HCV research. Several laboratories reported an HCV strain that replicates and release infectious particles in cell culture (HCVcc) (225, 415, 447). The strain was cloned from a genotype 2a virus isolated from a Japanese patient with severe acute HCV infection. This unique clone was referred to as Japanese Fulminant Hepatitis 1 (JFH-1). The efficient replication of HCVcc meant that the full lifecycle of the virus could be realized in vitro. Unlike all previous HCV genomes tested JFH-1 infection of hepatoma cells resulted in the release of progeny virus capable of infecting naive cells. Importantly, HCVcc was infectious for chimpanzees and mice transplanted with human hepatocytes (227). JFH-1 replication was not robust in certain cell lines which were susceptible to HCVpp infection suggesting that the limitation was not occurring at entry but rather at the level of replication. HCVcc confirmed major findings made using HCVpp including the identification of HCV co-receptors and continues to increase our understanding of the virus lifecycle. The successful isolation of JFH-1 paved the way for the development of several chimeric HCVcc constructs representing diverse genotypes (143, 144, 360). In conclusion, our understanding of HCV has been hindered for many years primarily because of a lack of robust model systems to study the virus lifecycle. The development of in vitro systems has greatly enhanced our understanding of key aspects in the virus lifecycle.

1.5 Mechanisms(s) of virus entry

Viruses gain entry into a host cell by binding to specific receptors or attachment molecules expressed on the cell membrane. Following attachment bound virus particles internalizes by one of two major routes; namely fusion of the viral envelope with the plasma membrane or uptake via endocytotic vesicles. The final stage of entry is the uncoating of the viral genome which is necessary for replication in the appropriate cellular environment (reviewed in (241)). Entry into a host cell is a complex process where the virus is likely to encounter environmental and immunological barriers; however, viruses have evolved to prime their target cells for entry. For example, studies of the entry mechanisms of murine leukaemia virus (MLV) have shown "virus surfing" an actin-dependent lateral transport of virus particles towards target cells, this conformational change in the cells cytoskeleton prepares the cell for next stage of virus entry be it receptor attachment or membrane fusion (214, 371). Receptor distribution restrict the cellular entry of some viruses, to overcome this viruses interact with signaling molecules which act in two distinct ways. 1) Remodeling the cell to potentiate entry (281); 2) utilizing signaling molecules as chaperones to cellular receptors (91). An example of the latter is the entry process of group B coxsackieviruses (CBV), CBV utilize the tight junction component CAR as a receptor. However, CAR is unattainable to CBV as it approaches the apical cell surface, realizing this CBV engage an apically expressed protein called decay-accelerating factor (DAF). DAF engagement induces signaling events which mediate the translocation of DAF to tight junctions where CAR is accessible to CBV; successful interaction CAR allows CBV to enter the cell (85, 241).

1.6 HCV entry

HCV targets hepatocytes by a complex multi-step process involving four host molecules or receptors to initiate productive infection. Although significant progress has been made over the past few years, the precise mechanism(s) of HCV entry is still unknown. Nevertheless, it is likely that entry is a balanced interplay between, co-receptor interactions in the correct cellular domain and virus induced host cell signalling. This section will outline our current understanding of HCV entry.

HCV attachment factors

In biology, a receptor is defined as a specific molecule expressed on the membrane of a cell to which complementary ligands such as antibodies, hormones and pathogens bind. The definition of a virus receptor is open to interpretation as there are so-called low affinity molecules expressed at the cell surface which viruses utilize to aid in tethering but do not initiate infection or internalize the virus. For example, vaccinia virus binds to cytoskeletal components and uses them as chaperones to secure binding to its major receptors; therefore, this initial targeting of the cytoskeleton is not considered as receptor binding but is essential to bring virus particles close to its receptors (94). These low affinity molecules are commonly referred to as attachment factors. HCV associates with several attachment factors before engaging receptor molecules expressed on target cells. The following sections outline the attachment factors required for HCV engagement of its receptor molecules.

C-type lectins

HCV travels from the initial site of infection to the liver. Virus particles approach the liver via the sinusoidal endothelium which is highly fenestrated and acts as a molecular sieve that filters debris between the blood and hepatocytes. Leaving the circulation HCV interacts with attachment factors expressed on the sinusoidal endothelium. Studies have shown that liver sinusoidal endothelial cells (LSEC) express liver and dendritic specific intracellular molecule 3-grabbing non-integrins (L-SIGN and DC-SIGN). L-SIGN and DC-SIGN are type II membrane proteins belonging to the C-type lectin family of proteins, they play a major role in liver sinusoidal and dendritic cell interaction(s) with T-cells due to their ability to bind intercellular adhesion molecules (ICAMs) (79). L-SIGN and DC-SIGN mediate the attachment of many viruses including HIV, feline caronavirus and dengue virus (5, 335, 417), more recent evidence demonstrated that both molecules bind HCV E2, suggesting a role to capture virus particles from the blood and transcytose them to the underlying hepatocytes (206, 234, 321). Importantly, L-SIGN and DC-SIGN engagement of HCV was inhibited using anti-L-SIGN and DC-SIGN antibodies (136, 235, 322) suggesting a specific interaction. Nevertheless, since both molecules are not expressed on hepatocytes, their role may involve capturing virus at the sinusoidal endothelium/dentritic cells and transcytosing them to the underlying hepatocytes (206, 234, 321).

Glycosaminoglycans (GAGs)

GAGs are cell surface polysaccharides ubiquitously expressed throughout the body and are post translationally linked to proteoglycans (34). Heparan

sulphates (HS) are highly sulphated GAGs expressed on proteglycans at the cell surface and offer a ubiquitous target for viral attachment. Indeed studies have shown that several viruses including dengue and sindbis associate with HS (167, 448). Once HCV has traversed the sinusoidal endothelium, it is believed that HS recruits virus from LSECs (22, 149, 234, 242, 279), and concentrate them at the basolateral surface of hepatocytes. This interaction is mediated by the virus encoded glycoprotein E2 via the HVR1 region (21, 437). In vitro, soluble forms of HS inhibit HCVpp infection of cells as does treatment of cells with heparanase supporting an association between HCV and GAGs (409). However, a study by Callens et al, showed that E2 and HS association inhibited HCVpp entry (56) raising questions as to the exact role of HS in the HCV lifecycle.

Low density lipoprotein receptors

In vivo HCV exist in high and low density fractions that are closely associated with apoliproteins B and E (64, 168, 178, 181), high density lipoproteins (HDL), low density lipoproteins (LDL) and very low density lipoproteins (VLDL) (10, 138, 285, 295, 324). As such, HCV represents a lipo-viro-particle (LVP) due its high lipid content. The liver is the primary site of VLDL assembly with key roles in regulating plasma lipoprotein concentrations. (305). Hepatocyte lipid receptors such as low density lipoprotein receptor (LDL-R) have been proposed as a candidate attachment molecule for HCV (242, 274, 279, 295, 307). In vivo, successful interaction between LDL and LDL-R initiates cholesterol endocytosis and trafficking. Serum derived HCV interacts with LDL-R resulting in enhanced cellular binding and endocytosis. Furthermore, HCV

endocytosis was inhibited by specific LDL-R antibodies and competition from LDL-R ligands including LDL and VLDL (3). These findings were unsuccessfully reproduced using HCVpp, suggesting that the LDL-R pathway is dependent on HCV association with lipoproteins (428). Ectopic expression of LDL-R in cells expressing all the other attachment factors does not confer susceptibility to HCV infection, suggesting that other factors are required to mediate HCV entry into hepatocytes.

HCV entry factors

Following a series of successful interactions with attachment factors, HCV particle uptake into hepatocytes is dependent on four receptor molecules. It is believed that HCV initially interacts with SR-BI, followed by CD81-Claudin-1 complexes and Occludin (108, 189, 440) . However, the exact nature and timing of these interactions is not well understood. Visualising HCV internalisation has been complicated by the heterogeneous nature of the virus particle, in terms of shape density, and its association with lipids. The following section outlines our current understanding of the complex yet fascinating process of HCV entry via its receptor molecules.

Scavenger Receptor Class B member I

Once HCV has traversed the sinusoidal endothelium and becomes concentrated at the basolateral hepatocyte membrane, the exact sequence of virus-receptor engagement is not fully understood; however, the lipid-rich nature of HCV particles favours an initial interaction with the scavenger receptor class BI (SR-BI) protein. SR-BI is a 509 amino acid glycoprotein with a C-terminal cytoplasmic tail, an N terminal domain and two transmembrane domains separated by a large extracellular loop (LEL)

(79). SR-BI functions as a multi-ligand lipoprotein receptor that is ubiquitously expressed throughout the body but is predominantly found in the liver and adrenal glands (79). It facilitates the binding and transfer of lipids from HDL, LDL and VLDL accounting for its varied roles in cholesterol metabolism including the removal of unesterified cholesterol and steroidogenesis (55, 200). In hepatocytes SR-BI mediates the selective uptake of cholesteryl ester from HDL and incorporates it into the plasma membrane to maintain lipid homeostasis between hepatocytes and plasma (61).

SR-BI is highly expressed on the sinusoidal face or basolateral membranes of hepatocytes consistent with the hypothesis that HCV enters the liver by interacting with basolateral expressed receptor molecules adjacent the hepatic portal blood flow (156). SR-BI was identified as an HCV entry receptor in 2002 by Scarselli and colleagues based on their observation that sE2 binds efficiently to SR-BI in HepG2 cells (357). To validate their findings and determine species specificity, Scarselli and colleagues transfected Chinese hamster ovary (CHO) cells with human SR-BI (hSR-BI). Only cells expressing hSR-BI efficiently bound sE2 demonstrating that hSR-BI is required for HCV E2 interaction (357). More specifically, this interaction was mapped to the first hypervariable region (HVR1) of HCV E2 as binding of sE2 was impaired by deletion of the HVR1 (357). Other studies have shown that HCVpp lacking the HVR1 were poorly infectious suggesting that this region is critical for entry (23). Importantly, anti-SR-BI antibodies and siRNA knockdown of SR-BI successfully reduced HCV infection in a genotype specific manner as some genotypes demonstrated increased sensitivity to SR-BI neutralization (62, 99, 146, 412).

Lipoprotein ligands were shown to modulate SR-BI-E2 interactions, where HDL enhanced virus uptake (409, 410) and offered protection against anti-E2 neutralizing antibodies to promote HCV entry (410). Conversely, oxidised LDL inhibited HCV infection in an SR-BI dependent manner (99, 413), this inhibition of infection did not occur by disrupting SR-BI-E2 association but through potential changes in the biophysical properties of the virus (412). These studies suggest the relationship between HCV and SR-BI is more complex than a simple virus-receptor interaction but is highly dependent on the lipid exchange function of SR-BI. Several studies have sought to map the exact role of SR-BI in the virus lifecycle. Bankwitz et al., reported that deletion of HVR1 decreased SR-BI dependence and increased HCV binding to CD81 (19). This finding is consistent with our observation that a single mutation at residue G451 in HCV E2 reduced SR-BI dependence and increased CD81 binding (147). Indeed, HVR1 masks conserved binding epitopes in CD81 to protect them from neutralizing antibodies (19); and mutation of specific N-linked glycans on E2 at positions 417, 532 and 635 increased E2–CD81 association (163). Taken together, these studies suggest that a conformational change in E2 is required to promote CD81 association. This conformational change may be mediated directly by HCV engagement of SR-BI, although this is yet to be determined.

The exact nature of E2-SR-BI interaction is unknown; however, it was reported that HCV E2 links directly to SR-BI (165). This association may in turn induce a membranous or cytoplasmic rearrangement that brings the SR-BI-virus complex in close proximity to other entry receptors. An SR-BI mutant that negates interaction with PDZK-1, a cytoplasmic adapter

protein that regulates SR-BI expression and localization, did not affect HCV entry (98). Conversely, mutations in the SR-BI C-terminus prevented its palmitoylation and association with lipid raft microdomains resulting in decreased HCV entry (98, 148); these findings suggest that SR-BI localization to specific membrane microdomains plays a role in HCV entry. Several reports have shown that SR-BI localizes to plasma membrane lipid rafts (15, 342), these are low density membrane microdomains enriched with cholesterol and are crucial for transport and endocytotic events that could potentiate virus internalization or targeting of co-receptors molecules via SR-BI binding (reviewed in (241)).

SR-BI may also play a role in HCV internalization due to its ability to endocytose its natural ligands via its C-terminal cytoplamic tail (429). Ectopic expression of SR-BII an mRNA splice variant of SR-BI that differs only by its C-terminus induced a rapid internalization of HDL (106) but inhibited HCVpp entry compared to SR-BI (98). This data demonstrate that SR-BI and not SR-BII is essential for HCV entry. Interestingly, the introduction of SR-BII dileucine endocytic motif in the C-terminal tail of SR-BI promotes SR-BI/HDL internalization but reduced HCV entry (98, 105), suggesting that determinants within the SR-BI cytoplasmic tail that controls endocytosis is different from those controlling HCV entry. Furthermore, these findings indicate that if SR-BI does induce HCV endocytosis it does not occur in a binary SR-BI virus interaction manner but may occur through SR-BI engagement of other HCV co-receptors.

To determine whether an association exists between HCV receptor expression levels and viral replication kinetics post liver transplant, Mensa

and colleagues studied entry receptor levels 24hrs post transplantation (263). The authors noted a significant association between SR-BI expression levels and HCV RNA, suggesting that SR-BI levels may limit HCV entry and replication in the new allograft. However, the authors did not discriminate between endothelial or hepatocyte SR-BI expression, which may lead to an alternate conclusion that SR-BI on the sinusoidal endothelium, defines HCV clearance rates. Further studies are needed to determine the role of hepatocyte SR-BI expression levels in defining HCV entry into the liver, especially given the interest in therapeutically targeting SR-BI to limit HCV infection post transplant (389, 424)

Tetraspanin CD81

It is believed that HCV engagement of SR-BI induces a conformational change in HCV E2 that allows its association with CD81. CD81 is a member of the tetraspanin family of proteins that includes CD9 and CD151, tetraspanins are type III glycoproteins ubiquitously expressed throughout the human body. They are organized into tetraspanin webs, which allow them to interact with other tetraspanins or integrins (305). They have multiple regulatory roles in cell signaling pathways including proliferation, migration and adhesion (244). CD81 is a 26-kDa protein made up of four hydrophobic transmembrane helices separating two extracellular (EC) loops, defined as EC1 and EC2. It has varied roles in signaling events including immune cell activation and morphology. Furthermore, CD81 is essential for Plasmodium infection of hepatocytes (217, 376). CD81 was the first molecule reported to interact with sE2 and was therefore proposed as a putative candidate receptor (314). HCV entry is highly dependent on

CD81 since anti-CD81 antibodies can neutralize diverse genotype transmission (50). CD81 EC2 binds HCV E2 via three domains; including amino acids 480–493, 544–551 and 612–619, along with several individual residues W420, Y527, W529, G530, and D535 (89, 296, 297). Importantly, sE2-CD81 interaction is species specific as sE2 only interacts with cells from human and not mouse origin. Furthermore, antibodies against CD81 or HCV patient sera inhibited the sE2 interaction (314, 427). Additional studies showed that siRNA knockdown of CD81, anti-CD81 monoclonal antibodies and recombinant forms of CD81 EC2 ablated HCVpp infection of primary human hepatocytes and hepatoma cells (26, 84, 443). Moreover, ectopic expression of CD81 in non permissive HepG2 cells induced susceptibility to HCVpp infection (254, 260).

Anti-CD81 antibodies or HCV E2 engagement of CD81 has been reported to activate Rho GTPase family members Rac, Rho and CDC42 (cell division cycle 42) and MAPK (mitogen-activated protein kinase) signaling cascades (48), to induce actin remodeling that allowed the lateral movement of CD81 necessary for HCV entry. However, we observed high levels of MAPK activation in a number of hepatoma cells and inhibiting these pathways with a variety of kinase inhibitors had no significant effect on HCV entry (113), highlighting the caveats of studying signaling pathways in transformed tumour cell lines. Further work is required to study the consequences of CD81 ligation in primary hepatocytes. CD81 has no endogenous ligand and does not possess an internalization motif accounting for its slow internalization rate (32, 308). However, recent data from our lab suggest a role for CD81 trafficking in HCV entry. CD81 antibodies and HCV engagement promotes CD81 internalization in a

clathrin mediated endocytosis dependent manner. Furthermore, anti-CD81 antibodies neutralized HCV infection post internalization suggesting an intracellular site for CD81 neutralization. These data suggest that HCV engagement of CD81 may promote its endocytosis which in turn potentiates virus entry (Farquhar et al, manuscript submitted).

CD81 is expressed on the basolateral membranes of hepatocytes where it co-localises with SR-BI and Claudin-1 (341). To understand how receptor complexes coordinate HCV entry, Harris et al, (156) utilized fluorescence resonance energy transfer (FRET) imaging techniques to identify CD81-CD81 and CD81-Claudin-1 protein complexes. Treatment of hepatoma cells with recombinant HCV E1E2 gycoproteins did not modulate FRET association between co-receptor complexes suggesting that FRET occurs in the absence of viral proteins. However, an anti-CD81 monoclonal antibody reduced FRET between CD81-CD81 but not CD81-Claudin-1 associations highlighting differences between homo and heterotypic co-receptor complexes in HCV entry (156). These data suggest that the correct localization and association of CD81 with other co-receptor molecules coordinates HCV entry.

A recent study implicated CD81 in HCV replication, HCV RNA replication occurred in cells expressing high levels of CD81. In contrast, cells expressing low CD81 levels demonstrated reduced RNA replication. Interestingly, over expression of CD81 increased HCV RNA synthesis, these findings suggest diverse and multiple roles for CD81 in the HCV lifecycle (445). CD81 interacts with two immunoglobulin proteins EWI-F and EWI-2 (66, 444) that link CD81 to the actin cytoskeleton by interacting with

Ezrin-Radixin-Meosin (ERM) protein (354). Expression of a EWI-2 cleavage product designated EWI-2wint (without its N terminus) abrogated HCVpp and HCVcc infection of hepatoma cells by blocking CD81-E2 interaction (346, 363). However, the role of EWI-2 in HCV entry is unclear as it is not expressed by primary human hepatocytes.

CD81 expression levels affect the efficiency of HCV infection as a minimum threshold of CD81 at the cell surface is necessary to render Huh-7 hepatoma cells susceptible to virus infection (199). Cells expressing SR-BI and CD81 failed to support HCV entry suggesting that additional receptor molecule(s) are required.

Claudin-1

Crucial to the functioning of all organs in the human body is the compartmentalization and directional trafficking of solutes in a specific manner. For example, the liver regulates the directional flow of bile by separating it from the blood flow (222). This is achieved by tissue polarization; hepatocytes have distinct membrane surfaces termed apical and basolateral. Each surface have a specific protein expression profile suitable to the tasks it performs (418). Tissue polarity is regulated by tight junction proteins, in the liver tight junctions separates the apical canalicular membrane where bile flow takes place from the basolateral sinusoidal membranes adjoining the blood flow. Tight junctions are multi-protein complexes that seal the paracellular space between adjacent cells in a way that prevents the free movement of solutes between distinct membranes (299). Sealing of the paracellular space is achieved through a series of interactions between transmembrane proteins including Occludin,

Claudin's, and junctional adhesion molecules (JAM). Tight junctions interact with the cells cytoskeletal structure; an association mediated through scaffolding or signaling partners such as the Zona Occludens (ZO-1/2) and Cingulin (4, 16). Figure 1-11 depicts transmembrane tight junction components.

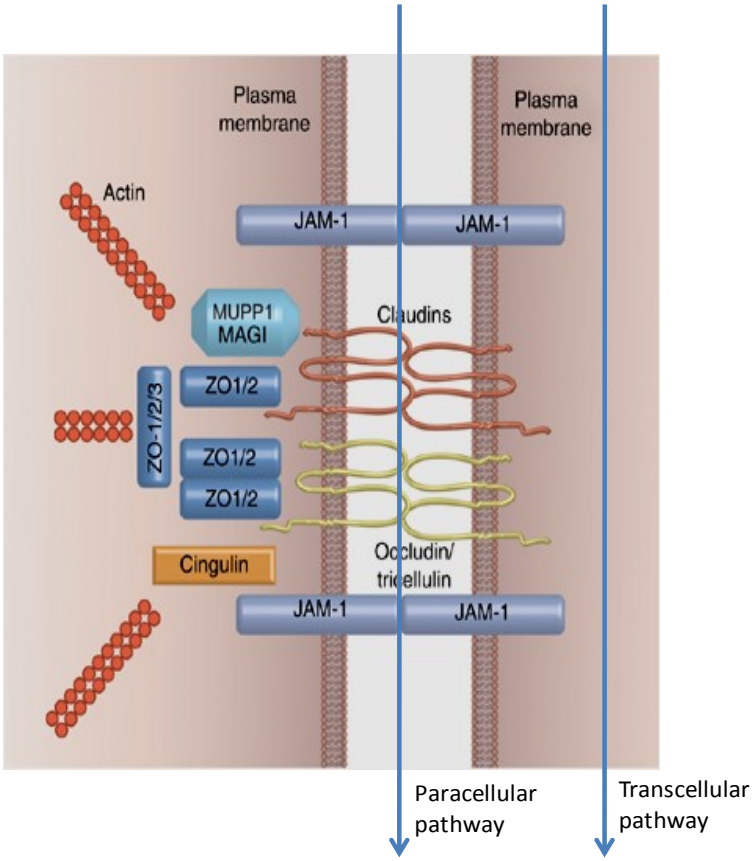

Figure 1-11. Organization of tight junction components.

Cartoon shows tight junction components and scaffolding partners that provide a link to the cytoskeleton. Arrows depict the movement of solutes via a paracellular or transcellular pathway, modified from (286).

Claudin-1 is 21 kDa in size and belongs to the Claudin family of transmembrane proteins. There are 24 members of the Claudin family that are highly conserved and share a basic structure consisting of four transmembrane domains that anchors a large and small extracellular loop (EC1 and EC2, respectively). EC1 is responsible for sealing of the paracellular space and the formation of ion channels, whereas EC2 is associated with the correct conformation and positioning of the protein (11). The cytoplasmic terminus of Claudin-1 has a PDZ-binding domain through which Claudin-1 interacts with the zona occludens that tether Claudin-1 to the cytoskeleton. Perturbation of this interaction leads to aberrant tight junctions; a phenotype associated with malignant tumours (251). Claudin-1 is predominantly expressed at the apical membrane of hepatocytes; however, a pool of Claudin-1 is observed at the basolateral membranes and this portion is believed to play a role in HCV entry (341).

In 2007, Evans and colleagues identified Claudin-1 as the third HCV co-receptor. The authors showed that the human embryonic kidney cell line (293T) that expresses SR-BI and CD81 but not Claudin-1 was resistant to HCV infection subsequent to Claudin-1 transduction (108). Importantly, silencing of Claudin-1 in permissive hepatoma cells ablated HCV entry (108, 446). However, Claudin-1 expression levels did not modulate HCV infectivity suggesting a putative indirect role for this molecule in the entry process. Generation of chimeric Claudin-1 molecules expressing domains of Claudin-7 showed that Claudin-1 EC1 domain is required for functional receptor activity. Claudin-1 and -7 share a highly conserved EC1 domain that differs by 5 residues only, mapping of these sites demonstrate that residues E48 and I32 define Claudin-1 co-receptor activity (108). To

further confirm the role of the EC1 in HCV entry, a Flag epitope was inserted into this region resulting in the inhibition of HCVpp entry using an anti-Flag antibody. Furthermore, the use of anti-Flag and anti-CD81 antibodies to inhibit HCVpp entry at various time points suggested that HCV-CD81 interaction precedes Claudin-1 engagement (108). Nevertheless, the precise role of Claudin-1 in HCV entry is not yet determined as no direct association between Claudin-1 and the viral glycoproteins has been reported to date. Several studies have suggested that Claudin-1 plays a role in HCV internalization as anti-Claudin-1 antibodies neutralized viral infection post attachment (123, 202). Indeed, a study has shown that Claudin-1 endocytose and fuse with Rab5 expressing early endosomes, indicative of a putative pathway for HCV to hijack during its internalization (113). Recent data from our group showed increased Claudin-1 endocytosis induced by HCV infection, suggesting that HCV modulate Claudin-1 internalization during entry (Farquhar et al, manuscript submitted).

Claudin's share a similar topology with tetraspanins and associate with CD81 at the plasma membrane. Data from our lab using FRET showed the formation of Claudin-1-CD81 complexes in the membranes of hepatoma cells and hepatocytes in the liver tissue. Perturbation with a protein kinase A (PKA) antagonist (112) and anti-CD81 antibodies (156) decreased FRET between these two molecules and inhibited HCVcc and HCVpp infection. More recent observations has shown that the Claudin-1-CD81 association is localized to the basolateral membrane of polarized HepG2 cells, whereas tight junction or apical associated pools of Claudin-1 demonstrated minimal

association with CD81, suggesting that Claudin-1-CD81 association at the basolateral membrane potentiates HCV infection (154).

Haid and colleagues developed a receptor complementation system in Huh 6 hepatoma cells that express low levels of endogenous Claudin-1 to assess the functional properties of Claudin-1 (151). Naive Huh 6 cells were resistant to HCV infection; however, expression of human, hamster or rat Claudin-1 supported HCV entry. In contrast, expression of mouse Claudin-1 showed moderate effects. The differences between mouse, human and rodent (hamster and rat) Claudin-1 were mapped to mouse-specific residues in the EC2. The authors suggested that these determinants could prevent optimal interaction with other co-receptors thus limiting efficient HCV infection and identified Claudin-1 as a contributory factor to HCV species specificity (151).

Two additional Claudin family members; Claudin-6 and 9 were also implicated in HCV entry (261, 446). Expression of Claudin-1, 6 and 9 but not other Claudin's rendered 293T cells susceptible to HCVpp entry. However, Claudin-6 and 9 expression levels in the liver and primary human hepatocytes is moderate and their role in particle entry is unclear, studies to characterise their interaction with HCV are ongoing.

Occludin

Whilst the presence of SR-BI, CD81 and Claudin-1 are essential for HCV infection; when expressed together they do not allow HCV infection of non-permissive cells. Benedicto and colleagues demonstrated that HCV E2 glycoprotein perturbed the cellular distribution of tight junction proteins in Huh-7 hepatomas resulting in the intracellular co-localization of Occludin

(30). This study represents the first indication of a putative role for Occludin in HCV entry although it was not fully grasped at the time. The role of Occludin was not formally identified until a year later when two independent studies implicated it in the virus lifecycle. In the first study, a short hairpin RNA (shRNA) library was used to reduce Claudin-1, Occludin, and ZO-1 expression. Reduction of all four proteins inhibited HCVpp and HCVcc infection. However, knockdown of ZO-1 alone had no effect on HCV entry, whereas modulation of Claudin-1 and more specifically Occludin reduced HCVpp entry (229). Ploss and colleagues expanded further on the role of Occludin in HCV entry (317). Expression of human Occludin and human CD81 in murine cells expressing endogenous SR-BI and Claudin-1 allowed for productive HCV infection. Conversely, silencing of Occludin expression in permissive Huh-7.5 cells reduced HCV entry (317).

Occludin is 60 kDa in size and consists of four transmembrane domains with two extracellular loops. Similar to Claudin-1, Occludin regulates the tight junction barrier and is tethered to the cytoskeleton through interactions with binding partners such as ZO-1 and Cingulin (117).

One of the greatest challenges in HCV research is the lack of a small animal model that supports HCV infection in which vaccine candidates can be evaluated. Apart from humans, the chimpanzee is the only known host for HCV replication and is not widely available for research use. The observation that Occludin allows HCV to infect murine cells is an exciting prospect because at least one species specific barrier has been removed to support the development of small transgenic animal models for HCV research (17, 312, 317, 319). Using a panel of inter-species chimeras and

alanine scanning mutagenesis of the extracellular domain of Occludin Michta et al, reported that the latter half of the extracellular 2 domain is critical for HCV entry and a further 2 cysteine residues flanking this region may facilitate interactions by forming a specific loop conformation mediated by disulfide bonding (271). Mapping the regions of Occludin essential for HCV entry represents significant progress in understanding its role in HCV entry. Occludin is predominantly expressed at the apical membrane of hepatocytes in normal liver concomitant with minimal expression at the basolateral surface (259). Recent data from our laboratory showed that perturbing Occludin localization with cell penetrating Occludin peptides (109) promotes HCV entry and suggests a role for intracellular Occludin in HCV entry (Mee et al, manuscript submitted). This data is consistent with one study demonstrating a post binding role in HCV entry (31). Furthermore, an observed co-localization of Occludin, CD81 and Claudin-1 in early endosomes supports a model where HCV exploits the dynamic intracellular trafficking of receptor proteins (Mee et al, manuscript submitted). Figure 1-12 shows the HCV receptor complex.

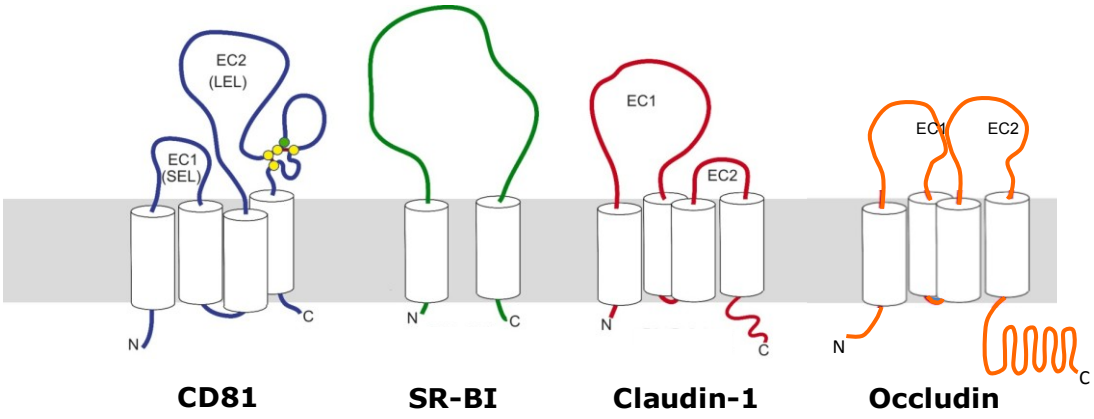

Receptor	HCV E2	HCV E2	?	?
Role	Internalization	Attachment	Internalization	Internalization

Figure 1-12. HCV receptor molecules.

CD81, Claudin-1 and Occludin receptor activity is dependent on residues in EC2 EC1 and EC2 domains respectively. SR-BI receptor activity is dependent on residues within its C-terminus. CD81 and SR-BI interacts directly with HCV E2 glycoprotein and aid in virus internalization and attachment respectively. The role of Claudin-1 and Occludin in the virus lifecycle is unclear as no direct association with HCV has been reported. However, it is believed that both proteins are important for virus internalization. Modified from (400).

1.7 HCV endocytosis and fusion

Following successful attachment to cell surface receptors, HCV particles internalize by crossing the cell membrane. HCV enters the cell via clathrin mediated endocytosis in a low pH compartment, (reviewed in (241)). This was demonstrated by silencing the clathrin heavy chain protein involved in endocytosis and blocking clathrin polymerization which inhibited HCVpp and HCVcc entry (38, 81, 262). Furthermore, inhibitors of endosomal acidification blocked HCVpp infection of hepatoma cells confirming a role this pathway (38, 81, 172). There is a 20 minute delay between HCV endocytosis and genome penetration suggesting that low pH is not sufficient to trigger fusion and other molecular events such as receptor engagement maybe required. This finding was substantiated by the observation that low pH pre-treatment of HCV particles had no effect on HCVcc infectivity (402). Indeed, studies have shown that clathrin mediated endocytosis transport viruses in conjunction with their receptors (reviewed in (241)).

Imaging studies have shown colocalization of HCV and Rab5, an early endosomal marker suggesting that HCV is delivered to early and not late endosomes. As such HCV entry is reduced in Huh-7 cells expressing dominant Rab5 GTPase mutants that interferes with cargo delivery to early enodsomes compared to cells expressing a Rab7 GTPase mutants which perturbs delivery to late endosomes (262). The acidic pH inside early endosomes triggers virus uncoating and penetration; penetration occurs via membrane fusion initiated by fusion peptides in the envelope glycoproteins (379). Fusion peptides are hydrophobic domains that are

inserted into the host cell membrane to induce the formation a hair-pin structure that brings the virus into close proximity to the lipid bilayer (192, 193). HCV fuses to the host lipid membrane to allow trafficking of the viral RNA into the cytoplasm.

Fusion of viral envelopes and cellular membranes is mediated by two classes of fusion proteins, namely class I and class II (241). Analysis of HCV glycoproteins revealed a folding pattern reminiscent of class II fusion proteins (137). Class II fusion proteins potentiate virus penetration following endocytosis in a low pH endosomal compartment as low pH is necessary for exposure of the fusion peptide (193). Clathrin and other proteins assemble at the cell membrane to form clathrin coated pits in a dynamin dependent manner (276). Clathrin coated pits are matured in early endosomes by shedding of the protein coat and acidification. Subsequent to HCV entry, the low pH of the endosome induces a conformational change that enables HCV glycoprotein fusion with the endosomal membrane resulting in the release of the viral genome into the cytoplasm. To date the precise mechanisms of HCV fusion are unclear; however it has been suggested that fusion resembles other flaviviruses due to pH and temperature dependence (162, 439).

1.8 HCV replication, assembly and release

Release of the RNA genome into the cytosol is closely followed by translation and replication. As previously discussed HCV consists of a single strand positive sense RNA genome composed of a 5' non coding region (NCR), an open reading frame that encodes a large poly protein precursor of about 3000 amino acids and a 3' NCR. The 5' NCR contains an internal ribosome entry site (IRES) that is responsible for cap-dependent translation of the viral RNA (13, 51, 275, 343). Studies have shown that the liver specific micro-RNA (mIR-122) binds to the 5' NCR to enhance HCV replication (182, 309, 334) suggesting that HCV exploits cellular micro-RNA pathways to further its lifecycle. The 3' NCR consists of a poly (U/UC), a 98 RNA nucleotide element called the X-tail and a short variable region, which is indispensible for replication of the viral genome (275).

HCV translation is initiated through the formation of a complex between the IRES and a 40s ribosomal unit followed closely by the assembly of a 48s complex at the AUG start codon after interacting with the eukaryotic initiation factor-3 (eIF3) (294). Translation of the open reading frame results in the large polyprotein precursor that is post translationally modified by host and viral proteases into mature structural (core, E1 and E2), a small ion channel (p7) and non-structural proteins (NS2, NS3, NS4A, NS4B, NS5A and NS5B) (228). The structural proteins and p7 peptide are cleaved by endoplasmic reticulum (ER) peptidases; separation of the core protein by host peptidases results in an immature 23 kDa core protein that undergoes further processing to yield a mature 21 kDa core which is anchored to the ER membrane and on the surface of lipid droplets

where it aids in virus packaging and assembly of new capsids (257). Core protein association with lipid droplets has been suggested to modulate lipid metabolism resulting in the development of hepatic steatosis often seen in patients with HCV infection (14). The envelope glycoproteins E1 and E2 form heterodimers that are retained in the ER by their C-terminal hydrophobic domain, their N-terminal ectodomains translocate to the ER lumen where they are glycosylated to form a non-covalent complex which is believed to be the building block for the new viral envelope (100). ER retention mediate the interaction of E1 and E2 with the core protein, as such it is believed that the viral nucleocapsids derived from the core protein buds through the ER membrane where they acquire their lipid bilayer envelopes. p7 is a 63 amino acid hydrophobic polypeptide that is located between the structural and non-structural proteins in the HCV genome; although it is not yet classified as a structural or non-structural protein. p7 has been designated the virion ion channel capable of mediating cation flow across a membrane. However, more recent studies have shown an essential role for p7 in HCV assembly and release by regulating pH gradient in intracellular compartments resulting in HCV particle maturation (78, 145, 394, 426).

Whilst the structural proteins are the building blocks for the new virion; the non-structural proteins replicates the RNA genome. Cleavage of the non-structural region is achieved through the NS2-3 autoprotease which cleaves at the NS2/3 junction and the NS3-4A serine protease which allows full processing of the remaining non-structural proteins (reviewed in (47, 228)). The NS2-3 autoprotease is essential for full virus replication; its enzymatic activity resides in the C-terminus of NS2 and the N-terminal of

NS3. Cleavage of the polyprotein between NS2 and 3 liberates NS3 which serves as an RNA helicase capable of unwinding double stranded RNA molecules in a 3’ to 5’ direction. Liberated NS3 is in complex with NS4A that functions as a cofactor for the NS3 serine protease (423). Studies have shown that NS3-4A catalyses the mitochondrial antiviral signalling protein (MAVS) which is important for inducing interferon response. Processing of MAVS by HCV proteases leads to impaired function and provides a means for HCV to escape the host immune response (220). HCV polyprotein cleavage sites are depicted in Figure 1-13.

Positive sense RNA viruses replicate their genomes via the formation of a membrane associated replication complex composed of viral proteins, altered cellular membranes and the replicating RNA (237). HCV replication occurs at ER membrane sites which have been modified by NS4B into cellular protrusions or scaffolds known as membranous webs. This process is closely intertwined with the host lipid metabolism as studies have shown that replication is stimulated and inhibited by fatty acids and antagonists of fatty acid synthesis, respectively (435). The replication cycle continues with the synthesis of a complementary negative strand RNA template from the original viral genome. This negative strand template is used to produce nascent HCV genomes, both steps are governed by NS5B which is the virus RNA-dependent-RNA polymerase; a highly error prone proof reading enzyme that results in nascent divergent virus variants (29, 430). NS5B has been studied extensively and is a major target for antiviral strategies due in part to the solving of its crystal structure. Also known as a tail anchored protein, NS5B is anchored to the ER lumen via a 21 amino acid

residue sequence in its C-terminal, which serves as a docking site for protein interactions (361).

NS5A is a phosphoprotein that can be found in a basally phosphorylated (56 kDA) or a hyperphosphorylated (59 kDa) form (329). Studies have shown that that NS5A potentiates HCV replication via interactions with NS5B and various cellular pathways (374, 403). NS5A consists of three distinct structural domains, namely domain I, II and III (396). Foster et al demonstrated that all three domains bind HCV RNA which is essential for genome replication (126). Further studies have shown that a single serine residue deletion in domain III inhibits phosphorylation of the casein kinase II domain motif in NS5A and inhibits the production of infectious virus particles (395). Additional evidence has demonstrated a role of NS5A in HCV particle assembly (12, 395), mutations in domains I and III prevented NS5A targeting of lipid droplets containing the core protein, leading to a reduction in secreted virus particles (273). NS5A also dampens the host immune response and promotes viral resistance by inactivating the double stranded RNA kinase PKR (132). Furthermore, NS5A induces oxidative stress (142) suggesting an integral role in HCV associated liver disease. The role of NS5A in the HCV lifecycle is still the focus of ongoing investigations. Figure 1-13 depicts HCV genome organization and polyprotein cleavage.

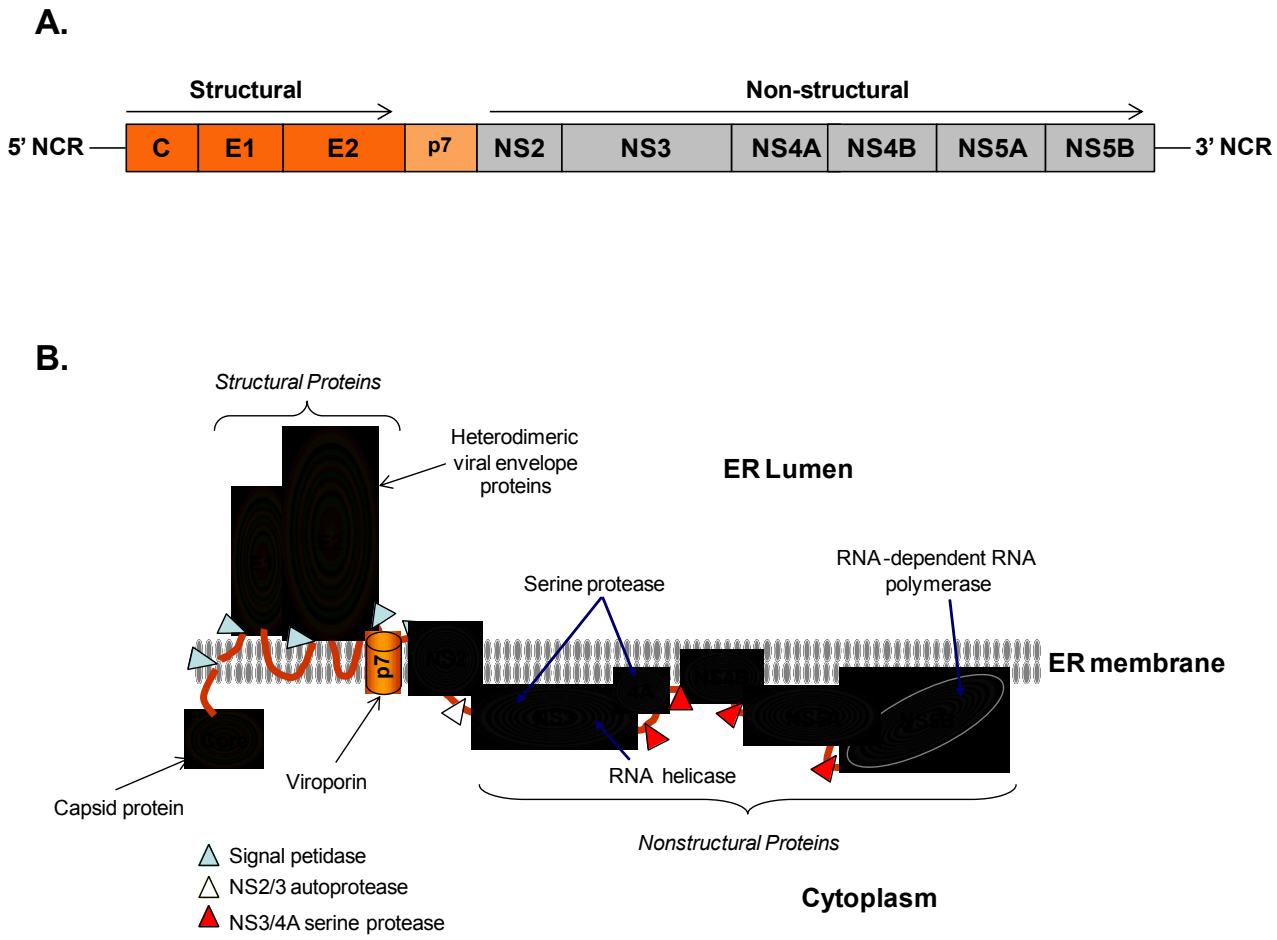

Figure 1-13. HCV genome organization.

A. The genome is organized into 3 structural proteins, a small ion channel and 6 non-structural proteins. **B.** The genome is cleaved by host and viral enzymes resulting in cleavage products shown in an endoplasmic reticulum (ER) membrane web. Arrow heads depicts cleavage sites and the function of each protein where known is shown.

Little is known about the late steps in the viral lifecycle; however, as discussed the non-structural proteins are recruited to lipid droplets sites coated by the core protein (256, 392) where RNA replication occurs at specialized ER sites to provide genomes for packaging into capsid structures composed of the core protein. In this manner, it is believed that lipid droplet associated membranes are sites of HCV particle assembly. In hepatocytes, lipid droplets constitute the bulk of lipids incorporated into VLDLs (421). Lipoproteins deliver dietary lipids to tissues throughout the body and it is believed that HCV utilizes this pathway to secrete infectious virus particles. Infectious HCV particles are characteristically low density around 50-70nm in diameter and complexed with lipoproteins. Inhibition of VLDL assembly with using microsomal transfer protein (MTP) inhibitors and depletion of apolipoproteins ApoB and ApoE blocked the release of HCV particles (64, 138, 173) to demonstrate that HCV release is associated with VLDL production. The assembly of VLDL occurs in two stages; firstly, nascent ApoB particles are lipidated by MTP to produce immature precursor lipoparticles. The second stage involves the addition of precursor lipoparticles to other lipoprotein components such as triacylglycerol and ApoE that gives rise to mature VLDL particles (140). After packaging of the viral genome into capsids formed by the core protein HCV assembly occurs through an unknown pathway in which the envelope glycoproteins are added to the capsids and combine with the VLDL pathway to release so called lipoviroparticles from the cell (255). Figure 1-14 depicts the HCV lifecycle.

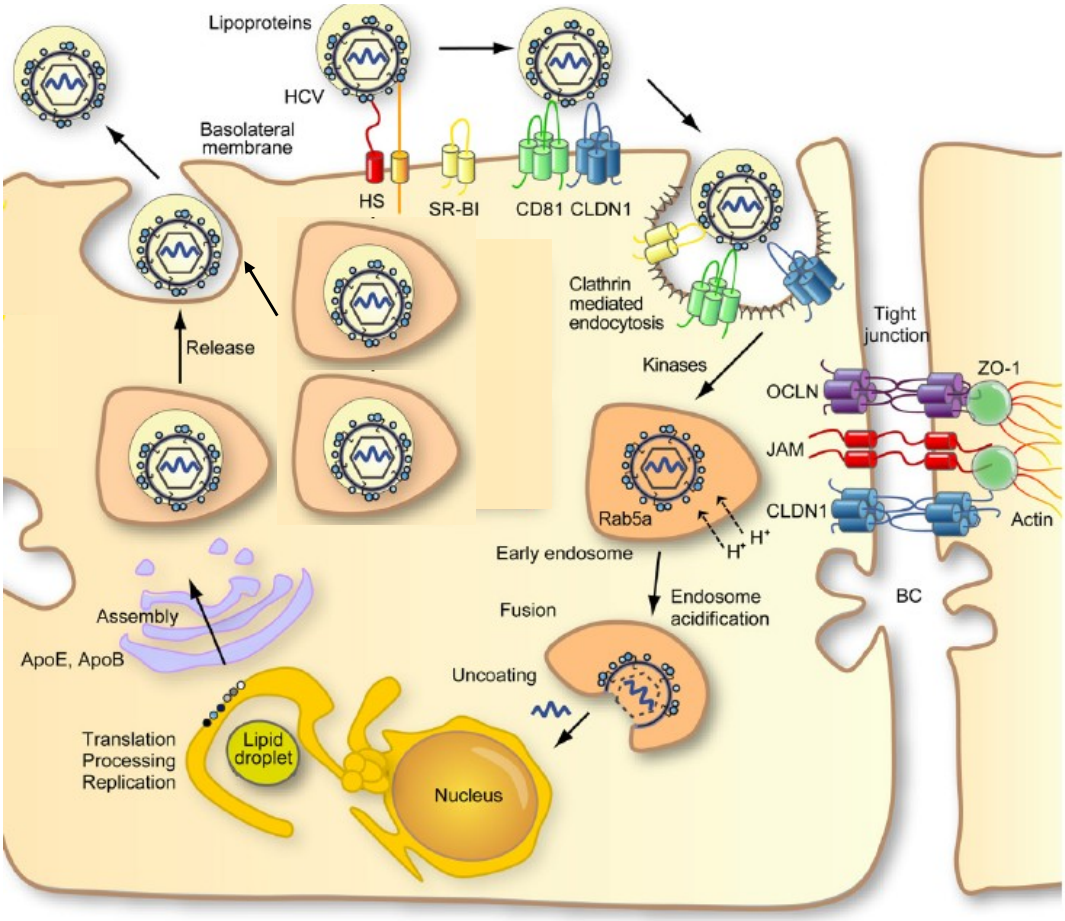

Figure 1-14. The HCV lifecycle.

HCV interacts with attachment molecules (heparin sulphate [HS] and low density lipoprotein receptor [LDLR]) on the basolateral membrane of hepatocytes. This is followed by a series of interactions with SR-BI, CD81-Claudin-1 complex and Occludin to potentiate virus internalization in a clathrin mediated manner. Fusion to the endomsomal membrane is followed by release of the viral genome into the cytoplasm where translation and replication occurs on ER membrane webs. HCV particle assembly is associated with apolipoproteins (ApoE and ApoB) synthesis, accounting for the lipid nature of virus particles released from cells. Tight junction proteins (junctional adhesion molecule [JAM], Zona Occludens [ZO-1], Claudin-1 [CLDN1] and Occludin [OCLN] are shown sealing the bile canalicular lumen (BC). Cartoon modified from (439).

1.9 Project aims

The work presented here provides insights into the mechanisms of HCV perturbation of hepatocellular homeostasis. HCV infection leads to chronic liver sequelae including HCC via undefined mechanism(s). Virus infection is a leading indicator for liver transplantation often culminating in graft failure due to exacerbated reinfection in the post-operative period. It has been suggested that glucocorticoids enhances HCV infection of the newly transplanted liver. However, the mechanism(s) governing this phenotype remains undefined. As such steroid treatment is still administered to HCV liver transplant patients.

Hepatocytes demonstrate a complex polarity, making in vitro studies to recapitulate in vivo HCV infection difficult. Current in vitro infection models are based on HCC derived cell lines which do not reflect normal hepatocyte physiology. Primary hepatocytes are perceived as a physiological in vitro model for HCV infection. However, there are relatively few reports describing HCV infection of primary hepatocytes due to difficulties in procuring liver specimens. Herein, we have obtained primary hepatocytes; allowing for the study of HCV infection in a relevant cell culture model.

The project objectives are as follows;

- To investigate whether HCV infection of primary hepatocytes and hepatoma cell lines are comparable. We aim to validate the use of hepatoma models as physiologically relevant for the study of HCV entry and replication.
- To provide insights into the role of HCV in driving HCC pathogenesis.

- To elucidate the underlying mechanism(s) of glucocorticoid exacerbation of HCV infection and liver injury in the post-operative period.

2. MATERIALS AND METHODS

2.1 Cell lines and tissue culture.

Hepatoma cells were maintained in Dulbecco's modified Eagle's medium (DMEM) (Gibco, USA), supplemented with 10% foetal bovine serum (FBS), 1% L-Glutamine, 1% nonessential amino acids and 50units/ml penicillin/streptomycin (Gibco) at 37°C, 20% O_2 and 5% CO_2. For hypoxic conditions cells were maintained at 37°C, 1% O_2 and 5% CO_2.

Name	Tissue	Growth Media	Source
Huh -7.5	Human Hepatoma	DMEM	C Rice, Rockefellar University, NY, USA
HepG2	Human Hepatoblastoma	DMEM	American Type Culture Collection
HepG2-CD81	Human Hepatoblastoma	DMEM	In House
HepG2 (E1E2)	Human Hepatoblastoma	DMEM	In House
HepG2 (VSV-G)	Human Hepatoblastoma	DMEM	In House
Hep3B	Human Hepatoma	DMEM	C Rice, Rockefellar University, NY, USA
293-T	Human Embryonic Kidney	DMEM	American Type Culture Collection
Primary hepatocytes	Human Liver	Williams E	Ragai Mitry, Kings College London, UK

Table 2-1. List of cell lines used.

2 . 1.1 Isolation of primary human hepatocytes

Primary human hepatocytes were a kind gift from Dr Ragai Mitry (Kings College, London). Cells were obtained from unused donor liver tissue rejected for transplantation due to long ischaemia time. Isolation and preservation were performed in accordance with good laboratory practice guidelines using pharmaceutical grade reagents to ensure reproducibility (272). Appropriate ethical approval and signed consent forms were obtained prior to tissue processing.

For hepatocyte isolation the liver tissue was digested; in doing so, the major blood vessels were cannulated and sutured to prevent fluid leakage

during perfusion, the minor blood vessels were also sutured. Thereafter, a short connector was fitted to the free end of each cannula and attached to perfusion tubes on a perfusion pump with bottles containing perfusion solution 1 [P1] (500mls Hanks Balanced Salt Solution without calcium or magnesium [Cambrex Bioscience, UK], 1ml 250mM EGTA [Sigma, UK], 2.5mls of 1M HEPES [Sigma, UK]). Bottles containing P1 were incubated in a water bath at 37°C.

P1 was used to prime the perfusion lines and the perfusion pump was set to 60-80 ml/minute flow. The perfusion pump was switched on and the liver perfused with using P1, P2 (Hanks Balanced Salt solution) and P3 (Minimal Essential Eagles Medium, containing 25mM HEPES without phenol red and calcium [Lonza, UK], 0.5g collagenase P [Roche Diagnostics, UK]). Digested tissues were transferred to sterile containers and the cannulae and sutures removed. Thereafter, the tissue was immersed in ice-cold wash solution (Minimal Essential Eagles Medium, 25mM HEPES and 50g Bovine Serum Albumin [Sigma, UK]) and minced with scalpels or scissors to release hepatocytes. Liberated hepatocytes were filtrated using two single layers of sterile swabs. The filtered cell suspension was aliquoted into 50ml Falcon tubes (Becton Dickinson) and pelleted by centrifugation at 50 x g and 4°C for 4 minutes. The supernatant was discarded and each pellet resuspended in ice-cold wash solution and the centrifugation process was repeated twice. The viability of freshly isolated hepatocytes was determined by trypan blue exclusion. Briefly, a small aliquot of cells were diluted 1:2 with trypan blue solution and cell viability was determined using a haemocytometer and light microscope.

2 . 1.2 Cryopreservation of isolated primary human hepatocytes

Cryopreservation ensures the availability of hepatocytes for long term use or continuous usage. The following protocol for hepatocyte preservation is based on an optimized, clinically approved protocol from the hepatocyte transplantation unit at Kings College London (328).

The cryopreservation solution consists of ViaSpan™ reagent (Bristol-Myers Squibb, Sweden) + 5% glucose (Hamlin Pharmaceutical Ltd, UK) and 10% DMSO (WAK-Chemie, Medical GmbH, Germany). Isolated hepatocytes were added to the cryopreservation solution at a density of 1.5×10^7 cells/ml. A 50ml syringe was used to deliver hepatocyte suspension to ice cold (2-8°C) cryopreservation bags. The bags were sealed and transferred to a control rate freezer for preservation. The stepwise freezing programme is shown in table 2-2.

At the end of the freezing process, cryopreserved cells were transported on dry ice to a liquid nitrogen tank for long term storage.

Start temperature (°C)	Rate (°C/min)	Time	End temperature (°C)
8	-1.0	8 minutes	0
0	HOLD	8 minutes	0
0	-2.0	4 minutes	-8
-8	-3.5	33 seconds	-28
-28	-2.5	2 minutes	-33
-33	+2.5	2 minutes	-28
-28	-1.0	32 minutes	-60
-60	-10.0	4 minutes	-100
-100	-20.0	2 minutes	-140

Table 2-2. Stepwise control freezing for the cryopreservation of primary human hepatocytes, modified from (272).

2.1.3 Thawing of cryopreserved hepatocytes

Thawing reagent was prepared by adding 20% ice-cold Human Serum Albumin (Baxter AG, UK) to Minimal Essential Eagles Medium containing 25mM HEPES without phenol red and calcium (Lonza, UK) at 1:100 dilution. Thawing was initiated by immersing cryopreserved bags containing hepatocytes into a water bath with sterile water set to 37°C. Thereafter, cryo-bags were sprayed with 70% ethanol, transferred to a laminar flow hood and cut opened using sterile scissors or blades. The cell suspension was placed into 50ml falcon tubes. Cells were pelleted at 50 x g, 4°C for 5 minutes. The supernatant was discarded and cells were resuspended in thawing reagent + 25% Percoll (GE Healthcare, UK) followed by centrifugation at 50 x g, 4°C for 20 minutes to separate viable cells from non-viable cells. The cell pellet was resuspended in thawing reagent and cell viability determined by trypan blue exclusion and haemocytometer counting. Hepatocytes were maintained at 37°C and 5% CO_2 in Williams Essential Eagles Medium (Sigma, UK) supplemented with 10% human serum, 1% L-Glutamine, 50units/ml penicillin/streptomycin (Gibco), 1M HEPES, 1% Insulin, (Sigma, UK).

2.2 Antibodies, cytokines and treatments

Primary Antibodies					
Antibody Name	**Antigen**	**Type**	**Specificity**	**Species**	**Source**
Anti-Claudin-1 (JAY.8)	Human Claudin-1	Purified IgG	Polyclonal	Rabbit	Zymed, CA
Anti-Claudin-1	Human Claudin-1	Purified IgG	Polyclonal	Rat	R&D System, Europe
Anti-Occludin (Z-T22)	Human Occludin	Purified IgG	Polyclonal	Rabbit	Zymed, CA
Anti-CD81 (2s131)	Human CD81	Purified IgG	Monoclonal	Mouse	In House
Anti-SR-BI (PF-71,-71,-73)	Human SR-BI	Purified IgG	Monoclonal	Human	Pfizer, UK
Anti-SR-B1 (Clone 25)	Human SR-BI	Purified IgG	Monoclonal	Mouse	BD Biosciences, UK
Anti-E-cadherin	Human E-cadherin	Purified IgG	Monoclonal	Mouse	Invitrogen, CA
Anti-von Willebrand Factor	Human von Willebrand	Purified IgG	Polyclonal	Rabbit	Dako, UK
Anti-E2 (3/11, 9/27)	HCV E2	Purified IgG	Monoclonal	Rat	In House
9E10	HCV NS5A	Hybridoma Supernatant	Monoclonal	Mouse	Charles Rice, Rokefellar University, NY
Anti-MRP-2	Human MRP-2	Purified	Monoclonal	Mouse	Abcam, UK
Anti-VSV-G	VSV Glycoprotein	Purified IgG	Monoclonal	Mouse	Abcam, UK
Anti-HIF-1α (Clone 67)	Human HIF-1α	Purified	Monoclonal	Mouse	Novus Biologicals, Europe
Anti-TGFβ (ID11)	Human TGFβ	Purified IgG	Monoclonal	Mouse	R&D Systems, Europe
Anti-VEGF (VG76e)	Human VEGF	Purified IgG	Monoclonal	Mouse	Roy Bicknell, University of Birmingham
Anti-Snail	Human Snail	Purified IgG	Polyclonal	Rabbit	Abcam, UK
Anti-Twist (2C1a)	Human Twist	Purified IgG	Monoclonal	Mouse	Abcam, UK
Anti-β-actin	Human β-actin	Purified IgG	Monoclonal	Mouse	Sigma Aldrich, MO, USA
Anti-GR receptor	Human	Purified IgG	Monoclonal	Mouse	Invitrogen, CA
Secondary Antibodies					
Rabbit Alexa Fluor 488	Rabbit IgG	Purified IgG (H+L)	Polyclonal	Goat	Molecular Probes, Invitrogen, CA
Mouse Alexa Fluor 488	Mouse IgG	Purified IgG (H+L)	Polyclonal	Goat	Molecular Probes, Invitrogen, CA
Rat Alex Fluor 488	Rat IgG	Purified IgG (H+L)	Polyclonal	Goat	Molecular Probes, Invitrogen, CA
Human Alexa Fluor 488	Human IgG	Purified IgG (H+L)	Polyclonal	Goat	Molecular Probes, Invitrogen, CA
Rabbit Alexa Fluor 594	Rabbit IgG	Purified IgG (H+L)	Polyclonal	Goat	Molecular Probes, Invitrogen, CA
Rabbit Alexa Fluor 633	Mouse IgG	Purified IgG (H+L)	Polyclonal	Goat	Molecular Probes, Invitrogen, CA
Mouse/Rabbit Universal	Mouse/Rabbit IgG	Purified IgG	Universal	Goat	Vector Laboratories, CA
Anti-Rabbit HRP	Rabbit IgG	Purified IgG	Polyclonal	Donkey	GE Healthcare, PA
Anti-Mouse HRP	Mouse IgG	Purified IgG	Polyclonal	Sheep	GE Healthcare, PA
Anti-Rat HRP	Rat IgG	Purified IgG	Polyclonal	Goat	Jackson Immuno Research, UK

Table 2-3. List of antibodies used.

Primary antibodies		
Antibody	**Application**	**Working concentration (µg/ml)**
9E10	IF	2
Anti-Claudin-1	IF, WB, IHC, FC	1
Rabbit anti-Occludin	IF, WB, IHC, FC	1
Anti-SR-BI	IF, WB, IHC, FC	1
Anti-CD81	IF, WB, FC	1
Anti-E-cadherin	IF, WB	1
Anti-von Willebrand Factor	IF	5
Anti-E2	IF, WB, FC	2
Anti-MRP-2	IF	2
Anti-VSV-G	IF, FC	2
Anti-HIF-1α	IF, IHC	5
Anti-Snail	IF, WB	1
Anti-Twist	IF, WB	1
Anti-Glucocorticoid receptor	IF	2
Anti-β-actin	WB	0.5
Anti-TGFβ	Blocking	1.5
Anti-VEGF	Blocking	1.5
Secondary Antibodies		
Alexa Fluor 488, 594, 633	IF, IHC, FC	1/500
Anti-Mouse/Rabbit Universal	IHC	1/200
Anti-Mouse HRP	WB	1/1000
Anti-Rabbit HRP	WB	1/1000
Anti-Rat HRP	WB	1/1000

Table 2-4. Antibody concentrations used.

IF, indirect immunofluorescence; FC, flow cytometry; WB, western blotting; IHC, immunohistochemistry.

Name	Source	Working concentration	Median toxicity
Dexamethasone	Sigma, UK	100nM	260nM
Geneticin (G418) Sulfate	Invitrogen, CA, USA	1mg/ml	3mg/ml
HIF-1α inhibitor (NSC-134574)	Margret Ashcroft, University College London	1μM	2μM
ITX 5061	Itherx, CA, USA	5μM	1mM
Mitomycin C	Sigma, UK	10μg/ml	20μg/ml
Prednisolone	Sigma, UK	100nM	500nM
RU-486	Sigma, UK	5μg/ml	10μg/ml
Interferon gamma	R&D Systems, USA	Various	NA
Tumour necrosis factor alpha	R&D Systems, USA	Various	NA
TGFβ	R&D Systems, USA	10ng/ml	NA
VEGF-A	R&D Systems, USA	10ng/ml	NA

Table 2-5. Cytokines, growth factors and drugs used in this study.

Drug toxicity was measured using an MTT Cell Proliferation Assay Kit (section 2.3.5).

2.3 Routine techniques

2 . 3.1 Flow cytometry

Flow cytometry was used to quantify total or plasma membrane expression of proteins of interest. Cells were grown in tissue culture flasks (Corning, NY, USA) and trypsinized (Gibco) for 3-5 minutes at 37°C. Thereafter, cells were resuspended in 10% DMEM and counted using a haemocytometer. Cells were pelleted in a 5804R centrifuge (Eppendorf, Germany) at 1200 revolutions per minute (rpm) for 3 minutes and diluted to $2x10^5$ cells/ml in PBS + 0.5% bovine serum albumin (BSA) (Sigma, UK).

For intracellular/total protein detection, cells were incubated in 3% paraformaldehyde (PFA) on ice (TAAB, UK) for 20 minutes followed by a PBS wash and resuspension in PBS + 0.5% BSA. To permeabilize, fixed cells were resuspended in PBS + 0.5% BSA + 0.01% saponin (Sigma) and all subsequent steps carried out in this buffer. For live (surface) staining, cells were resuspended in PBS containing 0.1% sodium azide and no permeabilization was required.

To block non-specific antibody binding, cells were incubated for 30 minutes at room temperature. Antibody staining was performed in 96 well U-bottomed microplates (Corning, NY, USA) with $2x10^5$ cells/well. Briefly, 100µl of cell suspension was transferred to each well and cells pelleted by centrifugation at 1200rpm for 3 minutes, followed by resuspension in 70-100µl of primary antibody diluted in PBS + 0.5% BSA (+0.01% saponin) or PBS + 0.5% BSA (+ 0.1% sodium azide). Species matched IgGs were used as controls throughout.

Primary antibody incubation was carried out for 45 minutes and cells were washed three times with PBS and resuspended in 70-100µl of fluorescent conjugated antibodies, antibody working dilutions are listed in table 2-4.

Cells were incubated in the dark for 45 minutes to prevent photo-bleaching and washed three times in PBS as above. For live cell staining cells were fixed prior to analysis, protein expression was measured using a Facscalibur flow cytometer (Becton Dickinson, Europe), and the data analyzed using FlowJo software (Tree Star, OR, USA).

2 . 3.2 Indirect immunofluorescence

Fluorescent microscopy

To visualize cellular protein expression by immunofluorescence cells were seeded at 4 $x10^4$ cells/ml in 24 well plates (Becton Dickinson). Cells were fixed prior to staining by incubation with ice-cold methanol (Fisher Scientific, UK) or 4% PFA (TAAB, UK) for 5 minutes and 20 minutes, respectively. Thereafter, cells were blocked for 20 minutes with PBS + 0.5% BSA followed by a permeabilizing step with PBS + 0.5% BSA and 0.01% of permeabilization detergent (saponin or Triton X-100). Primary antibody staining was performed by incubation for 1 hour at room temperature with antibody or control isotype diluted in the appropriate buffer. The antibody concentrations used in this study are listed in table 2-4.

After 1 hour the antibody diluents were removed by aspiration followed by a PBS wash, this process was repeated twice. Secondary antibody staining

was achieved with a fluorescent conjugated antibody diluted in the appropriate buffer and incubation in the dark at room temperature for 1 hour.

Cells were washed in PBS as described, the nuclei were counterstained by incubation in 4',6-diamidino-2-phenylindole [DAPI] 10μg/ml (Sigma, UK) for 1 minute at room temperature in dark. Finally, stained cells were visualised using a fluorescent microscope (Nikon TE200, Japan) and images were taken using a digital camera (Hammatsu, Japan).

Laser scanning confocal microscopy

To visualize cellular protein expression by confocal microscopy cells were seeded at 4 $x10^4$ cells/cm^2 into 24 well plates containing 13μm glass coverslips. Prior to cell seeding, coverslips were sterilized in 70% ethanol and washed once with PBS. Cell staining was achieved as described in fluorescence microscopy. Coverslips were mounted onto glass slides using Prolong Gold Antifade mounting reagent (Invitrogen, CA).

Laser scanning confocal microscopy was performed using a Zeiss Metahead Confocal (Zeiss, Germany) utilizing the 63x water-immersion objective. The background fluorescence of each sample was corrected based on the fluorescent levels of the isotype matched control samples.

2 . 3.3 Enzyme linked immunosorbent assay (ELISA)

Human VEGF and TGFβ levels were quantified using ELISA development kits specific for each growth factor (Peprotech, USA) according to the manufacturer's instructions. 100μl of a capture antibody (rabbit anti-

human VEGF or TGFβ diluted in PBS to 100µg/ml) was added to wells of a 96 well microplate, the plates were sealed and incubated overnight at room temperature. Thereafter, the liquid was removed and wells washed 4 times with excess wash buffer (0.05% Tween-20 in PBS). Any residual wash buffer was removed by inverting the plate with gentle tapping on a paper towel after the last wash.

300µl of blocking buffer (1% BSA in PBS) was added to each well followed by incubation at room temperature for 1 hour, after which the wells were washed 4 times. 100µl of conditioned media harvested from hepatoma or primary human hepatocytes after 24 hours in culture or 24 hours post infection was diluted 1:2 in diluent buffer (PBS + 0.05% Tween-20 + 0.1% BSA) and added to each well followed by incubation at room temperature for 2 hours. Wells incubated with buffer alone served as negative controls.

Wells were washed 4 times and 100µl of an Avidin-HRP conjugated antibody diluted 1:1000 in diluent buffer was added to each well followed by incubation at room temperature for 30 minutes. Wells were washed 4 times followed by incubation at room temperature with TMB liquid substrate (BioFix, USA) at 50µl/well for 5-10 minutes. HCV stop solution (BioFix) was used once colour development had occurred and absorbance measured with an ELISA plate reader (Thermo Scientific, USA) at 650nm.

Albumin ELISA

96 well microplates were coated with goat anti-human albumin (0.5mg/ml) (Bethyl Laboratories, USA) diluted in coating buffer (0.5M Na_2CO_3, pH 9.6) and incubated for 4 hours at 37°C. Wells were washed with washing buffer

(500mM Tris, 0.14M NaCl, 0.05% Tween-20, pH 8.0). Wells were blocked by adding 100µl of blocking solution (500mM Tris, 0.14M NaCl, 1% BSA, pH 8.0). Wells were washed 3 times and standards were diluted in sample buffer (50mM Tris, 0,14M NaCl, 1% BSA, 0.05% Tween20, pH 8.0) as tabulated below.

Step	Albumin ng/ml	Calibrator RS10-110-3	Sample Diluent
1	10000	2 µl	5000 µl
2	400	100 µl from step 1	2400 µl
3	200	250µl from step 2	250µl
4	100	250µl from step 3	250µl
5	50	250µl from step 4	250µl
6	25	250µl from step 5	250µl
7	12.5	250µl from step 6	250µl
8	6.25	250µl from step 7	250µl
9	0		250µl

Sample media was harvested from primary human hepatocytes (4×10^4 cells) at 24 hour intervals and diluted 1:2 in sample buffer. The growth media was refreshed daily to ensure that albumin read out was reflective of each time point. Standards ranging from 400-6.25ng/ml and samples were added at 50µl/well in triplicates followed by incubation for 4 hours at 37°C. After which wells were washed 4 times and incubated with 50µl goat anti-albumin HRP (Bethyl Laboratories) diluted 1:1000 in sample buffer for 4 hours at 37°C. Thereafter, wells were washed 4 times and 50µl of TMB substrate (BioFix) added for 5-10 minutes. The assay was stopped by the addition of 1M H_2SO_4. The absorbance was read at 450nm using an ELISA plate reader, albumin levels in each sample was determined using a linear plot of the albumin standard absorbance values. Albumin ELISA was performed with the kind help of Sukhdeep Galsinh.

2 . 3.4 Western blotting

Cell lysates were prepared from adherent cells (control or HCV infected) seeded at 4 x 10^4 cells/well in 6 well plates and maintained in culture for 24 hours. Cells were treated overnight with HIF-1α inhibitor (NSC-134574) 1μm or prednisolone (100nM) diluted in DMEM or Williams E media. The culture media was removed and cells washed in PBS. All subsequent steps were carried out using ice-cold buffers to prevent protein denaturation. 2mls of ice-cold PBS was added to each well and adherent cells remove using a cell scraper (Corning, UK). The cell suspension was transferred to universal tubes and pelleted by centrifugation at 1500 rpm at 4°C for 5 minutes. The supernatant was discarded and the pellet resuspended in lysis buffer (PBS, 1% Brij97, 20mM/L Tris [pH 7.5], 300 mM/L $CaCl_2$, and 2mM/L $MgCl_2$) supplemented with protease and phosphate inhibitors (Roche, UK) and incubated on ice for 30 minutes. The lysate was centrifuged at 15000rpm for 20 minutes at 4°C to separate nuclei and unsolubilized cell membranes from protein. The supernatant was collected and stored at -20°C.

Protein concentration was determined using the BCA Protein Assay Kit (Thermo Scientific, USA) according to the manufacturer's instructions. Briefly, 100μl of each sample or BSA standard were mixed with 200μl of BCA Working Reagent in a 96 well plate in triplicates. After which the plate was incubated at 37°C for 30 minutes. The plate was allowed to cool at room temperature and the absorbance read at 490nm using an ELISA plate reader.

The protein concentration of each sample was determined using a standard curve prepared by plotting the average blank corrected 490nm measurement for each BSA standard versus its concentration in µg/ml.

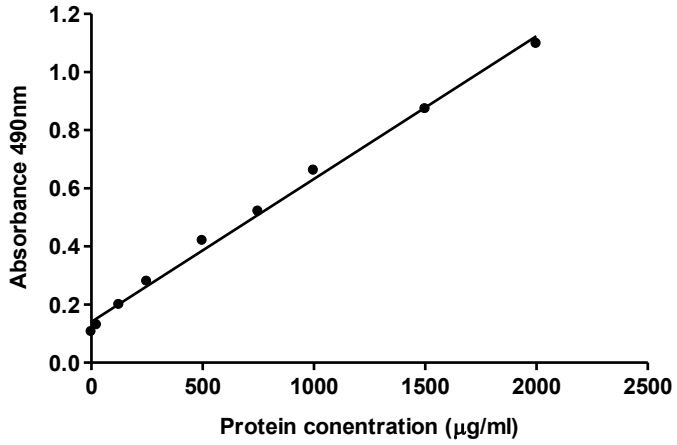

Fugure 2-1. BCA protein assay standard curve.

Sodium dodecyl sulphate polyacrylamide gel electrophoresis (SDS-PAGE).

Proteins were separated on 8% SDS gels. Samples were prepared by adding defined amounts of protein to 3x Laemmli loading dye (H_2O, 30% v/v Glycerol, 6% w/v SDS, 0.02% v/v Bromophenol Blue and 0.2M Tris-HCV; pH 6.8). With (reducing conditions) or without (non-reducing conditions for CD81 detection) 10% 2-β-mercaptoethanol. The total volume was adjusted to 25µl with H_2O and samples were denatured by heating at 95°C for 5 minutes followed by cooling at room temperature before loading.

Proteins were separated by gel electrophoresis using the Mini Protean 3 System (Bio-Rad Laboratories, USA) according to the manufacturer's instructions. Briefly, 20µg of protein lysates were loaded onto 8% sodium

dodecyl sulphate-polyacrylamide gels and gels run at 200 volts constant for 20-30 minutes.

Proteins were transferred to polyvinylidene membranes (Millipore, USA) using a Mini Trans-Blot Electrophoresis Transfer System (Bio-Rad). Briefly, polyvinylidene membranes were cut to appropriate sizes to match the diameter of the gel and pre-treated with methanol for 2 minutes, rinsed with H_2O and incubated in transfer buffer (25mM Trizma Base, 0.2M Glycince, 200ml methanol and 10% SDS) at room temperature for 5 minutes. Gels were equilibrated in transfer buffer to prevent shrinking and transfer was carried out at 350mA for 90 minutes at room temperature.

Immuno-blotting and chemiluminescent detection of proteins.

Following successful transfer, membranes were placed in 50ml falcon tubes; to block non-specific antibody binding, membranes were incubated in antibody buffer (10mM Trizma base, 0.1M Sodium Chloride, 10% v/v Tween-20 and 5% Marvel dry milk) for 45 minutes at room temperature.

The antibody blocking buffer was removed and the membranes were incubated in primary antibodies (table 2-4) diluted with antibody buffer overnight in 50ml falcon tubes and gentle agitation on a tube roller (Barloworld Scientific, UK) at 4°C.

The following day membranes were washed 4 times for 5 minutes with washing buffer (10mM Trizma base, 0.1M Sodium Chloride and 10% v/v Tween; pH 7.5). Incubation with HRP-conjugated secondary antibodies was carried out for 1.5 hours at 4°C followed by excess washing.

Chemiluminescent detection of HRP-conjugated antibodies was achieved with an ECL Western Blotting Detection System (Amersham, UK). Briefly, membranes were incubated in ECL detection reagent for 1 minute,

wrapped in plastic and exposed to CL-Xposure X-Ray Films (Thermo Scientific) for 1-10 minutes.

Co-immunoprecipitation

Cells were lysed as described in western blotting and lysates were pre-cleared by adding 50-100µl of an irrelevant isotype control antibody, followed by incubation on ice for 1 hour. Thereafter, 100µl of protein G sepharose beads (GE Healthcare, UK) was added to each lysate, followed by incubation at 4°C on a tube roller for 1 hour. The lysate-bead mixture was centrifuged at 2500 rpm for 10 minutes at 4°C. The supernatant was harvested for immunoprecipitation and the pellet discarded.

In separate tubes 2mg/ml of anti-E2 antibodies or an isotype control were added to 100µl of pre-cleared lysates followed by incubation at 4°C overnight with gentle agitation. Thereafter, 100µl of protein G beads was added to each sample and the mixture was incubated at 4°C for 4 hours under gentle agitation.

After 4 hours the tubes were centrifuged at 3,000 rpm for 1 minute and washed three times in ice-cold lysis buffer by centrifugation (PBS, 1% Brij97, 20mM/L Tris [pH 7.5], 300 mM/L $CaCl_2$, and 2mM/L $MgCl_2$) supplemented with protease and phosphate inhibitors. After each centrifugation, the supernatants were discarded and the beads coupled with antibody/protein complex were kept.

After the final wash supernatants were removed and beads resuspended in 30-50µl of loading buffer and boiled at 95°C for 5 minutes to dissociate protein G beads from the antibody/protein complex. The tubes were

centrifuged and the supernatants kept for SDS-PAGE and chemiluminescent detection. Membranes were probed with antibodies against HCV E2, CD81 and Occludin, a positive signal showed that HCV E2 antibody successfully immunoprecipitated the above proteins to demonstrate a specific interaction.

2 . 3.5 Cell proliferation assay

Cell proliferation was determined using the CellTiter Solution Cell Proliferation (MTT) Assay (Promega). In essence, cells were seeded at 4 x 10^4 cells/well in a 96 well microplate containing DMEM +3% FBS and incubated overnight. Thereafter, cells were treated with or without Mitomycin C [10μg/ml] or γ-irradiation for 20 minutes [32mSv] using a Gammacell 3000 Elan. 24 hours later cells were washed with PBS and 200μl of MTT reagent was added per well.

Cells were incubated at 37°C for 1 hour and 100μl of the supernatant was transferred to wells of a 96 well plate. The absorbance was read at 490nm using an ELISA plate reader. Final proliferation values were determined by subtracting the absorbance recorded from a control empty well.

2.4 Transfections and virus based work

2 . 4.1 Plasmids

Name	Source
HCVcc J6/JFH-1	Charles Rice, Rokefellar University, NY
HCVcc SA13/JFH-1	Jens Bukh, Copenhagen Hospital, Denmark
JFH-1 and H77 Replicons	Tajika Wakita, National Institute of Infectious Diseases, Tokyo
H77 E1E2	Zie Zhang, Rokefellar University, NY
JFH-1 E1E2	Zie Zhang, Rokefellar University, NY
OH8 E1E2	Zie Zhang, Rokefellar University, NY
Con-1 E1E2	Zie Zhang, Rokefellar University, NY
H91A6 E1E2	In House
Johns Hopkins (JHU) E1E2 clones	Stuart Ray, Johns Hopkins Centre , USA
VSV-G	Aaron Diamond AIDS Research Centre
Luciferase Reporter	Aaron Diamond AIDS Research Centre
HIV Gag-pol	Aaron Diamond AIDS Research Centre
TRIP Occludin	In House

Table 2-6. List of plasmids used in this study.

2 . 4.2 Generation of HCV pseudoparticles (HCVpp)

The HCVpp system is based on a replication deficient HIV gag-pol core that carries the HCV E1E2 glycoproteins. Infection is quantified by detecting a GFP or Luciferase reporter gene packaged into the HCVpp. As the particles do not encode any HCV non-structural proteins they are incapable of replication and only imitate the entry process of HCV.

HCVpp particles were generated by transfecting 293-T cells seeded at 5 x 10^5 cells/ml into 6 well plates coated with 0.1mg/ml poly-L-lysine (Sigma, UK) in DMEM +10% FBS and no penicillin/streptomycin 24 hours before transfection. The media was removed and replaced with penicillin/streptomycin free DMEM +3% FBS 1hour before the addition of DNA.

Cells were transfected using Fugene (Roche); briefly, 6µl of Fugene reagent was mixed with 100µl Optimem (Gibco) and added to a cocktail of

plasmids encoding HCV E1E2 (600ng), HIV gag-pol (600ng) and a luciferase reporter (600ng). For VSV-Gpp or a no-envelope control, the Fugene/Optimem mix was added to plasmids encoding these respective genes instead of HCV E1E2.

The Fugene/DNA mix was incubated at room temperature for 25 minutes and then added to cells. Cells were incubated with transfection mixture for 8 hours at 37°C, the media was removed and cells refreshed with DMEM +3% FBS and penicillin/streptomycin.

Culture media containing HCVpp was harvested 48-72 hours later, the media was clarified by centrifugation at 2000rpm for 5 minutes and used to infect target primary hepatocytes or hepatoma cells immediately.

Luciferase infection assay

Target cells were seeded at a density of 4 x 10^4 in 96 well microplates and inoculated for 8 hours (unless stated otherwise) with HCVpp diluted 1:2 in DMEM +3% FBS and penicillin/streptomycin. Thereafter, the inoculums were removed and cells replenished with fresh media. Luciferase activity was detected at 72 hours post infection (unless otherwise stated) using a Luciferase Assay System (Promega). Briefly, 1x lysis buffer was prepared according to the manufacturer's instructions and stored at -20°C. Luciferase assay reagent was prepared by adding 10mls of assay buffer to a vial containing lyosophilized luciferase substrate.

The media was removed from cells followed by a PBS wash; 50µl of lysis buffer was added to cells followed by incubation for 2 hours at -20°C. After 2 hours the plates were allowed to thaw at room temperature resulting in complete lysis of the cells. 40µl of cell lysate was added to wells of a white polystyrene 96-well fluorescent assay plate (Corning, USA) and mixed with

40µl of luciferase substrate reagent and luciferase activity detected with a 5 second delay using a Centro LB960 Luminometer (Berthold Technologies, UK). The luciferase activity was detected as relative light units (RLU) and the no-envelope signal which is typically in the order of 2 x 10^3 RLU was subtracted from each HCVpp/VSV-Gpp signal.

To ascertain the effects of cell division on HCVpp luciferase activity, target cells were seeded as described into 96 well microplates and treated with Mitomycin C 10µg/ml or γ-irradiated for 20 minutes using a Gammacell 3000 Elan (MDS Nordian, Canada) at 32 mSv/minute. 24 hours later the media was removed and cells infected with HCVpp or VSV-Gpp.

To determine the effects of HCV neutralizing reagents (anti-CD81 and ITX 5061) or HIF-1α inhibitor on virus entry, target cells were treated prior to infection with anti-CD81 (5µg/ml) for 3 hours or ITX 5061 (10µM) and HIF-1α inhibitor (1µM) overnight. At these concentrations anti-CD81 and ITX 5061 were reported to neutralize HCVpp entry (154, 389).

2 . 4.3 Generation of TRIP viruses

The TRIP system consists of a retrovirus gene expression vector that produces virus particles via a replication deficient HIV gag-pol core bearing the envelope glycoprotein of vesicular stomatitis virus (VSV-G). TRIP virus particles can incorporate a gene of interest as an RNA transcript. Subsequent transduction of cells results in reverse transcription of the target gene and insertion into the host genome (441). In this study, transduced cells were not subjected to antibiotic selection; however, they maintained exogenous gene expression for up to 4 weeks.

TRIP particles were produced by Fugene transfection of 293T cells seeded at $5x10^5$ cells/well in DMEM +3% FBS in 6-well culture microplates coated with 0.1 mg/ml poly-L-lysine. The following day, VSV-G (400ng), HIV gag-pol (600ng) and 600ng of gene of interest (human-Occludin or human-CD81) were introduced into the cells by overnight transfection at 37°C.

Thereafter, the culture media was replaced with DMEM +3% FBS and penicillin/streptomycin. Culture media containing TRIP virus particles was harvested 48-72 hours later and clarified by centrifugation at 2000rpm for 5 minutes to pellet any contaminating 293T cells.

Harvested supernatants were pooled and stored at 4°C where it was stable for up to 24 hours. Huh-7.5 cells seeded at 4 x 10^4 cells/well in 6 well plates 24 hours before transduction were transduced with TRIP supernatants diluted 1:2 in 3% DMEM containing 1.6µg/ml polybrene (Sigma) overnight. Transduction efficiency was determined 72 hours later by monitoring gene expression by flow cytometry or immunofluorescence staining.

2.4.4 Generation of HepG2 cells expressing viral glycoproteins

Successful expression of HCV and VSV-G glycoproteins was achieved by Magnet Assisted Transfection (Fisher Scientific, UK) according to the manufacturer's instructions. Briefly, the DNA of interest is coupled to charged nanoparticles. A mixture containing the DNA:nanoparticle complex is added to target cells and a strong magnetic force is applied beneath cells. The magnetic force pulls the DNA:nanoparticle complex onto the cells

resulting in close contact with the cell membrane followed by endocytosis. Successful endocytosis results in expression of target gene.

Herein, diverse HCV E1E2 glycoprotein strains (H77, JFH-1, OH8 and Con-1) encoded on pCCAGs plasmids containing a G418 resistance marker were delivered into HepG2 cells. Cells were seeded at 4 x 10^4/ml onto 24 well plates coated with collagen, followed by incubation overnight at 37°C in DMEM +10% FBS and penicillin/streptomycin. Thereafter, the media was replaced with antibiotic free DMEM +3% FBS. 600ng of pCCAGs plasmid containing HCV E1E2 or VSV-G was added to 100µl of serum free DMEM followed by incubation at room temperature for 5 minutes.

The DNA/DMEM mixture was supplemented with 50µl of the manufactures transfection reagent which contains charged nanoparticles. The mixture was incubated at room temperature for 1 hour and used to treat target cells. Cells were placed onto a magnet and incubated at 37°C overnight. The following day the media was replaced with DMEM +3% FBS and antibiotics and cells allowed to incubate for a further 72hours. Thereafter, cells were treated with G418 (1mg/ml) in DMEM + 3% FBS. Following multiple rounds of G418 selection stable cell populations expressing HCV or VSV-G glycoproteins remained and gene expression was confirmed by flow cytometry. The resulting cell clones were designated H77 E1E2, JFH E1E2, OH8 E1E2, Con-1 E1E2 and VSV-G.

2 . 4.5 Generation of cell culture HCV (HCVcc)

HCVcc viruses are based on the non-structural (replicase) proteins of HCV JFH-1 strain, a unique isolate that is able to produce infectious particles in Huh-7.5 cells (415). All subsequent HCVcc strains incorporate JFH-1 non-structural proteins and differ only by the structural proteins.

RNA Synthesis

RNA transcripts of HCV genomes SA13 and J6/JFH-1 were produced using the T7 RNA Polymerase Kit (Promega, UK) according to the manufacturer's instructions. Essentially, 5µg's of plasmid containing a cDNA clone of the HCV genome was linearised by restriction digest using the Xbal enzyme (New England Biolabs, UK). 1µg of the linearized plasmid was used as template for RNA transcription; this was achieved by incubating the reaction mix (T7 RNA polymerase mix from the manufacturer's kit) at 37°C for 4 hours. Thereafter, the RNA was purified using the RNAeasy MiniElute Kit (Qiagen, Netherlands) according the manufacturer's instructions. RNA quality was assessed by gel electrophoresis on a 1% agarose gel (Bioline, UK). RNA yields were quantified using a spectophotometer (Amersham, UK) with typical yields between 100-1500ng/µl.

Electroporation

Early passage (passage 1-35) Huh 7.5 cells were grown in T175 tissue culture flasks until 80-90% confluent. Cells were trypsinized and resuspended in DMEM. Thereafter, cells were washed in ice-cold PBS and pelleted by centrifugation at 2500rpm for 5mins at 1°C; this process was repeated and pellets were resuspended in ice-cold PBS at $1.5x10^7$ cells/ml.

400µl of the cell suspension was mixed with 5µg of HCV genomic RNA and transferred to electroporation curvettes (Sigma). Electroporation was carried out at 600 volts in an Electro Square Porator (Harvard Apparatus, USA). Electroporated cells were allowed to stand for 5 minutes at room temperature to rest before transferring them into 10mls of pre-warmed IMDM +10% human serum, 1% L-glutamine and penicillin/streptomycin.

8mls of the cell suspension was transferred to a T75 tissue culture flask and the remainder placed into wells of a 24 well tissue culture plate for the monitoring of HCV protein expression. Cells were incubated at 37°C in a category 3 containment laboratory and the media was replaced with DMEM +3% FBS the following day.

At 72 hours post electroporation, viral replication was quantified by staining the cells seeded in 24 well plates for NS5A using immunofluorescence as described in section 2.3.2 with mouse 9E10 anti-NS5A monocloanal antibody (mAb). Providing 60-80% of cells expressed NS5A, HCVcc particles were harvested from the T75 flasks between 4 and 14 days post electroporation after which cells were discarded. Briefly, cells were cultured in 4mls serum free DMEM and media containing secreted virions harvested at 4 hour intervals and pooled. Harvested virus was clarified by centrifugation at 3000rpm for 5 minutes and stored at -80°C.

HCVcc infection assay

All HCVcc infection in this study was performed as follows (unless stated otherwise); harvested virus was used to infect target primary human hepatocytes or hepatoma cells seeded at 4 x 10^4 cells/ml on a 48 well tissue culture plate 24 hours before infection. To infect cells, the media

was removed and replaced with 100µl of HCVcc virus diluted in DMEM +3% FBS, L-glutamine and penicillin/streptomycin.

Cells were incubated for 8 hours at 37°C, the HCVcc inoculum was removed and cells washed with PBS to remove any unbound virus. The cells were refed with 300µl of DMEM +3% FBS, L-glutamine and penicillin/streptomycin and infection allowed to proceed for 48-72 hours at 37°C as stated in the figure legends.

Cells were methanol fixed and NS5A positive cells were determined by immunofluorescence with 9E10 antibody as described above. Viral infectivity was enumerated by counting NS5A foci or individual infected cells using a fluorescence microscope. Alternatively HCVcc infection levels were quantified by quantitative reverse transcriptase polymerase chain reaction, see section 2.5.1.

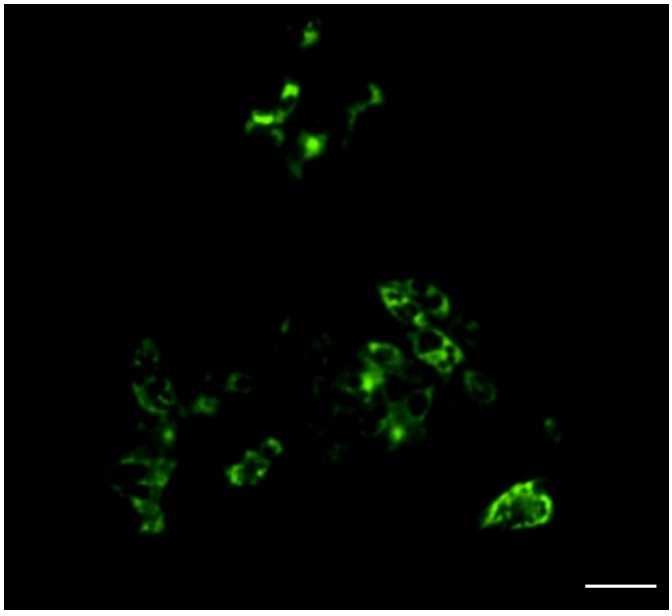

Figure 2-2. HCV NS5A positive foci.

Huh-7.5 cells were infected with HCVcc J6/JFH-1, at 72 hours post infection cells were methanol fixed and stained for HCV NS5A (green) using 9E10 monoclonal antibody and an Alexa Flour 488 secondary antibody. Scale bar represents 10µm.

Cell to cell transmission assay

To determine whether prednisolone increases HCV cell-cell transmission we employed an infectious co-culture assay (50). Huh-7.5 target cells were seeded at a density of 12.5 x 10^4 cells/well on collagen coated 12 well plates. To ascertain a role for prednisolone in HCV cell-cell transmission cells were seeded in the presence of prednisolone (100nM), RU-486 (5µg/ml) or a combination of both compounds overnight.

HCVcc J6/JFH-1 infected producer cells (infected as described in HCVcc infection assay) were labelled with CMFDA (5µM) by incubation at 37°C in DMEM +3% FBS for 30 minutes. Thereafter, producer cells were washed with PBS and removed from the tissue culture plastic with trypsin. 12.5 x 10^4 labelled producer cells were seeded into co-culture with target cells. Final co-culture contained a 1:1 ratio of producer and target cells, each well totalling 25 x 10^4 cells/well in DMEM + 3% FBS.

48 hours later supernatants were collected and used in a standard infectious assay to quantify cell free infectivity. Cells were trypsinized and seeded into 96 well round bottom plates, followed by centrifugation at 10,000rpm for 3 minutes and fixing for 5 minutes with 1% PFA. Cell-cell transmission from producer to target cells was measured by staining for HCV NS5A and analysed by flow cytometry (Figure 2-3). This allowed determination of de novo transmission events.

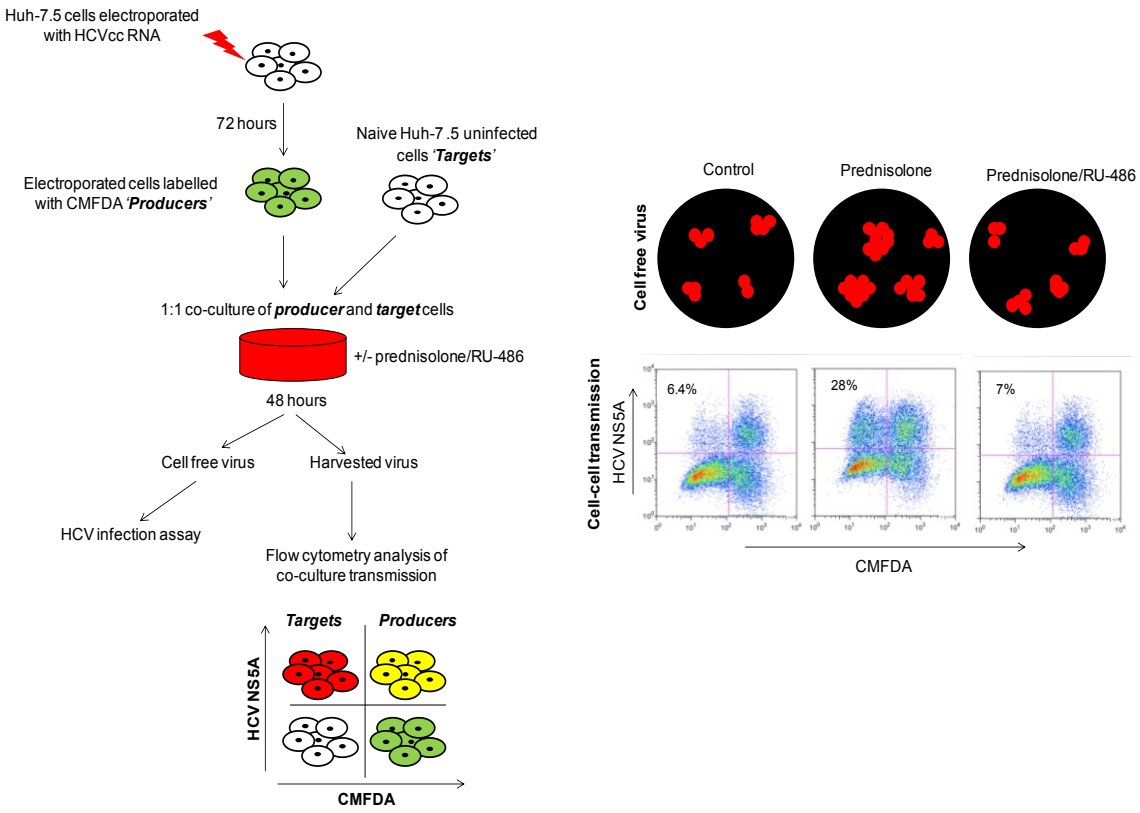

Figure 2-3. Cartoon of HCV co-culture assay to determine cell-cell transmission.

Target and producer cells were co-cultured as described; 48 hours later cells were fixed and stained with a labelled antibody (red) against NS5A followed by flow cytometry analysis. The supernatants were used to confirm cell-free infection. The flow cytometry scatter plot is divided into 4 populations; infected targets (red), infected producers (yellow), uninfected targets (unstained) and uninfected producers (green). This allows us to generate plots of HCV transmission in the presence or absence of prednisolone or RU-486. A general overview of the results that can be obtained is given on the right, where red dots represent NS5A foci. Prednisolone treatment is associated with an increase in foci size which is indicative of enhanced cell-cell transmission.

2.5 Specific assays

2 . 5.1 Quantitative RT-PCR (qRT-PCR)

HCV genome copy number was measured by qRT-PCR, using a Cells Direct Kit (Invitrogen) according to the manufacturer's instructions. Cells were infected as per a standard infection assay (section 2.4.5) in the presence or absence of prednisolone (100nM), RU-486 (5µg/ml) and HIF-1α inhibitor (1µM). Alternatively, cells were infected in a Hypoxic incubator (New Brunswick Scientific, UK) set to 1% O_2 and 5 % CO_2. 72 hours post infection cells were lysed and total RNA purified using the MiniElute RNA Extraction Kit (Qiagen) as per the manufacturer's instructions. The qRT-PCR reaction mixture was made up with specific primers targeting the Core protein (Primer Design, UK) and GAPDH house-keeping gene control primers (Invitrogen).

qRT-PCR was carried out in a MicroAmp 96 well optimal reaction plate (Applied Biosystems, USA) with samples tested in triplicates. A standard curve was devised with in vitro transcribed HCV RNA of known copy number. The reaction was performed in a quantitative PCR machine (Stratagene, USA) and the data analysed using the associated MXpro software.

The PCR reaction was performed using the following program;

30 minutes	50°C
5 minutes	95°C
15 seconds	95°C} 50 cycles
60 seconds	60°C} 50 cycles

Quantification of HCV receptor mRNA levels

To quantify HCV receptor mRNA levels in hepatoma and primary human hepatocytes; cells were seeded at a density 4 x 10^4/ml of a 24 well plate. For primary cells, total cellular RNA was purified as above at 1, 2 and 3 days post seeding. For Huh-7.5 cells RNA was purified at day 1 which is optimal of HCVcc infection of these cells. Purified RNA samples were amplified as described above for CD81, SR-BI, Claudin-1 and Occludin using the Cells Direct Kit and specific primers. In all reactions, the house-keeping gene GAPDH was included as an internal endogenous control for RNA quantification.

Quantification of hepatocyte differentiation phenotype

Primary human hepatocytes from 3 donors were seeded at 4 x 10^4/ml of a 24 well plate and allowed to grow for a period of 12 days. Each day cells were lysed and total RNA purified. Hepatocyte differentiation was determined using the reaction mix from the Cells Direct Kit according to the manufacturer's instructions and primers specific for hepatocyte differentiation markers (alpha-Fetoprotein, HnF4α and CYP3a4). GAPDH was used as an internal reaction control. The amplification reaction was performed as described above. qRT-PCR reactions were performed with the help of Sukhdeep Galsinh and Nicola Fletcher.

2 . 5.2 Determination of HepG2 polarity

Polarity is regulated by tight junction proteins that separate apical and basolateral membrane domains. HepG2 polarity was determined by

enumerating the expression of the apically expressed multi-drug resistant protein (MRP-2) per 100 nuclei. HepG2 polarity increases overtime consistent with increased MRP-2 expression at the apical bile canalicular membrane.

Cells were seeded at 4 $x10^4$ cells/ml and allowed to grow for 1, 3, and 5 days in order to quantify polarity over time. Cells were fixed at each time point with 3% PFA at room temperature for 20 minutes. Cells were washed in PBS and permeabilized using 0.1% Triton X-100 + 0.5% BSA in PBS for 30 minutes. Primary and secondary antibody staining was achieved as described in fluorescent microscopy (section 2.3.2) using anti-MRP-2 (Abcam, UK) and Alexa-Fluor 488 conjugated antibodies. Antibodies were diluted in PBS +0.5% BSA and 0.1% Triton X-100.

Cell nuclei were visualized using DAPI and the polarity index determined by counting the number of MRP-2 positive apical structures per 100 nuclei from 5 representative fields of view using a Nikon Eclipse TE200 fluorescence microscope and phase contrast microscopy. Figure 2-4 A, shows MRP-2 expression in polarized HepG2 cells.

To ascertain the effects of HIF-1α inhibitor on polarity cells grown for 4 days were treated with the inhibitor (1μM) for 24 hours and polarity index measured immediately after. To ascertain the effects of HCV infection of polarity cells were infected 24 hours post seeding and the polarity index determined at 72 hours post infection.

2 . 5.3 Determination of tight junction integrity

Tight junction integrity assesses the functionality (integrity) of apically expressed bile canalicular structures. This is performed using a

fluorochrome which diffuses across the cell membrane and is trafficked to the bile canaliculi. Providing the canalicular structures are functional the fluorochrome is retained. However, permeable or leaky junctions results in diffusion of the fluorochrome to the medium.

HepG2 cells were grown for 5 days to achieve polarity, followed by incubation with 5mM 5-chloromethylfluorescein diacetate [CMFDA] (Invitrogen) at 37° C for 15 minutes to allow internalization and translocation to bile canalicular lumen. After washing extensively with PBS, the capacity of bile canaliculi lumens to retain CMFDA was enumerated using a fluorescence microscope and phase contrast microscopy. Figure 2-4 B shows CMFDA retention at the bile canaliculi in HepG2 cells.

To ascertain the effects of HIF-1α inhibitor (1μM), anti-TGFβ and VEGF (1.5μg/ml) neutralizing antibodies on tight junction integrity, cells were treated with the respective compounds 24 hours prior to tight junction integrity quantification. To assess the effects of cytokines on tight junction integrity cells grown for 4 days were treated with increasing concentrations of interferon-γ (IFNγ) and tumour necrosis factor-alpha (TNFα) for 24 hours. Tight junction integrity was determined as above.

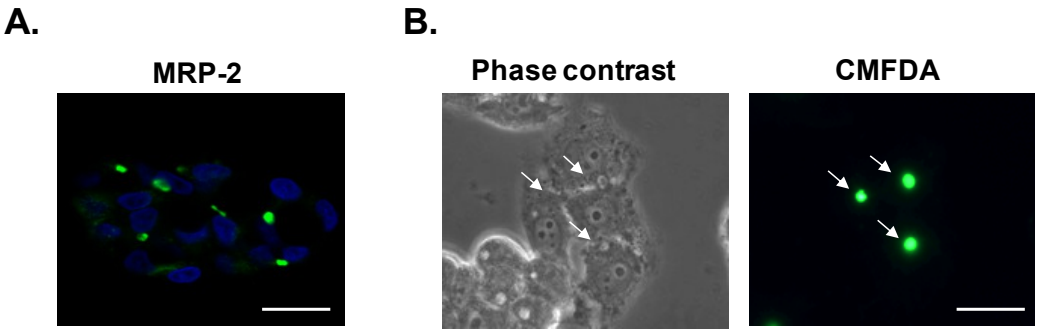

Figure 2-4. MRP-2 expression and CMFDA retention in HepG2 cells.

A. Immunofluorescent detection of MRP-2 (green) in HepG2 cells grown for 3 days, DAPI nuclear stain is shown (blue). **B.** Phase contrast and fluorescent images of bile canalicular structures retaining CMFDA (green). Arrows indicate bile canaliculi localization. Scale bars represent 20μm.

Measurement of tight junction remodeling

Tight junction formation is calcium dependent and its depletion perturbs junction formation. To study tight junction dynamics in parental and glycoprotein expressing HepG2 cells, we incubated cells in calcium free media (Minimum Essential Eagle Spinner Modification) +3% FBS, 1% non-essential amino acids and 0.5mM EGTA [Sigma] for 16 hours to deplete calcium from cells. Thereafter, the cells were supplemented with growth media containing calcium and tight junction formation was monitored over time by enumerating CMFDA retention at the bile canaliculi as described above.

2 . 5.4 Tight junction solubility to Triton X-100

Pools of tight junction proteins reside in detergent insoluble membranes, to study whether HCV glycoproteins affect tight junction solubility we treated cells with TX-100. Briefly, HepG2 cells were seeded at 4 x 10^4 cells/ml onto

24 well plates containing 13μm glass coverslips for 5 days to achieve polarization. Thereafter, the media was removed and cells washed in PBS followed by incubation with PBS containing 0.1% Triton X-100 for 2 minutes at room temperature.

The Triton X-100/PBS solution was removed and cells were washed 3 times in PBS to neutralize any residual Triton X-100. Thereafter, cells were fixed in ice-cold methanol for 5 minutes. Cells were washed with PBS and blocked for 1 hour at room temperature in PBS +1% BSA. Primary and secondary antibody staining was achieved as previously described in fluorescence microscopy. And mounting and confocal analysis was described in laser scanning confocal microscopy (section 2.3.2).

2 . 5.5 Reactive Oxygen Species (ROS) assay.

Accumulation of increase ROS is indicative of increased cellular oxidative stress; ROS was detected using a Fluorescence Assay Kit (Calibochem, Europe). The assay uses a cell-permeable fluorogenic probe 2', 7' Dicholorodihydrofluorescin diacetate (DCFH-DA). DCFH-DA is diffused into cells and is deacetylated by cellular enzymes to non-fluorescent DCFH which is readily oxidised to highly fluorescent DCF by ROS. The fluorescent intensity is proportional to the ROS levels within the cell.

We measured cellular ROS according to the manufacturer's instructions. Briefly, cells were seeded at 2 x 10^6 per well of a 6 well plate for 48 hours. The media was removed and cells washed 3 times with PBS, 500μl of RPMI media supplemented with 10% FBS (Gibco) was added to each well followed by the addition of DCFH-DA (100μl).

Cells were incubated in the dark at 37°C for 1 hour, after which the RPMI/DCFH-DA mixture was removed and the washing step was repeated. The fluorescent intensity was detected by flow cytometry and analysed with the Flow Jo software as described in section 2.3.1.

2 . 5.6 Cholesterol assay

Cellular cholesterol was measured using the Amplex Red Cholesterol Assay Kit (Invitrogen) according to the kit guidelines. Cells of interest were enumerated using a haemocytometer to a working density of 25 x 10^5 cells. Thereafter, cells were pelleted by centrifugation at 10,000rpm for 5 minutes and lysed with 250µl of 1x Reaction buffer. 50µl of the lysed samples were added to wells of a 96 well plate and cholesterol reference standards from the Amplex Red Kit was added to separate wells. All samples were added in triplicates; 50µl of Amplex Red Reagent was added to each sample followed by incubation at 37°C for 30 minutes. Fluorescence was read using an ELISA plate reader at excitation 530nm and emission detection 590nm. Cholesterol values were subtracted from the absorbance recorded for a control empty well. For each assay a standard curve was produced (Figure 2-5) using the cholesterol reference standards allowing cholesterol levels to be expressed as µM cholesterol per 1x10^5 cells.

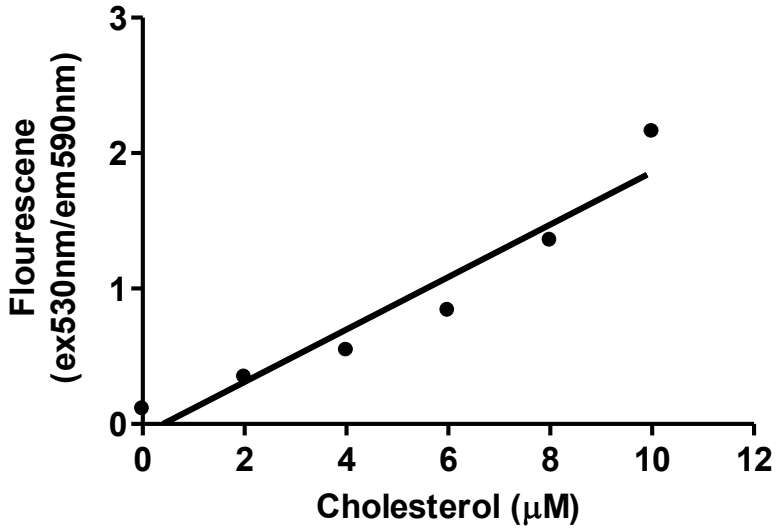

Figure 2-5. Cholesterol assay standard curve.

2 . 5.7 Invasion assay

Cells of interest were seeded at 4 x 10^4 cells/ml into T75 culture flasks for 24 hours followed by infection with HCVcc J6/JHF-1 (see section 2.4.5). 72 hours later cells were serum starved overnight. Cells were labelled with CMFDA by incubation at 37°C with 5μM CMFDA (DMEM +3% FBS) for 30 minutes. Labelled cells were washed with PBS followed by trypsinization. Cells were pelleted by centrifugation at 12000 rpm for 5min followed by resuspension with serum free DMEM.

Cells were counted using a haemocytometer and trypan blue exclusion. 4x10^4 cells (200μl) were seeded into the top well of a collagen coated (calf collagen, Sigma) 8μm pore transwell (BD Falcon, USA) in a 24 well tissue culture plate. Cells were also seeded onto a 24 well plate as a control. The bottom chamber was filled with 400μl serum free DMEM and cells were cultured for 24 hours at 37°C. Non-migrated cells (top chamber) were

mechanically removed with a cotton bud and confirmed under light microscope. Migrated and control cells were fixed with ice cold methanol for 5 minutes and stained for HCV NS5A (see section 2.4.5). Three fields of view per well were captured on a Nikon TE2000 fluorescence microscope. The number of invaded cells was enumerated per field of view. The proportion of infected invaded cells and those in the control wells were also determined.

To ascertain the effects of hypoxia and HIF-1α inhibitor on invasion, cells were cultured at 37°C in 1% CO_2 for 24 hours in the presence or absence of HIF-1α inhibitor (1μm) on 8μm pore transwells. To study the effects of anti-VEGF and TGFβ (1.5μg/ml) on invasion cells were cultured on 8μm pore transwells for 24 hours in the presence or absence of both compounds.

2 . 5.8 Migration assay

Cell migration was measured using a wound healing assay. Cells of interest were seeded at 5 x 10^5 cells/well into 12 well plates 24 hours prior to the start of the assay and serum starved overnight. A P200 tip was used to create a scratch wound in the cell monolayer and the media was refreshed with serum free DMEM. If treatment was required (HIF-1α inhibitor, anti-VEGF or anti-TGFβ) the media was refreshed with serum free DMEM containing the respective compounds. Images of the wound were taken immediately (0 hours). Cells were incubated at 37°C for 24 hours when further images were taken. To ensure the same area of the wound was being imaged at the different time points a black marker pen was used to

mark the exact location of the wound in each well. Images were taken using a Nikon TE2000 fluorescence microscope and area of wound at 0 and 24 hours determined using ILab 4.0 software (BD Biosciences).

To ascertain the effects of HCVcc infection on migration, cells were infected with J6/JFH-1 and 48 hours later a wound was created as above and media refreshed with serum free DMEM. Wound healing was measured as outlined.

2 . 5.9 Human liver tissue and immunohistochemistry

Formalin fixed needle biopsies or whole tissue blocks were obtained from patients undergoing liver transplantation for HCV, cirrhosis due to non alcoholic steatohepatitis (NASH), hepatitis B (HBV), primary biliary cirrhosis (PBC) and hepatocellular carcinoma (HCC). Disease in each case was characterized as early or late; diagnosed according to the severity of fibrosis where early = no/mild fibrosis (Ishak stage <2) and late = cirrhosis. Normal liver tissues were obtained from surplus donor liver used for reduced-size transplantation. All donors were anonymised and tissues were obtained from the Centre for Liver Research, University of Birmingham with regional ethics committee approval (reference number 06/Q702/61).

Representative 3µm tissue specimens were placed onto charged glass slides (Surgipath, UK) and stored at room temperature until ready to use. For immunohistochemistry, specimens were de-parafinized in Xylene (Surgipath, UK) for 10 minutes and rehydrated in H_2O. Thereafter, specimens were subjected to incubation in 0.3% hydrogen peroxide made

up in H_2O to block endogenous peroxidise activity, followed by agitated low-temperature epitope retrieval. Briefly, tissue specimens were placed in eDTA pH 8.0 (Binding Site, UK) and microwaved for 20 minutes. Slides were allowed to cool by standing for 10 minutes and washing in cold H_2O.

Slides were mounted onto a Shandon Sequencer (Thermo Scientific, UK) and blocked in 2% Casein (Vector Labs, USA) diluted in Tris-buffered saline pH 7.5. Specimens were incubated with antibodies specific for Claudin-1, Occludin, SR-BI and HIF-1α or an irrelevant isotype control. Final antibody concentrations are listed in Table 2-4 and were determined after titration of each antibody on the liver tissue. All antibodies were diluted in Tris-buffered saline with 0.1% Tween-20 (TBS-Tween) for 1 h at room temperature.

Specimens were washed with excess TBS-Tween three times followed by incubation for 1 hour in a secondary antibody reagent (ImPress Universal anti-mouse IgG/anti-rabbit IgG Peroxidise Kit) (Vector Labs, USA) according to the manufacturer's instructions. Briefly, two drops of reagent which equates to 200µl was added to each specimen. Specimens were washed with TBS-Tween as above; bound antibodies were visualized using ImPact DAB Diluent and Chromogen Kit (Vector Labs, USA) followed by counterstaining with hematoxylin (Surgipath). Slides were mounted after dehydration in Xylene for 5 minutes and sealed to 24mm coverslips with DPX mounting reagent (VWR, UK). Slides were dried in a laminar fume cupboard overnight and examined the following day.

Images were obtained using a Nikon Eclipse E400 microscope (Nikon). Acetone-fixed frozen sections of normal liver tissue were stained in a

comparable manner to confirm that the expression pattern of Claudin-1 and Occludin had not been altered during paraffin wax processing and formalin fixation (Figure 2-6).

Confocal analysis of human liver tissue

For confocal analysis; the methodology described in section 2.3.2 was employed. The tissue's endogenous autofluorescence was quenched by incubating specimens in Harris's Haematoxylin (Surgipath) for 5 minutes prior to Casein blocking and the addition of primary antibodies. Secondary antibody staining was achieved by incubation with conjugated Alexa 488 and 594 antibodies diluted 1:200 with TBS-Tween. Specimens were washed in TBS-Tween and incubated with DAPI for 15 minutes, after a final TBS-Tween wash specimens were mounted onto 24mm coverslips with Fluorescent Mounting Medium (Dako) and analysed by laser scanning confocal microscopy.

2 . 5.10 Statistical analysis

Statistical tests were performed using the Prism 5.0 software (GraphPad, CA). Results are expressed as mean ± 1 standard deviation, unless otherwise stated. Tests were performed using non-parametric means allowing for the prediction of statistical significance without assuming a particular data distribution. In other instances the Student's *t test* was employed. A probability (*P*) value of <0.05 was considered as statistically significant. The relevant tests and level of significance are noted in the figure legends.

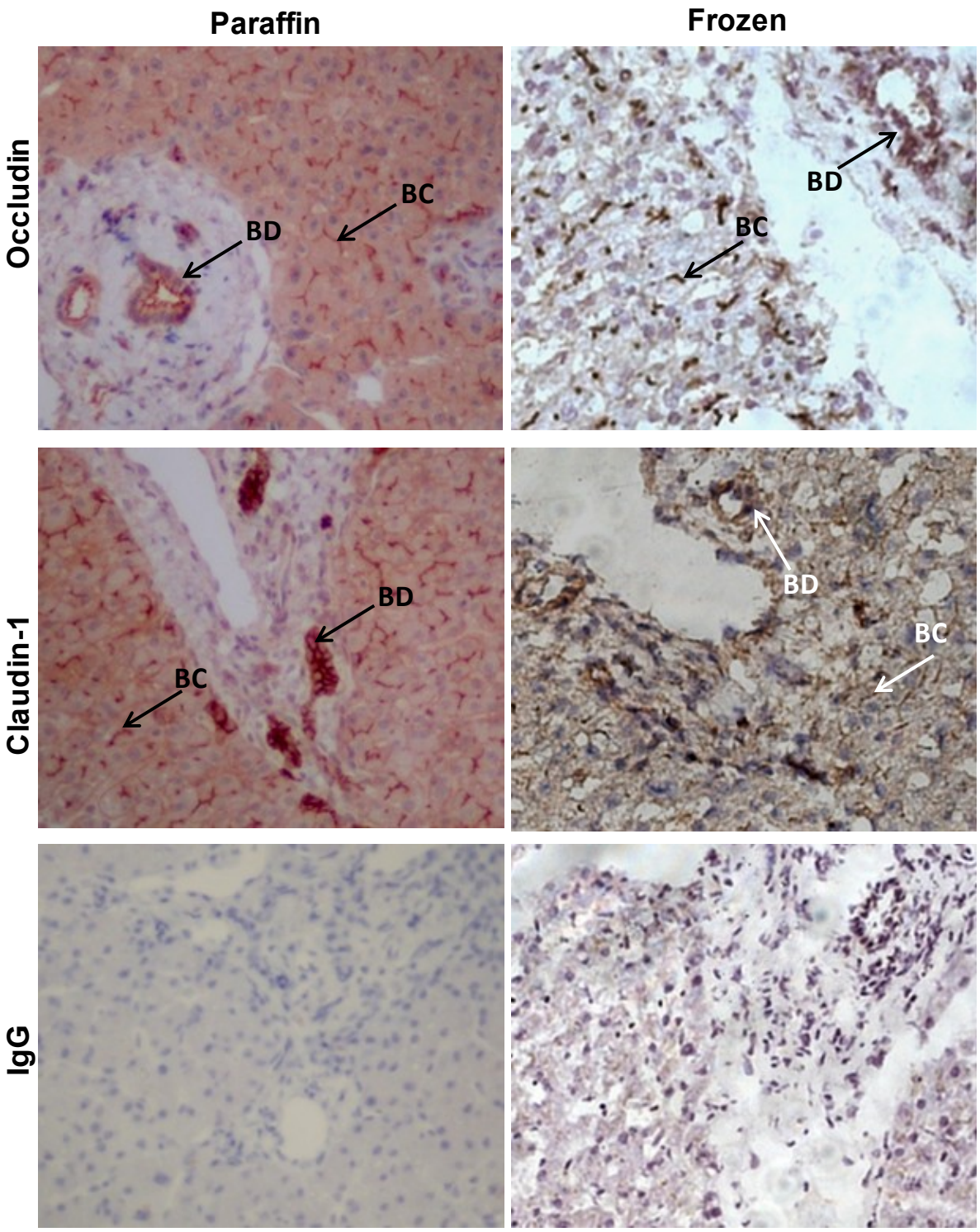

Figure 2-6. Tight junction protein expression in paraffin embedded and frozen liver specimens from normal liver tissue (x100).

IgG depicts an irrelevant isotype control. Arrows indicate Occludin and Claudin-1 expression at the bile canaliculi (BC) and on bile ducts (BD).

3. RESULTS

3.1 A comparative analysis of hepatoma cells and primary human hepatocytes to support HCV infection.

Our understanding of HCV entry and replication in vivo is limited due to the lack of small animal models to study the virus lifecycle. Primary human hepatocyte (PHH) cultures are believed to provide the 'gold standard' physiological model to study HCV infection of the human liver in vitro. Compared to many immortalized hepatic cell lines, PHHs demonstrate metabolic liver functions including urea and albumin production. Furthermore, they are highly differentiated, although this phenotype is short lived and elicits an anti-viral response to virus infection (310). These traits are uncommon in most transformed hepatic cell lines making PHHs a close physiological match to hepatocytes in vivo. However, there are relatively few reports studying HCV infection of PHHs due to the limited access to human liver tissue. Consequently, the majority of reports utilize transformed hepatoma cell lines to study virus entry and replication.

The development of HCVpp and HCVcc systems has enabled detailed and robust studies of HCV entry and replication, respectively (171, 225, 415). Both systems are capable of infecting poorly-differentiated human hepatoma cell lines such as Huh-7.5 (41). Huh-7.5 cells contain a mutation in the *RIG-I* gene, a key regulator of the interferon induction pathway (386). Consequently, HCV can establish and maintain prolonged infection of these cells. However, the tumour derived nature of Huh-7.5 cells results in cell division when cultured (101, 170, 436). In vivo, HCV dissemination occurs mainly in highly differentiated non-dividing hepatocytes (393).

Similarly, isolated PHHs in vitro do not divide although they are known to de-differentiate overtime. A comparative analysis of hepatoma infection models and PHHs to support entry and replication has not been performed. As such it is not known whether PHHs supports HCV infection that is comparable to hepatoma cell lines. We investigated HCV infection of hepatoma and PHHs with a view to validate hepatoma cells as relevant culture models to study the HCV lifecycle.

3.1.1 Phenotypic characteristics of primary human hepatocytes in culture.

Hepatocyte morphology was monitored over a period of 12 days; cells maintained a characteristic cobble stone like appearance for 10 days before de-differentiating to a more fibroblastic phenotype (Figure 3-1 A). We monitored liver specific metabolic function by measuring albumin secretion and expression of hepatocyte differentiation markers. Albumin secretion decreased over time consistent with the observed change in hepatocyte morphology (Figure 3-1 B). The expression of hepatocyte differentiation genes; including alpha-fetoprotein [α-FP], HnF4α and CYP3a4 (regulatory genes with crucial roles in maintaining hepatocyte phenotype) also declined over time albeit at varying levels (Figure 3-1 C). The decline in hepatocytic markers is in line with published data (310). Taken together, these data demonstrate the expression of hepatocyte phenotypic characteristics in PHHs from multiple donors that declined over time.

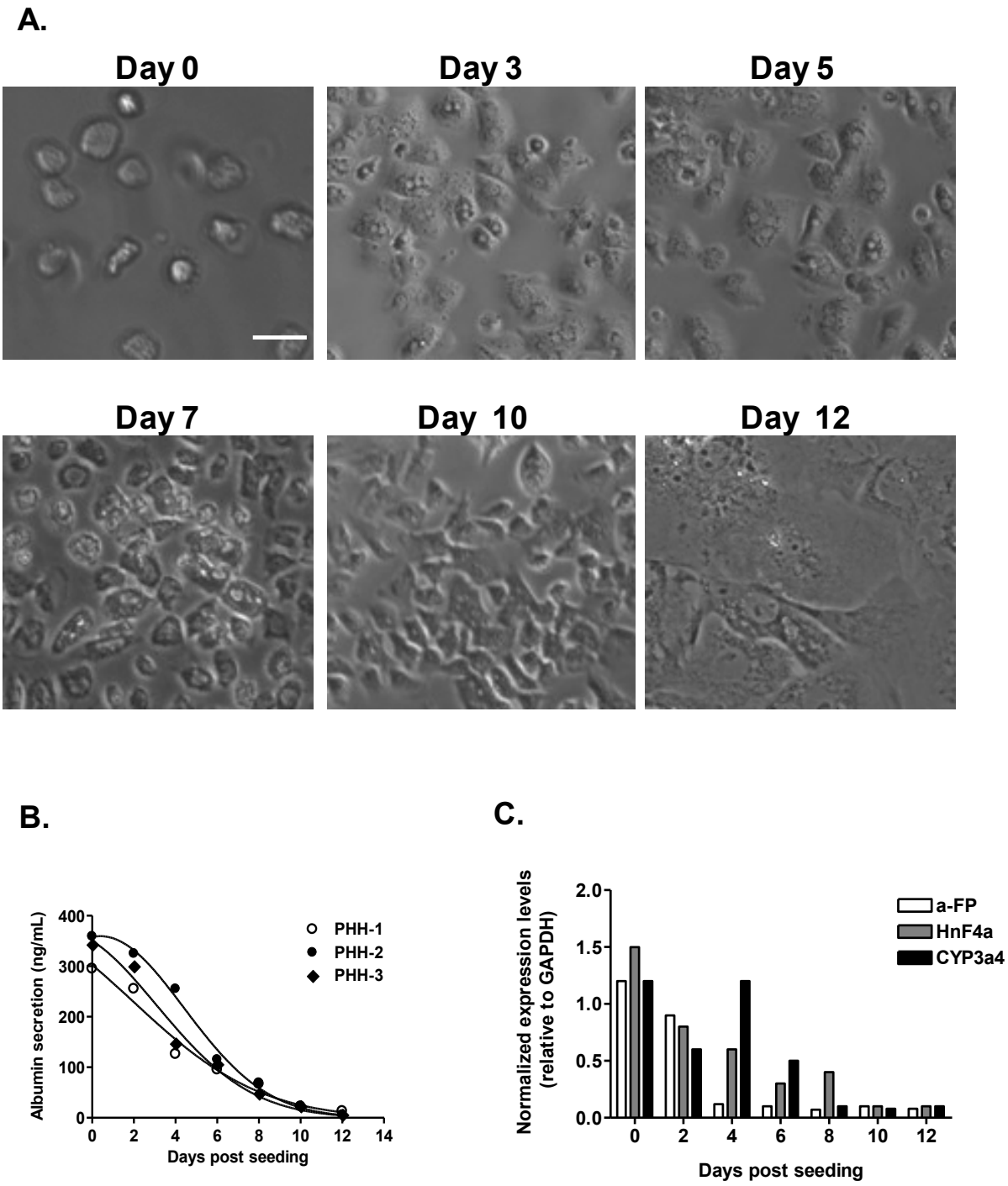

Figure 3-1. Phenotypic characteristics of primary human hepatocytes in culture.

A. Representative phase contrast images of cultured PHHs morphological appearance; the images represent hepatocytes from three donors, where the scale bar represents 10μm. **B.** ELISA detection of albumin production from 4x 10^4 cells, data shows 3 PHH donors. **C.** qRT-PCR quantification of hepatocyte gene expression, the data is representative of the 3 PHH donors from parts A and B and is presented relative to the housekeeping gene GAPDH.

3 . 1.2 Primary human hepatocytes support HCV glycoprotein-dependent virus entry (HCVpp).

HCVpp comprise a replication deficient retrovirus core and as such are only capable of a single round of infection (24, 171), allowing one to investigate the primary steps of HCV entry in isolation from downstream replication events. To optimise HCVpp infection of PHHs, cells were infected after 1, 2 and 3 days post seeding in the presence or absence of HCV entry inhibitors ITX5061 (ITX) that targets SR-BI (389) and anti-CD81 antibody (154) that blocks HCV engagement of CD81. PHHs were infected with lentiviral pseudotypes expressing HCV strain H77 genotype-1a glycoproteins (H77pp) or control vesicular stomatitis virus glycoprotein G (VSV-Gpp) for 72 hours and infection assessed by measuring luciferase activity, as previously reported (81, 171, 260). As a control cell line, we used Huh-7.5 cells which have been reported to support efficient HCV entry 1 day post seeding (171). H77pp infected PHHs resulted in 4- and 5-fold increased luciferase signals after 2 and 3 days post seeding respectively, compared to cells infected 1 day post seeding (Figure 3-2 A).

H77pp infected Huh-7.5 cells yielded 60-, 14- and 17-fold higher luciferase signals than PHHs at days 1, 2 and 3, respectively (Figure 3-2 A). ITX5061 and anti-CD81 inhibited H77pp infection of PHHs and Huh-7.5 cells at all time points confirming receptor-dependent entry. Importantly, VSV-Gpp infected both cell types at comparable levels regardless of time in culture and HCV entry inhibitors had no effect, demonstrating a HCV specific blocking effect (Figure 3-2 B). These data demonstrate that PHHs support optimal HCVpp entry at 2 days post seeding.

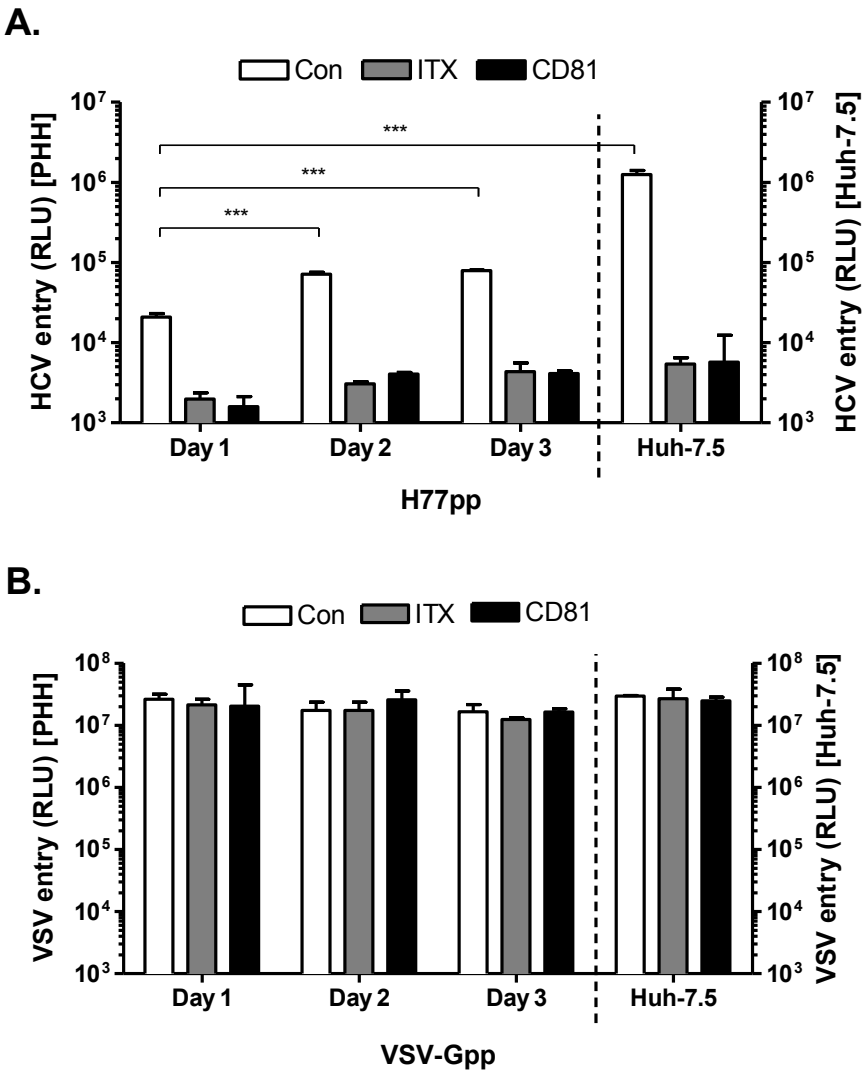

Figure 3-2. Optimization of HCVpp infection of primary human hepatocytes.

A. PHHs seeded at a density of $4x10^4$ cells/ml were infected with H77pp after 1, 2 and 3 days post seeding. Huh-7.5 cells seeded at the same density were infected 1 day post seeding which is the optimal time for HCVpp infection of these cells. White bar shows control untreated cells, grey bar depicts cells that were treated with HCV entry inhibitor ITX5061 (ITX) [5μM] and black bars show cells that were treated with anti-CD81 monoclonal antibody [2s131] (5μg/ml). **B.** VSV-Gpp infection of PHHs and Huh-7.5 cells. Pseudo-particle infectivity is presented as relative light units (RLU) from which a no envelope control value was subtracted. The no envelope RLU values were in the order of 2×10^3 for both cell types. Data is representative of 2 independent experiments performed in triplicate. Error bars indicate standard deviation from the mean (n=3). *** P = 0.0001 (t test).

3 . 1.3 HCV receptor expression and localization in primary human hepatocytes.

To ascertain whether optimal HCVpp entry into PHHs at day 2 reflects changes in HCV receptor levels, we monitored mRNA and protein expression and localization. Claudin-1 and Occludin demonstrated a predominantly intracellular staining pattern with discontinuous plasma membrane expression at day 1 (Figure 3-3 A). The plasma membrane expression of Claudin-1 and Occludin increased at days 2 and 3 in line with the HCV infection data. CD81 localized strongly to the plasma membrane on day 1; however, on days 2 and 3 CD81 membrane distribution was faint concomitant with increased intracellular staining (Figure 3-3 A). Our anti-SR-BI antibodies fail to detect SR-BI expression by confocal techniques. Nevertheless, PHHs express SR-BI as shown by western blotting and its expression level increased over time in culture (Figure 3-3 B). The levels of CD81, Claudin-1 and Occludin were also assessed by western blotting. CD81 expression was stable over time; in contrast, Claudin-1 and Occludin expression levels increased between day 1 and day 3 (Figure 3-3 B).

We also evaluated the mRNA levels of all four receptor proteins over time. As a control we compared the mRNA levels to those in Huh-7.5 cells at day 1 post seeding (Figure 3-3 C). HCV receptor mRNA levels increased over time in PHHs, comparable levels of SR-BI, Claudin-1 and Occludin mRNAs were detected at days 1-3. There was a modest increase in CD81 mRNA over time that was comparable to the levels seen in Huh-7.5 cells. At days 2 and 3 SR-BI, Claudin-1 and Occludin mRNA levels were comparable to Huh-7.5 cells (Figure 3-3 C). In summary, these data demonstrate that PHHs express all four receptor molecules required for HCV entry and

optimal H77pp entry at day 2 is consistent with increased receptor expression levels and localization at the plasma membrane.

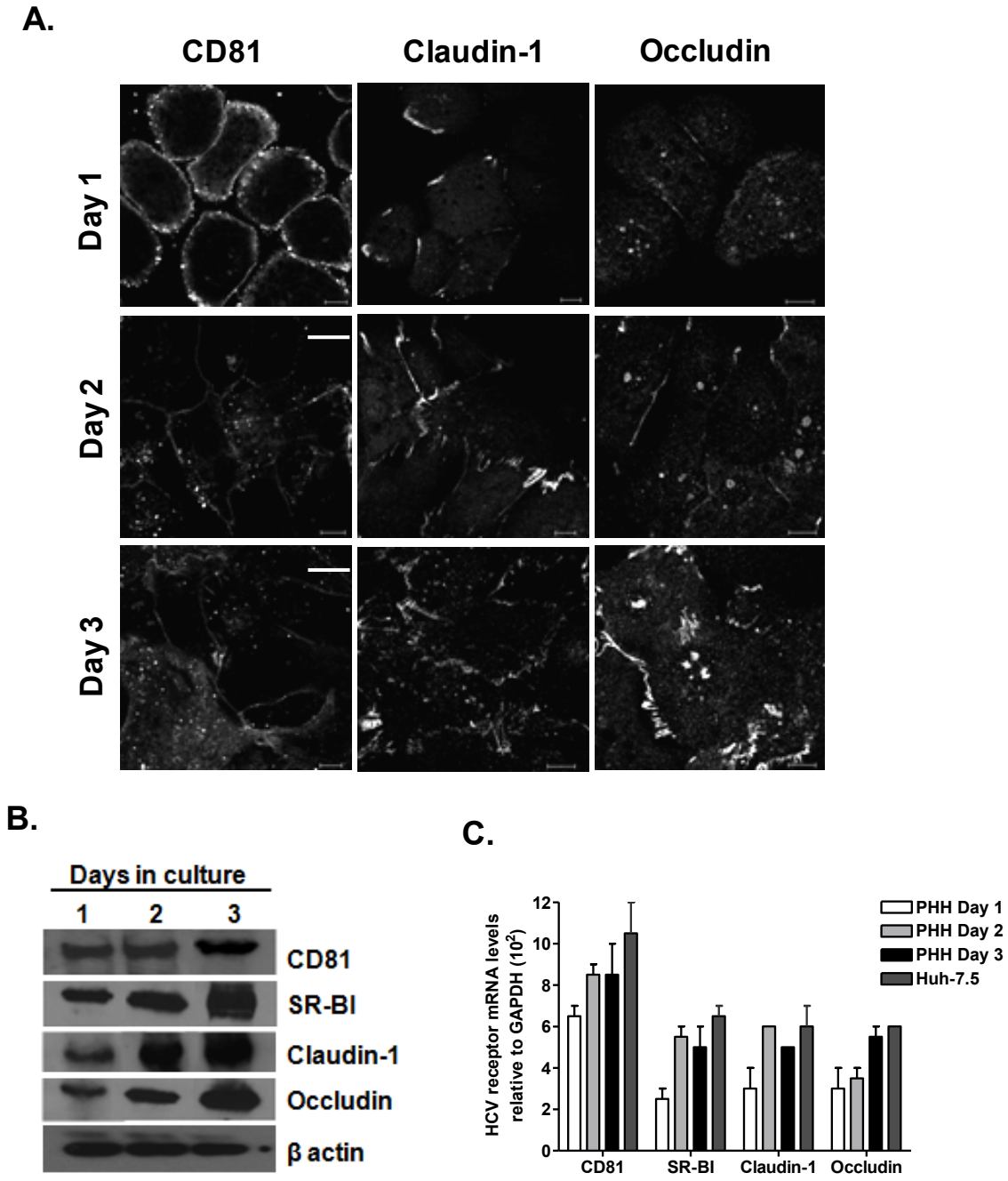

Figure 3-3. HCV receptor expression in primary human hepatocytes.

A. Confocal imaging of CD81, Claudin-1 and Occludin in PHHs cultured for 1, 2 and 3 days, scale bars represent 20μm. **B.** Western blot detection of HCV receptors over time in culture. **C.** HCV receptor mRNA levels in PHHs cultured for 1, 2 and 3 days and Huh-7.5 cells cultured for 1 day, where the data represents 2 independent experiments and presented relative to the housekeeping gene GAPDH. Error bars indicate mean from standard deviation (n=3).

3.1.4 Primary human hepatocytes support diverse HCVpp infection.

Previous studies have shown that HCVpp encoding glycoproteins from diverse HCV genotypes show different abilities to to infect hematoma cells, suggesting that genotypic differences define HCV-receptor interactions (122). To ascertain whether PHHs from multiple donors support diverse HCVpp infection we screened a panel of HCVpp glycoprotein variants (S11c1, S11c3, S28c1, S28c2 and S28c3) cloned from two patients S11 and S28 with acute genotype 1a and 1b infections, respectively (97). Cells were infected for 8 hours, unbound virus removed by washing and infectivity determined 72 hours later by measuring luciferase activity. PHHs from three independent donors (Figure 3-4 A-B) supported comparable levels of infection for all HCVpp strains tested, with typical luciferase values in the order of 7×10^4 relative light units (RLU). VSV-Gpp yielded 3 logs higher luciferase values and were comparable irrespective of PHH donor (Figure 3-4 B). These data demonstrate that PHHs from several donors support diverse HCVpp entry and donor variation has minimal effect on viral entry.

A.

Donor ID	Donor Age (yr)	Sex	Cause of Death	Comments
PHH-1	43	M	Intracranial bleeding	*NHBD
PHH-2	41	F	Intracranial bleeding	Steatotic
PHH-3	63	F	Intracranial haemorrhage	-

**NHBD = non-heart-beating donor*

B.

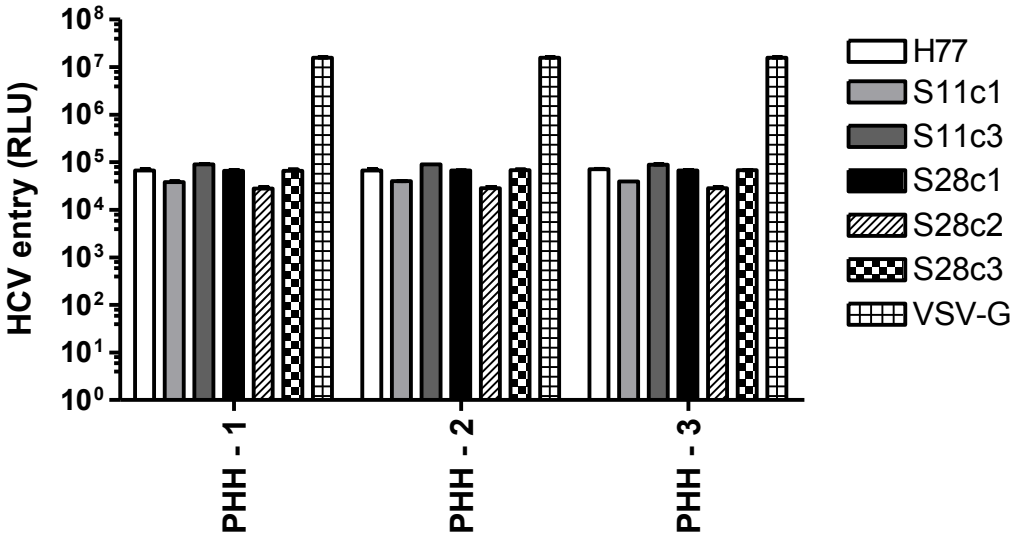

Figure 3-4. Diverse HCVpp infection of primary hepatocyte from 3 donors.

A. Primary hepatocyte donor information. **B.** PHHs from 3 donors were seeded at $4x10^4$ cells/ml and grown for 2 days in culture followed by infection with HCVpp strains or VSV-Gpp. Infection was analysed 72 hours later by measuring luciferase activity. Data is presented as relative light units (RLU) from which a no envelope control value was subtracted. The specific infectivities for HCVpp strains and VSV-Gpp were in the order of 7 $X10^4$ and 1.8 x 10^7 RLUs, respectively. The no envelope values were 2 x 10^3. Data represents standard deviation from the mean (n=3).

3 . 1.5 Comparison of HCVpp entry into primary human hepatocytes and hepatoma cells.

In addition to Huh-7.5's several other hepatoma cells including HepG2 and Hep3B cells have been reported to support HCV entry (254, 260, 349). Both Huh-7.5 and Hep3B cells express all four HCV receptor molecules; in contrast, HepG2 cells do not express CD81 making them non-permissive for infection (254). However, ectopic CD81 expression (HepG2-CD81) conferred susceptibility to HCV infection (254, 260). We compared HCVpp infection of different hepatoma cells to PHHs isolated from three independent donors (Figure 3-5 A). VSV-Gpp infection was comparable for all cell types except HepG2-CD81 cells which demonstrated a 10 fold reduction (Figure 3-5 B). HCVpp strains demonstrated a 1 log range in luciferase values in Huh-7.5 and Hep3B cells; however, this pattern was not seen with PHHs or HepG2-CD81 cells which showed comparable luciferase values (Figure 3-5 A). A non-parametric analysis of the median luciferase values from Huh-7.5 and Hep3B cells showed significant heterogeneity across the different HCVpp strains resulting in the log range ($P=0.0027$, Kruskal-Wallis test).

Variable HCVpp infection values, whether luciferase or GFP reporter viruses, have been interpreted to mean differences in HCV glycoprotein dependent entry. However, reporter gene signals are likely to be affected by cell division, leading to progeny daughter cells that will express the reporter gene. In the following section we describe the effects of cell division on HCVpp luciferase signals.

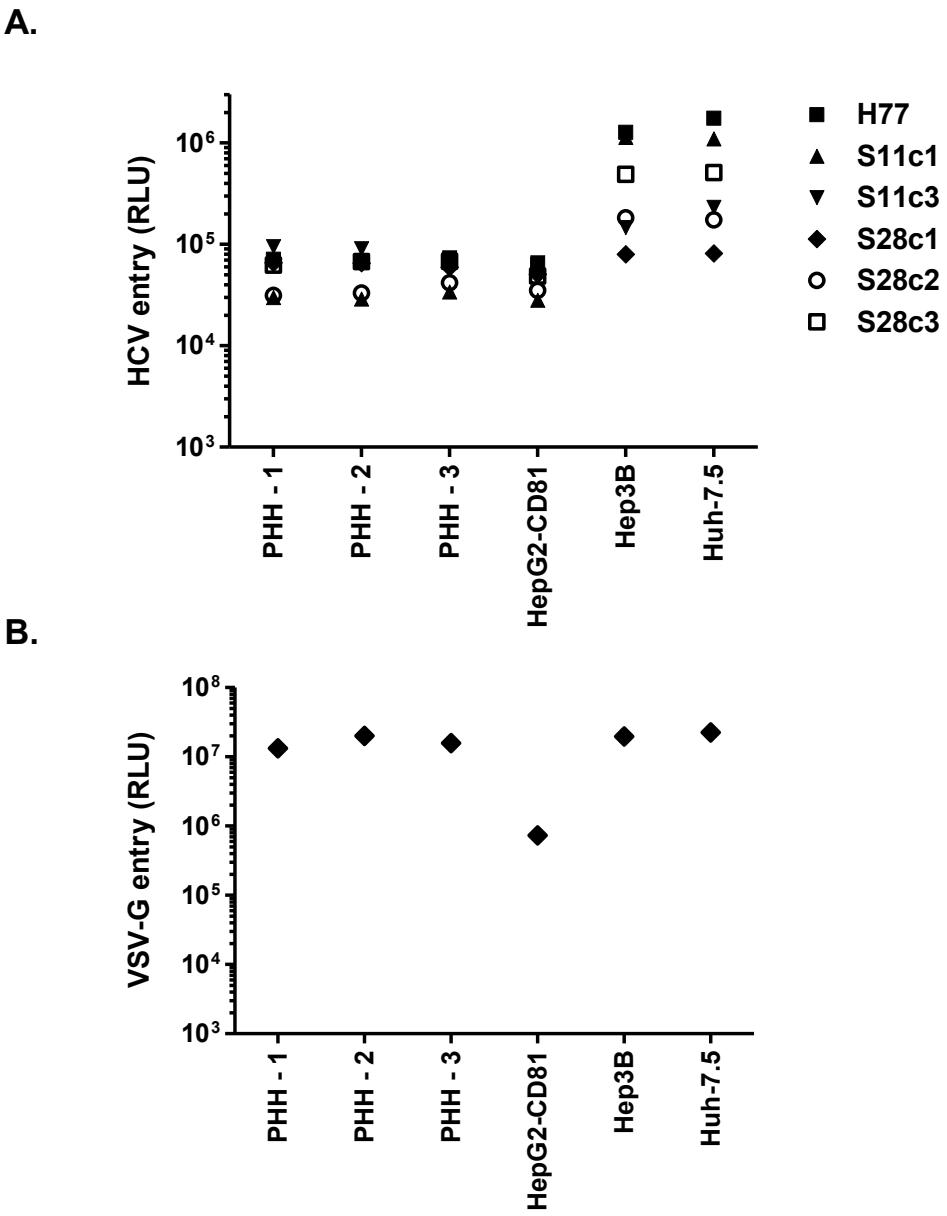

Figure 3-5. Comparison of HCVpp entry into primary human hepatocytes and hepatoma cells.

Primary hepatocytes from three donors (PHH-1, - 2 and -3) and hepatoma cell lines were compared for their permissivity to support HCVpp and VSV-Gpp infection. Cells were seeded at equal densities and infected with a panel of HCVpp strains (**A.**) or control VSV-Gpp (**B.**). HCVpp entry was measured 72 hours later by detection of the luciferase activity. Data is presented as relative light units (RLU) from which a no envelope control value was subtracted. The median luciferase values were significantly different between HCVpp strains infecting hepatoma cells (**P = 0.0027, Kruskal-Wallis test).

3 . 1.6 The effect of cell division on HCVpp reporter signals.

We investigated whether cell division affects HCVpp luciferase signals. In contrast to PHHs, hepatoma cells divide in culture with a doubling time in the order of 24-27h (101, 436). Division of an infected cell may result in two progeny daughter cells bearing the reporter virus. We measured cell division with an MTT (3-[4, 5-dimethylthiazol-2-yl)-2, 5-diphenyltetrazolium bromide) assay; MTT is reduced by enzymes in metabolically active cells to generate a signal that can be read calorimetrically. A linear relationship exists between cell number and the signal produced which is represented as optical density (OD). Firstly, we determined the doubling ability of each cell type. Cells were seeded at an equal density and treated with mitomycin C or γ-irradiation which cross-links cellular DNA to render cells mitotically inactive. 24 hours later MTT activity of control and treated cells was measured. Huh-7.5 and Hep3B cells showed increased cell division compared to PHHs (Figure 3-6 A). Similarly HepG2-CD81 divided in culture over 24 hours although the rate of division was lower compared to Huh-7.5 and Hep3B cells. Mitomycin C or γ-irradiation treatment of hepatoma cells decreased cell division that was indistinguishable from PHHs (Figure 3-6 A). Importantly, both treatments had minimal effects on PHHs (Figure 3-6 A). To ascertain whether cell proliferation affects HCVpp luciferase signal, cells were treated with mitomycin C or γ-irradiation followed by HCVpp infection and luciferase activity measured 72 hours later. Mitomycin C and γ-irradiation had minimal effects on HCVpp luciferase signals in PHHs consistent with their non-dividing nature (Figure 3-6 B). Treatment of HepG2-CD81 cells reduced HCVpp luciferase signals by 25% compared to control untreated

cells (Figure 3-6 C) consistent with the reduced doubling rate of these cells. In contrast, both treatments reduced the luciferase activity of most viral strains by 50% in Huh-7.5 and Hep3B cells resulting in luciferase signals that were comparable to PHHs and HepG2-CD81, with the exception of H77 and S11c1pp where the luciferase activity was reduced by 25% (Figure 3-6 D-E). These data suggest that factor(s) other than cell division potentiate H77 and S11c1pp infection of Huh-7.5 and Hep3B cells. In summary, we demonstrate that cell division increases HCVpp luciferase signals in Huh-7.5 and Hep3B cells independent of viral glycoprotein diversity. Inhibition of cell division reduced HCVpp luciferase signals to levels seen in PHHs with the exception of H77 and S11c1pp.

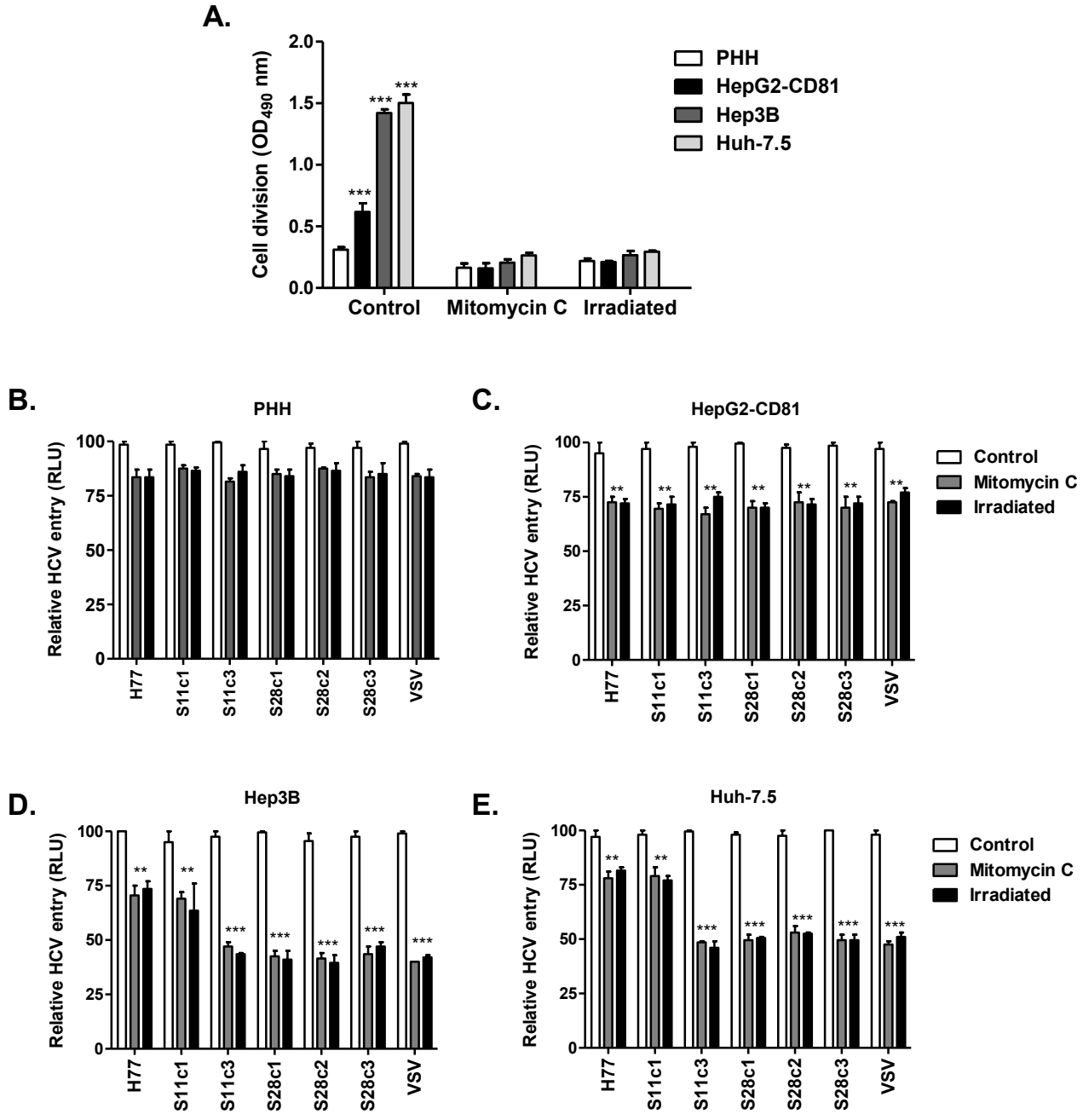

Figure 3-6. The effect of cell division of HCVpp entry.

A. The effect of mitomycin C and γ-irradiation on cell division. Cells were treated with mitomycin C (10μg/ml) or γ-irradiation (32mSV); 24 hours later cell proliferation was assessed. **B-E.** The effect of cell division on HCVpp infection. Control and treated cells were infected with HCVpp or VSV-Gpp and luciferase activity measured 72 hours later. Data is presented as relative light units (RLU) from which a no envelope signal was subtracted and plotted relative to control untreated cells. Data represents 2 independent experiments performed in triplicate, error bars indicate the standard deviation from the mean (n=3) **P = 0.01, *** P = 0.001 (t test).

3 . 1.7 HCVpp decay affects infection rates.

We noted elevated luciferase signals for H77 and S11c1pp infection of Huh-7.5 and Hep3B cells independent of cell proliferation. This was not apparent with other HCVpp strains suggesting that properties unique to H77 and S11c1 glycoproteins were responsible for the effect. Data from our lab has shown that HCVcc particles are highly labile at 37°C with a half life of 2-3 hours (Michelle Farquhar, unpublished observations). However, the labile nature of HCVpp particles has not been investigated; we therefore studied whether H77 and S11c1pp degrades slower at cultured conditions (37°C) compared to other HCVpp strains resulting in increased luciferase signals.

We compared the decay rates of H77, S11c1, S11c3 and S28c1pp; VSV-Gpp was used as control. S11c3 and S28c1pp were used as comparisons because both viral strains demonstrated comparable luciferase signals in all cell types after cell division was inhibited (Figure 3-6). HCVpp strains and VSV-Gpp were incubated in 3% DMEM at 37°C for 0, 12, 24, 36 and 48 hours. Viruses from each time point were used to infect hepatoma and PHHs for 4 hours. Unbound virus was removed by washing and luciferase activity measured 48 hours later. The infectivity of all HCVpp strains tested decreased over time, consistent with prolonged incubation at 37°C (Figure 3-7 A-D). All viral strains demonstrated a similar decay slope; however, when we compared the half-lives, S11c3 and S28c1 had a half-life of around 6 hours for all cell types tested (Figure 3-7 E). In contrast, H77 and S11c1pp strains showed an extended infectivity half-life of 11 hours for Huh-7.5 and Hep3B cells compared to 5 hours for PHH and HepG2-CD81 cells. The decline in VSV-G infectivity was comparable for all cell types

(Figure 3-7 A-E). In summary, these data show that H77 and S11c1pp degrades slower on Huh-7.5 and Hep3B cells which may explain the increased luciferase signals for both viral strains in these cell lines.

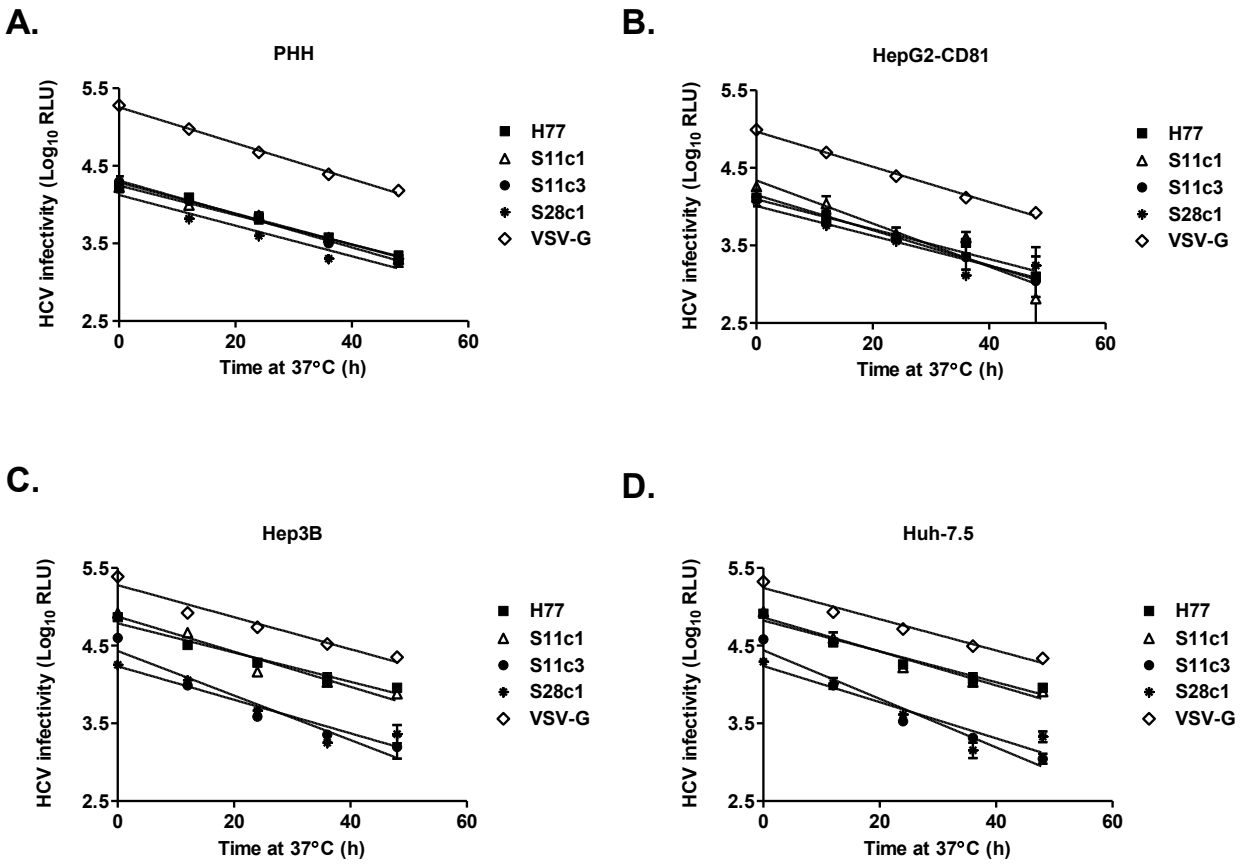

E.

	H77	S11c1	S11c3	S28c1	VSV-G
PHH	6.31	6.17	6.23	6.34	20.54
HepG2-CD81	7.35	7.39	7.50	6.87	17.32
Huh-7.5	11.88	11.30	5.5 1	5.36	20.82
Hep3B	11.35	11.42	5.0	5.72	20.69

Figure 3-7 The effect of degradation on HCVpp infectivity.

HCVpp and VSV-G viruses were incubated at 37°C for different time points (0, 12, 24, 36 and 48 hours) and their infectivity for PHHs, HepG2-CD81 and Huh-7.5 cells evaluated. **A-D** shows virus infectivity over time plotted as relative light units (RLU). **E.** Shows the half-life of each virus strain. Data represents 3 independent experiments performed in triplicate and error bars indicate the mean from the standard deviation (n=3). A no envelope signal was subtracted from each value.

3 . 1.8 Primary human hepatocytes support HCVcc replication.

The data presented thus far describes HCV infection at the level of entry only. To ascertain whether PHHs support HCV replication, we utilized the HCVcc system that allows us to study virus replication and assembly of infectious particles in vitro (225, 415). To determine the optimal time point for HCVcc infection of PHHs, cells were infected at 1, 2 and 3 days post seeding with HCVcc genotype 1b strain J6/JFH-1. SR-BI inhibitor (ITX5061) and anti-CD81 monoclonal antibody were included to evaluate receptor dependency and Huh-7.5 cells at day 1 in culture were used as controls. Infection was quantified by qRT-PCR 72 hours later and the data presented as HCV genome copies relative to the house-keeping gene GAPDH. PHHs support J6/JFH-1 infection in a SR-BI and CD81 dependent manner (Figure 3-8 A). JFH-1 infection of PHHs was optimal at day 2 post seeding where the level of HCV RNA was 100-fold lower than Huh-7.5 cells (Figure 3-8 A). HCVcc replication is associated with the secretion of infectious virus particles into the culture media which can be harvested and used to infect naive target cells. Media was harvested from infected PHHs and control Huh-7.5 cells at 72 hours post infection and their infectivity for naïve Huh-7.5 cells tested. Figure 3-8 B shows that PHH secrete fewer infectious virus particles compared to Huh-7.5 cells. However, after normalizing extracellular infectious virus to viral genomic burden PHHs secrete comparable levels of infectious virus to Huh-7.5 cells (Figure 3-8 C).

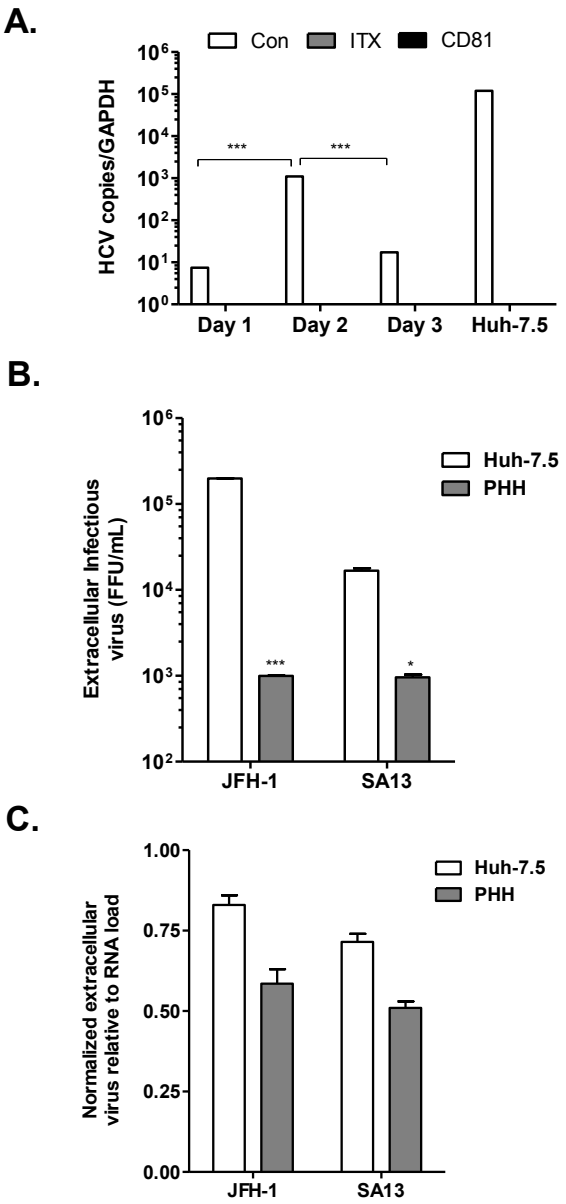

Figure 3-8. Primary human hepatocytes support HCVcc replication.

A. PHHs and Huh-7.5 cells treated with ITX 5061 (ITX) [5μM] or anti-CD81 (5μg/ml) were infected with HCVcc J6/JFH-1 at 1, 2 and 3 days post seeding to determine optimal time point for infection. As a control Huh-7.5 cells at day 1 in culture were infected, 72 hours later the HCV RNA burden was quantified. Data is presented as HCV copy numbers relative to GAPDH. **B.** Extracellular virus secreted from PHHs (infected at day 2 in culture) and Huh-7.5 (infected at day 1 in culture) with HCVcc stains J6/JFH-1 or SA13/JFH-1 were used to infect naive Huh-7.5 cells and infection quantified 72 hours later by staining for the virus antigen NS5A. Data is presented as focus forming units/ml (FFU/ml). **C.** The HCV RNA burden of both cell types was normalized to the level of secreted virus to show virus release from both cell types. *** P = 0.001, * P = 0.05 (t test).

3 . 1.9 Donor variation affects HCVcc replication in primary human hepatocytes.

We have shown comparable HCVpp infection of PHHs from three donors, suggesting that donor variation does not affect HCV infection at the level of entry. To ascertain whether PHHs from the same donors support comparable HCVcc replication, cells were infected with HCVcc strain J6/JFH-1 (genotype 1b) or strain SA13/JFH-1 (genotype 5a). 72 hours later the cells were lysed for qRT-PCR quantification of HCV genomic copy numbers. Figure 3-9 shows that HCV RNA levels were significantly higher in PHHs from donor 2 (PHH-2) compared to cells from donors 1 and 3, suggesting that donor variation affects HCV replication.

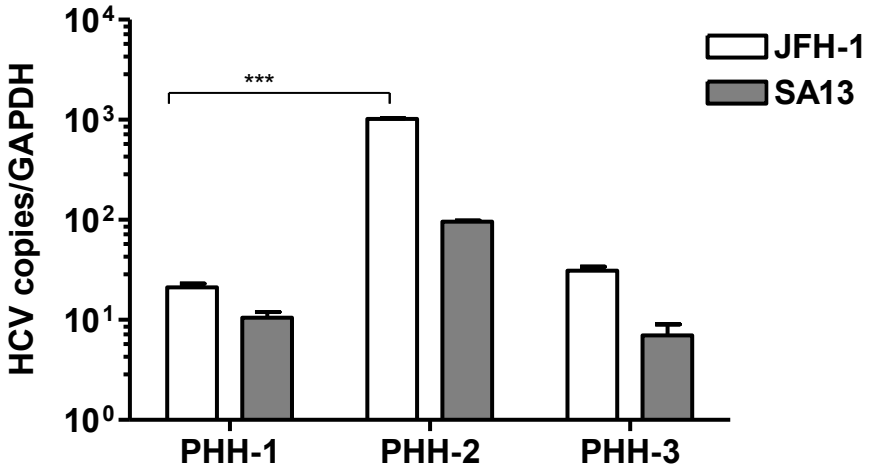

Figure 3-9 The effects of donor variation on HCVcc replication.

PHHs from 3 donors were infected 2 days post seeding with HCV strains J6/JFH-1 and SA13/JFH-1. The genomic RNA burden was quantified by qRT-PCR 72 hours later. Data is presented as HCV genomic copy number relative to the house keeping gene GAPDH. ***P = 0.001 (t test).

3.2 Discussion

The advent of HCVpp and HCVcc systems has enabled studies on the complete viral lifecycle in hepatoma cells. The next major challenge is to unify observations made using these systems with physiological relevant cell culture models. To date a comparative analysis of HCV infection of PHHs and hepatoma cell lines has not been reported. Here, we have utilized the HCVpp and HCVcc systems to compare virus entry and replication in PHHs and several hepatoma cell lines. Several studies have documented the use of PHHs for HCV studies (60, 127, 337); however, the performance of primary cell cultures has varied from one lab to another due to differences in culture conditions or inherent donor variability (141).

A major hindrance for HCV research is the limited availability of PHHs for experimental use. We have obtained cryopreserved PHHs isolated under good laboratory practice guidelines that improve uniformity and reproducibility (272). These PHHs are routinely used in a clinical setting for transplantation purposes (328). Cultured PHHs demonstrated hepatocyte metabolic function and differentiation features for up to 10 days and supported HCVpp infection in a SR-BI and CD81 dependent manner that was optimal at day 2 post seeding. This was consistent with increased SR-BI expression and localization at the cell membrane and a reduction in CD81 expression. These data suggest that thresholds of membrane-expressed pools of HCV receptors are required for maximal infection of PHHs. Indeed, studies have shown that Claudin-1 (434) and SR-BI (364) become enriched at sites of cell-cell contacts as cells become more confluent in culture which in turn enhances HCV infection. Although PHHs

are non-dividing, areas of cell-cell contact increase over time in culture as the cells spread.

HCVpp variants expressing glycoproteins cloned from recent seroconverters (97) infect PHHs from several donors at comparable levels suggesting that the initial stages of HCV infection are not restricted by donor differences. In contrast, HCVcc replication differed in hepatocytes from the different donors to corroborate a previous report (69). Marukian et al, (245), utilized primary human fetal cells from several donors to study the induction of interferon stimulated genes (ISGs) following HCVcc infection. The authors demonstrate variable induction of type III interferons and ISGs among donors. Stimulation of ISGs limit HCV spread in a donor dependent manner suggesting that inherent differences in the innate immune response may affect the outcome of HCV replication. These data provide a potential explanation for differences we observed in HCVcc replication in hepatocytes from different donors.

HCVpp infected PHHs at a lower level than Huh-7.5 and Hep3B cells. Interestingly, HCVpp infection of PHHs was almost indistinguishable from the levels of infection seen in HepG2-CD81 cells. HepG2-CD81 cells are considered to be more physiologically relevant compared to Huh-7.5 cells due to their ability to maintain hepatocyte features such as polarity and detoxifying enzymatic functions (88). The HCVpp system only allows for pseudo-particle infection of 1 target cell and does not transmit to neighbouring cells. Our data indicate that progeny daughter cells may acquire the luciferase gene via hepatoma cell division, resulting in increased luciferase values which are normally interpreted as authentic

HCV entry. However, inactivation of cell division by mitomycin C or γ-irradiation resulted in HCVpp infection of Huh-7.5 and Hep3B cells that was reduced by 50% for all strains tested and was comparable to the levels seen in HepG2-CD81 and PHHs except for strains H77 and S11c1pp which were reduced by 25%.

Our data shows that H77 and S11c1pp particles demonstrate reduced degradation at 37°C compared to other HCVpp strains. Both viruses had a half-life of 11.8 and 11.3 hours respectively for Huh-7.5 and Hep3B cells compared to 5.5 and 5.3 hours for S11c3 and S28c1pp. In contrast, all virus strains demonstrated comparable half-lives to infect PHHs and HepG2-CD81 cells. These data provide further insights into the increased permissivity of Huh-7.5 and Hep3B cells to HCVpp infection. Viruses are susceptible to environmental changes including pH and temperature. Such changes can induce structural rearrangements of the viral capsid leading to instability and degradation, reviewed in (247). Kamili and colleagues (186) showed that HCV plasma was still infectious after storage at room temperature for 16 hours. More recently, Song et al, (380) showed that HCVcc in culture was still infectious in a genotype specific manner after incubation at room temperature or 37°C for 16 days. Together, these data suggest that HCV particles demonstrate increased conformational stability over time which may be affected by genotype specific differences that are unknown. The properties governing virus decay are unclear; however, studies have shown the formation of virus aggregates, a phenomenon where virus particles aggregate via hydrophobic interactions in response to environmental changes (197, 339, 340). This feature reduced the efficacy of neutralizing antibodies and prevented virus degradation. Our data

suggest the tantalizing possibility that fractions of H77 and S11c1pp form aggregates that slows degradation. The mechanisms governing reduced HCVpp decay on Huh-7.5 and Hep3B cells warrants further study as it is unclear why two viral strains are preferentially infectious for these cell types.

We previously reported that CD81 and Claudin-1 co-receptor complexes in HepG2 cells play an essential role in HCV entry (154, 155); it is unknown whether HCV receptors interact in a comparable manner in other hepatoma and PHHs. Recent data from our lab using fluorescent recovery after photo bleaching (FRAP) and single particle tracking imaging techniques show the dynamic diffusion of HCV receptors through the plasma membranes of HepG2-CD81 cells (Harris et al, manuscript in preparation). However, further studies are required to ascertain whether HCV receptor dynamics are similar in other cell types including PHHs. Additional data from our group suggest that HCV receptor endocytosis is important for virus entry. Indeed, HCV receptor specific antibodies or infection induced the internalization of HCV receptors in Huh-7.5 cells in a time dependent manner (Farquhar et al, submitted manuscript). It remains to be seen whether the kinetics of HCV induced receptor internalization is comparable in PHHs; an interesting area for future studies.

A recent study by Podevin et al (320) showed that the expression and maintenance of hepatocyte differentiation makers is important for HCVcc replication in PHHs. Due to increased cell death caused by virus infection we were unable to study HCV replication in primary culture beyond day 5 to ascertain the true effects of hepatocyte differentiation on virus

replication. Although PHHs support lower levels of HCVcc replication compared to Huh-7.5 cells we observed increased virus replication at day 2, which could partly represent increased virus transmission in the infected culture or correct receptor expression and distribution. However, unlike infected Huh-7.5 cells where one can identify and enumerate viral antigen expressing cells, PHHs are highly autofluorescent making it difficult to measure the frequency of infected cells using fluorescent based techniques. Ploss and colleagues recently reported restricted HCV spread in micro-cultures of PHHs (318). The authors argued that virus spread may have been restricted by an inherent or acquired refractory nature of some cells in the population or heterogeneous expression of host factors critical for virus entry. Whilst the above reasons are valid, it is difficult to ascertain whether some cells are refractile and we did not detect regions of significant heterogeneous viral receptor distribution in our cells.

PHHs supported the release of extracellular virus that was infectious for Huh-7.5 cells. Normalization of HCV RNA burden to extracellular virus showed that PHHs secrete comparable levels of infectious virus to Huh-7.5 cells. Virus particles secreted from PHHs were reported to demonstrate a lower buoyant density (320) characteristic of particles associated with low density lipoproteins that are produced during in vivo infection (226). These properties were lost after culture in Huh-7.5 cells suggesting that genuine virus production can only be recapitulated with PHHs. It would be interesting to establish whether secreted virus from cryopreserved PHHs demonstrate authentic HCV properties, a potential avenue for future studies.

To conclude, we demonstrate that hepatoma proliferation led to increased HCVpp luciferase signals that was previously interpreted as increased virus entry. Inhibition of cell proliferation resulted in comparable virus entry into PHHs and hepatoma cell lines with the exception of H77 and S11c1pp, both viruses demonstrated increased stability for Huh-7.5 and Hep3B cells. These data indicate the need for caution when interpreting absolute HCVpp infection of dividing hepatoma cells. Importantly, PHHs support HCVcc replication and release comparable levels of infectious virus to permissive Huh-7.5 cells. In the absent of a small animal model to study HCV infection, PHHs are thought to be the most physiologically relevant cell culture model representing authentic HCV infection in vivo. However, they are difficult to obtain and last for a short time in culture making long term HCV studies impossible. Our study validates the use of immortalized hepatoma models as viable tools for HCV infection studies in vitro providing proliferation rates and virus particle properties are accounted for when interpreting HCV infection of hepatoma cells.

4. RESULTS

4.1 Mechanism(s) of hepatitis c virus perturbation of hepatocellular polarity.

Hepatitis C virus (HCV) induces chronic liver injury that can lead to progressive fibrosis and is one of the leading causes of HCC (111). HCV replicates in the cytoplasm of hepatocytes without integration into the host genome. The role of HCV infection in the carcinogenic process is unclear, in part due to the limited availability of small animal models that support HCV replication and technical difficulties in detecting HCV antigen expressing cells in the human liver (221). Reports demonstrating that HCV encoded proteins interact with cell cycle regulators and tumour suppressors, along with the development of HCC in some HCV transgenic lineages, suggest that HCV proteins may be directly oncogenic (reviewed in (253). Furthermore, HCV associated HCC has been reported to be associated with increased recurrence after liver resection (174) suggesting that HCV may drive the malignant process and metastasis.

As previously discussed HCV utilizes the tight junction proteins Claudin-1 (108) and Occludin (316) to enter target cells. Tight junctions are crucial for the establishment and maintenance of cell polarity and aberrant tight junctions are a feature of many malignant tumours including HCC (82, 293). Previous studies have shown that HCV glycoproteins induced a relocalization of Occludin to intracellular sites in Huh-7 cells (30) suggesting that infection modulates tight junction localization. However, due to the non-polarizing nature of Huh-7 cells (259), the authors were unable to study the functional consequences of viral glycoprotein on cell

polarity. In this chapter we utilize HepG2 cells which polarize in culture (88, 260) to study the functional consequences of HCV infection and glycoprotein expression on polarity.

4.1.1 HCV glycoproteins perturb tight junction protein expression and localization.

To investigate the functional effect(s) of HCV E1E2 glycoproteins on hepatocellular polarity we transfected HepG2-CD81 cells to stably express HCV strain H77 (genotype 1a), JFH-1 (genotype 2a) glycoproteins or control vesicular stomatitis virus encoded glycoprotein-G (VSV-G). Stable cell populations expressing the respective glycoproteins were selected for study where the majority of cells expressed HCV E2 at comparable levels to HCVcc infected hepatoma cells. The majority of infected cells also expressed the viral antigen NS5A (Figure 4-1 A and B). Tight junction protein localization and expression in parental and transfected HepG2 was assessed by confocal microscopy, western blotting and flow cytometry. Occludin localized as discrete bands surrounding the bile canaliculi in parental and VSV-G expressing cells, whereas in H77 and JFH-1 E1E2 expressing cells Occludin localization was modulated and showed reduced expression levels by western and flow cytometry (Figure 4-1 C and Figure 4-2 A and B). Claudin-1 was detected at both the bile canalicular and basolateral membranes. HCV glycoproteins promoted Claudin-1 expression levels with no discernable effect on protein localization (Figure 4-1 C and Figure 4-2 A and B). In contrast, HCV glycoproteins had no detectable effect on the expression levels of HCV entry factors CD81 and SR-BI.

To confirm Occludin relocalization to the basolateral membrane in HCV glycoprotein expressing cells, we studied tight junction solubility to detergent treatment. Tight junction-associated proteins reside in Triton X-100 detergent resistant microdomains (288) such that bile canalicular-localized Claudin-1 and Occludin in parental and VSV-G HepG2-CD81 cells

was detergent insoluble, whereas basolateral pools of Claudin-1 were Triton X-100 soluble (Figure 4-2 C). In contrast, Occludin was soluble to Triton X-100 in HCV glycoprotein expressing cells, confirming protein re-localization from the apical bile canaliculi membrane to the basolateral membrane.

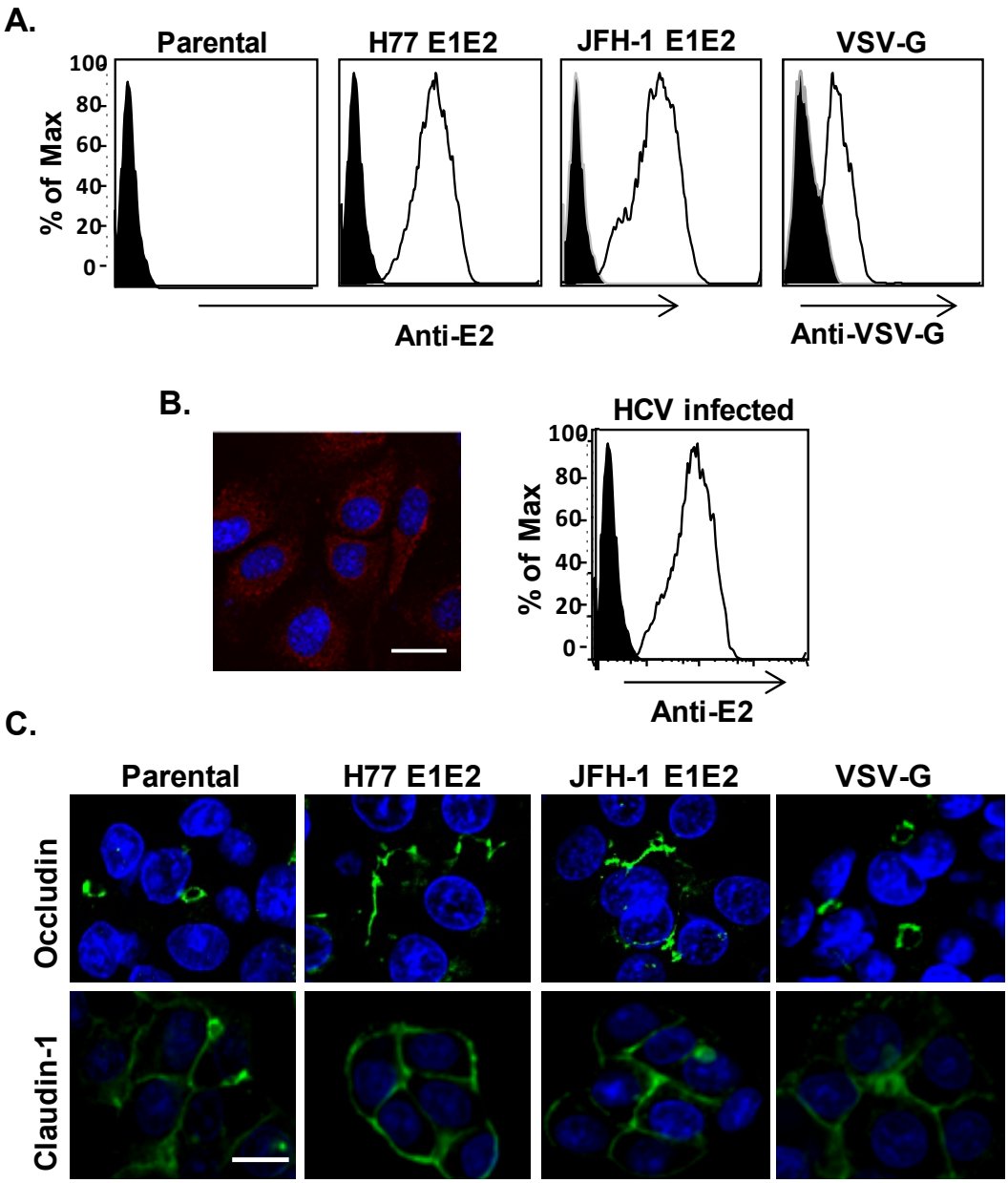

Figure 4-1. HCV glycoproteins perturb tight junction expression and localization.

A. Flow cytometric detection of HCV E2 and VSV-G, cells were stained with anti-E2 (3/11) or anti-VSV-G. The filled histograms depict an irrelevant isotype control and unfilled histograms shows E2 and VSV-G expression, respectively. **B.** E2 expression in HCV infected Huh-7.5 cells, image shows HCV NS5A protein expression (red) used as a marker HCV infection where 80% of cells in culture were infected. Unfilled histogram shows E2 expression in the infected culture and filled histogram depicts an irrelevant isotype control. **C**. Confocal imaging of Occludin and Claudin-1 (green) localization in parental, HCV glycoprotein and VSV-G expressing cells, where cell nuclei are counterstained with DAPI (blue); scale bar represents 20 μm.

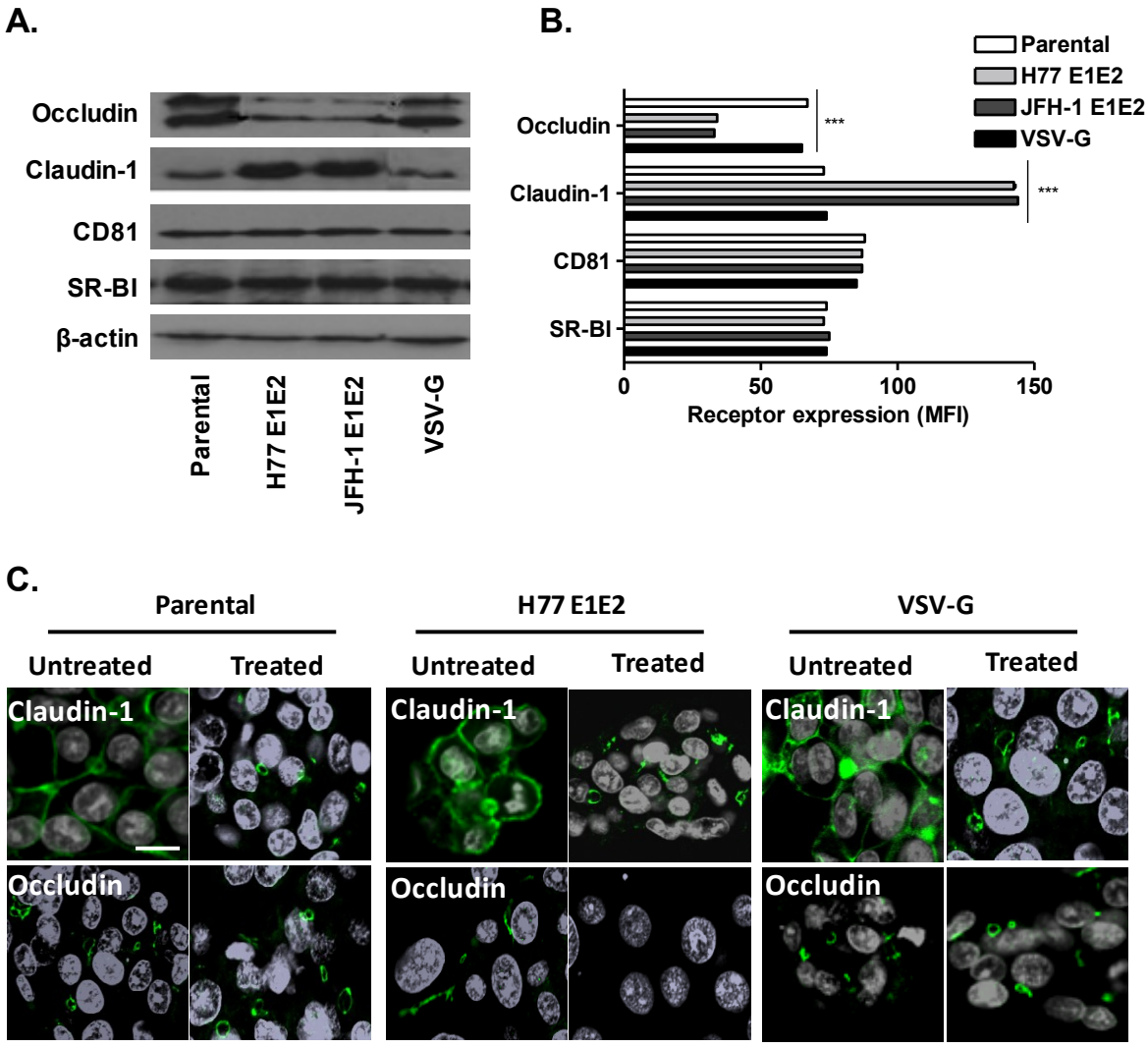

Figure 4-2. HCV receptor expression levels in parental and glycoprotein expressing HepG2-CD81 cells.

A. Quantification of HCV receptor levels in parental and glycoprotein expressing cells by western blotting. Antibodies specific for Occludin, Claudin-1, CD81 and SR-BI were used to show receptor expression levels. **B.** Flow cytometry detection of HCV receptor expression levels, where data is presented as mean fluorescent intensity (MFI) from which an irrelevant isotype control value was subtracted. **C.** Detergent solubility of tight junction proteins; cells were grown for 5 days in culture to polarize followed by treatment with 0.01% triton X-100. Confocal imaging of Claudin-1 and Occludin (green) distribution is shown in triton X-100 treated or untreated cells. The cell nucleus is shown in grey and the scale bar represents 20μm. ***P = 0.001.

4 . 1.2 Tight junction protein localization in normal and diseased liver tissue.

To optimise staining conditions for tight junction protein expression in the liver tissue, a serial dilution of antibodies specific for Claudin-1 and Occludin was performed. Final antibody working concentrations are listed in (Table 2-4). The staining pattern of Occludin and Claudin-1 in paraffin embedded specimens were compared to acetone fixed frozen tissues to ensure that formalin fixation and paraffin processing did not alter the expression pattern. Both proteins demonstrated comparable distribution in paraffin embedded and frozen sections (Figure 2-6).

We utilized formalin fixed paraffin sections to investigate Occludin and Claudin-1 localization in normal liver tissue; sections were stained with antibodies specific for each protein. Hepatocytes and bile ducts express Occludin and Claudin-1; Occludin was only detected at the bile canalicular membrane of hepatocytes (Figure 4-3). In contrast, Claudin-1 staining was apparent at both the apical-canalicular and basolateral-sinusoidal membranes with the dominant expression pattern at the apical-canalicular membrane (Figure 4-3). These results demonstrate that hepatocytes of the liver express Occludin and Claudin-1 consistent with HCV tropism and previous reports (341).

To investigate whether HCV infection perturb Occludin and Claudin-1 localization in vivo, formalin fixed paraffin embedded specimens of human liver samples from normal, HCV infected, non-alcoholic steatohepatitis (NASH) and hepatitis B virus (HBV) infected donors with early and late stage liver disease, diagnosed according to the severity of fibrosis, where

early = no/mild fibrosis (Ishak stage <2) and late = cirrhosis were stained for tight junction proteins.

Occludin demonstrated increased basolateral localization in all inflamed liver tissue samples, consistent with a reduction in apical canalicular expression compared to normal liver tissue (Figure 4-4 A and B). Similarly Claudin-1 demonstrated increased basolateral distribution consistent with a reduction in apical canalicular expression as the disease progress from early to late stage (Figure 4-5 A and B). A wide spread reorganization of Occludin and Cladin-1 was observed in all samples, independent of disease aetiology, suggesting an indirect inflammatory response that is not specific to the HCV infected liver.

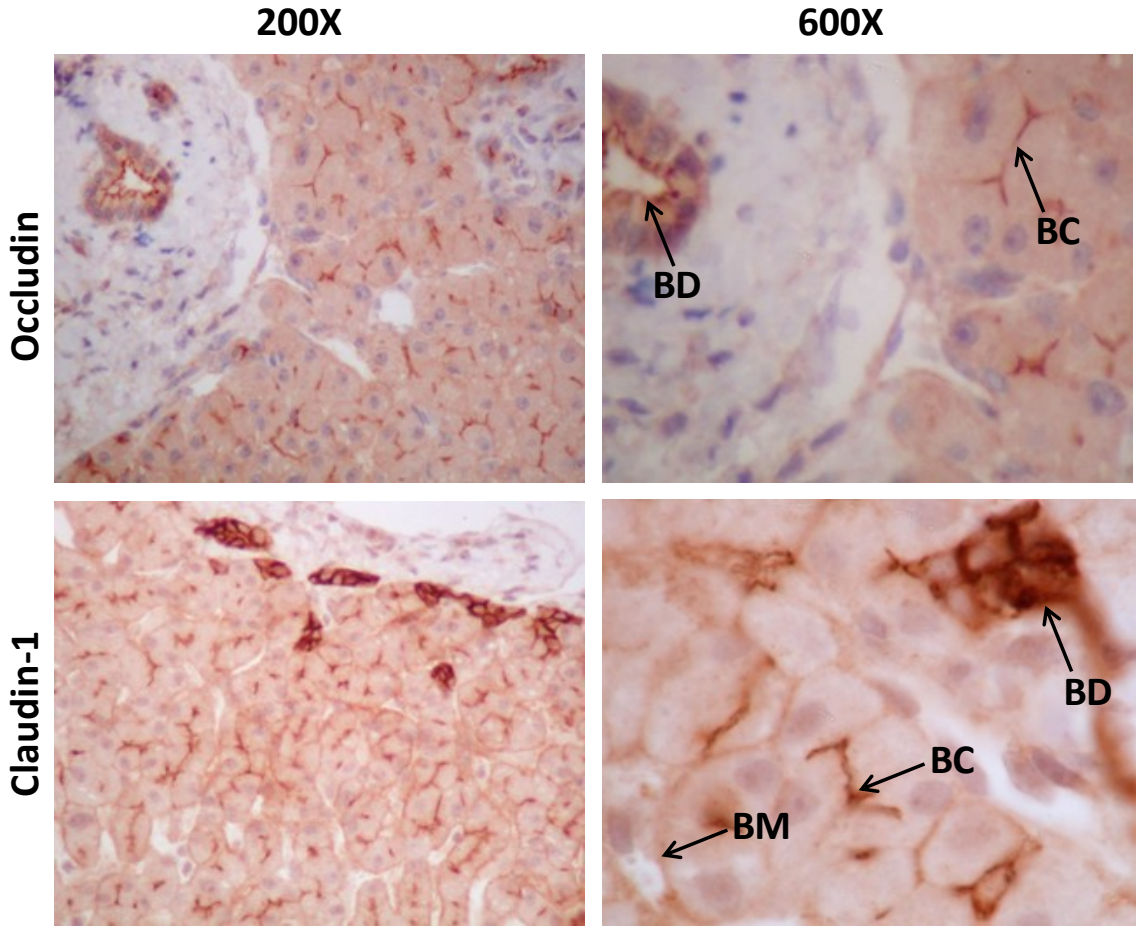

Figure 4-3. Tight junction protein localization in normal liver tissue.

Representative immunohistochemical staining (5 cases) of Occludin and Claudin-1 in normal liver tissue at x200 and 600 magnification. Arrows indicate Occludin and Claudin-1 expression on the bile canalicular (BC)) and basolateral membranes (BM) of hepatocytes, BD shows the expression of each protein on bile ducts.

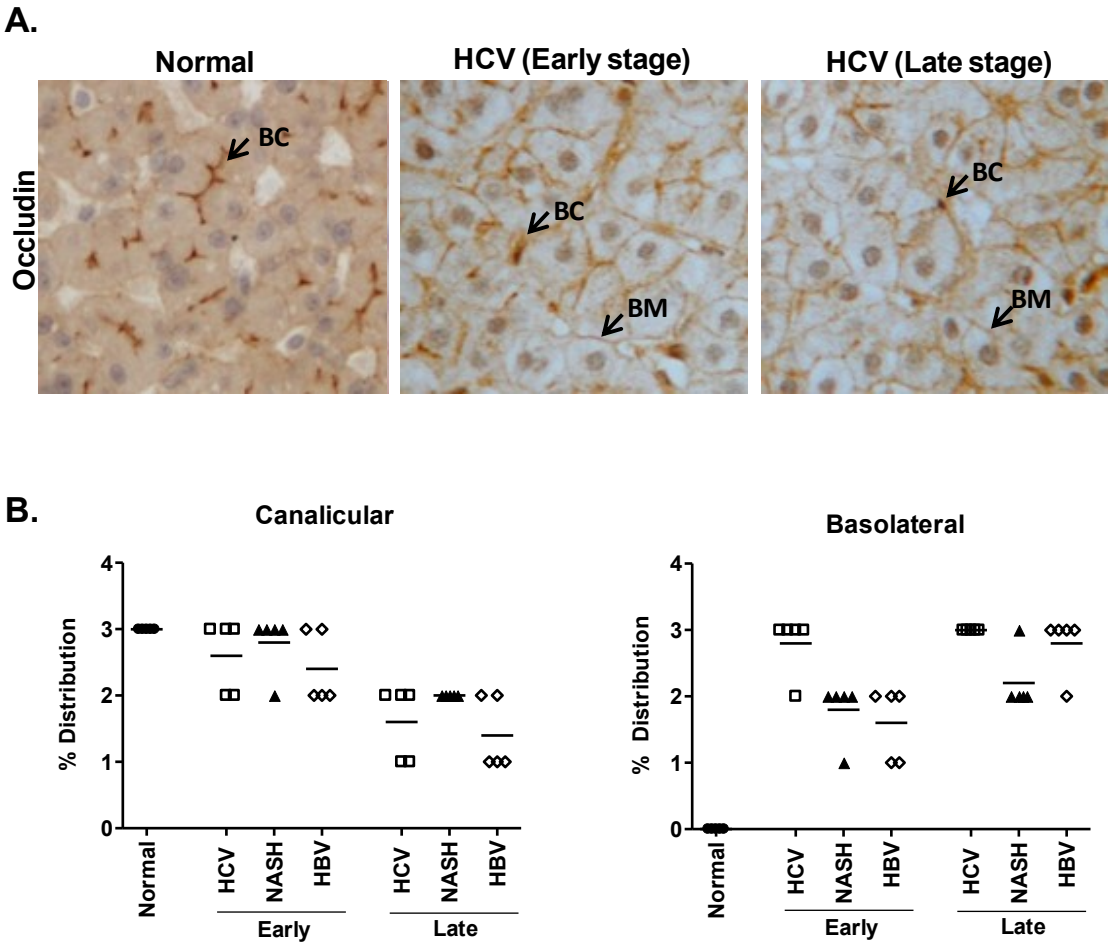

Figure 4-4. Occludin localization in normal and diseased liver tissue.

A. Representative immunohistochemical stains of Occludin localization in normal, early and late stage HCV infected liver (x200). Arrow indicates Occludin at bile canalicular (BC) or basolateral (BM) hepatocyte membranes. **B.** The canalicular and basolateral distribution of Occludin in 5 cases of normal, HCV infected, NASH inflamed and HBV infected tissue were graded as follows: 0=<5%; 1=5-33%; 2=33-66% and 3=>66%. The basolateral distribution in all inflamed phenotypes was significantly higher compared to normal tissue. *$P < 0.01$, *(Dunn's test).*

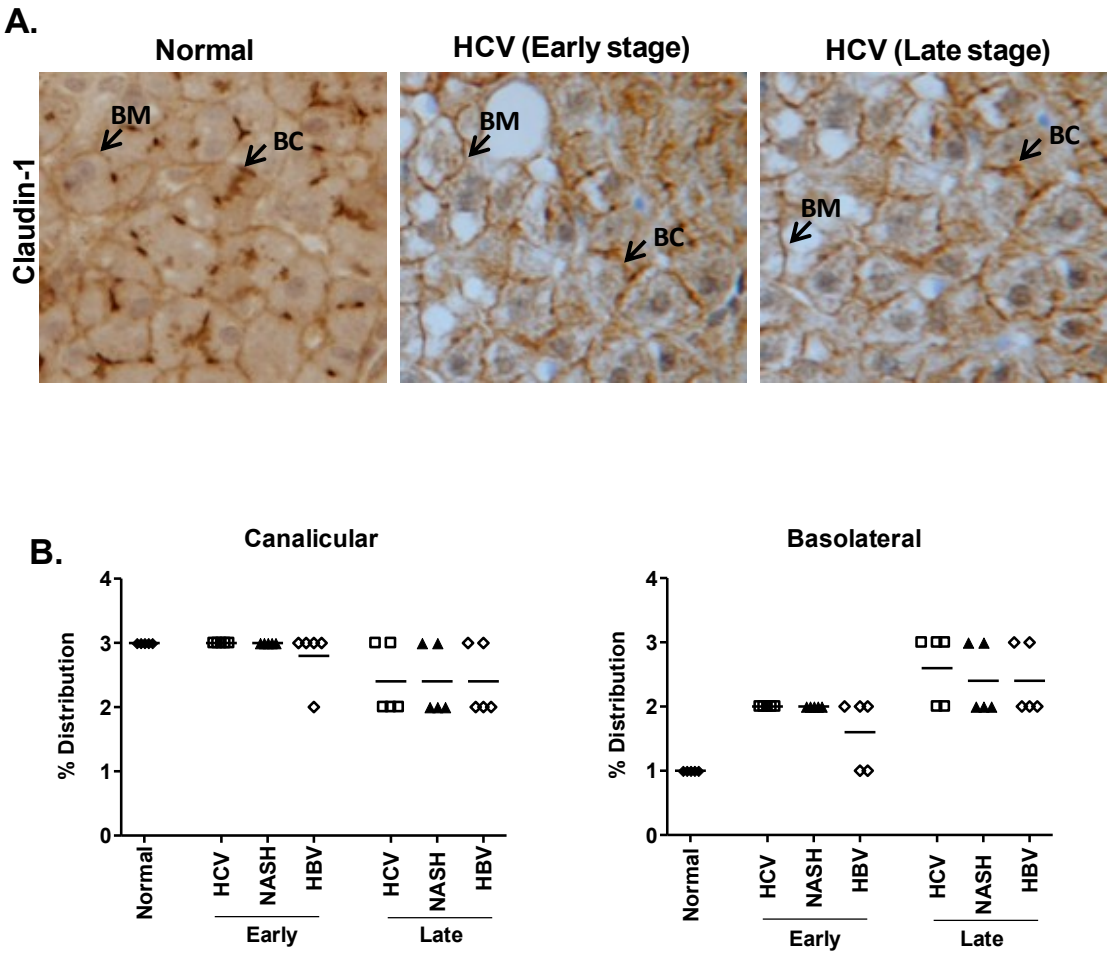

Figure 4-5. Claudin-1 localization in normal and diseased liver tissue.

A. Representative immunohistochemical stains of Claudin-1 in normal, early and late stage HCV infected liver (x200). Arrow indicates Claudin-1 at bile canalicular (BC) or basolateral (BM) hepatocyte membranes. **B.** The canalicular and basolateral distribution of Claudin-1 in 5 cases of normal, HCV infected, NASH inflamed and HBV infected tissue were graded as follows: 0=<5%; 1=5-33%; 2=33-66% and 3=>66%. The basolateral distribution in all inflamed phenotypes was significantly higher compared to normal tissue. **P < 0.01, (Dunn's test).*

4 . 1.3 HCV glycoproteins modulate HepG2 polarity and tight junction integrity.

HepG2 cells polarize overtime in culture and provide a model system to study the effects of HCV on hepatocellular polarization. Since HCV glycoproteins perturbed Occludin and Claudin-1 expression we wanted to investigate the potential consequences for cell polarization. HepG2 polarity can be quantified by enumerating the frequency of cells expressing apical MRP-2 positive bile canaliculi structures per 100 nuclei to give a polarity index (Figure 2-4 A). HepG2 cells form an increasing number of bile canaliculi overtime with approximately 39 bile canaliculi structures detected per 100 cells 5 days post seeding (Figure 4-6 A). Since a minimum of two cells is required to form a bile canaliculus, 39 bile canaliculi per 100 cells corresponds to at least 78% of cells demonstrating a polarized phenotype after 5 days in culture. We show that H77 and JFH-1 glycoproteins significantly reduced HepG2 polarity compared to parental and VSV-G cells (Figure 4-6 A). Furthermore, both HCV glycoprotein strains reduced the ability of MRP-2 expressing bile canaliculi to retain fluorescent CMFDA dye, demonstrating an increased permeability and loss of tight junction integrity compared to parental and VSV-G expressing cells (Figure 4-6 B).

To ascertain whether diverse HCV glycoproteins modulate polarity in a comparable manner to H77 and JFH-1 E1E2, cells were transfected with HCV strains Con-1 (genotype 1b), J6 (1a) and OH8 (1b). Diverse HCV gycoproteins significantly reduced polarity in a comparable manner to H77 and JFH-1 glycoproteins (Figure 4-6 C). Wild type HepG2 cells do not express CD81 and the data presented thus far describes experiments

performed using HepG2 cells transduced to express CD81 (HepG2-CD81). To investigate whether HCV glycoproteins perturbed HepG2 polarity independent of CD81 expression, we studied the effects of HCV H77 and JFH-1 glycoproteins on polarity in wild type and HepG2-CD81 cells (Figure 4-6 D). HCV glycoproteins significantly reduced polarity irrespective of CD81 expression. These data demonstrate that our observations of altered protein expression and impaired tight junction function are independent of HCV engagement of CD81.

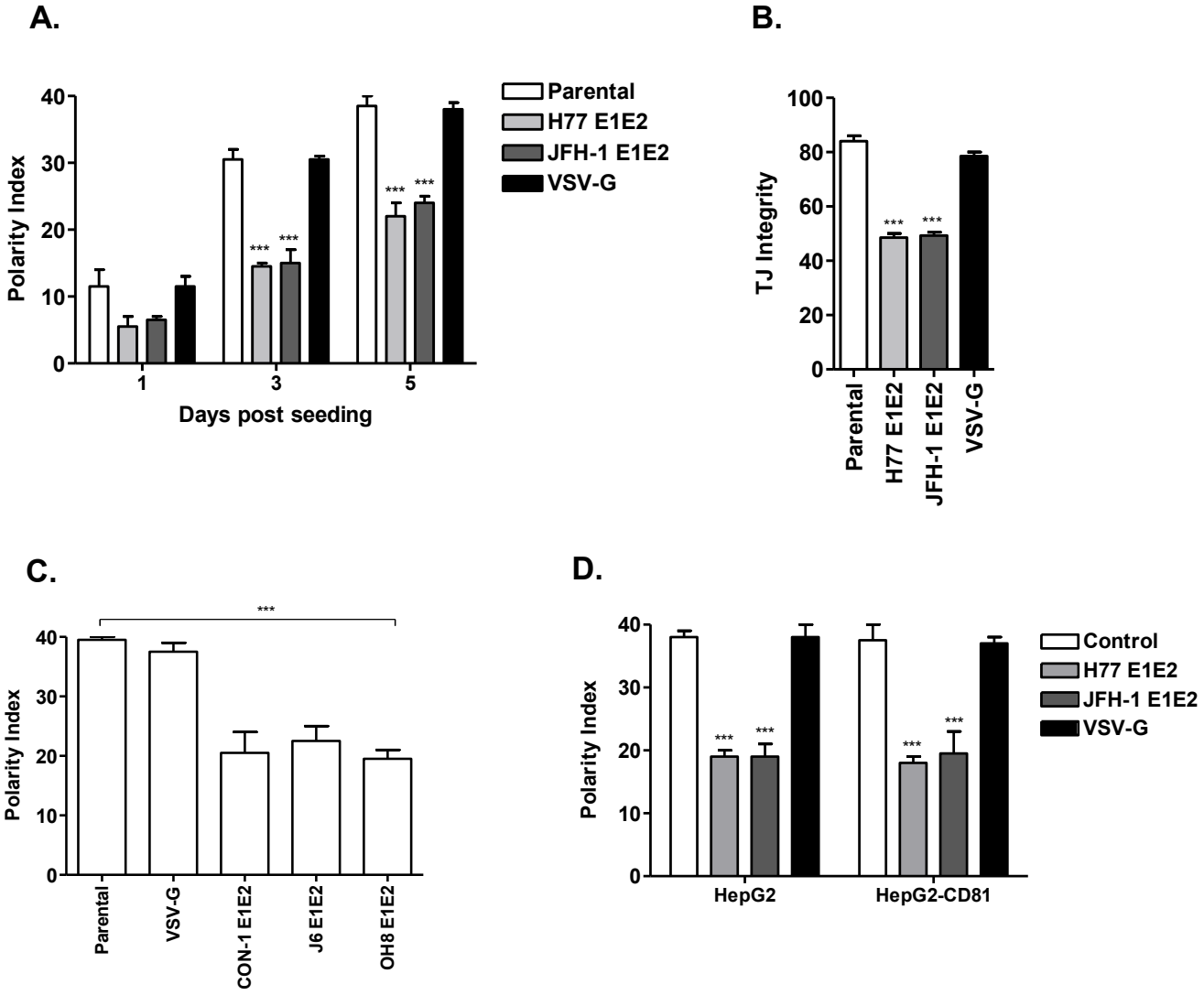

Figure 4-6. HCV glycoproteins perturb HepG2 polarity and tight junction integrity.

A. HepG2-CD81 cells were grown in culture for 1, 3 and 5 days and their polarity assessed by enumerating the number of MRP-2 positive bile canaliculi per 100 nuclei in 5 independent fields of view to achieve the polarity index. **B.** HepG2-CD81 cells were allowed to polarize for 5 days and tight junction (TJ) integrity quantified by determining the number of canalicular structures retaining CMFDA. **C.** HepG2-CD81 cells transfected with diverse HCV glycoproteins were grown for 5 days their polarity index quantified. **D.** Polarity index of wild type (HepG2) and HepG2-CD81 cells transfected with HCV E1E2 or VSV-G glycoproteins ***P < 0.001 (t test).

4 . 1.4 HCV glycoproteins perturb tight junction formation and increase sensitivity to the permeating effects of cytokines.

Tight junction formation and maintenance is calcium dependent and depletion of cellular calcium leads to a reversible loss of epithelial permeability allowing one to study the kinetics of tight junction formation. We monitored tight junction formation by enumerating CMFDA retention at the bile canaliculi in parental, HCV gycoprotein and VSV-G transfected cells overtime. Tight junction integrity in parental or VSV-G expressing cells was restored by 50% within 5.6h following calcium addition, with complete restoration observed by 10h (Figure 4-7 A). In contrast, HCV glycoprotein expressing cells demonstrated a significant delay in tight junction restoring, with a 50% recovery time of 8h (Figure 4-7 A).

Cytokine-mediated changes in epithelial permeability cause a variety of inflammatory disorders (58). To investigate whether HCV glycoproteins modulate HepG2 sensitivity to the permeating effect(s) of cytokines, parental and viral glycoprotein expressing HepG2 cells were incubated with increasing concentrations of TNFα and IFNγ for 24h (Figure 4-7 B). HepG2 cells expressing HCV glycoproteins demonstrated an increased sensitivity to TNFα compared to parental or VSV-G expressing cells, with significantly lower concentrations of TNFα required to break 50% of tight junctions in these cells (Figure 4-7 B). In contrast, HCV glycoprotein expressing cells demonstrated comparable sensitivity to IFNγ mediated effects on tight junction integrity to parental and VSV-G expressing cells. The mechanism underlying TNFα and IFNγ perturbation of hepatocellular permeability is unknown; however, studies with other epithelial and endothelial cell types suggest different mechanisms of action involving actin restructuring and

myosin light chain kinase activation, respectively (57). In summary, these data highlight a role for the viral glycoproteins in perturbing tight junction protein function that may result in an abnormal ‘leaky’ hepatic barrier in vivo.

A.

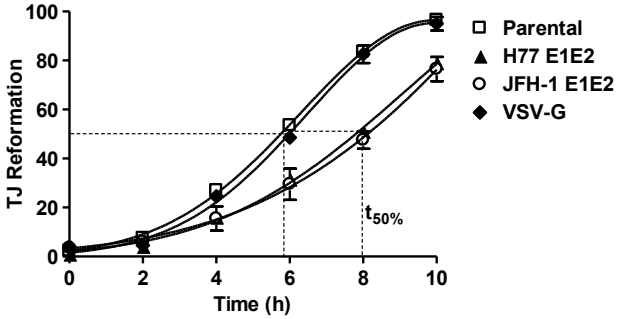

B.

Cell line	INFγ (IC_{50})	TNFα (IC_{50})
Parental	73 ± 6	71 ± 8
H77 E1E2	64 ± 4	34 ± 5*
JFH-1 E1E2	66 ± 7	36 ± 2*
VSV-G	70 ± 5	69 ± 3

Figure 4-7. Tight junction dynamics in glycoprotein expressing cells.

A. Tight junction (TJ) reformation in parental and glycoprotein expressing HepG2-CD81 cells. Polarized cells (5 days in culture) were depleted of calcium for 16h, media containing calcium was added and the cells monitored for their ability to retain CMFDA. $T_{50\%}$ is the time required for 50% of bile canalicular structures to re-form; which was 5.6h for parental/VSV-G cells and 8h for HCV glycoprotein expressing cells. **B** Polarized cells were treated with increasing concentrations of TNFα or IFNγ and tight junction permeability assessed by CMFDA retention. Table shows the concentration of TNFα and or IFNγ required to permeabilize 50% (IC_{50}) of tight junctions in HepG2 cells expressing strain H77 and JFH-1 glycoproteins compared to parental and VSV-G cells. *P < 0.05.

4 . 1.5 HCV glycoproteins perturb hepatocellular polarity via indirect mechanism(s).

Benedicto and colleagues (30) showed that a direct association between HCV glycoproteins and Occludin perturbed Occludin localization at the plasma membrane in infected Huh-7 cells. To investigate whether there is a direct interaction between HCV glycoproteins and Occludin in our HepG2 clones, we co-immunoprecipitated lysates from glycoprotein expressing or HCVcc J6/JFH-1 infected cells. Previous reports have shown a direct interaction between CD81 and HCV E2 glycoprotein (254), as such CD81-E2 association was used as control. Our data showed a direct association between E2 and CD81 in HCV glycoprotein expressing and infected cells compared to parental and VSV-G cells. In contrast, we failed to detect an association between Occludin and E2 in glycoprotein expressing or infected cells, suggesting that HCV glycoproteins modulate hepatocellular polarity via indirect means (Figure 4-8).

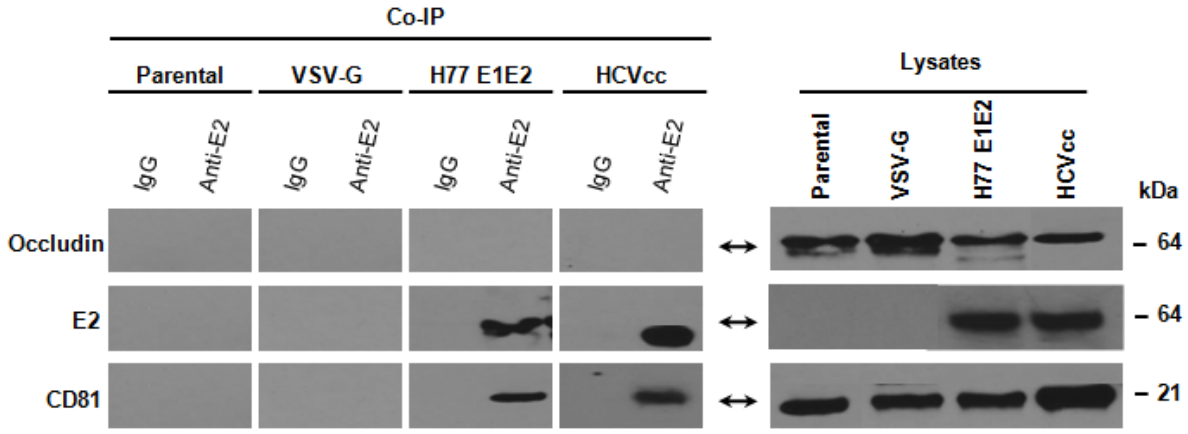

Figure 4-8. HCV E2 glycoprotein does not interact with Occludin.

Lysates from glycoprotein or HCVcc J6/JFH-1 infected cells were immunoprecipitated with anti-E2 monoclonal antibody (3/11) or an isotype matched control (IgG). Figure shows western blot analysis of immunoprecipitated lysates for E2, Occludin and CD81 protein using specific antibodies for each protein. Arrows indicate the specific band for each protein with molecular weight shown in kilo Daltons (kDa).

4 . 1.6 Mechanism(s) of HCV glycoprotein modulation of hepatocellular polarity.

Recent studies have demonstrated that HCV infection induces an ER-stress response leading to mitochondrial dysfunction and the generation of reactive oxygen species (ROS) (280). ROS have been reported to stabilize HIF-1α (280) and activate PI3K, MAPK and NF-kB pathways that promote VEGF and TGFβ expression (224, 326). To ascertain whether HCV glycoproteins increase ROS expression; we studied parental, glycoprotein expressing and infected hepatoma cells for ROS expression by flow cytometry. Increased levels of ROS were observed in HCV glycoprotein expressing cells (Figure 4-9). HepG2 cells expressing VSV-G demonstrated increased ROS production although the levels were significantly less compared to cells expressing HCV glycoproteins (Figure 4-9). Importantly, these results were confirmed with HCVcc J6/JFH-1 infected Huh-7.5 cells. These findings suggest that HCV glycoproteins have the potential to modulate hepatocellular polarity through an oxidative stress pathway.

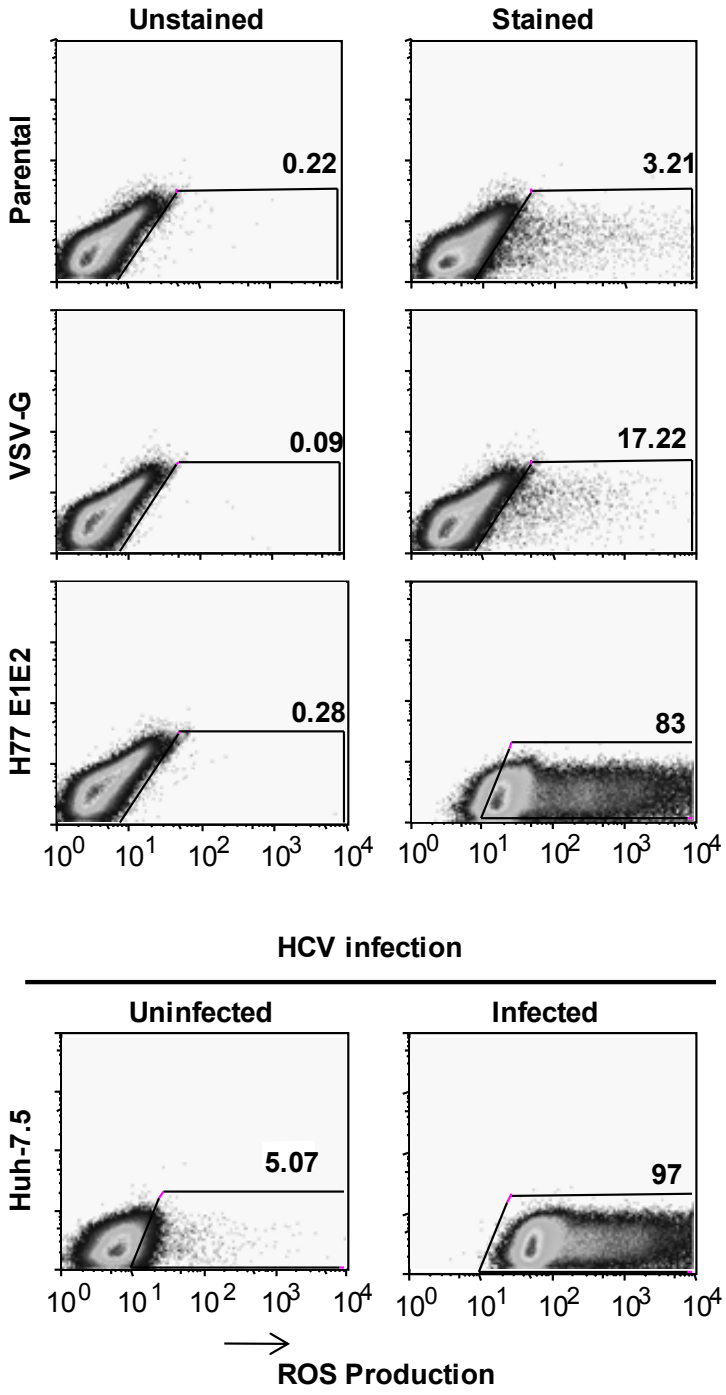

Figure 4-9. ROS production in HCV glycoprotein expressing cells.

ROS production was determined using a cell-permeable fluorogenic probe (DCFH-DA), which diffuses into cells and is deacetylcated by cellular esterases into the non-fluorescent DCFH when ROS levels are low. In the presence of elevated ROS, DCFH is rapidly oxidized to highly fluorescent DCFH. Fluorescence levels were quantified by flow cytometry.

4 . 1.7 Stabilization of HIF-1α in HCV glycoprotein expressing cells.

Since ROS expression is associated with HIF-1α stabilization; we investigated whether HCV glycoproteins stabilizes HIF-1α. HIF-1α is a transcription factor that regulates many genes including VEGF and TGFβ that are involved in tumour invasion and metastasis (264, 280). Parental and glycoprotein expressing cells plated at comparable seeding densities were stained for HIF-1α and media analysed for cytokine expression. HCV glycoproteins stabilize HIF-1α under normoxic conditions (Figure 4-10 A) and led to a significant increase in VEGF and TGFβ expression (Figure 4-10 B). Individual neutralizing antibodies targeting VEGF or TGFβ partially restored tight junction integrity in glycoprotein expressing HepG2 cells, whereas neutralizing both cytokines gave a phenotype that was indistinguishable from parental HepG2 cells (Figure 4-10 C).

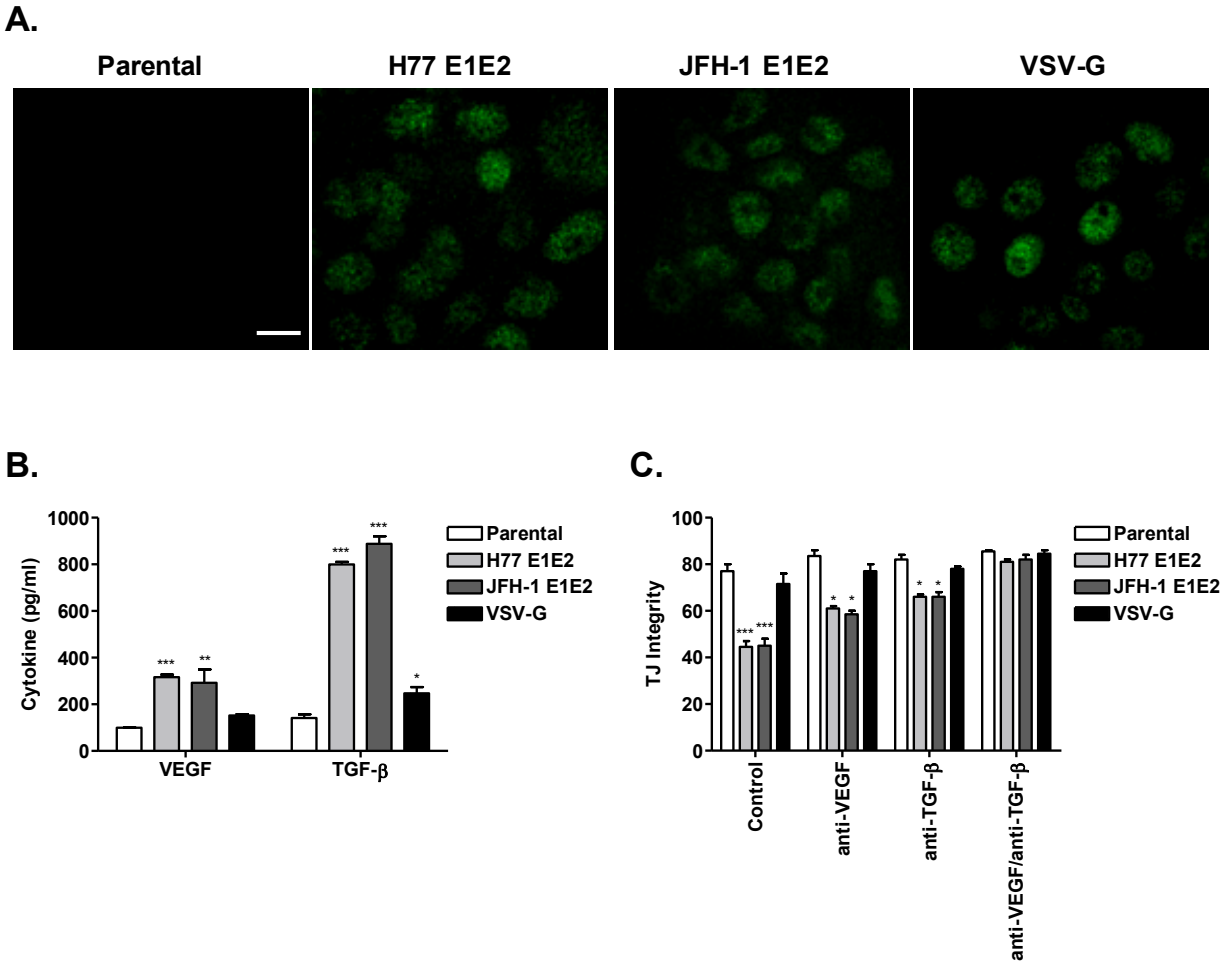

Figure 4-10. Stabilization of HIF-1α in HCV glycoprotein expressing cells.

A. HCV glycoproteins and VSV-G stabilize HIF-1α: nuclear HIF-1α was visualized with anti-HIF-1α mAb (green) and confocal microscopy; scale bar represents 20μm. **B.** Media was harvested from parental and glycoprotein expressing cells and screened for VEGF and TGF-β expression, where the data shows cytokine production per $4x10^4$ cells over a 24h time period. **C.** Cells were allowed to polarize over 5 days and treated with anti-VEGF (1.5μg/ml) or anti-TGF-β (1.5μg/ml) neutralizing antibodies for 24h and tight junction integrity enumerated. *P < 0.05, **P < 0.01, ***P < 0.001 (t test).

Since VEGF and TGFβ are regulated by HIF-1α (264, 280), we evaluated the effects of HIF-1α inhibitor NSC-134754 (NSC) on polarity and tight junction integrity. NSC was identified as a novel compound that inhibits hypoxia or growth factor induction of HIF-1α (67). Different concentrations of NSC were studied to ascertain its effect on cell growth and HIF-1α expression, at 1μM concentration NSC inhibited HIF-1α and had minimal effects on cell growth (67).

We demonstrate HIF-1α stabilization in HepG2-CD81 cells propagated under hypoxic conditions (1% O_2). Importantly, 1μM NSC treatment reduced HIF-1α expression (Figure 4-11 A) and restored polarity and tight junction integrity in HCV glycoprotein expressing cells (Figure 4-11 B), suggesting that HCV glycoproteins modulate HepG2 polarity indirectly via a HIF-1α driven VEGF and TGFß-dependent pathway.

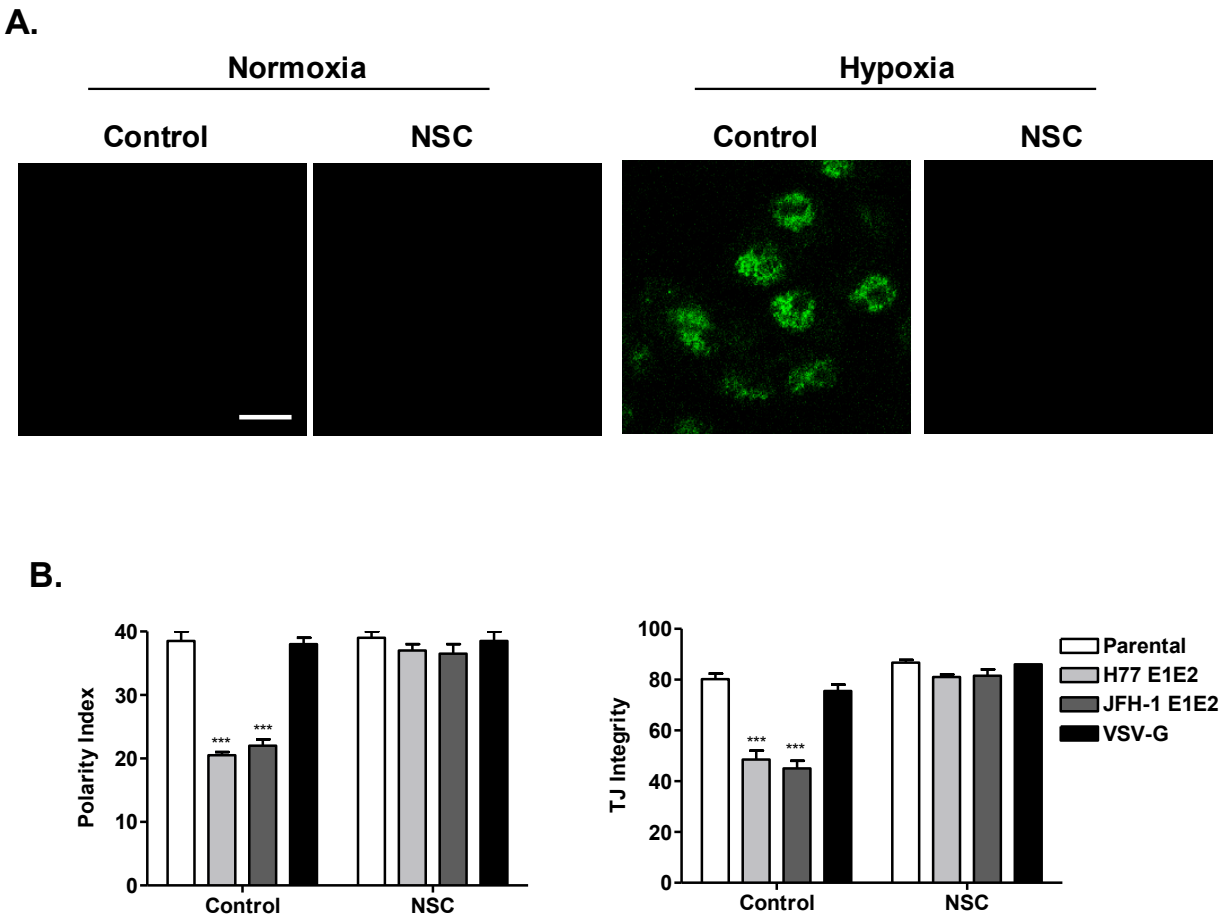

Figure 4-11. The effects of HIF-1α on HepG2 polarity.

A. Confocal images of HIF-1α expression (green) in control or NSC (1μM) treated HepG2-CD81 cells grown under hypoxic (1% O_2) or normoxic conditions (20% O_2), scale bar represents 20μm. **B.** Cells were treated with HIF-1α inhibitor NSC (1μM) for 24h and the polarity index and tight junction integrity quantified. ***P < 0.001 (t test).

4.1.8 HCVcc infection stabilizes HIF-1α and perturbs Occludin localization.

Thus far, the majority of our observations have been based on regulated viral protein expression. To confirm our findings in the context of HCV infection, we used HCVcc strain J6/JFH to infect HepG2-CD81 cells and assessed the effects of virus infection on tight junction localization and HIF-1α stabilization. We confirmed that HCVcc infection stabilized HIF-1α and induced a relocalization of Occludin to the basolateral membrane, consistent with reduced polarity and tight junction integrity (Figure 4-12 A and B). Furthermore, infection of Huh-7.5, HepG2-CD81 and PHHs increased VEGF and TGF-β expression (Figure 4-12 C). We also observed hepatocellular HIF-1α expression in chronic HCV infected liver tissue (Figure 4-13), demonstrating a focal nuclear staining pattern that was consistent with the staining pattern seen in HCC liver tissue. This staining pattern was not observed in normal or primary billiary cirrhosis (PBC) liver samples suggesting that HIF-1α is stabilized during HCV infection in vivo. In summary, we found that HCV infection stabilized HIF-1α leading to altered tight junction protein localization.

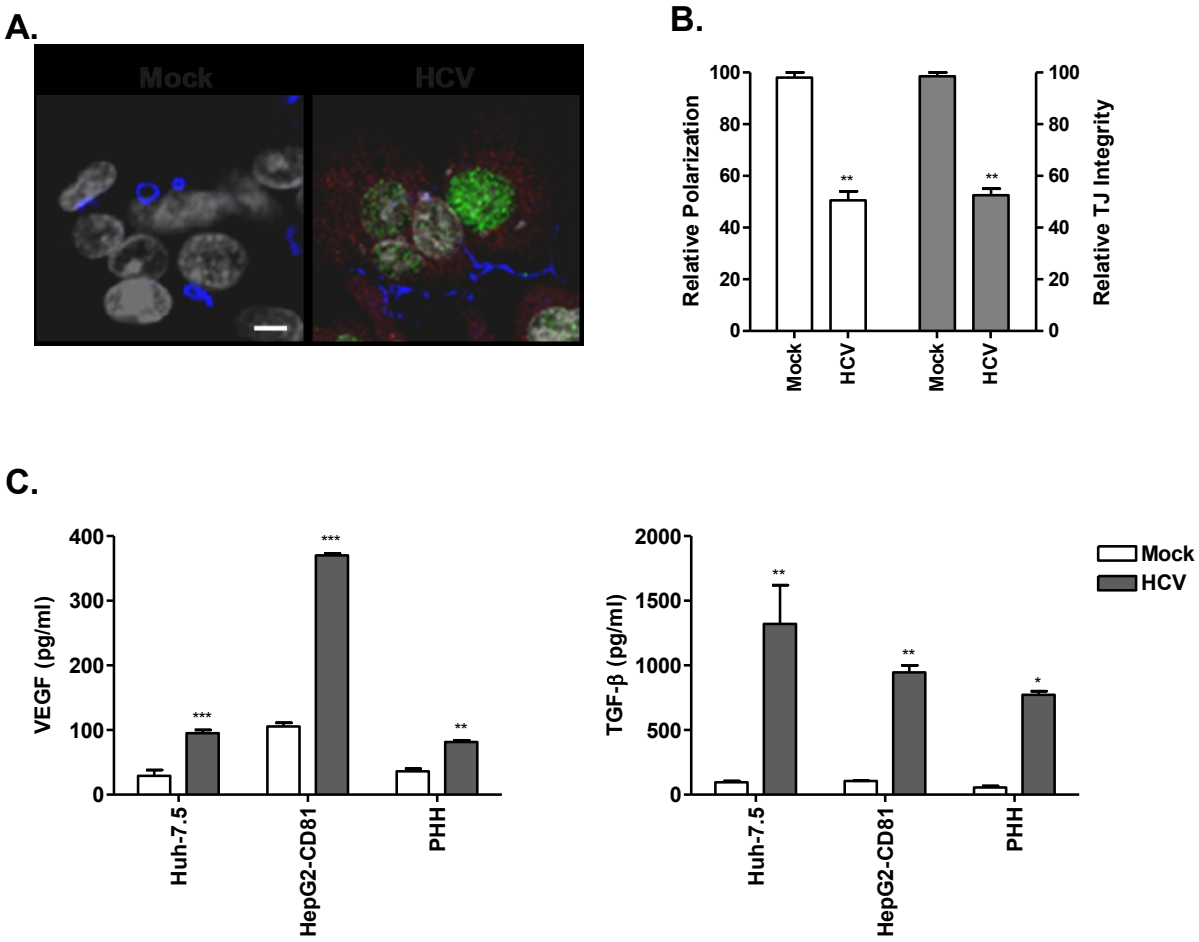

Figure 4-12. HCVcc infection stabilizes HIF-1α.

A. HCVcc J6/JFH infection (viral NS5A antigen is shown in red) of HepG2-CD81 cells stabilized HIF-1α (green) and perturbed Occludin (turquoise) localization, scale bar depicts 20μm. **B.** Polarity and tight junction integrity (TJ) in infected HepG2-CD81 cells; the data is presented relative to uninfected (mock) cells. **C.** VEGF and TGFβ expression in mock and HCVcc J6/JFH-1 infected Huh-7.5, HepG2-CD81 and PHHs, where the HCV RNA burdens were 2.4 x 10^6, 3.8 x 10^5 and 4.1 x 10^5 HCV RNA copies/10^4 cells, respectively. *P < 0.05, **P < 0.01, ***P < 0.001 (t test).

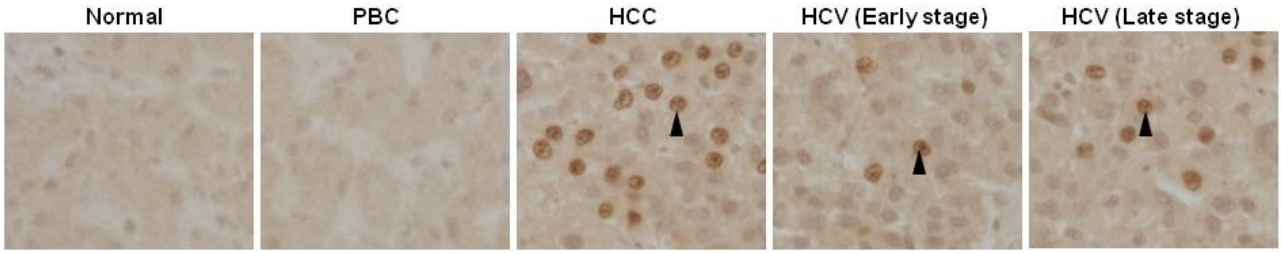

Figure 4-13. HIF-1α expression in normal and diseased liver tissue.

Immunohistochemical staining of HIF-1α in normal, primary billary cirrhosis (PBC), hepatocellular carcinoma (HCC) and HCV infected liver samples, where the arrow head indicates nuclear HIF-1α localization. Images are representative of 5 independent cases from each disease category.

4 . 1.9 Increased migration and de-differentiation in HCV glycoprotein expressing cells.

Our observation that HCV promotes TGFβ expression, a growth factor linked to aggressive tumors (265), led us to assess the effect(s) of infection and viral glycoprotein expression on hepatoma migration. HCV glycoprotein expressing HepG2 clones showed a significantly increased migratory capacity compared to parental or VSV-G expressing cells. Furthermore, expression of the cell adhesion molecule, E-Cadherin, was reduced (Figure 4-14 A and B), consistent with a mesenchymal phenotype. To ascertain whether the viral glycoproteins promote a de-differentiation process reminiscent of epithelial to mesenchymal transition (EMT) which is associated with increase migration (248, 398, 432), we investigated the expression of EMT associated transcription factors, Snail and Twist (303). Both viral glycoproteins promoted Snail and Twist expression (Figure 4-14 B). Importantly, neutralizing TGFβ or treating cells with HIF-1α inhibitor NSC reduced the migration of HCV glycoprotein expressing cells to levels seen with parental and VSV-G expressing cells (Figure 4-14 C). In contrast, neutralizing VEGF had no detectable effect on hepatoma migration (Figure 4-14 C), consistent with experiments showing that exogenous TGFβ promotes HepG2 migration and VEGF had no detectable effect (Figure 4-14 D).

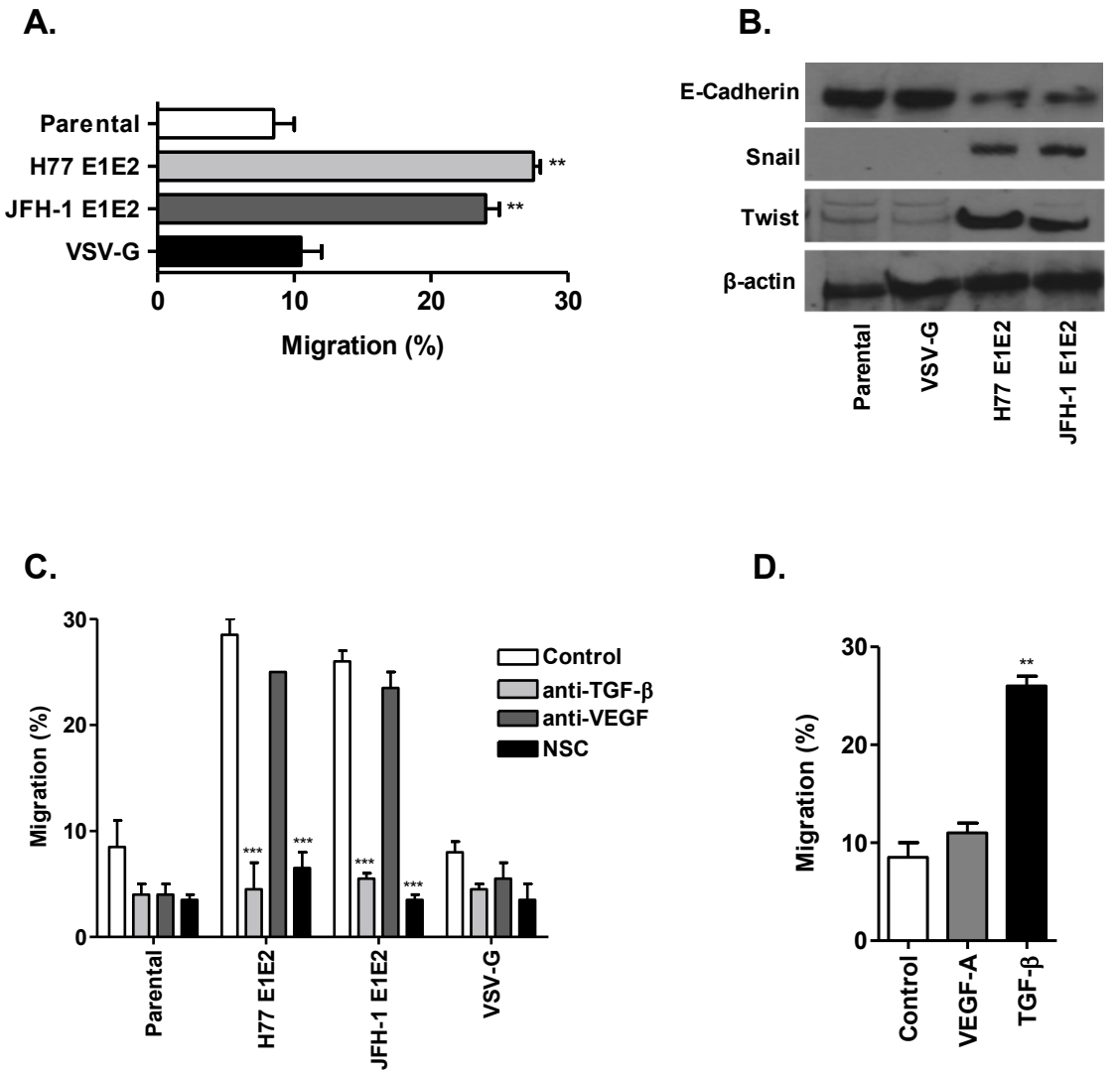

Figure 4-14. HCV glycoprotein promotes HepG2 migration and de-differentiation.

A. Increased migration of HCV glycoprotein expressing HepG2 cells; where migration was determined over a 24h period in a scratch-wound assay. Data is presented as percentage migration. **B.** Western blot detection of E-cadherin and EMT transcription factors Snail and Twist. **C.** The effect of anti-VEGF (1.5μg/ml), anti-TGF-β (1.5μg/ml) neutralizing antibodies and HIF-1α inhibitor NSC (1μM) on HepG2 migration. Cells were treated with the respective compounds for 24h and the difference in migration calculated using a scratch wound assay. **D.** The effect of recombinant VEGF and TGFβ on HepG2 migration, parental HepG2 cells were treated with the respective compounds for 24 hours and their migration assessed via a scratch wound assay. **P < 0.01, ***P < 0.001 (t test).

4 . 1.10 HCV infection promotes hepatoma migration and differentiation.

To confirm our observations of increased migration and expression of EMT transcription factors with full-length infectious virus, we assessed the effect(s) of HCVcc infection on hepatoma migration using two model systems: a scratch wound assay that measures cell migration within the context of a monolayer and a collagen invasion assay that quantifies hepatoma migration through an extracellular matrix. Infection significantly increased HepG2-CD81 and Huh-7.5 migration in both assays (Figure 4-15 A and B) and promoted Snail and Twist expression in hepatoma and PHHs (Figure 4-15 C). Furthermore, inhibiting HIF-1α restored the migratory capacity of infected hepatoma cells and ablated nuclear Snail and Twist expression (Figure 4-15 A-D), demonstrating a HIF-1α dependent process.

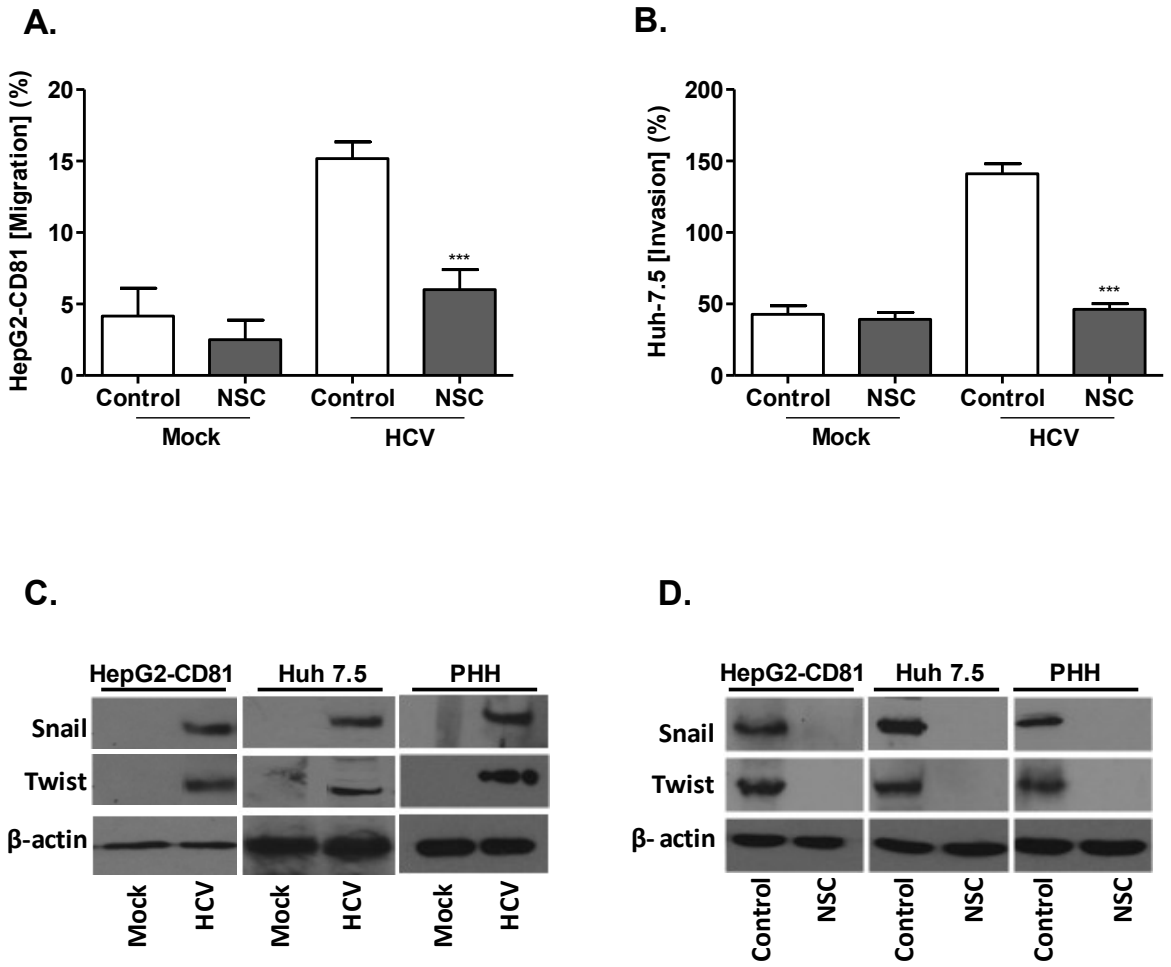

Figure 4-15. Increased migration and expression of EMT transcription factors in HCVcc infected cells.

HepG2-CD81 **(A)** and Huh-7.5 cells **(B)** were infected with HCVcc J6/JFH-1 and their migratory capacity assessed after 48h in a scratch wound and collagen invasion assay respectively, in the presence or absence of NSC (1μM). Data is presented relative to control untreated cells. HepG2-CD81 cells are less permissive for HCVcc infection compared to Huh-7.5 cells and the mean level of NS5A positive infected cells per well was 1.7×10^3 and 9×10^4, respectively. **C.** Western blot detection of Snail and Twist in mock and HCV infected hepatoma and primary human hepatocytes (PHHs) **D.** NSC treatment (1μM) ablated Snail and Twist expression. The infected PHHs contained 4.1×10^5 HCV RNA copies/10^4 cells. $^{**}P < 0.01$.

HIF-1α regulates EMT transcription factors through direct and indirect mechanisms (reviewed in (303, 359). Directly, HIF-1α binds to the hypoxic responsive element in EMT transcription genes to initiate expression. Indirectly, HIF-1α may upregulate additional target genes which in turn activate EMT signalling. Oft et al (289), showed that exogenous TGFβ triggers EMT in cancer cells, confirming that HIF-1α driven indirect signals from the micro-environment can activate this pathway. To investigate whether HIF-1α directly or indirectly promote Snail and Twist expression; Huh-7.5 cells were infected with HCVcc at a low multiplicity of infection (0.01) to achieve distinct populations of infected and uninfected cells. We then assessed the distribution of HIF-1α, Snail and Twist in the culture. HIF-1α was only detected in cells expressing the HCV antigen NS5A (Figure 4-16 A), consistent with the focal HIF-1α staining observed in HCV infected liver tissue which may indicate regions of viral antigen expression in vivo (Figure 4-16 B). In contrast, the majority of cells in the infected population expressed Snail and Twist, independent of viral antigen expression, suggesting a bystander effect that may be mediated by HIF-1α upregulation of TGFβ (Figure 4-16 A). We studied the effects of neutralizing TGFβ and VEGF antibodies on Snail and Twist expression in the infected population. Neutralization of VEGF had no effect on Snail and Twist expression. In contrast, anti-TGFβ ablated the nuclear expression of both transcription factors to confirm a HIF-1α targeting of TGFβ effect (Figure 4-17).

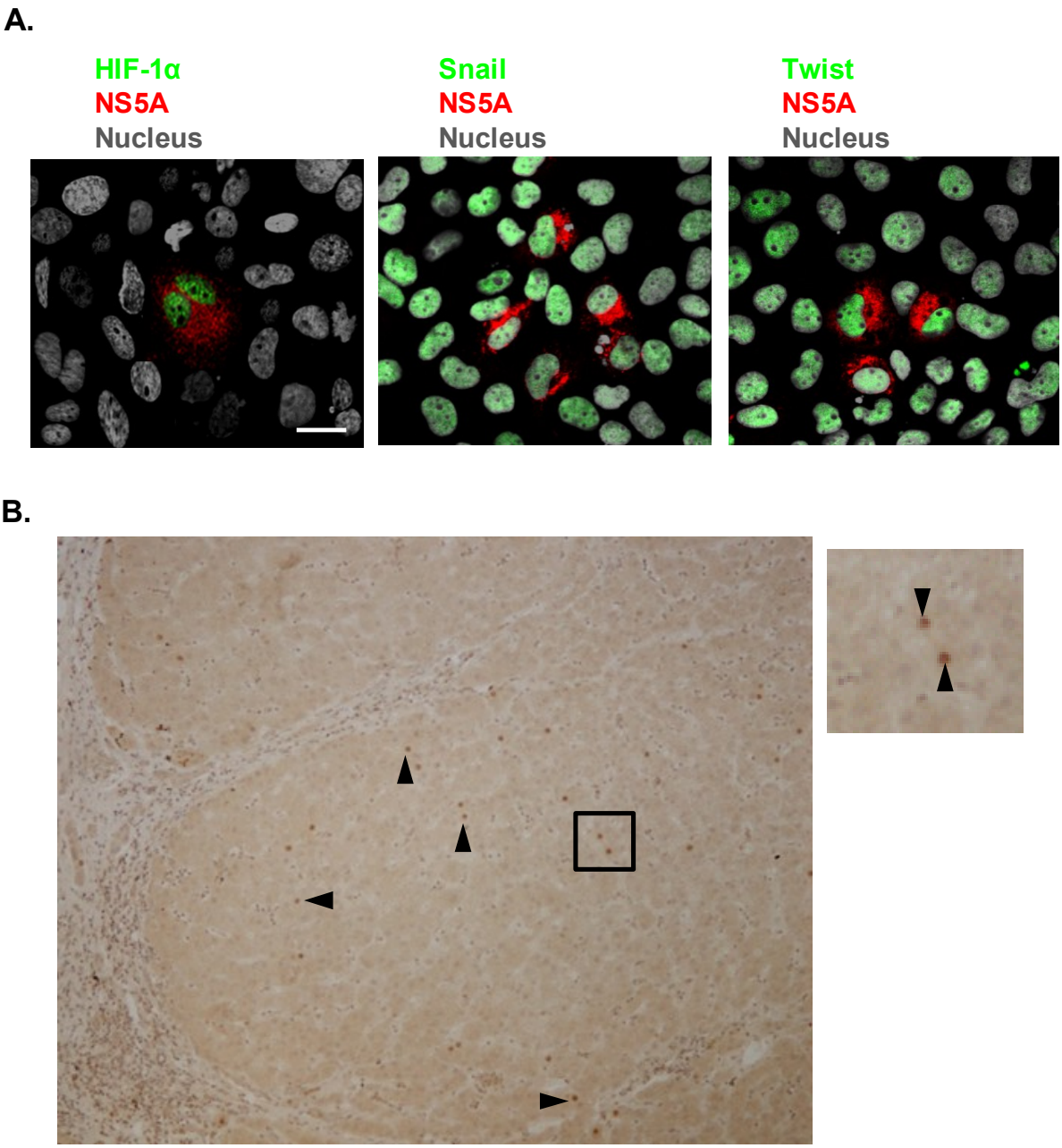

Figure 4-16. HIF-1α, Snail and Twist distribution in HCV infected cells.

A. Huh-7.5 cells were infected with HCVcc J6/JFH-1 at a low multiplicity of infection (0.01) for 48h to study HIF-1α, Snail, Twist and viral antigen NS5A expression. Cells were fixed and co-stained for NS5A (red), HIF-1α, Snail and Twist (green), and nuclei counterstained with DAPI (grey); scale bar represents 20μm. **B.** HIF-1α localization in HCV infected liver tissue. Representative image of HIF-1α distribution in a HCV cirrhotic nodule, arrow heads indicate the nuclear localization of HIF-1α. Box shows a magnified area from the image.

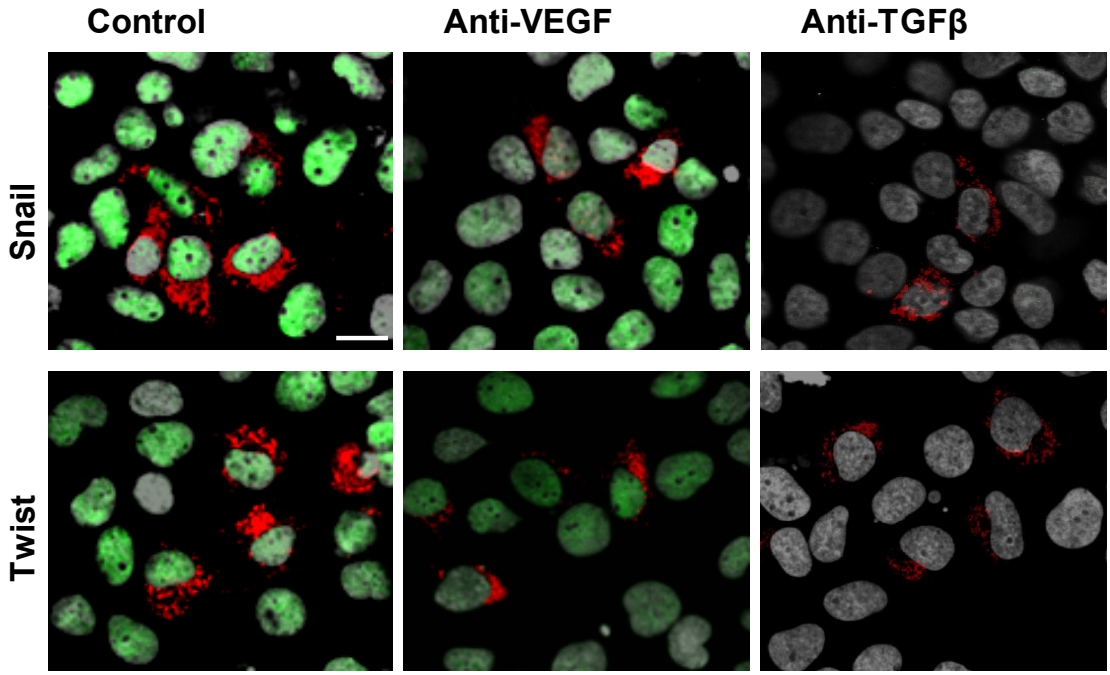

Figure 4-17. The effects of TGFβ on Snail and Twist expression.

Huh-7.5 cells were infected with HCVcc J6/JFH-1 at a low multiplicity of infection (0.01) for 48h in the presence or absence anti-VEGF (1.5μg/ml) and anti-TGFβ (1.5μg/ml). Cells were fixed and co-stained for the viral antigen NS5A (red), Snail and Twist (green), and nuclei counterstained with DAPI (grey); scale bar represents 20μm.

4 . 1.11 A role for HIF-1α in the HCV lifecycle.

Our observation that HCV stabilized HIF-1α, suggest that HCV induces a cellular state of low oxygen which affects cellular metabolic pathways. Indeed previous reports have shown cellular reprogramming induced by HCV including, perturbation of glycolysis and the pentose phosphate pathway which favours biosynthetic activities to support virus replication (90). We investigated the effects of hypoxia on HCV replication, hypoxia significantly increased HCVcc infection of Huh-7.5 and HepG2-CD81 cells and treatment of infected cultures with NSC reduced viral infection (Figure 4-18 A and B). We confirmed these findings using primary human hepatocytes as treatment of infected hepatoma and PHHs with NSC significantly reduced HCV genomic RNA burden (Figure 4-18 C), demonstrating a positive regulatory role for this transcription factor in HCV infection. To ascertain whether HIF-1α regulates HCV infection at the level of entry, we investigated the effect of hypoxia on HCVpp entry into Huh-7.5, HepG2-CD81 and PHHs. As control we studied VSV-Gpp entry. Hypoxia had minimal effects on H77 and VSV-Gpp infection; moreover, HIF-1α inhibitor NSC had no effect confirming a positive regulatory role for HIF-1α during HCV replication (Figure 4-19 A and B). Taken together, these data provide a new paradigm for HCV to modulate HIF-1α dependent pathways that promote HCV replication and underlie virus induced HCC growth.

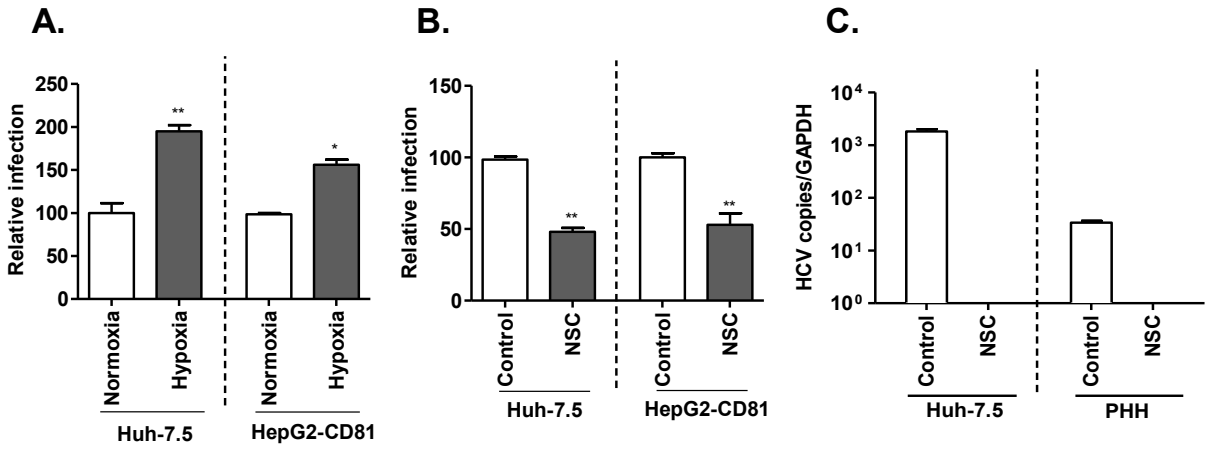

Figure 4-18. The effects of HIF-1α on HCVcc replication.

A. The effect of hypoxia on HCV infection of hepatoma cells; cells were infected with HCVcc J6/JFH-1 virus under hypoxic (1% O_2) or normoxic (20% O_2) conditions and infection determined 48h later by enumerating NS5A antigen expressing cells, data is presented relative to normoxic conditions. **B.** Treatment of infected cells with HIF-1α inhibitor NSC (1μM) reduced viral infection; data is presented relative to untreated (control) cells. **C.** HCV replication in Huh-7.5 cells and PHHs in the presence or absence of HIF-1α inhibitor NSC (1μM). Data is presented as HCV copy numbers relative to the housekeeping gene GAPDH.*$P < 0.05$, **$P < 0.01$ (t-test).

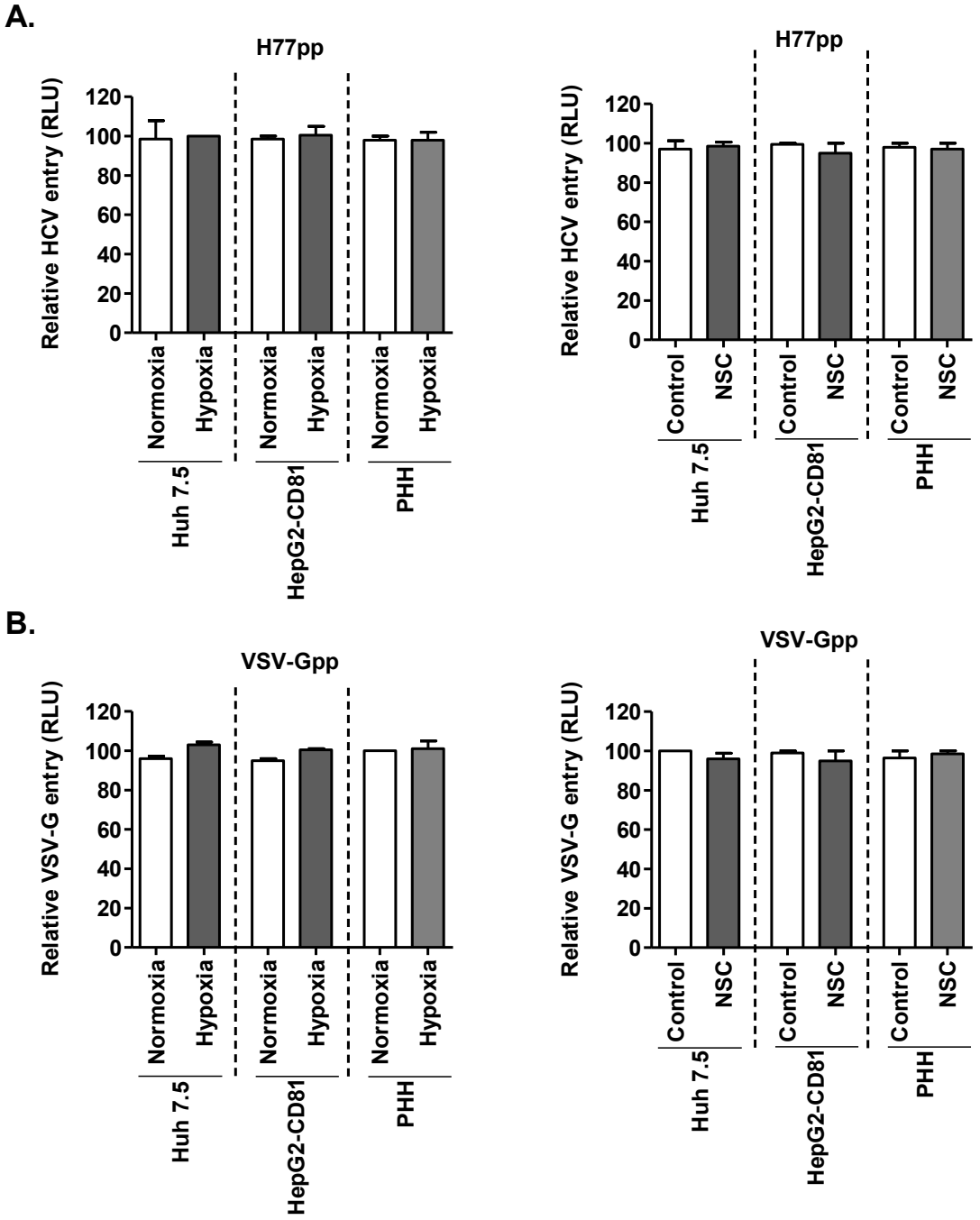

Figure 4-19. The effects of HIF-1α on HCVpp entry.

A. The effect of hypoxia on HCVpp entry; PHHs and hepatoma cells were infected with H77pp under hypoxic (1% O_2) or normoxic (20% O_2) conditions in the presence or absence of HIF-1α inhibitor NSC (1μM) and luciferase activity, shown as relative light units (RLU) was measured 72 hours later. Data is presented relative to normoxic conditions or control untreated cells. **B.** The effects of hypoxia on VSV-Gpp entry; data is presented relative to normoxic conditions or control untreated cells. H77pp infectivity values were 1 x 10^6, 7 x10^4 and 6 x10^4 for Huh-7.5, PHHs and HepG2-CD81 respectively. VSV-Gpp infection values were 2 x10^7 for Huh-7.5 and PHHs and 7 x 10^5 for HepG2-CD81 cells.

4.2 Discussion

Our studies show that HCV infection and the viral encoded glycoproteins reduce hepatoma polarity and increase cell migration by stabilizing HIF-1α expression and upregulating downstream effectors, VEGF and TGFβ. Neutralization of both growth factors or inhibition of HIF-1α restored the polarity and reduced the migratory capacity of infected cells. Furthermore, inhibiting HIF-1α significantly reduced HCV replication in both hepatoma cell lines and primary hepatocytes, highlighting a dual role for this transcription factor in hepatoma migration and the viral lifecycle.

HIF-1α expression has been reported to associate with EMT, a reversible developmental process where epithelial cells reduce intercellular adhesion and acquire fibroblastoid properties that promote an invasive and metastatic phenotype (398, 406). EMT is reported to play a major role in the invasive and metastatic potential of human cancers (73, 152). EMT transcription factors Snail and Twist are expressed in 40-70% of HCCs and correlate with evidence for adherens junction disruption and worse prognosis (387, 432). Similarly, ectopic expression of Snail or Twist in hepatoma cell lines with low endogenous expression enhances cell motility and invasiveness (248, 432). Yang and co-authors reported that increased Twist expression was more frequently observed in HCC associated with HCV infection than with other liver diseases (432). The poor prognosis of HCC is largely due to the invasive nature of the tumour, with frequent intrahepatic and extrahepatic metastases (231). Therapeutic options for patients with HCC are limited. Curative approaches, including surgical resection and liver transplantation are attempted in approximately 30% of patients, and even in these cases the rate of cancer recurrence is in the

order of 60-70% within 5 years (230). Our findings provide a potential explanation for the clinical observation that HCV associated HCC is frequently more aggressive (174). Our data showing that HCV glycoprotein expression and infection promotes Snail and Twist expression highlights a potential mechanism for HCV to accelerate the malignant process.

HCV infection is one of the leading indications for liver transplantation and the number of patients requiring transplantation for chronic hepatitis C is increasing. HCV infects the newly transplanted liver in all cases, leading to a more rapidly progressive disease and frequent graft loss (332). Recurrent HCV is recognised as one of the major challenges facing liver transplantation in the next decade (350). Currently available antiviral treatments are poorly tolerated and have limited efficacy in patients after transplant and novel therapies are urgently required. Injury to the liver at the time of transplantation (i.e. ischaemia reperfusion injury, IRI) has been associated with more aggressive recurrent HCV disease (252); however, the factors governing viral replication rate(s) in the newly transplanted liver are poorly understood. Our demonstration that hypoxia, a key event during hepatic IRI, increases virus replication provides a potential explanation for these clinical observations and highlights the potential value of short term anti-oxidant or HIF-1α inhibitor treatment at the time of liver transplantation to limit HCV replication.

Recent reports demonstrate that HCV promotes TGFβ expression by inducing reactive oxygen species and activating p38MAPK, JNK, ERK and NF-κB pathways (224, 326), consistent with reports of increased TGFβ levels in HCV infected patients (36). TGFβ promotes EMT and is thought to

play a major role in the dissemination of malignant hepatocytes during HCC progression (129, 139). Our current data showing a role for TGFβ in the increased migratory capacity of HCV infected hepatoma cells support a role for HCV in promoting tumour spread rather than a direct role in the oncogenic process *per se.* We failed to observe any morphological fibroblast features of infected or HCV glycoprotein expressing hepatoma cells, suggesting a partial de-differentiation process in vitro. Mazocca et al. recently reported that inhibition of TGFβ receptor I kinase blocked HCC growth, supporting a rationale for therapeutic targeting of TGFβ signalling in HCC (250).

Our observation that VEGF and TGFβ perturb tight junction function supports our in vivo observations demonstrating a widespread reorganization of Occludin in diseased human liver. In contrast, Benedicto and colleagues reported that HCV glycoproteins directly associate with Occludin and alter protein trafficking in Huh-7 cells (30). We failed to co-immunoprecipitate Occludin with the HCV glycoproteins in a variety of cell lines transduced to express HCV E1E2 or in HCV infected cells, in agreement with a recent report (270). Importantly, VEGF or TGFβ had no detectable effect on the expression or localization of Occludin in Huh-7 cells, suggesting that these cells are refractory to these cytokines (258).

In summary, we have shown that HIF-1α is involved in stimulating VEGF and TGFβ that alter hepatocyte behaviour and promote malignancy in the HCV infected microenvironment. We have also demonstrated a role for HIF-1α in HCV infection. These findings highlight a potential role of HIF-1α inhibitors as therapeutics in patients with both HCC and HCV infection.

5. RESULTS

5.1 The effects of glucocorticoids on HCV infection and hepatocellular biology.

HCV infects the newly transplanted liver in all cases, leading to rapid and progressive disease culminating in frequent graft loss. There is a significant reduction in peripheral HCV RNA levels in the first 24 hours following liver transplantation followed by a rapid increase in viral load due to infection of the new graft (65, 263, 416). This exacerbated infection is likely to contribute to rapid liver failure that compromises patient and graft survival. The underlying mechanisms for the more aggressive nature of HCV infection and deterioration of the new graft are unclear; however, several factors including donor age and HCV genotype have been implicated with the progressive nature of the virus post liver transplantation (110, 164). Several studies have called into question the use of glucocorticoid immunosuppressive drugs for HCV infected patients undergoing liver transplantation. High doses and repeat usage of glucocorticoids such as prednisolone, cyclosporin A and hydrocortisone have been linked to increased fibrosis and poor long-term graft survival (33, 134). More recently, Ciesek and colleagues reported that glucocorticoid treatment of hepatoma cells increased HCV replication (76). Despite these observations, steroids continue to be used in the liver transplant, largely since the mechanism(s) of steroid associated exacerbation of HCV infection are unknown. In this chapter, we shed light on the potential mechanism(s) of glucocorticoid enhanced HCV infection and the consequences for hepatocyte biology.

5.1.1 Prednisolone increases HCVpp entry into hepatoma and primary human hepatocytes.

We evaluated the effects of prednisolone on HCVpp entry into hepatoma and PHHs. Cells were treated overnight with increasing concentrations of prednisolone and infected the following day with H77pp. We also evaluated the effects of prednisolone on cell viability using an MTT assay (Figure 5-1 A). Prednisolone increased H77pp entry into Huh-7.5 and PHHs in a dose dependent manner whilst having minimal effect on cell viability. The dose dependent response plateau at 100nm in both cell types suggesting a threshold for prednisolone mediated boost in H77pp entry. Prednisolone enhanced H77pp entry 3- and 4.5- folds in PHHs and Huh-7.5 cells respectively, and had no effect on VSV-Gpp entry (Figure 5-1 B and C). To confirm prednisolone mediated boost in H77pp entry, cells were treated with Mifepristone (RU-486) a glucocorticoid receptor (GR) antagonist that binds the receptor with high affinity (238). RU-486 had no effect on virus entry and ablated the enhancing effects of prednisolone (Figure 5-1 B), demonstrating a role for glucocorticoid signalling in HCV entry.

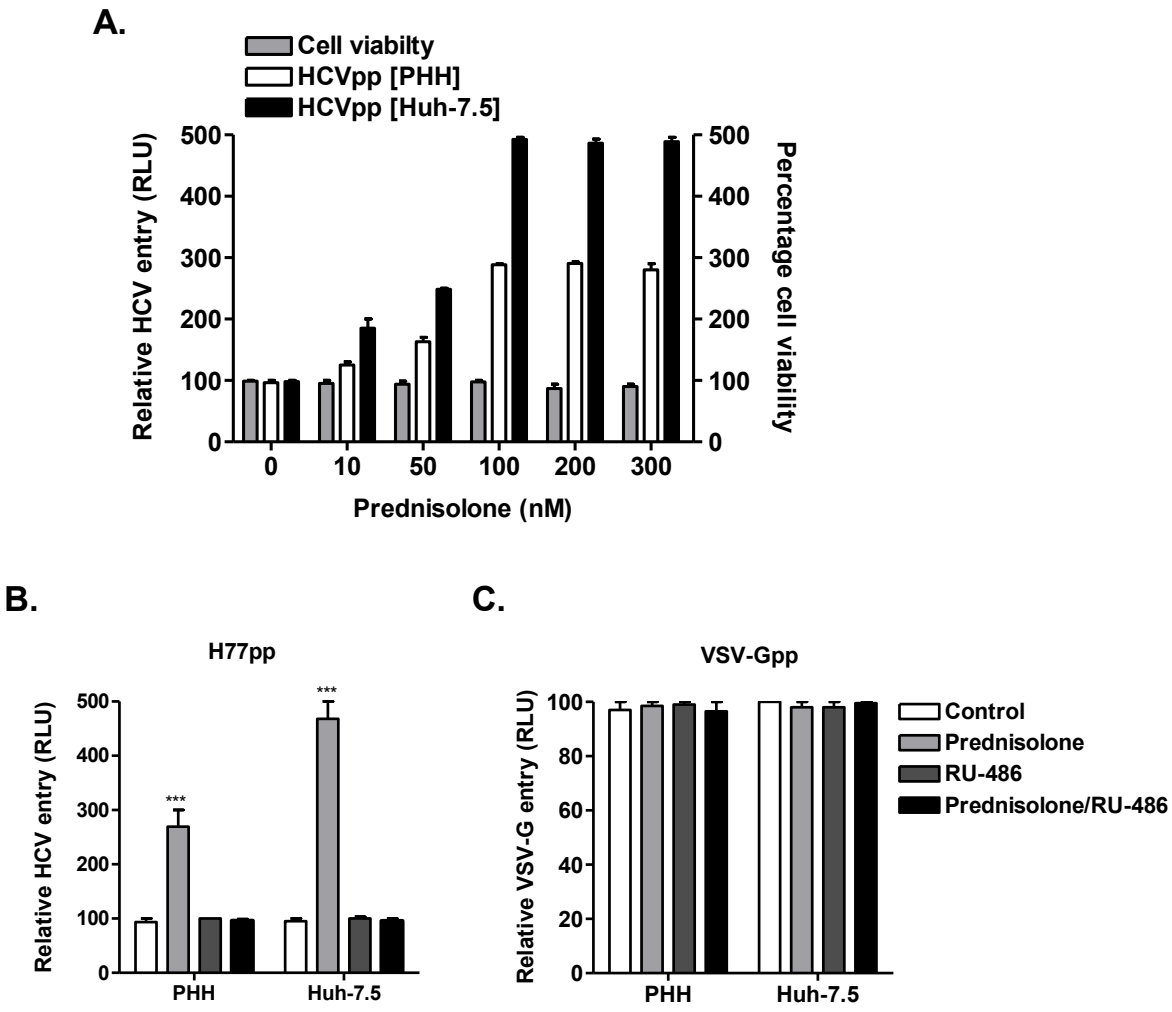

Figure 5-1. Prednisolone increases HCVpp infection of primary human hepatocytes and Huh-7.5 cells.

A. The effect of prednisolone on HCVpp entry and cell viability. PHHs were infected after 2 days in culture and Huh-7.5 cells after 1 day. Cells were treated with increasing concentrations of prednisolone overnight followed by infection with H77pp or the measurement of cell viability using an MTT assay. Infected cells were lysed after 72 hours and luciferase activity measured. Data is plotted relative to control untreated cells and presented as relative light units (RLU). **B-C.** Cells were treated overnight with prednisolone (100nM) or RU-486 (5µg/ml) and infected with H77 or VSV-Gpp. Infected cells were lysed after 72 hours and luciferase activity measured. Data is presented as virus infectivity relative to control untreated cells. H77pp infection of PHH was 7.0 x 10^4 and 2.4 x 10^5 RLUs in control and prednisolone treated cells respectively. For Huh-7.5 cells H77pp infection was 1.2 x 10^6 and 5.7 x 10^6 respectively. VSV-Gpp infection of both cell types was 2.3 x 10^7 RLUs and prednisolone treatment had no effect. *** P <0.001 (t test).

5 . 1.2 Prednisolone increases HCVcc replication.

There are conflicting reports regarding the effects of prednisolone on distinct phases of the virus lifecycle. For example a study by Ciesek et al reported that prednisolone enhanced HCV entry and reduced replication (76). In contrast, Henry and colleagues reported increased HCV replication as a result of prednisolone treatment (164). The discrepancies between these two studies could be the result of differences in Huh-7 clones and viral strains used; we aimed to expand on these studies by confirming our findings in PHHs. We studied the effects of prednisolone on HCV strain J6/JFH-1 replication in PHHs and Huh-7.5 cells. Prednisolone significantly increased HCVcc RNA levels in both cell types (Figure 5-2 A). To confirm a positive role for prednisolone in the viral replication cycle we studied the effect of prednisolone on HCV replicon RNA levels; which are genetic elements that replicate autonomously (20) and allow the study of genome replication without particle assembly. Cells expressing full length HCV JFH-1 and subgenomic (comprising the non-structural proteins NS3-NS5) replicons were treated overnight with prednisolone/RU-486 and HCV RNA levels measured by qRT-PCR. Prednisolone increased the levels of HCV RNA in both cell types (Figure 5–2 B), demonstrating that prednisolone acts on the entry and replication phases of the virus life cycle.

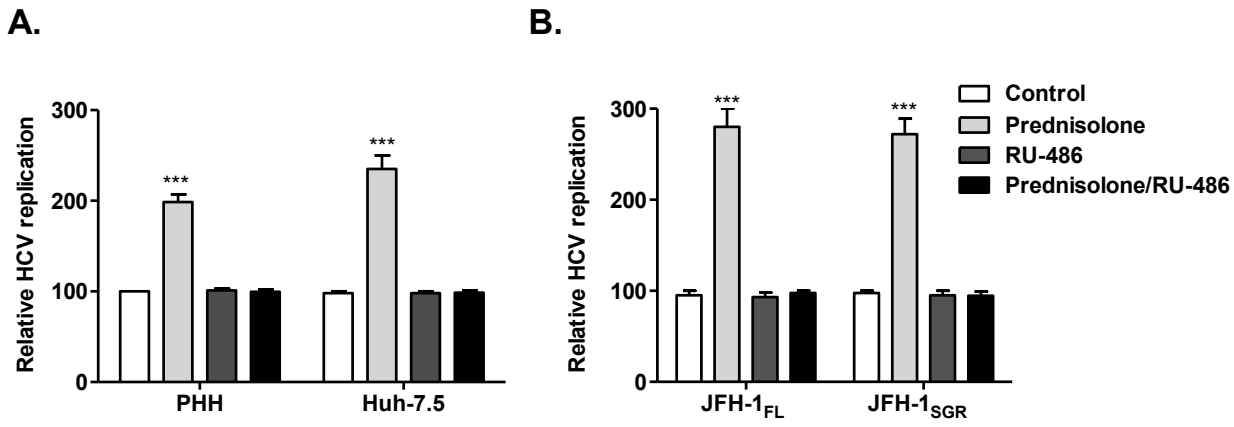

Figure 5-2. Prednisolone enhances HCVcc replication.

A. HCVcc replication in PHHs and Huh-7.5 cells. Cells were treated overnight with prednisolone (100nM), RU-486 (5µg/ml) or a combination of both compounds and infected with J6/JFH-1. Infection was analysed 72 hours later by qRT-PCR. Data represents HCV genomic burden relative to control untreated cells. PHHs contained 3.7 x 10^5 HCV RNA copies/10^4 cells and prednisolone treatment increased HCV RNA copy number to 7.1 x 10^5 RNA copies/10^4 cells. Huh-7.5 cells contained 1.6 x 10^6 and 4 x 10^6 HCV RNA copies in control and prednisolone treated cells respectively. **B.** Huh-7 cells expressing full length (JFH-1_{FL}) or sub-genomic (JFH-1_{SGR}) HCV replicons were treated with prednisolone or RU-486 overnight. Data represents HCV RNA levels relative to control untreated cells, where the RNA copy numbers for JFH-1_{FL} were 5.4 x 10^5 and 1.3 x 10^6 in control and prednisolone treated cells respectively. JFH-1_{SGR} cells contained 3.9 x 10^5 and 1.4 x 10^6 RNA copies in control and prednisolone treated cells respectively. ***P < 0.001 (t test).

5 . 1.3 The effect of prednisolone on cell-cell HCV transmission.

HCVcc infection can be quantified by staining for the viral expressed antigen NS5A that is distributed focally in an infected culture (225). We noted an increase in focal size in prednisolone treated cells infected with J6/JFH-1 and even though this phenotype was apparent in untreated cells it was more defined in treated cells (Figure 5–3 A). Larger focus sizes are generally indicative of enhanced cell-cell transmission or secondary infection of neighbouring cells. We quantified the differences in focus size by enumerating the number of infected cells per focus in treated and untreated cells. Focus size were classified as small (1-2 cells/focus); medium (3-15); large (16-40) and very large (41-100) (Figure 5-3 B). Prednisolone increased the frequency of large and very large foci; whereas RU-486 had no effect of the number of infected cells within each foci. Treatment of cells with both compounds reduced the frequency of large and very large foci to comparable levels seen in untreated cells, confirming a GR dependent effect (Figure 5–3 B). In prednisolone treated cells around 75% of infected cells resided in large or very large foci compared to 25% in untreated cells, suggesting increased cell-cell transmission.

We and others have reported that HCV can initiate infection by cell-free particle release and direct cell-cell contact dependent route of transmission (50, 401, 422). To examine whether prednisolone can increase cell-cell transmission, naive Huh-7.5 cells were pre-treated with prednisolone overnight followed by co-culture with J6/JFH-1 infected Huh-7.5 cells, 48 hours later cell-cell transmission from infected to naive cells was measured by flow cytometry quantification of NS5A antigen expressing cells.

Prednisolone enhanced HCV cell-cell transmission (Figure 5–3 C), consistent with our observation of increased focus size (Figure 5–3 B). RU-486 alone had no effect on virus transmission and ablated the effects of prednisolone (Figure 5-3 C). These data show that prednisolone may potentiate cell-cell HCV transmission; however, further studies are required to ascertain this as the efflux of CMFDA from the cells may be altered by prednisolone.

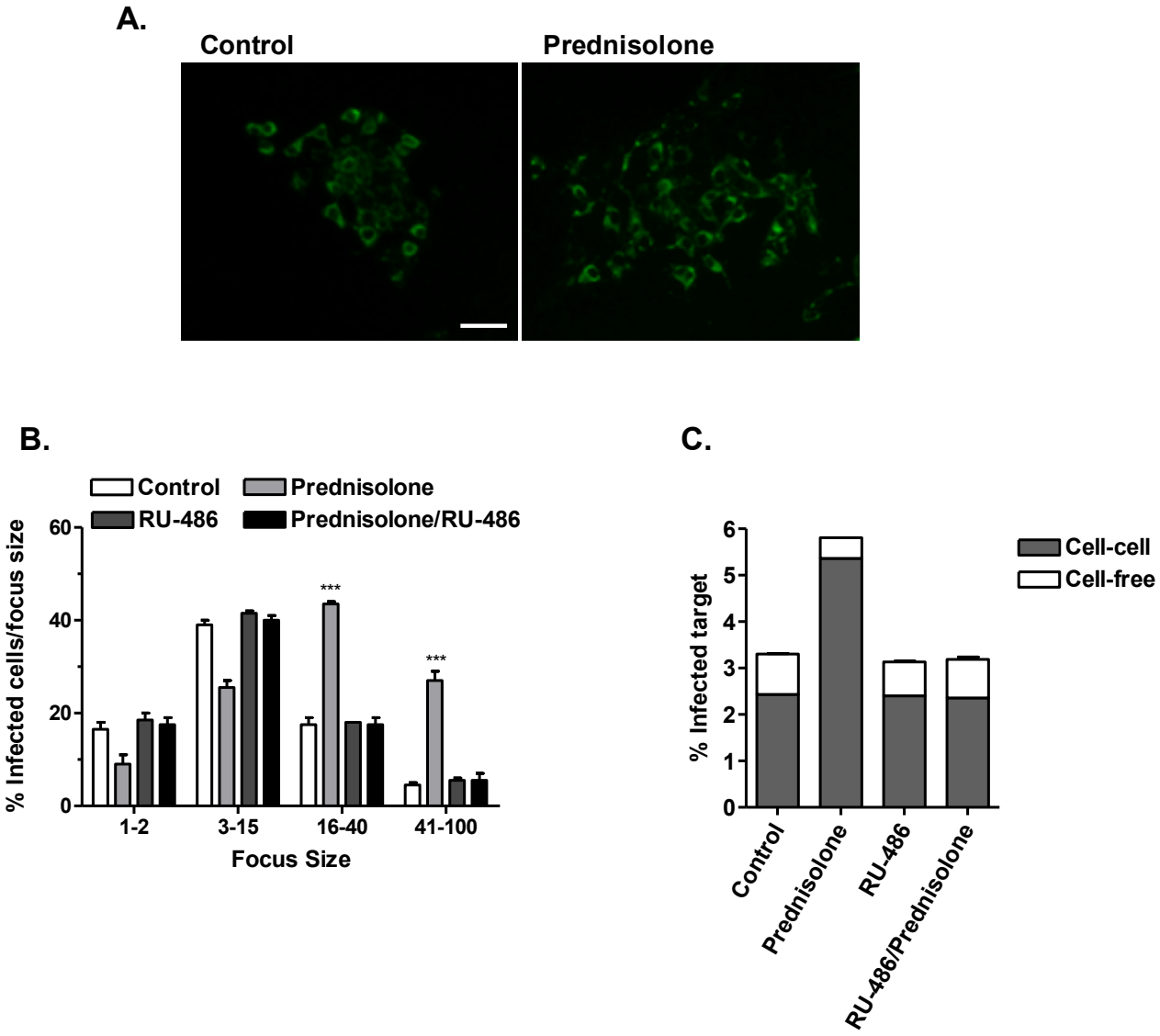

Figure 5-3. Evidence of HCV cell-cell transmission in prednisolone treated cells.

A. Huh-7.5 cells treated overnight with prednisolone (100nM) and infected with J6/JFH-1 for 48 hours. Images show foci formation in infected cells. Foci were detected by staining for HCV NS5A protein (green). Scale bar represents 20μm. **B.** Focus size was distributed across 4 categories according to the number of infected cells/focus (1-2, 3-15, 16-40 and 41-100). The % total of infected cells that is present within category is shown. 75% of infected cells resided in large or very large foci in prednisolone treated cells compared to 25% for RU-486 or control cells. **C.** Prednisolone enhances HCV cell-cell transmission; Huh-7.5 naive target cells were treated with prednisolone overnight and co-cultured in a 1:1 ratio with J6/JFH-1 infected producer cells labelled with CMFDA (80% of producer cells expressed NS5A). 48 hours later virus transmission from producer to target cells was measured using a flow cytometry based assay. Data represents 2 independent experiments. ***P = <0.001.

5 . 1.4 Prednisolone increases SR-BI and Occludin expression.

We previously reported that SR-BI over expression in hepatoma cells promoted HCV foci size (146) and enhanced cell-cell HCV transmission (50). This finding suggests that an increase in HCV receptor expression levels promotes HCV transmission. Our observation that prednisolone increased cell-cell transmission is reminiscent of the enhanced HCV transmission observed in cells transduced to over-express SR-BI reported by Grove et al (146), we therefore investigated the effects of prednisolone on HCV receptor expression levels. Western blot analysis demonstrated increased SR-BI and Occludin expression in PHHs and Huh-7.5 cells treated with prednisolone; in contrast CD81 and Claudin-1 expression levels were unaffected (Figure 5-4 A). In addition, flow cytometric staining showed increased SR-BI cell surface expression (Figure 5-4 B); unfortunately, due to the lack of antibodies recognising extracellular epitopes of Occludin we were unable to confirm its expression at the cell surface by flow cytometry.

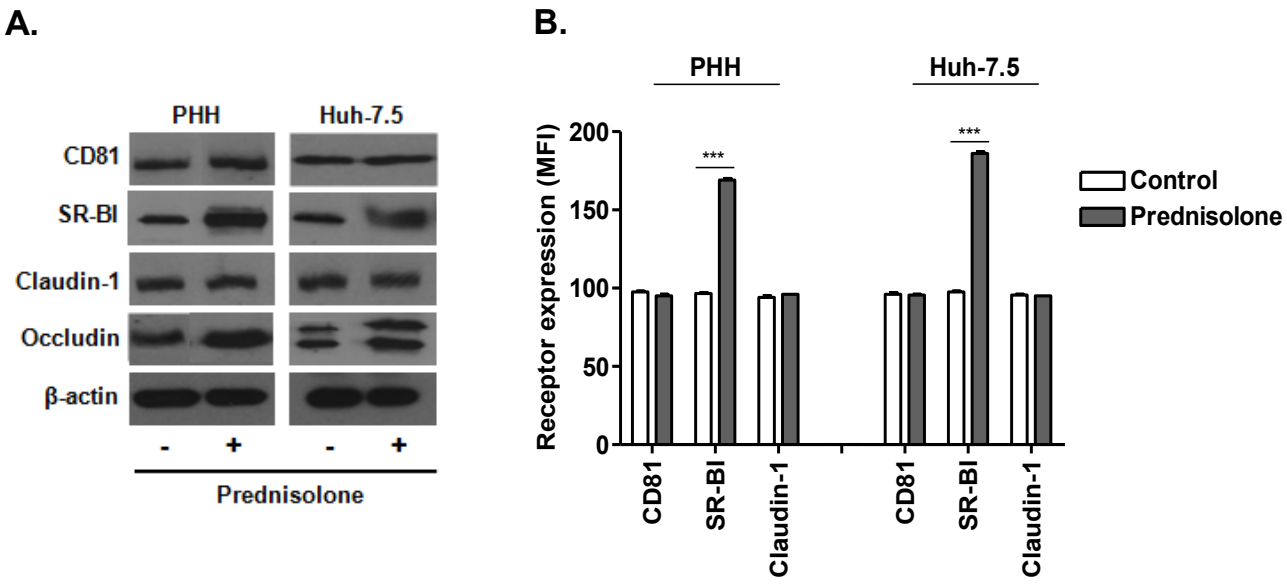

Figure 5-4. Prednisolone upregulates SR-BI and Occludin expression.

A. Western blot detection of HCV receptors in control and prednisolone (100nM overnight) treated PHHs and Huh-7.5 cells. **B.** Flow cytometric analysis of HCV receptor expression at the cell surface in control and prednisolone treated PHHs and Huh-7.5 cells. We do not have antibodies to detect Occludin at the cell surface and were unable to confirm its upregulation by flow cytometry. Data is presented as mean fluorescent intensity (MFI) from which an isotype specific control value was subtracted. ***P = <0.001.

5 . 1.5 Prednisolone enhanced HCV infection is SR-BI dependent.

We investigated whether prednisolone mediated increase in HCV infection is dependent on up-regulation of host factors SR-BI and Occludin. Firstly, we investigated the role of SR-BI using an anti-SR-BI neutralizing antibody and a small molecule inhibitor of SR-BI (ITX 5061) (389). ITX 5061 is a clinical stage small molecule compound that promotes HDL levels in animals and patients by targeting the SR-BI pathway. Recently ITX 5061 has entered clinical trials for its efficacy to inhibit HCV infection of the graft in patients undergoing liver transplantation. In vitro ITX 5061 is thought to inhibit HCV entry by blocking virus engagement of SR-BI. Prednisolone treated cells were infected with H77 or control VSV-Gpp and the effects of anti-SR-BI and ITX 5061 on virus infection evaluated. Both compounds reduced H77pp infection by almost 95% whereas VSV-Gpp infectivity was unaffected (Figure 5-5 A). Furthermore, we evaluated both compounds for their ability to reduce HCVcc infection of prednisolone treated cells and found similar results (Figure 5 -5 B).

We do not have neutralizing agents to study the role of Occludin in HCV infection; therefore to study HCV dependency on Occludin expression levels we transduced Huh-7.5 cells with GFP tagged Occludin via a TRIP lentivirus vector. Lentiviral transduction increased Occludin expression to comparable levels seen following prednisolone treatment (Figure 5-6 A). Confocal microscopy assessment of Occludin localization in transduced cells, showed increased staining at the plasma membrane with some evidence of intracellular staining, consistent with the pattern seen in prednisolone treated cells (Figure 5-6 B). HCVpp and HCVcc infection of

Huh-7.5 cells was unaffected by increased Occludin expression (Figure 5-6 C). In summary, we show that Occludin over expression does not affect HCVpp entry, indicating that the prednisolone mediated boost is SR-BI dependent.

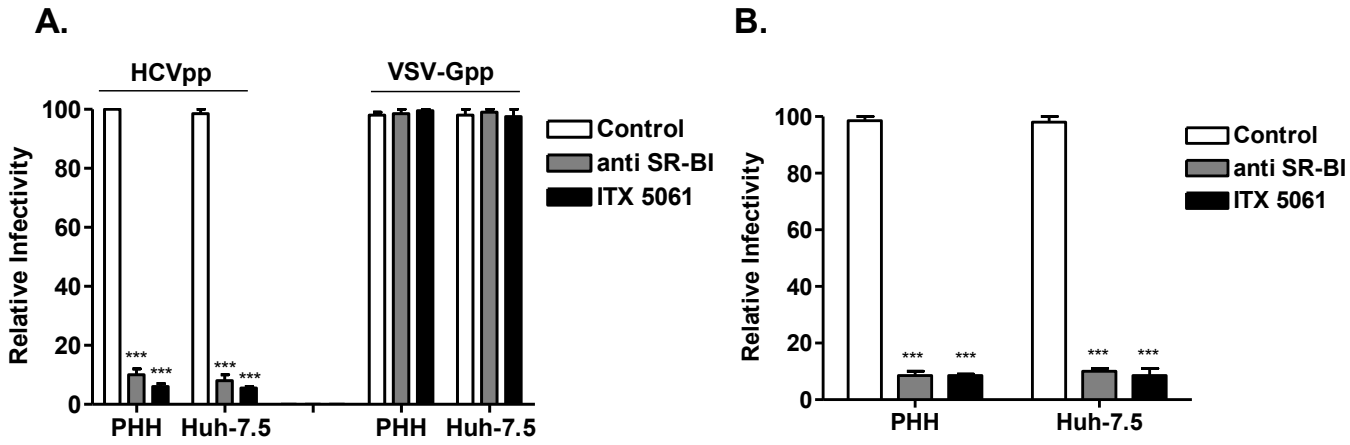

Figure 5-5. Prednisolone enhanced HCV entry is SR-BI dependent.

A. PHHs and Huh-7.5 cells treated with prednisolone (100nm overnight) were infected with H77 or VSV-Gpp in the presence of SR-BI inhibitors ITX 5061 (5μM) and anti SR-BI (5μg/ml). Virus infection is presented relative to control cells where the specific infectivity of H77pp was 2 x 10^5 and 1.6 x 10^6 relative light units (RLU) in PHHs and Huh-7.5 cells respectively. VSV-Gpp infection was 2.5 x 10^7 and 2.7 x 10^7 RLUs respectively for PHHs and Huh-7.5 cells. **B.** PHHs and Huh-7.5 cells treated with prednisolone were infected with HCVcc J6/JFH-1 in the presence of HCV entry inhibitors anti SR-BI and ITX 5061. Data represent HCV genomic copies and is presented relative to control cells. PHHs and Huh-7.5 cells contained 6.7 x 10^5 and 3.6 x 10^6 RNA copies/10^4 cells respectively. ***P = <0.001 (t test).

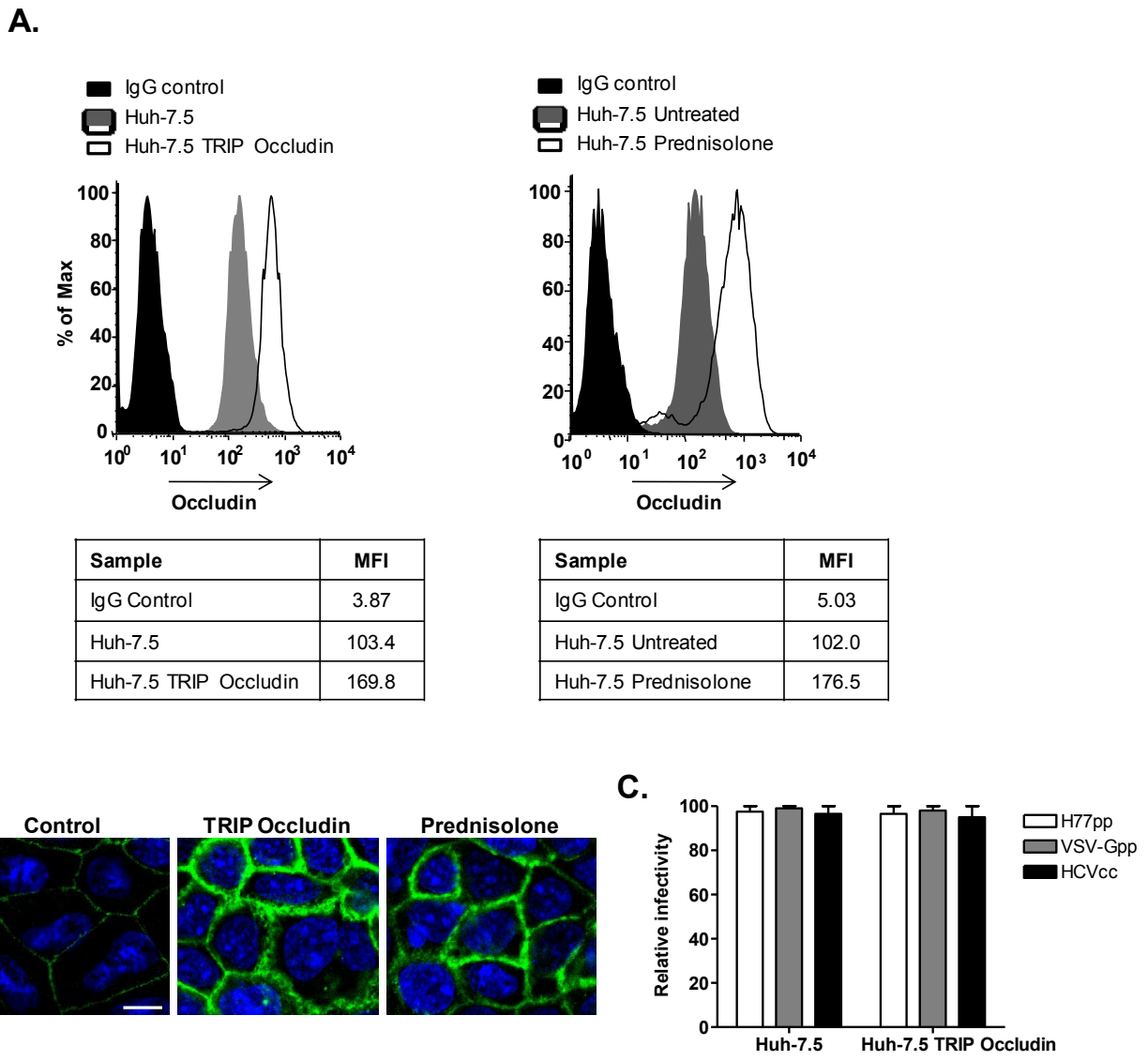

Sample	MFI
IgG Control	3.87
Huh-7.5	103.4
Huh-7.5 TRIP Occludin	169.8

Sample	MFI
IgG Control	5.03
Huh-7.5 Untreated	102.0
Huh-7.5 Prednisolone	176.5

Figure 5-6. The role of Occludin in prednisolone enhanced HCV infection.

A. Flow cytometric detection of Occludin in parental, TRIP and prednisolone treated Huh-7.5 cells. Data represents total Occludin expression in permeabilized cells. Tables show the mean fluorescent intensity (MFI) of Occludin and an isotype specific (IgG) control stain. **B.** Confocal images of Occludin (green) localization in Huh-7.5 cells, DAPI staining of the nucleus is shown in blue and the scale bar represents 20μm. **C.** HCV and VSV-Gpp infection of Huh-7.5 cells over expressing Occludin. Data is presented relative to parental Huh-7.5 cells. H77 and VSV-Gpp infection of cells was 1.0×10^6 and 2.3×10^7 relative light units (RLUs), respectively. HCVcc J6/JFH-1 infected cells contained 1.6×10^6 HCV RNA copies/10^4 cells.

5 . 1.6 The effects of prednisolone on pseudoparticles bearing diverse HCV glycoproteins.

We hypothesize that if SR-BI is the major receptor promoting HCV entry, then viruses with reduced sensitivity to prednisolone may infect independently of SR-BI. To this end, we measured the effect(s) of prednisolone on a range of HCVpp strains to infect PHHs and Huh-7.5 cells. We studied HCV glycoprotein clones from several patients; patient H (H77, H91A6) who has chronic HCV infection; patient S11 (S11c1, S11c3); patient S18 (S18c1, S18c2) and patient S28 (S28c1, S28c2 and S28c3) are all acutely infected. HCV glycoproteins from each patient were incorporated into the HCVpp system and screened for their ability to infect cells.

The majority of glycoprotein variants were sensitive to prednisolone treatment and showed an increased infection, albeit to varying levels (Figure 5-7 A). However, viruses expressing envelope glycoproteins H91A6 and S18c2 were resistant to prednisolone. Similar results were observed when cells were treated with dexamethasone an analogue of prednisolone (Figure 5-7 A). Furthermore, anti-SR-BI preferentially inhibited glycoprotein variants that were sensitive to prednisolone treatment, whilst having negligible effects on H91A6pp and S18c2pp entry (Figure 5-7 B). In summary, these data show that prednisolone enhances the entry of SR-BI dependent viral strains, lending further to an essential role for SR-BI expression levels in defining prednisolone enhancement of HCV entry.

A.

Virus	Prednisolone (nM)		Dexamethasone (nM)	
	PHH	Huh-7.5	PHH	Huh-7.5
H77	3	4	4	5
H91A6	0	0	0	0
S11c1	6	7	7	7
S11c3	5	6	4	5
S18c1	5	6	5	5
S18c2	1	1	1	1
S28c1	5	6	5	5
S28c2	2	2	1	2
S28c3	3	4	3	4
VSV-G	0	0	0	0

B.

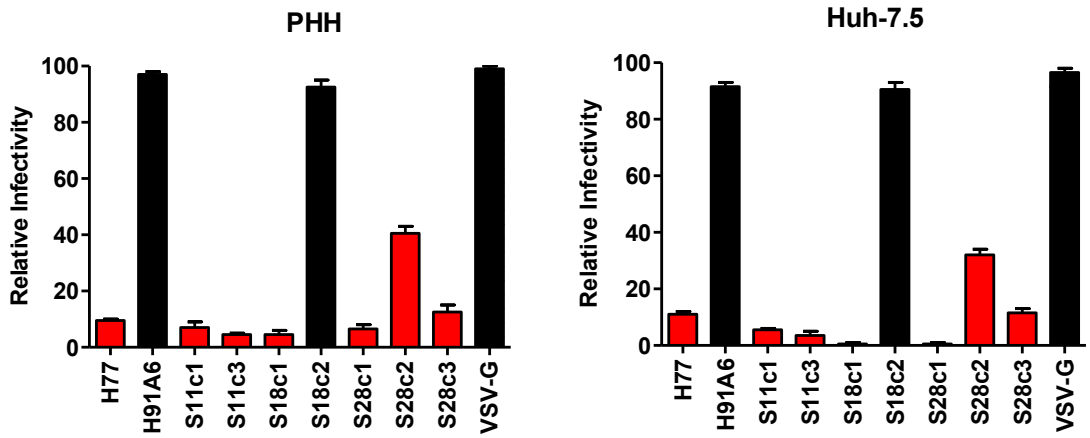

Figure 5-7. Diverse HCVpp sensitivity to prednisolone treatment.

A. The effects of prednisolone (100nM) and dexamethasone (100nM) overnight treatments on diverse HCVpp infection of PHHs and Huh-7.5 cells. Table shows the fold increase of HCVpp entry when cells were treated with the above compounds relative to untreated cells. Viruses highlighted in red demonstrated increased susceptibility to glucocorticoid treatment, whereas viruses highlighted in black showed a minimal boost effect. **B.** Anti-SR-BI (5µg/ml) neutralization of diverse HCVpp entry into PHHs and Huh-7.5 cells shows that HCVpp strains with reduced susceptibility (black bars) to glucocorticoid treatment were resistant to anti-SR-BI neutralization. Data is presented as HCVpp infectivity relative to control untreated cells.

5 . 1.7 Prednisolone enhances ITX 5061 neutralizing efficacy.

HCV infected patients are given steroid boluses as immune modulators immediately after liver transplantation which continues for up to 90 days to ensure immune tolerance of the new liver or graft (355). Since ITX 5061 is currently undergoing clinical trials as an HCV entry inhibitor in the liver transplant setting, we asked whether ITX 5061 function is altered in conjunction with prednisolone. We measured the levels of ITX 5061 required to neutralize HCVpp infection in the presence or absence of prednisolone treatment. As a control we evaluated the effect of prednisolone treatment on anti-CD81 monoclonal antibody neutralizing efficacy. ITX 5061 showed a dose-dependent inhibition of H77pp and S11c1pp infection with IC_{50} values of 0.8 and 1.1μM respectively, whereas in the presence of prednisolone ITX 5061 IC_{50} values were reduced to 0.3 and 0.5μM, respectively (Figure 5-8 A).

ITX 5061 had minimal effect on H91A6pp infection, consistent with our earlier observation of reduced SR-BI dependency (Figure 5-7 A). In contrast, prednisolone had no effect on the levels of anti-CD81 monoclonal antibody required to neutralize HCVpp strains (Figure 5-8 B). In summary, ITX 5061 is still effective to neutralize HCV infection in the presence of prednisolone. Furthermore, its neutralizing efficacy is enhanced by prednisolone treatment.

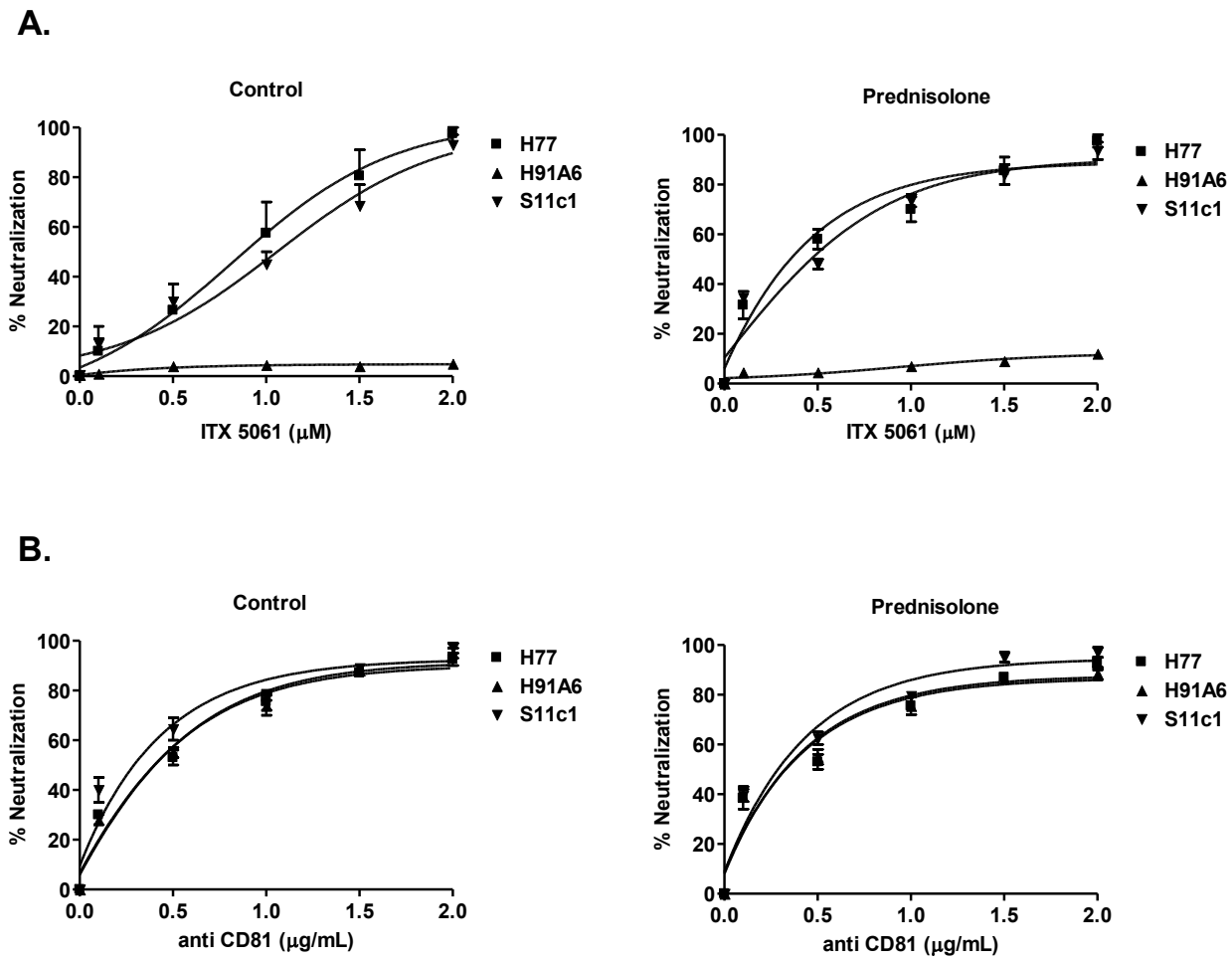

Figure 5-8. The effects of prednisolone on ITX 5061 efficacy.

A. ITX 5061 dose dependent neutralization of H77pp, H91A6pp and S11c1pp entry into Huh-7.5 cells. Cells were treated with prednisolone (100nM) overnight followed by treatment with increasing concentrations of ITX 5061 for 4 hours. Cells were infected with HCVpp strains and luciferase activity measured 72 hours later. The IC_{50} of ITX 5061 on H77pp infection was 0.8 ± 3 and 0.3 ± 1μM for control and prednisolone treated cells respectively. For S11c1pp ITX 5061 IC_{50} was 1.1 ± 4 and 0.5 ± 2μM in control and treated cells respectively. **B.** Anti-CD81 neutralization of H77pp, H91A6pp and S11c1pp entry in a dose dependent manner. Control and prednisolone cells were treated with anti-CD81 monoclonal antibody clone [2s131] for 4 hours followed by infection. Luciferase activity was determined 72 hours later. Data is presented as percentage neutralization. Anti-CD81 IC_{50} was 0.5 ± 2μg/ml irrespective of prednisolone treatment.

5 . 1.8 Heterogeneous SR-BI distribution in normal and HCV infected liver tissue.

Given our data showing the importance of SR-BI expression levels in HCV transmission in vitro we were interested to study SR-BI expression in the liver. Sequential paraffin embedded sections from normal and HCV infected livers were stained with a serial dilution of anti SR-BI monoclonal antibody to ascertain SR-BI expression levels across the parenchyma. Figure 5-9 shows representative images of sections stained with 1.0 and 0.06µg/ml dilutions of anti-SR-BI monoclonal antibody, where SR-BI is predominantly expressed on the sinusoidal endothelium consistent with published observations (341). Although there was a clear reduction in SR-BI staining with lower concentrations of monoclonal antibody, expression at the peri-portal and peri-septal regions of normal and HCV infected tissue respectively were visible, suggesting increased SR-BI expression in these regions (Figure 5-9). In addition, SR-BI expression in HCV infected liver was strong compared to normal liver (Figure 5-9), suggesting altered SR-BI expression during chronic HCV infection.

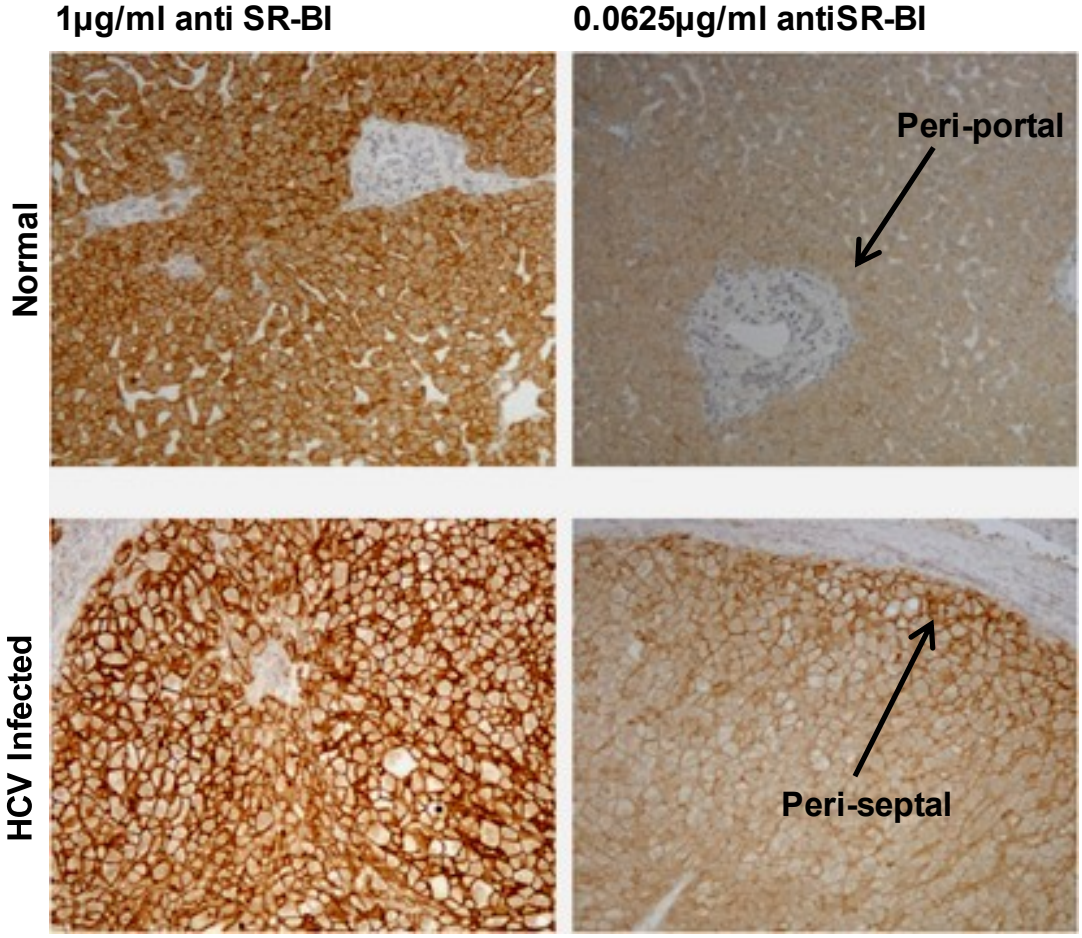

Figure 5-9. Immunohistochemical staining of SR-BI in normal and HCV infected liver tissue.

Representative image of SR-BI expression in normal and HCV infected livers (5 cases in each category) using two concentrations of anti SR-BI monoclonal antibody (x100). Arrows indicate enriched sites of SR-BI expression around peri-portal areas in normal liver and peri-septal areas of HCV infected liver.

5 . 1.9 The effects of glucocorticoids on SR-BI distribution in vivo.

To investigate whether glucocorticoid treatment alters SR-BI expression and distribution in the liver, we stained liver biopsies collected at defined times post transplant liver for SR-BI expression. Table 5-1 shows the patient history of and collection times of biopsies studied. Biopsies collected during liver reperfusion (time 0) before the patients were immunosuppressed, 2 weeks post liver transplantation when patients were in receipt of immunosuppression, and 12 months post liver transplantation, when immunosuppression was no longer administered, were studied. Biopsies (n=5 patients) from each time point were co-stained for von Willebrand factor (vWF) which is expressed on the sinusoidal endothelium and SR-BI which is expressed on hepatocytes and the sinusoidal endothelium. vWF enables us to distinguish between hepatocyte and sinusoidal SR-BI expression (Figure 5-10). At time 0 and 2 weeks post transplantation SR-BI was expressed on the sinusoidal endothelium and hepatocytes, however, by 12 months post transplantation SR-BI was predominantly expressed on the sinusoidal endothelium with minor hepatocellular staining (Figure 5-10). These data show hepatocyte SR-BI expression in biopsies from the reperfusion (time 0) and immunosuppressive (2 weeks) periods, suggesting that SR-BI distribution during initial stages after liver transplantation may promote HCV infection.

Patient ID	Diagnosis	Time 0	2 Weeks	12 months
1	PBC/ALD	No steroids	Prednisolone (20mg/day)	No steroids
2	AIH	No steroids	Prednisolone (20mg/day)	No steroids
3	NASH	No steroids	Prednisolone (20mg/day)	No steroids
4	PBC	No steroids	Prednisolone (20mg/day)	No steroids
5	ALD	No steroids	Prednisolone (20mg/day)	No steroids

Table 5-1. List of biopsies used in this study.

Biopsies (n=5) were taken at the reperfusion stage (time 0) before steroid treatment, 2 weeks post liver transplantation (steroid treatment) and 12 months later (no steroid treatment). Table also shows the disease aetiology of all patients; biopsies from HCV infected patients were excluded from the study to avoid any bias which may have resulted from virus infection. PBC; Primary Billiary Cirrhosis, ALD; Alcoholic Liver Disease, AIH; Auto Immune Hepatitis, and NASH; Non-Alcoholic Steatohepatitis.

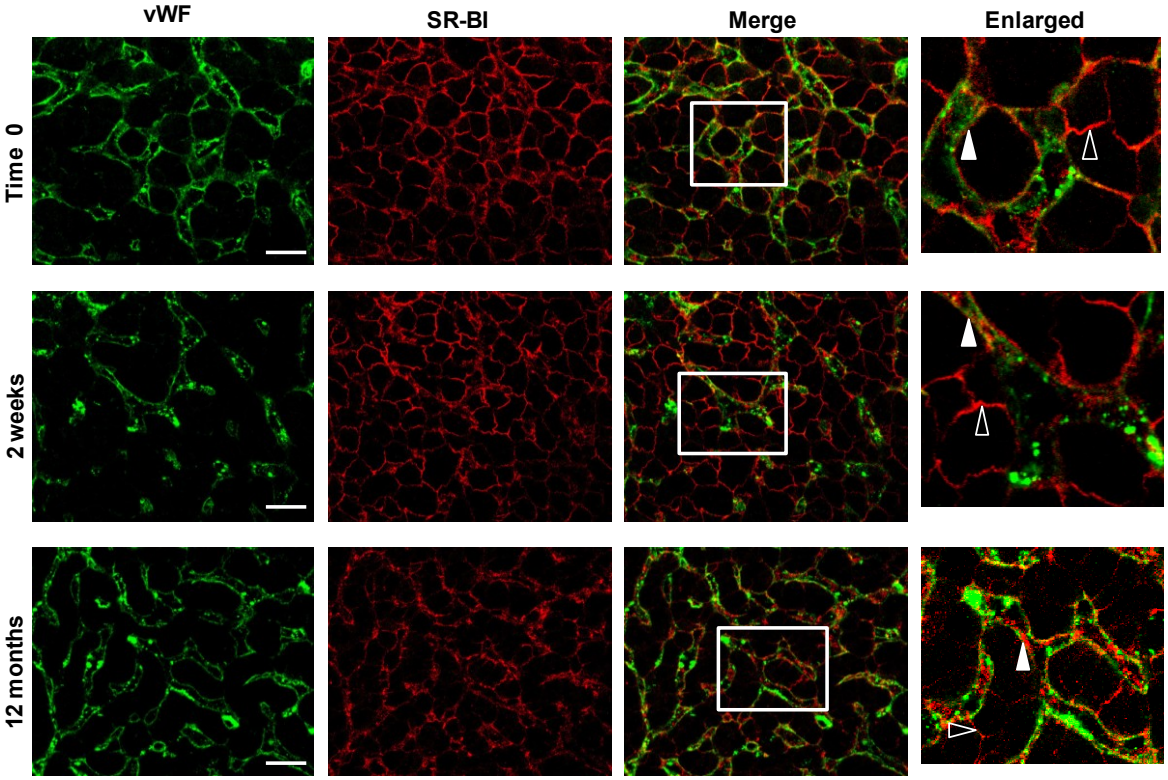

Figure 5-10. SR-BI distribution in specimens from liver transplant patients in receipt of glucocorticoid therapy.

Representative confocal images of SR-BI expression in biopsies obtained from 5 liver transplant patients before (time 0), during (2 weeks) and after (12 months) glucocorticoid treatment. Liver tissue at each time point was co-stained for the endothelial marker von Willebrand factor (vWF) (green) and SR-BI (red). Boxes indicate the area from which the enlarged images were taken. Hepatocyte (open arrow heads) and sinusoid (closed arrow heads) SR-BI staining is shown. Scale bar represents 20μm.

5 . 1.10 Hypoxia increases SR-BI expression in vitro.

In normal liver tissue SR-BI is predominantly expressed at the sinusoidal endothelium with minimal hepatocyte expression (341) and is therefore reflective of the 12 month biopsy. Our in vitro findings demonstrate a role for GR signaling in promoting SR-BI expression and we anticipated that increased hepatocyte SR-BI expression would be found in the 2 week biopsies only due to glucocorticoid treatment. Nevertheless, our observation of increased SR-BI expression on hepatocytes in time 0 specimens suggests that factors associated with graft reperfusion affects SR-BI expression. The liver sustains injury from ischemic preservation and reperfusion leading to parenchymal changes during the post-operative period. Ischemia reperfusion injury (IRI) is associated with increased serum aspartate transaminase (AST) levels. Normal AST levels ranges between 5-43 IU/L, AST levels of <400 IU/L 1 day post liver transplantation is associated with mild IRI and day 1 AST of >2000 IU/L is associated with severe IRI (283, 315). The majority of specimens studied, were from patients with severe IRI in the early post-operative period due to elevated AST (Table 5-2).

Patient ID	AST level (IU/L)
1	449 (day 1)
2	2188 (day 1)
3	3403 (day 1)
4	2210 (day 2)
5	987 (day 1)

Table 5-2. AST levels in the early post operative period.

IRI is associated with hypoxia due to diminished oxygen levels (59). To ascertain whether hypoxia modulate SR-BI expression; we quantified SR-BI expression in Huh-7.5 and liver sinusoidal endothelial cells (LSEC) grown under hypoxia and normoxia. Hypoxia increased SR-BI expression in Huh-7.5 and LSEC's (Figure 5-11). Interestingly, cultured Huh-7.5's showed higher levels of SR-BI expression compared to LSEC's; in contrast, SR-BI is predominantly expressed on the sinusoidal endothelium in vivo (341) suggesting that its expression on LSEC's is affected by isolation from the liver tissue. These data demonstrate that hypoxia promotes SR-BI expression levels in cells representing hepatocytes (Huh-7.5) and the sinusoidal endothelium (LSEC). Therefore, the increased hepatocyte SR-BI noted in the time 0 biopsy may be indicative of a cellular response to hypoxia.

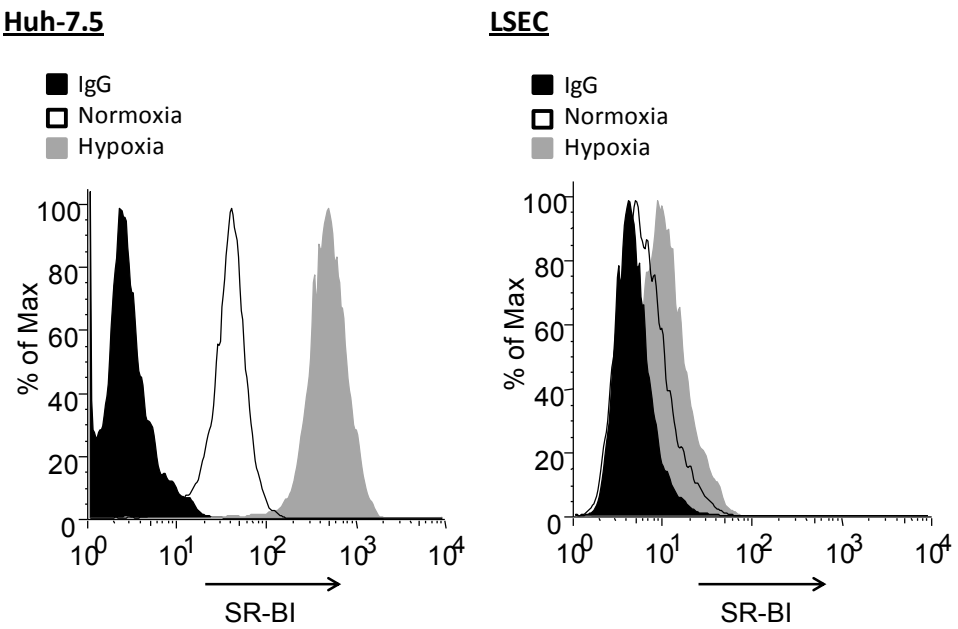

Sample	MFI
IgG Control	8.0
Normoxia	109.8
Hypoxia	186.4

Sample	MFI
IgG Control	10.2
Normoxia	37.8
Hypoxia	83.4

Figure 5-11. Hypoxia upregulates SR-BI expression in vitro.

Huh-7.5 and LSEC's were grown in hypoxic or normoxic conditions overnight and SR-BI expression monitored by flow cytometry. Histograms show SR-BI expression at the cell surface. Tables show the mean fluorescent intensities (MFI) of SR-BI and an isotype matched (IgG) control antibody stain.

5 . 1.11 Increased cholesterol production in prednisolone treated cells.

Studies have shown increased cholesterol levels in prednisolone treated transplant patients (42, 133, 150, 330). SR-BI has been reported to regulate various aspects of cholesterol metabolism; including the removal of unesterified cholesterol from the periphery leading to altered cholesterol distribution in the plasma membrane (243). Together, these data suggest a link between SR-BI, prednisolone and cellular cholesterol levels. We investigated whether prednisolone altered cellular cholesterol levels in vitro. Prednisolone significantly increased total cholesterol levels in PHHs and Huh-7.5 cells by 2-fold (Figure 5-12 A). Moreover, HCVcc infection increased PHH and Huh-7.5 cholesterol to comparable levels observed in prednisolone treated cells (Figure 5-12 B).

Since HCV infection increases cellular cholesterol, we hypothesized that virus infection may affect glucocorticoid receptor (GR) signaling. The glucocorticoid receptor resides in the cytoplasm in its dormant phase, steroid engagement of GR induces a relocalization to nucleus where it acts as a transcription factor regulating many target genes including cytokine production and cholesterol synthesis (Figure 5-13) (408). We studied whether HCV infection modulates GR signalling. Prednisolone treatment of Huh-7.5 cells induced a nuclear localization of GR and this was blocked by co-treatment with RU-486 (Figure 5-12 C). Furthermore, we observed nuclear GR expression in HCV infected Huh-7.5 cells compared to mock cells; interestingly, RU-486 treatment had no effect on GR localization in infected cells suggesting that HCV modulation of GR signaling occurs via unknown mechanism(s) (Figure 5-12 C). In summary, we show that HCV

infection perturbs GR signaling leading to increased cholesterol production. These findings may help to shed light on increased steatosis seen in HCV infected individuals.

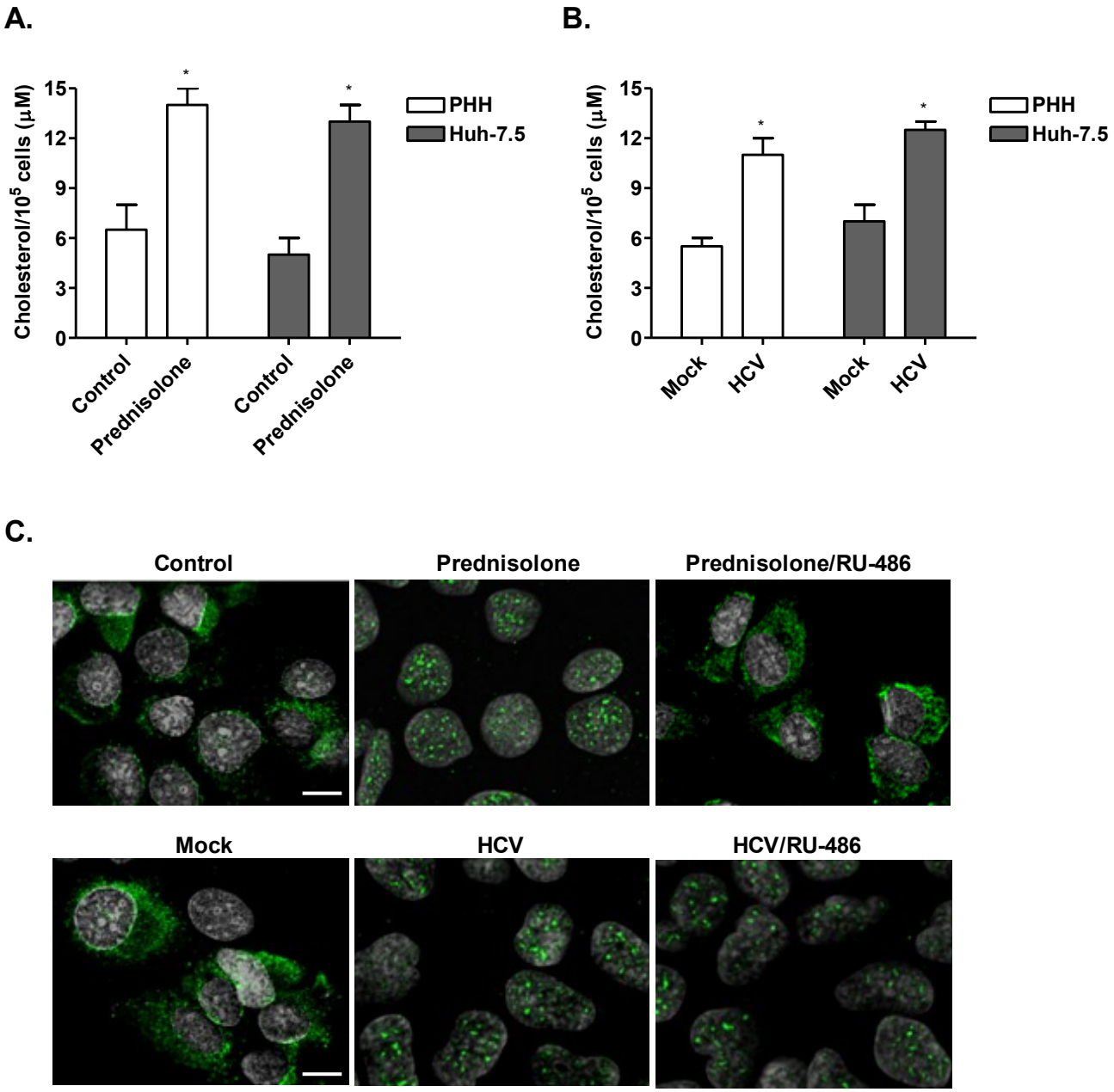

Figure 5-12. The effects of HCV infection on cholesterol efflux and glucocorticoid receptor signalling.

A. Prednisolone treatment (100nM) overnight increases cholesterol levels in PHHs and Huh-7.5 cells. Data is shown as the µM of cholesterol/10^5 cells. **B.** HCVcc J6/JFH-1 infection increases cellular cholesterol levels. Cells were infected for 48 hours and cholesterol measured. The infected cells contained 2.2 x 10^5 and 1.6 x 10^6 HCV RNA copies/10^5 cells for PHHs and Huh-7.5 cells respectively. **C.** Glucocorticoid receptor (green) localization in prednisolone treated and J6/JFH-1 infected Huh-7.5 cells, DAPI staining is depicted in grey and the scale bar represents 20µm. The infected cells were treated with RU-486 (5µg/ml) and contained 8 x 10^5 RNA copies/10^5 cells.

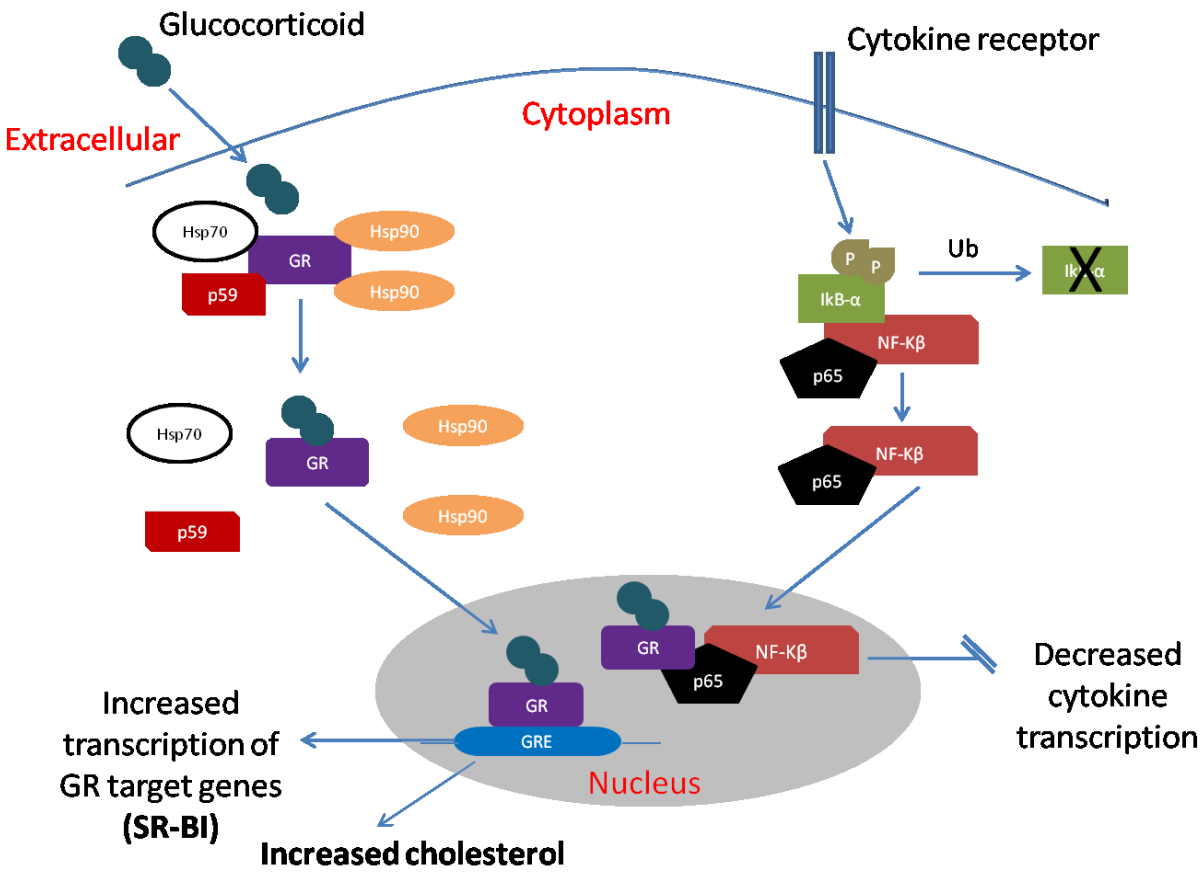

Figure 5-13. Schematic outline of the glucocorticoid receptor signalling.

5.2 Discussion

Prednisolone treatment of PHHs and Huh-7.5 cells increased their susceptibility to HCVpp and HCVcc infection in a SR-BI dependent manner. This was associated with increased GR signaling and cholesterol production. Moreover, SR-BI expression in the liver is heterogeneous suggesting a rate limiting role for this receptor in the HCV lifecycle.

A previous report suggested that enhanced HCV entry by prednisolone was mediated through SR-BI and Occludin (76). Although have we confirmed an increase in Occludin expression by prednisolone, over expression of Occludin in Huh-7.5 cells did not confer an increased susceptibility to HCV infection. In contrast, HCVpp strains demonstrating reduced SR-BI dependency were resistant to the effects of prednisolone. Furthermore, anti-SR-BI neutralizing antibody and HCV entry inhibitor ITX 5061 ablated HCV infection of prednisolone treated cells by up to 95%, suggesting a role for SR-BI in the prednisolone mediated effects. Studies have shown that the Occludin gene contains a glucocorticoid response element (GRE) explaining the increase in Occludin expression following steroid treatment (125, 153). There are no studies showing a GRE promoter region in SR-BI; however, SR-BI plays an integral role in the steroidogenic pathway by providing cholesterol substrate necessary for steroid synthesis (55, 397).

Glucocorticoids have been reported to increase epithelial Caco-2 cell polarity (43) and to protect the integrity of the blood brain barrier against the permeating effects of proinflammatory cytokines (124). These data suggest a role for glucocorticoids in the maintenance and regulation of epithelial polarity. We have previously shown that polarity restricts HCV

entry into HepG2 hepatoma cells (260). It is therefore interesting, that prednisolone would increase virus entry whilst protecting polarity. Since Huh-7.5 cells do not polarize (259), HepG2 cells were treated with prednisolone and the polarity index determined. Prednisolone had no effect on HepG2 polarity; in contrast prednisolone restricted the flux of 70kDa FITC dextran across a Caco2 monolayer, suggesting differential regulatory mechanism(s) of epithelial and hepatic polarity (data not shown).

Henry et al studied the effects of glucocorticoids on HCV replication and observed a decrease in virus replication in vitro. In contrast, glucocorticoid treatment increased viral RNA levels in vivo (164). The authors attributed this to a dampening of the immune system by steroid treatment and thus the effects were indirect. Our findings shed further light on the potential mechanistic of glucocorticoids enhanced HCV replication. We noted an increase in HCV RNA levels induced by prednisolone treatment of Huh-7.5 cells in the absence of a host immune response. This effect was coupled with increased GR signalling; GR activity is associated with enhanced lipid metabolism (reviewed in (302)), and lipidomic profiling of HCV infected cells show the perturbation of lipid species believed to play an important role in virus replication and assembly (90). Together, these data suggest that GR signaling modulates the lipid profile of infected cells which may in turn augment viral RNA replication.

Our laboratory previously reported that HCV can transmit in cell-cell contact dependent manner. Although all the viral receptors are necessary for this to occur, this mode of transmission is highly dependent on SR-BI expression levels (50). HCV strains with limited SR-BI dependence show

minimal cell-cell spread and disseminate predominantly via the cell-free route. These data support our current observation that prednisolone increased the infectivity of HCVpp expressing glycoproteins that were readily neutralized by anti SR-BI and ITX5061, whereas strains H91A6 and S18c2 that were insensitive to neutralizing agents targeting SR-BI were resistant to prednisolone. These findings support a model where strains that are highly dependent on SR-BI will transmit preferentially in a cell-cell fashion; furthermore, glucocorticoid treatment may favour the transmission of such viruses in the newly transplanted liver.

We observed heterogeneous SR-BI staining in the liver, with enriched areas adjacent to peri-portal areas which border the peripheral blood flow. Oxygen is supplied to the liver via the blood; our data showing enriched SR-BI near the blood flow suggest a putative role for oxygen levels in regulating SR-BI expression. HCV circulates in the peripheral blood before coming into contact with hepatocytes. Our observation of enriched SR-BI expression at peri-portal regions supports a model where HCV interacts with receptor complexes that are highly expressed on the basolateral hepatocellular membrane adjacent to the peripheral blood flow. HCV infects the liver allograft in 100% of cases concomitant with a rapid decline in peripheral HCV RNA levels in the first few days after liver transplantation (263). Several groups have monitored HCV replication kinetics in the liver immediately after transplantation and found an increase in HCV viral load as early as 12 hours post graft reperfusion, reaching pre-transplantation levels within 4 days in the majority of individuals and exceeding these levels by up to two logs by 12 weeks (75, 135, 325, 331, 333). Recent findings from our laboratory show two distinct patterns of HCV replication

kinetics in the post transplant setting; typified by a prolonged decline in HCV RNA levels followed by a late rebound 14 days later or an initial decline and rapid rebound 48 hours after liver transplant (Ian Rowe, personal communication). The increase in HCV viremia post-transplant suggests that viral replication is efficient and represents de novo infection of new target cells. Recently, Mensa and colleagues (263), studied SR-BI expression levels in the liver post liver transplantation and showed an association between increased SR-BI expression in the reperfusion biopsy and reduced peripheral HCV RNA levels in the first 24 hours following liver transplantation, suggesting that SR-BI levels modulate early infection kinetics.

SR-BI is a scavenger receptor molecule that mediates binding and lipid transfer from different classes of lipoproteins accounting for its role in cholesterol metabolism including the removal of peripheral unesterified cholesterol, steroidogenesis, bile acid synthesis and secretion (200). In vivo HCV particles associate with lipoproteins and cholesterol is a central component of lipoproteins suggesting an essential role in the virus life cycle. We noted increased cholesterol levels in HCV infected and prednisolone treated cells. Of note, SR-BI regulates the bidirectional flux of free cholesterol between lipoproteins and cells resulting in increased cellular cholesterol mass (191, 298). Increased cholesterol levels during HCV infection and a rapid decline in peripheral HCV RNA levels post-reperfusion suggest that enhanced SR-BI scavenging activity increases the uptake of HCV particles in the new allograft. Furthermore, steroid bolus is associated with increased cholesterol levels in transplant patients (150, 330), suggesting the intriguing possibility that glucocorticoids exacerbate

HCV infection by increasing cholesterol levels resulting in enhanced SR-BI expression and activity that is essential for cholesterol regulation. We noted reduced hepatocyte SR-BI distribution in biopsies from post transplant patients after the glucocorticoid administration period (12 months later) compared to biopsies taken at time 0 (graft reperfusion), and 2 weeks after liver transplantation which demonstrated a mixture of hepatocyte and sinusoidal endothelium SR-BI localization. At time 0 patients were steroid free and during the first 3 months patients were in receipt of immunosuppression therapy to prevent graft rejection by the immune system. These findings show comparable hepatocyte SR-BI distribution before and during glucocorticoid therapy representing a paradox as we anticipated increased hepatocyte SR-BI distribution in the steroid treatment period only. These data suggest that the outcome of HCV infection post liver transplant is multifactorial. For example, ischemia reperfusion injury (IRI); liver tissue damage caused by blood reperfusion during transplant has been linked to recurrent HCV disease (reviewed in (252)). In the previous chapter, we showed that hypoxia a key regulator of IRI promotes HCV replication suggesting that injury sustained during organ transplant potentiates HCV infection. Furthermore, it is likely that IRI upregulates hepatocyte SR-BI expression to comparable levels seen in biopsies from immunosuppressed patients. To date, there are no studies showing a hypoxia responsive region in the SR-BI genome; however, CD36 another member of the family of scavenger receptors contains a functional HIF-1 binding site which is upregulated during hypoxia (278) suggesting the possibility that the SR-BI promoter region contains a hypoxia responsive element (HRE). We show that hypoxia increases SR-BI

expression in Huh-7.5 and LSEC's to confirm a putative HRE in the SR-BI promoter.

Our observation that HCV infection perturbs GR signaling is intriguing and provides a potential explanation for hepatic steatosis observed in HCV patients (reviewed in, (175)). Glucocorticoid treatment precipitates steatohepatitis by increasing insulin resistance, diabetes and hypertriglycerridemia, resulting in severe scarring of the liver (96, 114). The mechanism underlying HCV perturbation of GR activity is unclear as GR antagonist RU-486 inhibited GR transcriptional activity in prednisolone treated cells but not HCV infected cells. A recent study by Sun et al showed increased GR transcriptional activity is associated with HIF-1α stabilization in oligodendrocytes (388), highlighting the possibility that HCV stabilization of HIF-1α modulates GR signaling events which in turn favours increased HCV replication kinetics. These findings provide avenues for future studies looking at the effects of HIF-1 inhibitors on GR transcriptional activity. In summary, these studies provide unique insights into the mechanisms of glucocorticoids induced exacerbation of HCV infection of the newly transplanted liver.

What are the clinical implications and outlook for these findings?

The kinetics of HCV infection is exacerbated post liver transplantation, culminating in graft failure within 5 years. Our findings suggest that high glucocorticoid doses may account for the increased viral load after liver transplant. Although the factors governing accelerated HCV re-infection of the liver are likely to be multiple, including host immune response, viral genotype and hypoxia. Reports have shown that non-steroid based

immunosuppression reduced the severity of recurrent hepatitis post transplant, suggesting a prominent role for glucocorticoids in augmenting HCV infection (76). However, steroid boli are continually prescribed as they provide the most potent way of combating immune intolerance leading to graft rejection. As such, a delicate balance is required to control rejection and viremia, on one hand lowering the steroid dose may reduce HCV infection but increases the likelihood of graft failure or rejection. Non-steroid based therapy such as Cyclosporin A may provide an alternative for the current regimen. HCV infection in the absence of glucocorticoids perturbs glucocorticoid receptor activity indicating that virus infection is capable of augmenting this pathway to potentially promote its lifecycle. In this regard, non-steroid immune modulators in conjunction with glucocorticoid receptor antagonists may prove beneficial to HCV transplanted patients. Nevertheless, the exact nature of glucocorticoid enhanced HCV infection or perturbation of hepatocyte biology requires further investigation which may in turn aid in the development of improved immunosuppressive drugs for HCV infected patients.

6. CONCLUDING REMARKS

6.1 HCV infection of primary human hepatocytes and hepatoma cells.

Significant progress has been made in the development of in vitro models to study the HCV lifecycle over the last two decades. As such, key aspects of HCV entry, replication, assembly and release have been reported. Our understanding of the HCV lifecycle has been shaped through the use of hepatocellular carcinoma cell lines that enable robust virus entry and replication. However, it is becoming clear that hepatoma cell lines such as Huh-7.5 cells may not reflect hepatocytes in vivo. Huh-7.5 cells fail to polarize in culture and do not induce an interferon response to virus infection (259, 386). It is believed that cultured PHHs represent a closely matched physiological model of hepatocytes in vivo. Nevertheless, there are few reports of HCV infection of PHHs; this is in part due to difficulties in obtaining them and their short lifespan in culture. To date, it is not known whether HCV infection of hepatoma cell lines is comparable to PHHs. In this study, we employed the HCVpp and HCVcc systems to investigate virus entry and replication respectively, in hepatoma and PHHs. We have demonstrated that PHHs support HCV entry and replication which was optimal at day 2 post seeding consistent with the formation of cellular contacts that increases HCV receptor expression at the cell surface. We were able to show comparable HCVpp entry kinetics in PHHs and hepatoma cell lines in the absence of hepatoma cell division. In vivo, hepatocytes are quiescent (393), importantly cultured PHHs maintains this phenotype. In contrast, hepatoma cells divide in culture; we provide the first evidence that cell division increases HCVpp luciferase signals which is regularly

reported as authentic virus entry. Our data suggest the need for caution when interpreting absolute HCVpp luciferase activity in dividing hepatoma cells. We propose a model whereby HCV infection of hepatocytes in vivo is restricted to a small percentage of hepatocytes, supported by Liang and colleagues who showed that only a small proportion of hepatocytes express HCV antigens in vivo, this may in part be due to a lack of cell division (221). Reagents that inactivate cell division resulted in comparable HCVpp entry in both cell types. Interestingly, H77pp and S11c1pp were highly stable on Huh-7.5 cells compared to PHHs in the absence of cell division. To date there are no reports on the effects of HCVpp stability in determining infection kinetics. Or data provides novel insights into cellular and viral factors that determine the outcome of HCVpp entry.

Importantly, PHHs supported HCVcc replication and released comparable infectious virus particles to Huh-7.5 cells. HCVcc strains demonstrated variable replication in PHHs from multiple donors. In contrast, donor variation did not affect HCVpp entry. These data suggest that inherent donor differences including variabilities in interferon response to virus infection affect HCV replication.

Overall, we have shown that in the absence of cell division, hepatoma cells represent a closely matched physiological model for HCV infection of hepatocytes. Our findings shed light on the mechanistic driving increased HCVpp luciferase activity in hepatoma cells and validate their use as robust in vitro models to study HCV infection.

6.2 HCV induced hepatocellular injury

We showed that HCV infection and glycoprotein expression modulate tight junction protein expression and localization resulting in reduced polarity and increased migration. Both phenotypes are associated with intrahepatic cholestasis and HCC malignancy (9, 166). Indeed, HCV infection is associated with cholestatic liver disease and HCC (115, 277). The role of HCV in the carcinogenic process is thought to be indirect as HCV is non-cytopathic (49). We show the promotion of EMT transcription factors Snail and Twist associated with HIF-1α stabilization and increased expression of its target genes VEGF and TGFβ. Neutralizing antibodies targeting TGFβ and not VEGF ablated Snail and Twist expression and restored polarity to demonstrate a HIF-1α driven TGFβ process.

During liver repair the liver reverts to an early developmental stage reminiscent of EMT induced by cytokines and growth factors. Growth factors associated with liver repair includes VEGF and TGFβ (393). Most EMT cells undergo MET to signal the end of the repair process enabling the liver to return to its normal homeostasis (72). Our data suggest that HCV infection induces liver injury via HIF-1α stabilization resulting in an inflammatory response including VEGF and TGFβ that primes the livers repair mechanisms including fibrogenesis induced by stellate cells. In a healthy liver, hepatocytes are highly ordered and compact; thus, they are likely to restrict virus transmission. HCV could become opportunistic during the repair process when some cells de-differentiate. Indeed, a recent study showed that a mesenchymal phenotype increases cellular permissiveness to HCV replication, consistent with previous data showing that HCV perturbation hepatocellular metabolism favours the viral lifecycle (71, 90).

Studies of oncogenic Epstein Barr virus (EBV) showed that EBV induced EMT does not promote the virus lifecycle per se but contributes to the metastatic nature of a tumour (169, 239). HIF-1α and TGFβ can directly induce EMT which is associated with carcinogenesis (184, 303, 433). Our data showing increased migration and virus replication in HIF-1α stabilized cells suggest a dual role for this transcription factor in the HCV lifecycle and hepatocellular migration. It is likely that HCV modulates the liver repair mechanisms by prolonging MET signaling resulting in sustained EMT which promotes HCC pathogenesis. These data suggest that HCV injures the liver via indirect means consistent with our observation that HCV gyclopropteins does not interact with Occludin. Furthermore, our study suggests that a cellular response to virus infection promotes signalling pathways that drives HCC. These data provide insights into the effects of HCV infection on hepatocyte biology. Figure 6-1 shows HIF-1α signaling induced by HCV infection.

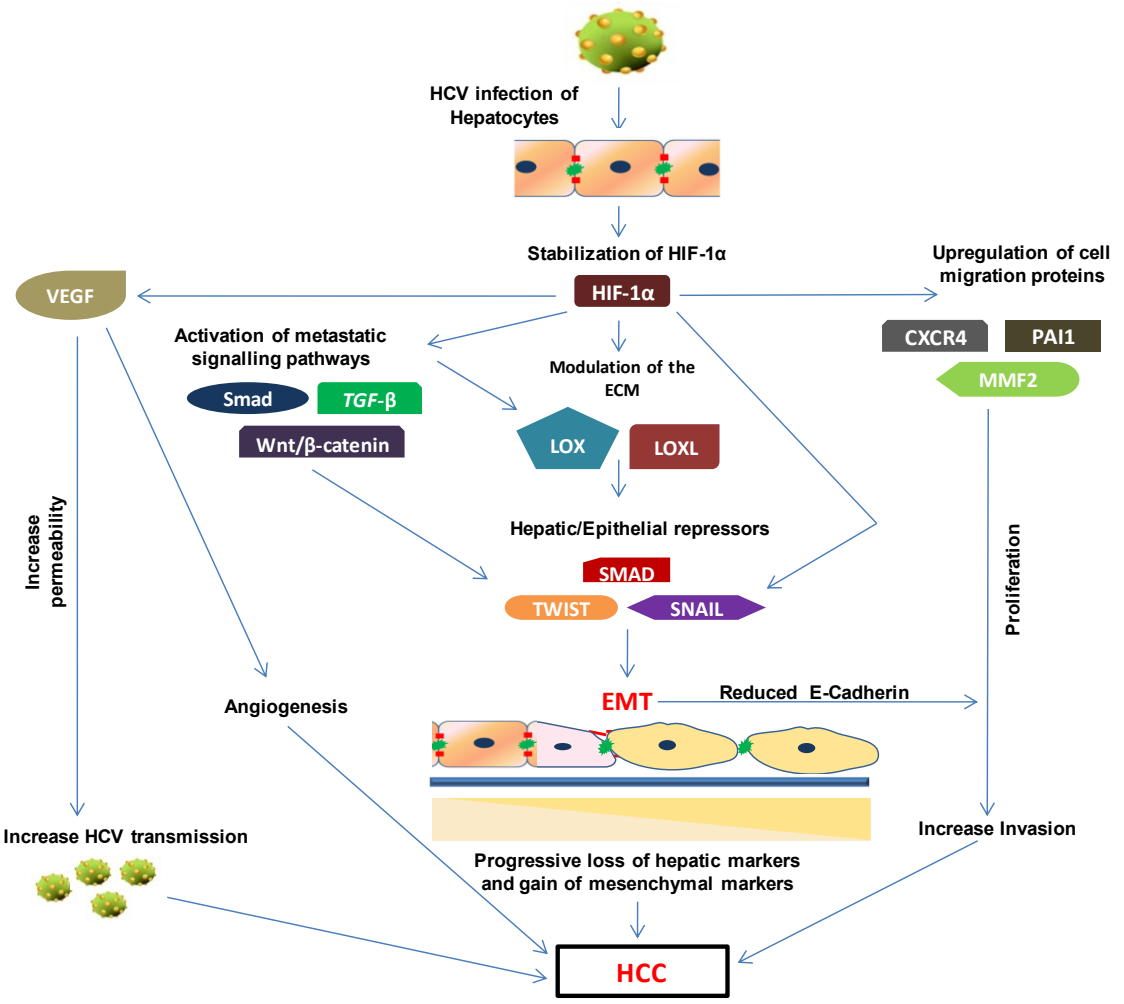

Figure 6-1. The cellular response to HCV infection.

HCV infection of hepatocytes stabilizes HIF-1α which induces the expression of many genes including those implicated in angiogenesis and HCV transmission (VEGF, TGFβ); proteins involved in metastatic signalling (TGFβ, Smad, Wnt/β catenin); extracellular matrix lysyl oxidase proteins (LOX and LOXL); EMT transcription factors (SNAIL and TWIST); regulators of cell proliferation and invasion, (chemokine receptor 4 [CXCR4], matrix metalloproteinase [MMF2] and the cell morphology protein [PaI1]. These HIF-1α driven pathways may act in concert or independently to drive HCC pathogenesis.

6.3 Glucocorticoid receptor transcription and HCV infection.

In order to prevent rejection of the new graft, HCV infected patients are treated with glucocorticoids post liver transplantation. It has been reported that glucocorticoids enhances HCV infection offering insights into rapid reinfection of the new allograft culminating in liver failure a few years post transplantation (77, 325). However, there are limited studies addressing the mechanisms of glucocorticoid induced exacerbation of HCV entry. We have shown that the glucocorticoid prednisolone enhanced HCV entry into hepatoma and PHHs by upregulating the viral receptor SR-BI. Glucocorticoid actions are mediated through the glucocorticoid receptor (GR) expressed in the cytoplasm. When activated by glucocorticoids, GR functions as a transcription factor for various genes including NF-ќB signalling and cholesterol production (2). We demonstrate that HCV infection perturbs GR localization concomitant with elevated cholesterol levels, increased HCV entry, replication and transmission. These data offers further insights into cellular pathways modulated by HCV to further its lifecycle and potentiate liver injury.

We studied liver biopsies from transplant patients taken before, during and after glucocorticoid treatment for SR-BI expression and localization. SR-BI demonstrated increased hepatocyte distribution in biopsies taken at graft reperfusion prior to glucocorticoid treatment and during the treatment period. In contrast, biopsies taken after glucocorticoid treatment showed a predominant sinusoidal endothelial SR-BI expression pattern. It is believed that hepatocyte expressed forms of HCV receptors in vivo potentiate HCV entry. Our data showing increased hepatocyte SR-BI expression prior to steroid treatment suggest that multiple factors in vivo may potentiate HCV

reinfection of the transplant liver. Graft reperfusion is associated with elevated AST resulting in IRI. In addition, IRI is regulated by HIF-1α suggesting the intriguing possibility that HIF-1α plays a role in virus uptake during the transplant setting (87). One study has shown that GR activity is regulated by HIF-1α (215), indicating that HCV stabilization of HIF-1α may prime GR dependent pathways resulting in a dampened immune response and increased viral receptor expression that favours HCV uptake and transmission. Furthermore, Kodama and colleagues have shown that GR transcriptional activity up-regulates HIF-1α dependent genes through an association with the transactivational domain of HIF-1α (195). Together, these data suggest that both transcriptional factors positively regulate each other in an HCV inflamed liver and will ultimately dictate the course of HCV pathogenesis. GR signaling is also associated with steatosis and insulin resistance (96) and similar traits have been reported in a significant percentage of HCV related liver disease (14, 351). Our observation that HCV infection modulates GR signaling suggests a role for GR is driving HCV associated steatosis.

Taken together, our findings validate the use of hepatoma cell lines as in vitro tools to study HCV infection. We provide insights on the mechanisms of HCV induced injury of the liver. HCV infection perturbs liver functions via HIF-1α and GR transcription activity. Both pathways de-regulate genes involved in metabolism, cell proliferation, cholesterol production, immune regulation, insulin resistance and hepatic carcinogenesis. In doing so, HCV primes the hepatic environment to favour virus replication and transmission. A detailed understanding of HCV pathology is required for the development of anti-virals and the prevention of HCV related liver

injury. We show that HIF-1α inhibitors neutralize the effects of virus infection on hepatocyte biology accompanied by reduced virus replication. HIF-1α inhibitors may therefore represent a novel therapeutic for HCV induced HCC. In addition, we show that GR antagonist RU-486 ablated the effects of GR transcription on HCV entry and hepatocyte biology offering hope for the use of GR antagonists to treat HCV related steatosis.

7. BIBLIOGRAPHY

1. **Acloque, H., M. S. Adams, K. Fishwick, M. Bronner-Fraser, and M. A. Nieto.** 2009. Epithelial-mesenchymal transitions: the importance of changing cell state in development and disease. J Clin Invest **119:**1438-49.
2. **Adcock, I. M., and G. Caramori.** 2001. Cross-talk between pro-inflammatory transcription factors and glucocorticoids. Immunol Cell Biol **79:**376-84.
3. **Agnello, V., G. Abel, M. Elfahal, G. B. Knight, and Q. X. Zhang.** 1999. Hepatitis C virus and other Flaviviridae viruses enter cells via low density lipoprotein receptor. Proceedings of the National Academy of Sciences of the United States of America **96:**12766-12771.
4. **Aijaz, S., M. S. Balda, and K. Matter.** 2006. Tight junctions: molecular architecture and function. Int Rev Cytol **248:**261-98.
5. **Alen, M. M., S. J. Kaptein, T. De Burghgraeve, J. Balzarini, J. Neyts, and D. Schols.** 2009. Antiviral activity of carbohydrate-binding agents and the role of DC-SIGN in dengue virus infection. Virology **387:**67-75.
6. **Alter, H. J., P. V. Holland, A. G. Morrow, R. H. Purcell, S. M. Feinstone, and Y. Moritsugu.** 1975. Clinical and serological analysis of transfusion-associated hepatitis. Lancet **2:**838-41.
7. **Alter, H. J., P. V. Holland, R. H. Purcell, J. J. Lander, S. M. Feinstone, A. G. Morrow, and P. J. Schmidt.** 1972. Posttransfusion hepatitis after exclusion of commercial and hepatitis-B antigen-positive donors. Ann Intern Med **77:**691-9.
8. **Aly, H. H., K. Watashi, M. Hijikata, H. Kaneko, Y. Takada, H. Egawa, S. Uemoto, and K. Shimotohno.** 2007. Serum-derived hepatitis C virus infectivity in interferon regulatory factor-7-suppressed human primary hepatocytes. J Hepatol **46:**26-36.
9. **Anderson, J. M.** 1996. Leaky junctions and cholestasis: a tight correlation. Gastroenterology **110:**1662-5.
10. **Andre, P., F. Komurian-Pradel, S. Deforges, M. Perret, J. L. Berland, M. Sodoyer, S. Pol, C. Brechot, G. Paranhos-Baccala, and V. Lotteau.** 2002. Characterization of low- and very-low-density hepatitis C virus RNA-containing particles. J Virol **76:**6919-28.
11. **Angelow, S., R. Ahlstrom, and A. S. Yu.** 2008. Biology of claudins. Am J Physiol Renal Physiol **295:**F867-76.
12. **Appel, N., M. Zayas, S. Miller, J. Krijnse-Locker, T. Schaller, P. Friebe, S. Kallis, U. Engel, and R. Bartenschlager.** 2008. Essential role of domain III of nonstructural protein 5A for hepatitis C virus infectious particle assembly. PLoS Pathog **4:**e1000035.
13. **Ashfaq, U. A., T. Javed, S. Rehman, Z. Nawaz, and S. Riazuddin.** 2011. An overview of HCV molecular biology, replication and immune responses. Virol J **8:**161.
14. **Asselah, T., L. Rubbia-Brandt, P. Marcellin, and F. Negro.** 2006. Steatosis in chronic hepatitis C: why does it really matter? Gut **55:**123-30.
15. **Babitt, J., B. Trigatti, A. Rigotti, E. J. Smart, R. G. Anderson, S. Xu, and M. Krieger.** 1997. Murine SR-BI, a high density lipoprotein receptor that mediates selective lipid uptake, is N-glycosylated and fatty acylated and colocalizes with plasma membrane caveolae. J Biol Chem **272:**13242-9.
16. **Balda, M. S., and K. Matter.** 2000. Transmembrane proteins of tight junctions. Semin Cell Dev Biol **11:**281-9.
17. **Balfe, P., and J. A. McKeating.** 2009. The complexities of hepatitis C virus entry. J Hepatol **51:**609-11.
18. **Balogun, M. A., M. E. Ramsay, L. M. Hesketh, N. Andrews, K. P. Osborne, N. J. Gay, and P. Morgan-Capner.** 2002. The prevalence of hepatitis C in England and Wales. J Infect **45:**219-26.

19. **Bankwitz, D., E. Steinmann, J. Bitzegeio, S. Ciesek, M. Friesland, E. Herrmann, M. B. Zeisel, T. F. Baumert, Z. Y. Keck, S. K. Foung, E. I. Pecheur, and T. Pietschmann.** 2010. Hepatitis C virus hypervariable region 1 modulates receptor interactions, conceals the CD81 binding site, and protects conserved neutralizing epitopes. J Virol **84:**5751-63.
20. **Bartenschlager, R., and V. Lohmann.** 2001. Novel cell culture systems for the hepatitis C virus. Antiviral Res **52:**1-17.
21. **Barth, H., C. Schafer, M. I. Adah, R. J. Linhardt, E. Depla, H. E. Blum, and T. F. Baumert.** 2002. Cellular binding of Hepatitis C virus envelope glycoprotein E2 requires cell surface heparan sulfate proteoglycans. Hepatology **36:**214a-214a.
22. **Barth, H., E. K. Schnober, F. Zhang, R. J. Linhardt, E. Depla, B. Boson, F. L. Cosset, A. H. Patel, H. E. Blum, and T. F. Baumert.** 2006. Viral and cellular determinants of the hepatitis C virus envelope-heparan sulfate interaction. J Virol **80:**10579-90.
23. **Bartosch, B., J. Dubuisson, and F. L. Cosset.** 2003. Infectious hepatitis C virus pseudo-particles containing functional E1-E2 envelope protein complexes. Journal of Experimental Medicine **197:**633-642.
24. **Bartosch, B., J. Dubuisson, and F. L. Cosset.** 2003. Infectious hepatitis C virus pseudo-particles containing functional E1-E2 envelope protein complexes. J Exp Med **197:**633-42.
25. **Bartosch, B., R. Thimme, H. E. Blum, and F. Zoulim.** 2009. Hepatitis C virus-induced hepatocarcinogenesis. J Hepatol **51:**810-20.
26. **Bartosch, B., A. Vitelli, C. Granier, C. Goujon, J. Dubuisson, S. Pascale, E. Scarselli, R. Cortese, A. Nicosia, and F. L. Cosset.** 2003. Cell entry of hepatitis C virus requires a set of co-receptors that include the CD81 tetraspanin and the SR-B1 scavenger receptor. J Biol Chem **278:**41624-30.
27. **Bartsch, H., and J. Nair.** 2004. Oxidative stress and lipid peroxidation-derived DNA-lesions in inflammation driven carcinogenesis. Cancer Detect Prev **28:**385-91.
28. **Battaglia, S., N. Benzoubir, S. Nobilet, P. Charneau, D. Samuel, A. L. Zignego, A. Atfi, C. Brechot, and M. F. Bourgeade.** 2009. Liver cancer-derived hepatitis C virus core proteins shift TGF-beta responses from tumor suppression to epithelial-mesenchymal transition. PLoS ONE **4:**e4355.
29. **Behrens, S. E., L. Tomei, and R. De Francesco.** 1996. Identification and properties of the RNA-dependent RNA polymerase of hepatitis C virus. EMBO J **15:**12-22.
30. **Benedicto, I., F. Molina-Jimenez, O. Barreiro, A. Madonado-Rodriguez, J. Prieto, R. Moreno-Otero, R. Aldabe, M. Lopez-Cabrera, and P. L. Majano.** 2008. Hepatitis C virus envelope components alter localization of hepatocyte tight junction-associated proteins and promote occludin retention in the endoplasmic reticulum. Hepatology **48:**1044-1053.
31. **Benedicto, I., F. Molina-Jimenez, B. Bartosch, F. L. Cosset, D. Lavillette, J. Prieto, R. Moreno-Otero, A. Valenzuela-Fernandez, R. Aldabe, M. Lopez-Cabrera, and P. L. Majano.** 2009. The tight junction-associated protein occludin is required for a postbinding step in hepatitis C virus entry and infection. J Virol **83:**8012-20.
32. **Berditchevski, F.** 2001. Complexes of tetraspanins with integrins: more than meets the eye. J Cell Sci **114:**4143-51.
33. **Berenguer, M., V. Aguilera, M. Prieto, F. San Juan, J. M. Rayon, S. Benlloch, and J. Berenguer.** 2006. Significant improvement in the outcome of HCV-infected transplant recipients by avoiding rapid steroid tapering and potent induction immunosuppression. J Hepatol **44:**717-22.
34. **Bernfield, M., M. Gotte, P. W. Park, O. Reizes, M. L. Fitzgerald, J. Lincecum, and M. Zako.** 1999. Functions of cell surface heparan sulfate proteoglycans. Annu Rev Biochem **68:**729-77.

35. **Bismuth, H.** 1982. Surgical anatomy and anatomical surgery of the liver. World J Surg **6:**3-9.
36. **Blackard, J. T., M. Kang, K. E. Sherman, M. J. Koziel, M. G. Peters, and R. T. Chung.** 2006. Effects of HCV treatment on cytokine expression during HCV/HIV coinfection. Journal of interferon & cytokine research : the official journal of the International Society for Interferon and Cytokine Research **26:**834-8.
37. **Blackham, S., A. Baillie, F. Al-Hababi, K. Remlinger, S. You, R. Hamatake, and M. J. McGarvey.** 2010. Gene expression profiling indicates the roles of host oxidative stress, apoptosis, lipid metabolism, and intracellular transport genes in the replication of hepatitis C virus. J Virol **84:**5404-14.
38. **Blanchard, E., S. Belouzard, L. Goueslain, T. Wakita, J. Dubuisson, C. Wychowski, and Y. Rouille.** 2006. Hepatitis C virus entry depends on clathrin-mediated endocytosis. J Virol **80:**6964-72.
39. **Blight, K. J., A. A. Kolykhalov, and C. M. Rice.** 2000. Efficient initiation of HCV RNA replication in cell culture. Science **290:**1972-1974.
40. **Blight, K. J., J. A. McKeating, J. Marcotrigiano, and C. M. Rice.** 2003. Efficient replication of hepatitis C virus genotype 1a RNAs in cell culture. J Virol **77:**3181-90.
41. **Blight, K. J., J. A. McKeating, and C. M. Rice.** 2002. Highly permissive cell lines for subgenomic and genomic hepatitis C virus RNA replication. J Virol **76:**13001-14.
42. **Boers, M., M. T. Nurmohamed, C. J. Doelman, L. R. Lard, A. C. Verhoeven, A. E. Voskuyl, T. W. Huizinga, R. J. van de Stadt, B. A. Dijkmans, and S. van der Linden.** 2003. Influence of glucocorticoids and disease activity on total and high density lipoprotein cholesterol in patients with rheumatoid arthritis. Ann Rheum Dis **62:**842-5.
43. **Boivin, M. A., D. Ye, J. C. Kennedy, R. Al-Sadi, C. Shepela, and T. Y. Ma.** 2007. Mechanism of glucocorticoid regulation of the intestinal tight junction barrier. Am J Physiol Gastrointest Liver Physiol **292:**G590-8.
44. **Boudreau, H. E., S. U. Emerson, A. Korzeniowska, M. A. Jendrysik, and T. L. Leto.** 2009. Hepatitis C virus (HCV) proteins induce NADPH oxidase 4 expression in a transforming growth factor beta-dependent manner: a new contributor to HCV-induced oxidative stress. J Virol **83:**12934-46.
45. **Bowen, D. G., and C. M. Walker.** 2005. Adaptive immune responses in acute and chronic hepatitis C virus infection. Nature **436:**946-52.
46. **Braet, F., J. Riches, W. Geerts, K. A. Jahn, E. Wisse, and P. Frederik.** 2009. Three-dimensional organization of fenestrae labyrinths in liver sinusoidal endothelial cells. Liver Int **29:**603-13.
47. **Branch, A. D., D. D. Stump, J. A. Gutierrez, F. Eng, and J. L. Walewski.** 2005. The hepatitis C virus alternate reading frame (ARF) and its family of novel products: the alternate reading frame protein/F-protein, the double-frameshift protein, and others. Semin Liver Dis **25:**105-17.
48. **Brazzoli, M., A. Bianchi, S. Filippini, A. Weiner, Q. Zhu, M. Pizza, and S. Crotta.** 2008. CD81 is a central regulator of cellular events required for hepatitis C virus infection of human hepatocytes. J Virol **82:**8316-29.
49. **Brillanti, S., M. Foli, S. Gaiani, C. Masci, M. Miglioli, and L. Barbara.** 1993. Persistent hepatitis C viraemia without liver disease. Lancet **341:**464-5.
50. **Brimacombe, C. L., J. Grove, L. W. Meredith, K. Hu, A. J. Syder, M. V. Flores, J. M. Timpe, S. E. Krieger, T. F. Baumert, T. L. Tellinghuisen, F. Wong-Staal, P. Balfe, and J. A. McKeating.** 2011. Neutralizing antibody-resistant hepatitis C virus cell-to-cell transmission. J Virol **85:**596-605.

51. **Buhler, S., and R. Bartenschlager.** 2011. [Molecular mechanisms of hepatitis C virus (HCV) replication - implications for the development of antiviral drugs]. Z Gastroenterol **49:**836-44.
52. **Burgel, B., M. Friesland, A. Koch, M. P. Manns, H. Wedemeyer, K. Weissenborn, W. J. Schulz-Schaeffer, T. Pietschmann, E. Steinmann, and S. Ciesek.** 2011. Hepatitis C virus enters human peripheral neuroblastoma cells - evidence for extra-hepatic cells sustaining hepatitis C virus penetration. J Viral Hepat **18:**562-70.
53. **Burr, A. W., K. Toole, C. Chapman, J. E. Hines, and A. D. Burt.** 1998. Anti-hepatocyte growth factor antibody inhibits hepatocyte proliferation during liver regeneration. J Pathol **185:**298-302.
54. **Busch, M. P.** 2001. Insights into the epidemiology, natural history and pathogenesis of hepatitis C virus infection from studies of infected donors and blood product recipients. Transfusion Clinique Et Biologique **8:**200-206.
55. **Cai, L., A. Ji, F. C. de Beer, L. R. Tannock, and D. R. van der Westhuyzen.** 2008. SR-BI protects against endotoxemia in mice through its roles in glucocorticoid production and hepatic clearance. J Clin Invest **118:**364-75.
56. **Callens, N., Y. Ciczora, B. Bartosch, N. Vu-Dac, F. L. Cosset, J. M. Pawlotsky, F. Penin, and J. Dubuisson.** 2005. Basic residues in hypervariable region 1 of hepatitis C virus envelope glycoprotein e2 contribute to virus entry. J Virol **79:**15331-41.
57. **Capaldo, C. T., and A. Nusrat.** 2009. Cytokine regulation of tight junctions. Biochimica Et Biophysica Acta-Biomembranes **1788:**864-871.
58. **Capaldo, C. T., and A. Nusrat.** 2009. Cytokine regulation of tight junctions. Biochim Biophys Acta **1788:**864-71.
59. **Cassavaugh, J., and K. M. Lounsbury.** 2011. Hypoxia-mediated biological control. J Cell Biochem **112:**735-44.
60. **Castet, V., C. Fournier, A. Soulier, R. Brillet, J. Coste, D. Larrey, D. Dhumeaux, P. Maurel, and J. M. Pawlotsky.** 2002. Alpha interferon inhibits hepatitis C virus replication in primary human hepatocytes infected in vitro. J Virol **76:**8189-99.
61. **Catanese, M. T., H. Ansuini, R. Graziani, T. Huby, M. Moreau, J. K. Ball, G. Paonessa, C. M. Rice, R. Cortese, A. Vitelli, and A. Nicosia.** 2010. Role of scavenger receptor class B type I in hepatitis C virus entry: kinetics and molecular determinants. J Virol **84:**34-43.
62. **Catanese, M. T., R. Graziani, T. von Hahn, M. Moreau, T. Huby, G. Paonessa, C. Santini, A. Luzzago, C. M. Rice, R. Cortese, A. Vitelli, and A. Nicosia.** 2007. High-avidity monoclonal antibodies against the human scavenger class B type I receptor efficiently block hepatitis C virus infection in the presence of high-density lipoprotein. Journal of Virology **81:**8063-8071.
63. **Cereijido, M., J. Valdes, L. Shoshani, and R. G. Contreras.** 1998. Role of tight junctions in establishing and maintaining cell polarity. Annu Rev Physiol **60:**161-77.
64. **Chang, K. S., J. Jiang, Z. Cai, and G. Luo.** 2007. Human apolipoprotein e is required for infectivity and production of hepatitis C virus in cell culture. J Virol **81:**13783-93.
65. **Charlton, M.** 2003. Liver biopsy, viral kinetics, and the impact of viremia on severity of hepatitis C virus recurrence. Liver Transpl **9:**S58-62.
66. **Charrin, S., F. Le Naour, V. Labas, M. Billard, J. P. Le Caer, J. F. Emile, M. A. Petit, C. Boucheix, and E. Rubinstein.** 2003. EWI-2 is a new component of the tetraspanin web in hepatocytes and lymphoid cells. Biochem J **373:**409-21.
67. **Chau, N. M., P. Rogers, W. Aherne, V. Carroll, I. Collins, E. McDonald, P. Workman, and M. Ashcroft.** 2005. Identification of novel small molecule inhibitors of hypoxia-inducible factor-1 that differentially block hypoxia-inducible factor-1 activity and hypoxia-inducible factor-1alpha induction in response to hypoxic stress and growth factors. Cancer Res **65:**4918-28.

68. **Chen, S. L., and T. R. Morgan.** 2006. The natural history of hepatitis C virus (HCV) infection. Int J Med Sci **3:**47-52.
69. **Chevaliez, S., and J. M. Pawlotsky.** 2007. Hepatitis C virus: virology, diagnosis and management of antiviral therapy. World J Gastroenterol **13:**2461-6.
70. **Chiappini, F., A. Barrier, R. Saffroy, M. C. Domart, N. Dagues, D. Azoulay, M. Sebagh, B. Franc, S. Chevalier, B. Debuire, S. Dudoit, and A. Lemoine.** 2006. Exploration of global gene expression in human liver steatosis by high-density oligonucleotide microarray. Lab Invest **86:**154-65.
71. **Choi, S. S., S. Bradrick, G. Qiang, A. Mostafavi, G. Chaturvedi, S. A. Weinman, A. M. Diehl, and R. Jhaveri.** 2011. Upregulation of Hedgehog pathway is associated with cellular permissiveness for hepatitis C virus replication. Hepatology.
72. **Choi, S. S., and A. M. Diehl.** 2009. Epithelial-to-mesenchymal transitions in the liver. Hepatology **50:**2007-2013.
73. **Choi, S. S., and A. M. Diehl.** 2009. Epithelial-to-mesenchymal transitions in the liver. Hepatology **50:**2007-13.
74. **Choo, Q. L., G. Kuo, A. J. Weiner, L. R. Overby, D. W. Bradley, and M. Houghton.** 1989. Isolation of a Cdna Clone Derived from a Blood-Borne Non-a, Non-B Viral-Hepatitis Genome. Science **244:**359-362.
75. **Ciccorossi, P., A. M. Maina, F. Oliveri, S. Petruccelli, G. Leandro, P. Colombatto, F. Moriconi, F. Mosca, F. Filipponi, F. Bonino, and M. R. Brunetto.** 2007. Viral load 1 week after liver transplantation, donor age and rejections correlate with the outcome of recurrent hepatitis C. Liver International **27:**612-619.
76. **Ciesek, S., E. Steinmann, M. Iken, M. Ott, F. A. Helfritz, I. Wappler, M. P. Manns, H. Wedemeyer, and T. Pietschmann.** 2010. Glucocorticosteroids increase cell entry by hepatitis C virus. Gastroenterology **138:**1875-84.
77. **Ciesek, S., E. Steinmann, M. Iken, M. Ott, F. A. Helfritz, I. Wappler, M. P. Manns, H. Wedemeyer, and T. Pietschmann.** 2010. Glucocorticosteroids increase cell entry by hepatitis C virus. Gastroenterology.
78. **Clarke, D., S. Griffin, L. Beales, C. S. Gelais, S. Burgess, M. Harris, and D. Rowlands.** 2006. Evidence for the formation of a heptameric ion channel complex by the hepatitis C virus p7 protein in vitro. J Biol Chem **281:**37057-68.
79. **Cocquerel, L., C. Voisset, and J. Dubuisson.** 2006. Hepatitis C virus entry: potential receptors and their biological functions. Journal of General Virology **87:**1075-1084.
80. **Cocquerel, L., C. Wychowski, F. Minner, F. Penin, and J. Dubuisson.** 2000. Charged residues in the transmembrane domains of hepatitis C virus glycoproteins play a major role in the processing, subcellular localization, and assembly of these envelope proteins. J Virol **74:**3623-33.
81. **Codran, A., C. Royer, D. Jaeck, M. Bastien-Valle, T. F. Baumert, M. P. Kieny, C. A. Pereira, and J. P. Martin.** 2006. Entry of hepatitis C virus pseudotypes into primary human hepatocytes by clathrin-dependent endocytosis. J Gen Virol **87:**2583-93.
82. **Cohn, M. L., V. N. Goncharuk, A. H. Diwan, P. S. Zhang, S. S. Shen, and V. G. Prieto.** 2005. Loss of claudin-1 expression in tumor-associated vessels correlates with acquisition of metastatic phenotype in melanocytic neoplasms. J Cutan Pathol **32:**533-6.
83. **Cooper, S., A. L. Erickson, E. J. Adams, J. Kansopon, A. J. Weiner, D. Y. Chien, M. Houghton, P. Parham, and C. M. Walker.** 1999. Analysis of a successful immune response against hepatitis C virus. Immunity **10:**439-49.
84. **Cormier, E. G., F. Tsamis, F. Kajumo, R. J. Durso, J. P. Gardner, and T. Dragic.** 2004. CD81 is an entry coreceptor for hepatitis C virus. Proceedings of the National Academy of Sciences of the United States of America **101:**7270-7274.

85. **Coyne, C. B., and J. M. Bergelson.** 2006. Virus-induced Abl and Fyn kinase signals permit coxsackievirus entry through epithelial tight junctions. Cell **124:**119-31.
86. **Date, M., K. Matsuzaki, M. Matsushita, Y. Tahashi, K. Sakitani, and K. Inoue.** 2000. Differential regulation of activin A for hepatocyte growth and fibronectin synthesis in rat liver injury. J Hepatol **32:**251-60.
87. **Debonera, F., X. Aldeguer, X. Shen, A. E. Gelman, F. Gao, X. Que, L. E. Greenbaum, E. E. Furth, R. Taub, and K. M. Olthoff.** 2001. Activation of interleukin-6/STAT3 and liver regeneration following transplantation. J Surg Res **96:**289-95.
88. **Decaens, C., M. Durand, B. Grosse, and D. Cassio.** 2008. Which in vitro models could be best used to study hepatocyte polarity? Biol Cell **100:**387-98.
89. **Dhillon, S., J. Witteveldt, D. Gatherer, A. M. Owsianka, M. B. Zeisel, M. N. Zahid, M. Rychlowska, S. K. Foung, T. F. Baumert, A. G. Angus, and A. H. Patel.** 2010. Mutations within a conserved region of the hepatitis C virus E2 glycoprotein that influence virus-receptor interactions and sensitivity to neutralizing antibodies. J Virol **84:**5494-507.
90. **Diamond, D. L., A. J. Syder, J. M. Jacobs, C. M. Sorensen, K. A. Walters, S. C. Proll, J. E. McDermott, M. A. Gritsenko, Q. Zhang, R. Zhao, T. O. Metz, D. G. Camp, 2nd, K. M. Waters, R. D. Smith, C. M. Rice, and M. G. Katze.** 2010. Temporal proteome and lipidome profiles reveal hepatitis C virus-associated reprogramming of hepatocellular metabolism and bioenergetics. PLoS Pathog **6:**e1000719.
91. **Diaz, F., and E. Rodriguez-Boulan.** 2006. Open sesame! Coxsackieviruses conspire to trespass the tight junctional gate. Dev Cell **10:**151-2.
92. **Diehl-Jones, W. L., and D. F. Askin.** 2002. The neonatal liver, Part 1: embryology, anatomy, and physiology. Neonatal Netw **21:**5-12.
93. **Diehl, A. M., M. Yin, J. Fleckenstein, S. Q. Yang, H. Z. Lin, D. A. Brenner, J. Westwick, G. Bagby, and S. Nelson.** 1994. Tumor necrosis factor-alpha induces c-jun during the regenerative response to liver injury. Am J Physiol **267:**G552-61.
94. **Doceul, V., M. Hollinshead, L. van der Linden, and G. L. Smith.** Repulsion of superinfecting virions: a mechanism for rapid virus spread. Science **327:**873-6.
95. **Dooley, J., and S. Sherlock.** 2011. Sherlock's diseases of the liver and biliary system, 12th ed. Wiley-Blackwell, Chichester, West Sussex.
96. **Dourakis, S. P., V. A. Sevastianos, and P. Kaliopi.** 2002. Acute severe steatohepatitis related to prednisolone therapy. Am J Gastroenterol **97:**1074-5.
97. **Dowd, K. A., D. M. Netski, X. H. Wang, A. L. Cox, and S. C. Ray.** 2009. Selection pressure from neutralizing antibodies drives sequence evolution during acute infection with hepatitis C virus. Gastroenterology **136:**2377-86.
98. **Dreux, M., V. L. Dao Thi, J. Fresquet, M. Guerin, Z. Julia, G. Verney, D. Durantel, F. Zoulim, D. Lavillette, F. L. Cosset, and B. Bartosch.** 2009. Receptor complementation and mutagenesis reveal SR-BI as an essential HCV entry factor and functionally imply its intra- and extra-cellular domains. PLoS Pathog **5:**e1000310.
99. **Dreux, M., T. Pietschmann, C. Granier, C. Voisset, S. Ricard-Blum, P. E. Mangeot, Z. Keck, S. Foung, N. Vu-Dac, J. Dubuisson, R. Bartenschlager, D. Lavillette, and F. L. Cosset.** 2006. High density lipoprotein inhibits hepatitis C virus-neutralizing antibodies by stimulating cell entry via activation of the scavenger receptor BI. J Biol Chem **281:**18285-95.
100. **Dubuisson, J., F. Penin, and D. Moradpour.** 2002. Interaction of hepatitis C virus proteins with host cell membranes and lipids. Trends Cell Biol **12:**517-23.
101. **Durantel, D., and F. Zoulim.** 2007. Going towards more relevant cell culture models to study the in vitro replication of serum-derived hepatitis C virus and virus/host cell interactions? J Hepatol **46:**1-5.

102. **Dusheiko, G., H. Schmilovitzweiss, D. Brown, F. Mcomish, P. L. Yap, S. Sherlock, N. Mcintyre, and P. Simmonds.** 1994. Hepatitis-C Virus Genotypes - an Investigation of Type-Specific Differences in Geographic Origin and Disease. Hepatology **19:**13-18.
103. **Dustin, L. B., and C. M. Rice.** 2007. Flying under the radar: the immunobiology of hepatitis C. Annu Rev Immunol **25:**71-99.
104. **Dutta, U., J. Kench, K. Byth, M. H. Khan, R. Lin, C. Liddle, and G. C. Farrell.** 1998. Hepatocellular proliferation and development of hepatocellular carcinoma: a case-control study in chronic hepatitis C. Hum Pathol **29:**1279-84.
105. **Eckhardt, E. R., L. Cai, S. Shetty, Z. Zhao, A. Szanto, N. R. Webb, and D. R. Van der Westhuyzen.** 2006. High density lipoprotein endocytosis by scavenger receptor SR-BII is clathrin-dependent and requires a carboxyl-terminal dileucine motif. J Biol Chem **281:**4348-53.
106. **Eckhardt, E. R., L. Cai, B. Sun, N. R. Webb, and D. R. van der Westhuyzen.** 2004. High density lipoprotein uptake by scavenger receptor SR-BII. J Biol Chem **279:**14372-81.
107. **El-Serag, H. B., and K. L. Rudolph.** 2007. Hepatocellular carcinoma: epidemiology and molecular carcinogenesis. Gastroenterology **132:**2557-76.
108. **Evans, M. J., T. von Hahn, D. M. Tscherne, A. J. Syder, M. Panis, B. Wolk, T. Hatziioannou, J. A. McKeating, P. D. Bieniasz, and C. M. Rice.** 2007. Claudin-1 is a hepatitis C virus co-receptor required for a late step in entry. Nature **446:**801-5.
109. **Everett, R. S., M. K. Vanhook, N. Barozzi, I. Toth, and L. G. Johnson.** 2006. Specific modulation of airway epithelial tight junctions by apical application of an occludin peptide. Mol Pharmacol **69:**492-500.
110. **Everson, G. T.** 2002. Impact of immunosuppressive therapy on recurrence of hepatitis C. Liver Transpl **8:**S19-27.
111. **Farazi, P. A., and R. A. DePinho.** 2006. Hepatocellular carcinoma pathogenesis: from genes to environment. Nat Rev Cancer **6:**674-87.
112. **Farquhar, M. J., H. J. Harris, M. Diskar, S. Jones, C. J. Mee, S. U. Nielsen, C. L. Brimacombe, S. Molina, G. L. Toms, P. Maurel, J. Howl, F. W. Herberg, S. C. van Ijzendoorn, P. Balfe, and J. A. McKeating.** 2008. Protein kinase A-dependent step(s) in hepatitis C virus entry and infectivity. J Virol **82:**8797-811.
113. **Farquhar, M. J., H. J. Harris, and J. A. McKeating.** 2011. Hepatitis C virus entry and the tetraspanin CD81. Biochem Soc Trans **39:**532-6.
114. **Farrell, G. C.** 2002. Drugs and steatohepatitis. Semin Liver Dis **22:**185-94.
115. **Fassio, E.** 2010. Hepatitis C and hepatocellular carcinoma. Ann Hepatol **9 Suppl:**119-22.
116. **Feld, J. J., and J. H. Hoofnagle.** 2005. Mechanism of action of interferon and ribavirin in treatment of hepatitis C. Nature **436:**967-72.
117. **Feldman, G. J., J. M. Mullin, and M. P. Ryan.** 2005. Occludin: structure, function and regulation. Adv Drug Deliv Rev **57:**883-917.
118. **Feldmann, G.** 1989. The cytoskeleton of the hepatocyte. Structure and functions. J Hepatol **8:**380-6.
119. **Ferri, C., G. Ferraccioli, D. Ferrari, M. Galeazzi, G. Lapadula, C. Montecucco, G. Triolo, G. Valentini, and G. Valesini.** 2008. Safety of anti-tumor necrosis factor-alpha therapy in patients with rheumatoid arthritis and chronic hepatitis C virus infection. J Rheumatol **35:**1944-9.
120. **Fish, S. M., R. Proujansky, and W. W. Reenstra.** 1999. Synergistic effects of interferon gamma and tumour necrosis factor alpha on T84 cell function. Gut **45:**191-198.
121. **Fletcher, N. F., J. P. Yang, M. J. Farquhar, K. Hu, C. Davis, Q. He, K. Dowd, S. C. Ray, S. E. Krieger, J. Neyts, T. F. Baumert, P. Balfe, J. A. McKeating, and F. Wong-Staal.**

2010. Hepatitis C virus infection of neuroepithelioma cell lines. Gastroenterology **139:**1365-74.

122. **Flint, M., T. von Hahn, J. Zhang, M. Farquhar, C. T. Jones, P. Balfe, C. M. Rice, and J. A. McKeating.** 2006. Diverse CD81 proteins support hepatitis C virus infection. J Virol **80:**11331-42.
123. **Fofana, I., S. E. Krieger, F. Grunert, S. Glauben, F. Xiao, S. Fafi-Kremer, E. Soulier, C. Royer, C. Thumann, C. J. Mee, J. A. McKeating, T. Dragic, P. Pessaux, F. Stoll-Keller, C. Schuster, J. Thompson, and T. F. Baumert.** 2010. Monoclonal anti-claudin 1 antibodies prevent hepatitis C virus infection of primary human hepatocytes. Gastroenterology **139:**953-64, 964 e1-4.
124. **Forster, C., M. Burek, I. A. Romero, B. Weksler, P. O. Couraud, and D. Drenckhahn.** 2008. Differential effects of hydrocortisone and TNFalpha on tight junction proteins in an in vitro model of the human blood-brain barrier. J Physiol **586:**1937-49.
125. **Forster, C., C. Silwedel, N. Golenhofen, M. Burek, S. Kietz, J. Mankertz, and D. Drenckhahn.** 2005. Occludin as direct target for glucocorticoid-induced improvement of blood-brain barrier properties in a murine in vitro system. J Physiol **565:**475-86.
126. **Foster, T. L., T. Belyaeva, N. J. Stonehouse, A. R. Pearson, and M. Harris.** 2010. All three domains of the hepatitis C virus nonstructural NS5A protein contribute to RNA binding. J Virol **84:**9267-77.
127. **Fournier, C., C. Sureau, J. Coste, J. Ducos, G. Pageaux, D. Larrey, J. Domergue, and P. Maurel.** 1998. In vitro infection of adult normal human hepatocytes in primary culture by hepatitis C virus. J Gen Virol **79 (Pt 10):**2367-74.
128. **Foy, E., K. Li, R. Sumpter, Jr., Y. M. Loo, C. L. Johnson, C. Wang, P. M. Fish, M. Yoneyama, T. Fujita, S. M. Lemon, and M. Gale, Jr.** 2005. Control of antiviral defenses through hepatitis C virus disruption of retinoic acid-inducible gene-I signaling. Proc Natl Acad Sci U S A **102:**2986-91.
129. **Fransvea, E., U. Angelotti, S. Antonaci, and G. Giannelli.** 2008. Blocking transforming growth factor-beta up-regulates E-cadherin and reduces migration and invasion of hepatocellular carcinoma cells. Hepatology **47:**1557-66.
130. **Gabriel, A., A. Ziolkowski, P. Radlowski, K. Tomaszek, and A. Dziambor.** 2008. Hepatocyte steatosis in HCV patients promotes fibrosis by enhancing TGF-beta liver expression. Hepatol Res **38:**141-6.
131. **Gale, M., Jr.** 2003. Effector genes of interferon action against hepatitis C virus. Hepatology **37:**975-8.
132. **Gale, M., Jr., C. M. Blakely, B. Kwieciszewski, S. L. Tan, M. Dossett, N. M. Tang, M. J. Korth, S. J. Polyak, D. R. Gretch, and M. G. Katze.** 1998. Control of PKR protein kinase by hepatitis C virus nonstructural 5A protein: molecular mechanisms of kinase regulation. Mol Cell Biol **18:**5208-18.
133. **Galman, C., B. Angelin, and M. Rudling.** 2002. Prolonged stimulation of the adrenals by corticotropin suppresses hepatic low-density lipoprotein and high-density lipoprotein receptors and increases plasma cholesterol. Endocrinology **143:**1809-16.
134. **Gane, E. J., B. C. Portmann, N. V. Naoumov, H. M. Smith, J. A. Underhill, P. T. Donaldson, G. Maertens, and R. Williams.** 1996. Long-term outcome of hepatitis C infection after liver transplantation. N Engl J Med **334:**815-20.
135. **Garcia-Retortillo, M., X. Forns, A. Feliu, E. Moitinho, J. Costa, M. Navasa, A. Rimola, and J. Rodes.** 2002. Hepatitis C virus kinetics during and immediately after liver transplantation. Hepatology **35:**680-7.
136. **Gardner, J. P., R. J. Durso, R. R. Arrigale, G. P. Donovan, P. J. Maddon, T. Dragic, and W. C. Olson.** 2003. L-SIGN (CD 209L) is a liver-specific capture receptor for hepatitis C virus. Proceedings of the National Academy of Sciences of the United States of America **100:**4498-4503.

137. **Garry, R. F., and S. Dash.** 2003. Proteomics computational analyses suggest that hepatitis C virus E1 and pestivirus E2 envelope glycoproteins are truncated class II fusion proteins. Virology **307:**255-65.
138. **Gastaminza, P., G. Cheng, S. Wieland, J. Zhong, W. Liao, and F. V. Chisari.** 2008. Cellular determinants of hepatitis C virus assembly, maturation, degradation, and secretion. J Virol **82:**2120-9.
139. **Giannelli, G., C. Bergamini, E. Fransvea, C. Sgarra, and S. Antonaci.** 2005. Laminin-5 with transforming growth factor-beta1 induces epithelial to mesenchymal transition in hepatocellular carcinoma. Gastroenterology **129:**1375-83.
140. **Gibbons, G. F., D. Wiggins, A. M. Brown, and A. M. Hebbachi.** 2004. Synthesis and function of hepatic very-low-density lipoprotein. Biochem Soc Trans **32:**59-64.
141. **Gondeau, C., L. Pichard-Garcia, and P. Maurel.** 2009. Cellular models for the screening and development of anti-hepatitis C virus agents. Pharmacology & Therapeutics **124:**1-22.
142. **Gong, G., G. Waris, R. Tanveer, and A. Siddiqui.** 2001. Human hepatitis C virus NS5A protein alters intracellular calcium levels, induces oxidative stress, and activates STAT-3 and NF-kappa B. Proc Natl Acad Sci U S A **98:**9599-604.
143. **Gottwein, J. M., T. K. Scheel, A. M. Hoegh, J. B. Lademann, J. Eugen-Olsen, G. Lisby, and J. Bukh.** 2007. Robust hepatitis C genotype 3a cell culture releasing adapted intergenotypic 3a/2a (S52/JFH1) viruses. Gastroenterology **133:**1614-26.
144. **Gottwein, J. M., T. K. Scheel, T. B. Jensen, J. B. Lademann, J. C. Prentoe, M. L. Knudsen, A. M. Hoegh, and J. Bukh.** 2009. Development and characterization of hepatitis C virus genotype 1-7 cell culture systems: role of CD81 and scavenger receptor class B type I and effect of antiviral drugs. Hepatology **49:**364-77.
145. **Griffin, S. D., L. P. Beales, D. S. Clarke, O. Worsfold, S. D. Evans, J. Jaeger, M. P. Harris, and D. J. Rowlands.** 2003. The p7 protein of hepatitis C virus forms an ion channel that is blocked by the antiviral drug, Amantadine. FEBS Lett **535:**34-8.
146. **Grove, J., T. Huby, Z. Stamataki, T. Vanwolleghem, P. Meuleman, M. Farquhar, A. Schwarz, M. Moreau, J. S. Owen, G. Leroux-Roels, P. Balfe, and J. A. McKeating.** 2007. Scavenger receptor BI and BII expression levels modulate hepatitis C virus infectivity. J Virol **81:**3162-9.
147. **Grove, J., S. Nielsen, J. Zhong, M. F. Bassendine, H. E. Drummer, P. Balfe, and J. A. McKeating.** 2008. Identification of a residue in hepatitis C virus E2 glycoprotein that determines scavenger receptor BI and CD81 receptor dependency and sensitivity to neutralizing antibodies. J Virol **82:**12020-9.
148. **Gu, X., B. Trigatti, S. Xu, S. Acton, J. Babitt, and M. Krieger.** 1998. The efficient cellular uptake of high density lipoprotein lipids via scavenger receptor class B type I requires not only receptor-mediated surface binding but also receptor-specific lipid transfer mediated by its extracellular domain. J Biol Chem **273:**26338-48.
149. **H, T.** 2008. A potential role of the heparan sulfate in the hepatitis C virus attachment. Acta Virol **52:**7-15.
150. **Hafstrom, I., M. Rohani, S. Deneberg, M. Wornert, T. Jogestrand, and J. Frostegard.** 2007. Effects of low-dose prednisolone on endothelial function, atherosclerosis, and traditional risk factors for atherosclerosis in patients with rheumatoid arthritis--a randomized study. J Rheumatol **34:**1810-6.
151. **Haid, S., M. P. Windisch, R. Bartenschlager, and T. Pietschmann.** Mouse-specific residues of claudin-1 limit hepatitis C virus genotype 2a infection in a human hepatocyte cell line. J Virol **84:**964-75.
152. **Hanahan, D., and R. A. Weinberg.** 2011. Hallmarks of cancer: the next generation. Cell **144:**646-74.

153. **Harke, N., J. Leers, S. Kietz, D. Drenckhahn, and C. Forster.** 2008. Glucocorticoids regulate the human occludin gene through a single imperfect palindromic glucocorticoid response element. Mol Cell Endocrinol **295:**39-47.
154. **Harris, H. J., C. Davis, J. G. Mullins, K. Hu, M. Goodall, M. J. Farquhar, C. J. Mee, K. McCaffrey, S. Young, H. Drummer, P. Balfe, and J. A. McKeating.** 2010. Claudin association with CD81 defines hepatitis C virus entry. J Biol Chem **285:**21092-102.
155. **Harris, H. J., M. J. Farquhar, C. J. Mee, C. Davis, G. M. Reynolds, A. Jennings, K. Hu, F. Yuan, H. Deng, S. G. Hubscher, J. H. Han, P. Balfe, and J. A. McKeating.** 2008. CD81 and claudin 1 coreceptor association: role in hepatitis C virus entry. J Virol **82:**5007-20.
156. **Harris, H. J., M. J. Farquhar, C. J. Mee, C. Davis, G. M. Reynolds, A. Jennings, K. Hu, F. Yuan, H. Deng, S. G. Hubscher, J. H. Han, P. Balfe, and J. A. McKeating.** 2008. CD81 and claudin 1 coreceptor association: Role in hepatitis C virus entry. Journal of Virology **82:**5007-5020.
157. **Hassan, M., D. Selimovic, H. Ghozlan, and O. Abdel-Kader.** 2009. Hepatitis C Virus Core Protein Triggers Hepatic Angiogenesis by a Mechanism Including Multiple Pathways. Hepatology **49:**1469-1482.
158. **Hassan, M., D. Selimovic, H. Ghozlan, and O. Abdel-Kader.** 2007. Induction of high-molecular-weight (HMW) tumor necrosis factor(TNF) alpha by hepatitis C virus (HCV) non-structural protein 3 (NS3) in liver cells is AP-1 and NF-kappaB-dependent activation. Cell Signal **19:**301-11.
159. **Havens, W. P.** 1944. Experimental production of hepatitis by feeding icterogenic materials. Proceedings of the Society of Experimental Biology and Medicine **57**.
160. **Havens, W. P., Jr.** 1956. Viral hepatitis: multiple attacks in a narcotic addict. Ann Intern Med **44:**199-203.
161. **Heathcote, J., and J. Main.** 2005. Treatment of hepatitis C. J Viral Hepat **12:**223-35.
162. **Heinz, F. X., K. Stiasny, and S. L. Allison.** 2004. The entry machinery of flaviviruses. Arch Virol Suppl**:**133-7.
163. **Helle, F., G. Vieyres, L. Elkrief, C. I. Popescu, C. Wychowski, V. Descamps, S. Castelain, P. Roingeard, G. Duverlie, and J. Dubuisson.** 2010. Role of N-linked glycans in the functions of hepatitis C virus envelope proteins incorporated into infectious virions. J Virol **84:**11905-15.
164. **Henry, S. D., H. J. Metselaar, J. Van Dijck, H. W. Tilanus, and L. J. Van Der Laan.** 2007. Impact of steroids on hepatitis C virus replication in vivo and in vitro. Ann N Y Acad Sci **1110:**439-47.
165. **Heo, T. H., S. M. Lee, B. Bartosch, F. L. Cosset, and C. Y. Kang.** 2006. Hepatitis C virus E2 links soluble human CD81 and SR-B1 protein. Virus Res **121:**58-64.
166. **Higashi, Y., S. Suzuki, T. Sakaguchi, T. Nakamura, S. Baba, H. C. Reinecker, S. Nakamura, and H. Konno.** 2007. Loss of claudin-1 expression correlates with malignancy of hepatocellular carcinoma. J Surg Res **139:**68-76.
167. **Hilgard, P., and R. Stockert.** 2000. Heparan sulfate proteoglycans initiate dengue virus infection of hepatocytes. Hepatology **32:**1069-77.
168. **Hishiki, T., Y. Shimizu, R. Tobita, K. Sugiyama, K. Ogawa, K. Funami, Y. Ohsaki, T. Fujimoto, H. Takaku, T. Wakita, T. F. Baumert, Y. Miyanari, and K. Shimotohno.** 2010. Infectivity of hepatitis C virus is influenced by association with apolipoprotein E isoforms. J Virol **84:**12048-57.
169. **Horikawa, T., J. Yang, S. Kondo, T. Yoshizaki, I. Joab, M. Furukawa, and J. S. Pagano.** 2007. Twist and epithelial-mesenchymal transition are induced by the EBV oncoprotein latent membrane protein 1 and are associated with metastatic nasopharyngeal carcinoma. Cancer Res **67:**1970-8.

170. **Hsu, I. C., T. Tokiwa, W. Bennett, R. A. Metcalf, J. A. Welsh, T. Sun, and C. C. Harris.** 1993. p53 gene mutation and integrated hepatitis B viral DNA sequences in human liver cancer cell lines. Carcinogenesis **14:**987-92.

171. **Hsu, M., J. Zhang, M. Flint, C. Logvinoff, C. Cheng-Mayer, C. M. Rice, and J. A. McKeating.** 2003. Hepatitis C virus glycoproteins mediate pH-dependent cell entry of pseudotyped retroviral particles. Proc Natl Acad Sci U S A **100:**7271-6.

172. **Hsu, M., J. Zhang, M. Flint, C. Logvinoff, C. Cheng-Mayer, C. M. Rice, and J. A. McKeating.** 2003. Hepatitis C virus glycoproteins mediate pH-dependent cell entry of pseudotyped retroviral particles. Proceedings of the National Academy of Sciences of the United States of America **100:**7271-7276.

173. **Huang, H., F. Sun, D. M. Owen, W. Li, Y. Chen, M. Gale, Jr., and J. Ye.** 2007. Hepatitis C virus production by human hepatocytes dependent on assembly and secretion of very low-density lipoproteins. Proc Natl Acad Sci U S A **104:**5848-53.

174. **Huang, Y. H., J. C. Wu, C. H. Chen, T. T. Chang, P. C. Lee, G. Y. Chau, W. Y. Lui, F. Y. Chang, and S. D. Lee.** 2005. Comparison of recurrence after hepatic resection in patients with hepatitis B vs. hepatitis C-related small hepatocellular carcinoma in hepatitis B virus endemic area. Liver international : official journal of the International Association for the Study of the Liver **25:**236-41.

175. **Hwang, S. J., and S. D. Lee.** 2011. Hepatic steatosis and hepatitis C: Still unhappy bedfellows? J Gastroenterol Hepatol **26 Suppl 1:**96-101.

176. **Ikeda, M., K. Sugiyama, T. Mizutani, T. Tanaka, K. Tanaka, H. Sekihara, K. Shimotohno, and N. Kato.** 1998. Human hepatocyte clonal cell lines that support persistent replication of hepatitis C virus. Virus Res **56:**157-67.

177. **Ikeda, M., M. Yi, K. Li, and S. M. Lemon.** 2002. Selectable subgenomic and genome-length dicistronic RNAs derived from an infectious molecular clone of the HCV-N strain of hepatitis C virus replicate efficiently in cultured Huh7 cells. J Virol **76:**2997-3006.

178. **Itzhaki, R. F., W. L. Irving, and M. A. Wozniak.** 2003. Apolipoprotein E and hepatitis C virus. Hepatology **38:**1060.

179. **Ivan, M., K. Kondo, H. Yang, W. Kim, J. Valiando, M. Ohh, A. Salic, J. M. Asara, W. S. Lane, and W. G. Kaelin, Jr.** 2001. HIFalpha targeted for VHL-mediated destruction by proline hydroxylation: implications for O2 sensing. Science **292:**464-8.

180. **Jaakkola, P., D. R. Mole, Y. M. Tian, M. I. Wilson, J. Gielbert, S. J. Gaskell, A. Kriegsheim, H. F. Hebestreit, M. Mukherji, C. J. Schofield, P. H. Maxwell, C. W. Pugh, and P. J. Ratcliffe.** 2001. Targeting of HIF-alpha to the von Hippel-Lindau ubiquitylation complex by O2-regulated prolyl hydroxylation. Science **292:**468-72.

181. **Jiang, J., and G. Luo.** 2009. Apolipoprotein E but not B is required for the formation of infectious hepatitis C virus particles. J Virol **83:**12680-91.

182. **Jopling, C. L., M. Yi, A. M. Lancaster, S. M. Lemon, and P. Sarnow.** 2005. Modulation of hepatitis C virus RNA abundance by a liver-specific MicroRNA. Science **309:**1577-81.

183. **Kabir, A., S. M. Alavian, and H. Keyvani.** 2006. Distribution of hepatitis C virus genotypes in patients infected by different sources and its correlation with clinical and virological parameters: a preliminary study. Comp Hepatol **5:**4.

184. **Kaimori, A., J. Potter, J. Y. Kaimori, C. Wang, E. Mezey, and A. Koteish.** 2007. Transforming growth factor-beta1 induces an epithelial-to-mesenchymal transition state in mouse hepatocytes in vitro. J Biol Chem **282:**22089-101.

185. **Kalluri, R., and R. A. Weinberg.** 2009. The basics of epithelial-mesenchymal transition. J Clin Invest **119:**1420-8.

186. **Kamili, S., K. Krawczynski, K. McCaustland, X. Li, and M. J. Alter.** 2007. Infectivity of hepatitis C virus in plasma after drying and storing at room temperature. Infect Control Hosp Epidemiol **28:**519-24.
187. **Kanazawa, N., N. Enomoto, M. Kurosaki, N. Sakamoto, N. Izumi, and C. Sato.** 2000. Repression of HCV-IRES-dependent protein translation by the activation of PKR with dsRNA. Gastroenterology **118:**A938-A938.
188. **Kanno, N., G. LeSage, S. Glaser, D. Alvaro, and G. Alpini.** 2000. Functional heterogeneity of the intrahepatic biliary epithelium. Hepatology **31:**555-61.
189. **Kapadia, S. B., H. Barth, T. Baumert, J. A. McKeating, and F. V. Chisari.** 2007. Initiation of hepatitis C virus infection is dependent on cholesterol and cooperativity between CD81 and scavenger receptor B type I. J Virol **81:**374-83.
190. **Kato, N., K. Sugiyama, K. Namba, H. Dansako, T. Nakamura, M. Takami, K. Naka, A. Nozaki, and K. Shimotohno.** 2003. Establishment of a hepatitis C virus subgenomic replicon derived from human hepatocytes infected in vitro. Biochem Biophys Res Commun **306:**756-66.
191. **Kellner-Weibel, G., M. de La Llera-Moya, M. A. Connelly, G. Stoudt, A. E. Christian, M. P. Haynes, D. L. Williams, and G. H. Rothblat.** 2000. Expression of scavenger receptor BI in COS-7 cells alters cholesterol content and distribution. Biochemistry **39:**221-9.
192. **Kielian, M.** 2006. Class II virus membrane fusion proteins. Virology **344:**38-47.
193. **Kielian, M., and F. A. Rey.** 2006. Virus membrane-fusion proteins: more than one way to make a hairpin. Nat Rev Microbiol **4:**67-76.
194. **Klenerman, P., M. Lucas, E. Barnes, and G. Harcourt.** 2002. Immunity to hepatitis C virus: stunned but not defeated. Microbes Infect **4:**57-65.
195. **Kodama, T., N. Shimizu, N. Yoshikawa, Y. Makino, R. Ouchida, K. Okamoto, T. Hisada, H. Nakamura, C. Morimoto, and H. Tanaka.** 2003. Role of the glucocorticoid receptor for regulation of hypoxia-dependent gene expression. J Biol Chem **278:**33384-91.
196. **Kolios, G., V. Valatas, and E. Kouroumalis.** 2006. Role of Kupffer cells in the pathogenesis of liver disease. World J Gastroenterol **12:**7413-20.
197. **Konz, J. O., A. L. Lee, J. A. Lewis, and S. L. Sagar.** 2005. Development of a purification process for adenovirus: controlling virus aggregation to improve the clearance of host cell DNA. Biotechnol Prog **21:**466-72.
198. **Koskinas, J., K. Petraki, N. Kavantzas, I. Rapti, D. Kountouras, and S. Hadziyannis.** 2005. Hepatic expression of the proliferative marker Ki-67 and p53 protein in HBV or HCV cirrhosis in relation to dysplastic liver cell changes and hepatocellular carcinoma. J Viral Hepat **12:**635-41.
199. **Koutsoudakis, G., E. Herrmann, S. Kallis, R. Bartenschlager, and T. Pietschmann.** 2007. The level of CD81 cell surface expression is a key determinant for productive entry of hepatitis C virus into host cells. J Virol **81:**588-98.
200. **Krieger, M.** 2001. Scavenger receptor class B type I is a multiligand HDL receptor that influences diverse physiologic systems. J Clin Invest **108:**793-7.
201. **Krieger, N., V. Lohmann, and R. Bartenschlager.** 2001. Enhancement of hepatitis C virus RNA replication by cell culture-adaptive mutations. J Virol **75:**4614-24.
202. **Krieger, S. E., M. B. Zeisel, C. Davis, C. Thumann, H. J. Harris, E. K. Schnober, C. Mee, E. Soulier, C. Royer, M. Lambotin, F. Grunert, V. L. Dao Thi, M. Dreux, F. L. Cosset, J. A. McKeating, C. Schuster, and T. F. Baumert.** 2010. Inhibition of hepatitis C virus infection by anti-claudin-1 antibodies is mediated by neutralization of E2-CD81-claudin-1 associations. Hepatology **51:**1144-57.
203. **Krugman, S., R. Ward, and J. P. Giles.** 1962. The natural history of infectious hepatitis. Am J Med **32:**717-28.

204. **Kwong, A. D., R. S. Kauffman, P. Hurter, and P. Mueller.** 2011. Discovery and development of telaprevir: an NS3-4A protease inhibitor for treating genotype 1 chronic hepatitis C virus. Nat Biotechnol **29:**993-1003.

205. **Lagging, L. M., K. Meyer, R. J. Owens, and R. Ray.** 1998. Functional role of hepatitis C virus chimeric glycoproteins in the infectivity of pseudotyped virus. J Virol **72:**3539-46.

206. **Lai, W. K., P. J. Sun, J. Zhang, A. Jennings, P. F. Lalor, S. Hubscher, J. A. McKeating, and D. H. Adams.** 2006. Expression of DC-SIGN and DC-SIGNR on human sinusoidal endothelium: a role for capturing hepatitis C virus particles. Am J Pathol **169:**200-8.

207. **Lalor, P. F., and D. H. Adams.** 2002. The liver: a model of organ-specific lymphocyte recruitment. Expert Rev Mol Med **4:**1-16.

208. **Lanford, R. E., B. Guerra, H. Lee, D. R. Averett, B. Pfeiffer, D. Chavez, L. Notvall, and C. Bigger.** 2003. Antiviral effect and virus-host interactions in response to alpha interferon, gamma interferon, poly(i)-poly(c), tumor necrosis factor alpha, and ribavirin in hepatitis C virus subgenomic replicons. J Virol **77:**1092-104.

209. **Lanford, R. E., C. Sureau, J. R. Jacob, R. White, and T. R. Fuerst.** 1994. Demonstration of in vitro infection of chimpanzee hepatocytes with hepatitis C virus using strand-specific RT/PCR. Virology **202:**606-14.

210. **Laskus, T., M. Radkowski, A. Piasek, M. Nowicki, A. Horban, J. Cianciara, and J. Rakela.** 2000. Hepatitis C virus in lymphoid cells of patients coinfected with human immunodeficiency virus type 1: evidence of active replication in monocytes/macrophages and lymphocytes. J Infect Dis **181:**442-8.

211. **Lauer, G. M., E. Barnes, M. Lucas, J. Timm, K. Ouchi, A. Y. Kim, C. L. Day, G. K. Robbins, D. R. Casson, M. Reiser, G. Dusheiko, T. M. Allen, R. T. Chung, B. D. Walker, and P. Klenerman.** 2004. High resolution analysis of cellular immune responses in resolved and persistent hepatitis C virus infection. Gastroenterology **127:**924-36.

212. **Law, M., T. Maruyama, J. Lewis, E. Giang, A. W. Tarr, Z. Stamataki, P. Gastaminza, F. V. Chisari, I. M. Jones, R. I. Fox, J. K. Ball, J. A. McKeating, N. M. Kneteman, and D. R. Burton.** 2008. Broadly neutralizing antibodies protect against hepatitis C virus quasispecies challenge. Nat Med **14:**25-7.

213. **Lee, T. K., R. T. Poon, A. P. Yuen, M. T. Ling, W. K. Kwok, X. H. Wang, Y. C. Wong, X. Y. Guan, K. Man, K. L. Chau, and S. T. Fan.** 2006. Twist overexpression correlates with hepatocellular carcinoma metastasis through induction of epithelial-mesenchymal transition. Clin Cancer Res **12:**5369-76.

214. **Lehmann, M. J., N. M. Sherer, C. B. Marks, M. Pypaert, and W. Mothes.** 2005. Actin- and myosin-driven movement of viruses along filopodia precedes their entry into cells. J Cell Biol **170:**317-25.

215. **Leonard, M. O., C. Godson, H. R. Brady, and C. T. Taylor.** 2005. Potentiation of glucocorticoid activity in hypoxia through induction of the glucocorticoid receptor. J Immunol **174:**2250-7.

216. **Leu, J. I., M. A. Crissey, J. P. Leu, G. Ciliberto, and R. Taub.** 2001. Interleukin-6-induced STAT3 and AP-1 amplify hepatocyte nuclear factor 1-mediated transactivation of hepatic genes, an adaptive response to liver injury. Mol Cell Biol **21:**414-24.

217. **Levy, S., S. C. Todd, and H. T. Maecker.** 1998. CD81 (TAPA-1): a molecule involved in signal transduction and cell adhesion in the immune system. Annu Rev Immunol **16:**89-109.

218. **Li, K., E. Foy, J. C. Ferreon, M. Nakamura, A. C. Ferreon, M. Ikeda, S. C. Ray, M. Gale, Jr., and S. M. Lemon.** 2005. Immune evasion by hepatitis C virus NS3/4A protease-mediated cleavage of the Toll-like receptor 3 adaptor protein TRIF. Proc Natl Acad Sci U S A **102:**2992-7.

219. **Li, T., D. Li, L. Cheng, H. Wu, Z. Gao, Z. Liu, W. Jiang, Y. H. Gao, F. Tian, L. Zhao, and S. Wang.** 2010. Epithelial-Mesenchymal Transition Induced by Hepatitis C Virus Core Protein in Cholangiocarcinoma. Ann Surg Oncol.

220. **Li, X. D., L. Sun, R. B. Seth, G. Pineda, and Z. J. Chen.** 2005. Hepatitis C virus protease NS3/4A cleaves mitochondrial antiviral signaling protein off the mitochondria to evade innate immunity. Proc Natl Acad Sci U S A **102:**17717-22.

221. **Liang, Y., T. Shilagard, S. Y. Xiao, N. Snyder, D. Lau, L. Cicalese, H. Weiss, G. Vargas, and S. M. Lemon.** 2009. Visualizing hepatitis C virus infections in human liver by two-photon microscopy. Gastroenterology **137:**1448-58.

222. **Lima, J. P.** 1980. [Anatomy and physiology of the liver secretory apparatus]. Arq Gastroenterol **17:**149-60.

223. **Lin, K., A. D. Kwong, and C. Lin.** 2004. Combination of a hepatitis C virus NS3-NS4A protease inhibitor and alpha interferon synergistically inhibits viral RNA replication and facilitates viral RNA clearance in replicon cells. Antimicrob Agents Chemother **48:**4784-92.

224. **Lin, W., W. L. Tsai, R. X. Shao, G. Wu, L. F. Peng, L. L. Barlow, W. J. Chung, L. Zhang, H. Zhao, J. Y. Jang, and R. T. Chung.** 2010. Hepatitis C virus regulates transforming growth factor beta1 production through the generation of reactive oxygen species in a nuclear factor kappaB-dependent manner. Gastroenterology **138:**2509-18, 2518 e1.

225. **Lindenbach, B. D., M. J. Evans, A. J. Syder, B. Wolk, T. L. Tellinghuisen, C. C. Liu, T. Maruyama, R. O. Hynes, D. R. Burton, J. A. McKeating, and C. M. Rice.** 2005. Complete replication of hepatitis C virus in cell culture. Science **309:**623-6.

226. **Lindenbach, B. D., P. Meuleman, A. Ploss, T. Vanwolleghem, A. J. Syder, J. A. McKeating, R. E. Lanford, S. M. Feinstone, M. E. Major, G. Leroux-Roels, and C. M. Rice.** 2006. Cell culture-grown hepatitis C virus is infectious in vivo and can be recultured in vitro. Proc Natl Acad Sci U S A **103:**3805-9.

227. **Lindenbach, B. D., P. Meuleman, A. Ploss, T. Vanwolleghem, A. J. Syder, J. A. McKeating, R. E. Lanford, S. M. Feinstone, M. E. Major, G. Leroux-Roels, and C. M. Rice.** 2006. Cell culture-grown hepatitis C virus is infectious in vivo and can be recultured in vitro. Proceedings of the National Academy of Sciences of the United States of America **103:**3805-3809.

228. **Lindenbach, B. D., and C. M. Rice.** 2005. Unravelling hepatitis C virus replication from genome to function. Nature **436:**933-938.

229. **Liu, S. F., W. Yang, L. Shen, J. R. Turner, C. B. Coyne, and T. Y. Wang.** 2009. Tight Junction Proteins Claudin-1 and Occludin Control Hepatitis C Virus Entry and Are Downregulated during Infection To Prevent Superinfection. Journal of Virology **83:**2011-2014.

230. **Llovet, J. M.** 2005. Updated treatment approach to hepatocellular carcinoma. Journal of gastroenterology **40:**225-35.

231. **Llovet, J. M., and J. Bruix.** 2008. Molecular targeted therapies in hepatocellular carcinoma. Hepatology **48:**1312-27.

232. **Logvinoff, C., M. E. Major, D. Oldach, S. Heyward, A. Talal, P. Balfe, S. M. Feinstone, H. Alter, C. M. Rice, and J. A. McKeating.** 2004. Neutralizing antibody response during acute and chronic hepatitis C virus infection. Proc Natl Acad Sci U S A **101:**10149-54.

233. **Lohmann, V., F. Korner, J. Koch, U. Herian, L. Theilmann, and R. Bartenschlager.** 1999. Replication of subgenomic hepatitis C virus RNAs in a hepatoma cell line. Science **285:**110-3.

234. **Lozach, P. Y., A. Amara, B. Bartosch, J. L. Virelizier, F. Arenzana-Seisdedos, F. L. Cosset, and R. Altmeyer.** 2004. C-type lectins L-SIGN and DC-SIGN capture and transmit infectious hepatitis C virus pseudotype particles. J Biol Chem **279:**32035-45.

235. **Lozach, P. Y., A. Amara, B. Bartosch, J. L. Virelizier, F. Arenzana-Seisdedos, F. L. Cosset, and R. Altmeyer.** 2004. C-type lectins L-SIGN and DC-SIGN capture and transmit infectious hepatitis C virus pseudotype particles. Journal of Biological Chemistry **279:**32035-32045.
236. **MacCallum, F.** 1944. Transmission of hepatitis to human volunteers. Lancet **2**.
237. **Mackenzie, J.** 2005. Wrapping things up about virus RNA replication. Traffic **6:**967-77.
238. **Mahajan, D. K., and S. N. London.** 1997. Mifepristone (RU486): a review. Fertil Steril **68:**967-76.
239. **Malizia, A. P., N. Lacey, D. Walls, J. J. Egan, and P. P. Doran.** 2009. CUX1/Wnt signaling regulates epithelial mesenchymal transition in EBV infected epithelial cells. Exp Cell Res **315:**1819-31.
240. **Marek, B., D. Kajdaniuk, U. Mazurek, E. Janczewska-Kazek, B. Kos-Kudla, B. Strzalka, A. Fila, D. Niedziolka, M. Beniowski, Z. Ostrowska, H. Borgiel-Marek, J. Kajdaniuk, L. Sieminska, M. Nowak, T. Wilczok, D. Pakula, and P. Filipczyk.** 2005. TGF-beta1 mRNA expression in liver biopsy specimens and TGF-beta1 serum levels in patients with chronic hepatitis C before and after antiviral therapy. J Clin Pharm Ther **30:**271-7.
241. **Marsh, M., and A. Helenius.** 2006. Virus entry: open sesame. Cell **124:**729-40.
242. **Martin, C., S. U. Nielsen, S. Ibrahim, M. F. Bassendine, and G. L. Toms.** 2008. Binding of liver derived, low density hepatitis C virus to human hepatoma cells. J Med Virol **80:**816-23.
243. **Martin, C. A., E. Longman, C. Wooding, S. J. Hoosdally, S. Ali, T. J. Aitman, D. A. Gutmann, P. S. Freemont, B. Byrne, and K. J. Linton.** 2007. Cd36, a class B scavenger receptor, functions as a monomer to bind acetylated and oxidized low-density lipoproteins. Protein Sci **16:**2531-41.
244. **Martin, F., D. M. Roth, D. A. Jans, C. W. Pouton, L. J. Partridge, P. N. Monk, and G. W. Moseley.** 2005. Tetraspanins in viral infections: a fundamental role in viral biology? J Virol **79:**10839-51.
245. **Marukian, S., L. Andrus, T. P. Sheahan, C. T. Jones, E. D. Charles, A. Ploss, C. M. Rice, and L. B. Dustin.** 2011. Hepatitis C virus induces interferon-lambda and interferon-stimulated genes in primary liver cultures. Hepatology.
246. **Mastellos, D., J. C. Papadimitriou, S. Franchini, P. A. Tsonis, and J. D. Lambris.** 2001. A novel role of complement: mice deficient in the fifth component of complement (C5) exhibit impaired liver regeneration. J Immunol **166:**2479-86.
247. **Mateu, M. G.** 2011. Virus engineering: functionalization and stabilization. Protein Eng Des Sel **24:**53-63.
248. **Matsuo, N., H. Shiraha, T. Fujikawa, N. Takaoka, N. Ueda, S. Tanaka, S. Nishina, Y. Nakanishi, M. Uemura, A. Takaki, S. Nakamura, Y. Kobayashi, K. Nouso, T. Yagi, and K. Yamamoto.** 2009. Twist expression promotes migration and invasion in hepatocellular carcinoma. BMC Cancer **9:**240.
249. **Mazzeo, C., F. Azzaroli, S. Giovanelli, A. Dormi, D. Festi, A. Colecchia, A. Miracolo, P. Natale, G. Nigro, A. Alberti, E. Roda, and G. Mazzella.** 2003. Ten year incidence of HCV infection in northern Italy and frequency of spontaneous viral clearance. Gut **52:**1030-4.
250. **Mazzocca, A., E. Fransvea, G. Lavezzari, S. Antonaci, and G. Giannelli.** 2009. Inhibition of transforming growth factor beta receptor I kinase blocks hepatocellular carcinoma growth through neo-angiogenesis regulation. Hepatology **50:**1140-51.
251. **McCarthy, K. M., S. A. Francis, J. M. McCormack, J. Lai, R. A. Rogers, I. B. Skare, R. D. Lynch, and E. E. Schneeberger.** 2000. Inducible expression of claudin-1-myc but not occludin-VSV-G results in aberrant tight junction strand formation in MDCK cells. J Cell Sci **113 Pt 19:**3387-98.

252. **McCaughan, G. W., N. A. Shackel, P. Bertolino, and D. G. Bowen.** 2009. Molecular and cellular aspects of hepatitis C virus reinfection after liver transplantation: how the early phase impacts on outcomes. Transplantation **87:**1105-11.
253. **McGivern, D. R., and S. M. Lemon.** 2011. Virus-specific mechanisms of carcinogenesis in hepatitis C virus associated liver cancer. Oncogene **30:**1969-83.
254. **McKeating, J. A., L. Q. Zhang, C. Logvinoff, M. Flint, J. Zhang, J. Yu, D. Butera, D. D. Ho, L. B. Dustin, C. M. Rice, and P. Balfe.** 2004. Diverse hepatitis C virus glycoproteins mediate viral infection in a CD81-dependent manner. J Virol **78:**8496-505.
255. **McLauchlan, J.** 2009. Hepatitis C virus: viral proteins on the move. Biochem Soc Trans **37:**986-90.
256. **McLauchlan, J.** 2009. Lipid droplets and hepatitis C virus infection. Biochim Biophys Acta **1791:**552-9.
257. **McLauchlan, J., M. K. Lemberg, G. Hope, and B. Martoglio.** 2002. Intramembrane proteolysis promotes trafficking of hepatitis C virus core protein to lipid droplets. EMBO J **21:**3980-8.
258. **Mee, C. J., M. J. Farquhar, H. J. Harris, K. Hu, W. Ramma, A. Ahmed, P. Maurel, R. Bicknell, P. Balfe, and J. A. McKeating.** 2010. Hepatitis C virus infection reduces hepatocellular polarity in a vascular endothelial growth factor-dependent manner. Gastroenterology **138:**1134-42.
259. **Mee, C. J., J. Grove, H. J. Harris, K. Hu, P. Balfe, and J. A. McKeating.** 2008. Effect of cell polarization on hepatitis C virus entry. J Virol **82:**461-70.
260. **Mee, C. J., H. J. Harris, M. J. Farquhar, G. Wilson, G. Reynolds, C. Davis, I. S. C. van, P. Balfe, and J. A. McKeating.** 2009. Polarization restricts hepatitis C virus entry into HepG2 hepatoma cells. J Virol **83:**6211-21.
261. **Meertens, L., C. Bertaux, L. Cukierman, E. Cormier, D. Lavillette, F. L. Cosset, and T. Dragic.** 2008. The tight junction proteins claudin-1, -6, and -9 are entry cofactors for hepatitis C virus. J Virol **82:**3555-60.
262. **Meertens, L., C. Bertaux, and T. Dragic.** 2006. Hepatitis C virus entry requires a critical postinternalization step and delivery to early endosomes via clathrin-coated vesicles. J Virol **80:**11571-8.
263. **Mensa, L., G. Crespo, M. J. Gastinger, J. Kabat, S. Perez-del-Pulgar, R. Miquel, S. U. Emerson, R. H. Purcell, and X. Forns.** 2011. Hepatitis C virus receptors claudin-1 and occludin after liver transplantation and influence on early viral kinetics. Hepatology **53:**1436-45.
264. **Meulmeester, E., and P. Ten Dijke.** 2011. The dynamic roles of TGF-beta in cancer. J Pathol **223:**205-18.
265. **Meulmeester, E., and P. Ten Dijke.** The dynamic roles of TGF-beta in cancer. J Pathol **223:**205-18.
266. **Meunier, J. C., R. E. Engle, K. Faulk, M. Zhao, B. Bartosch, H. Alter, S. U. Emerson, F. L. Cosset, R. H. Purcell, and J. Bukh.** 2005. Evidence for cross-genotype neutralization of hepatitis C virus pseudo-particles and enhancement of infectivity by apolipoprotein C1. Proc Natl Acad Sci U S A **102:**4560-5.
267. **Michalak, J. P., C. Wychowski, A. Choukhi, J. C. Meunier, S. Ung, C. M. Rice, and J. Dubuisson.** 1997. Characterization of truncated forms of hepatitis C virus glycoproteins. J Gen Virol **78 (Pt 9):**2299-306.
268. **Michalopoulos, G. K., and M. DeFrances.** 2005. Liver regeneration. Adv Biochem Eng Biotechnol **93:**101-34.
269. **Michalopoulos, G. K., and M. C. DeFrances.** 1997. Liver regeneration. Science **276:**60-6.

270. **Michta, M. L., S. E. Hopcraft, C. M. Narbus, Z. Kratovac, B. Israelow, M. Sourisseau, and M. J. Evans.** 2010. Species-specific regions of occludin required by hepatitis C virus for cell entry. Journal of virology **84:**11696-708.
271. **Michta, M. L., S. E. Hopcraft, C. M. Narbus, Z. Kratovac, B. Israelow, M. Sourisseau, and M. J. Evans.** 2010. Species-specific regions of occludin required by hepatitis C virus for cell entry. J Virol **84:**11696-708.
272. **Mitry, R. R.** 2009. Isolation of human hepatocytes. Methods Mol Biol **481:**17-23.
273. **Miyanari, Y., K. Atsuzawa, N. Usuda, K. Watashi, T. Hishiki, M. Zayas, R. Bartenschlager, T. Wakita, M. Hijikata, and K. Shimotohno.** 2007. The lipid droplet is an important organelle for hepatitis C virus production. Nat Cell Biol **9:**1089-97.
274. **Monazahian, M., I. Bohme, S. Bonk, A. Koch, C. Scholz, S. Grethe, and R. Thomssen.** 1999. Low density lipoprotein receptor as a candidate receptor for hepatitis C virus. J Med Virol **57:**223-9.
275. **Moradpour, D., F. Penin, and C. M. Rice.** 2007. Replication of hepatitis C virus. Nat Rev Microbiol **5:**453-63.
276. **Mousavi, S. A., L. Malerod, T. Berg, and R. Kjeken.** 2004. Clathrin-dependent endocytosis. Biochem J **377:**1-16.
277. **Munoz De Bustillo, E., C. Ibarrola, F. Colina, G. Castellano, A. Fuertes, A. Andres, J. M. Aguado, J. L. Rodicio, and J. M. Morales.** 1998. Fibrosing cholestatic hepatitis in hepatitis C virus-infected renal transplant recipients. J Am Soc Nephrol **9:**1109-13.
278. **Mwaikambo, B. R., C. Yang, S. Chemtob, and P. Hardy.** 2009. Hypoxia up-regulates CD36 expression and function via hypoxia-inducible factor-1- and phosphatidylinositol 3-kinase-dependent mechanisms. J Biol Chem **284:**26695-707.
279. **Nahmias, Y., M. Casali, L. Barbe, F. Berthiaume, and M. L. Yarmush.** 2006. Liver endothelial cells promote LDL-R expression and the uptake of HCV-like particles in primary rat and human hepatocytes. Hepatology **43:**257-65.
280. **Nasimuzzaman, M., G. Waris, D. Mikolon, D. G. Stupack, and A. Siddiqui.** 2007. Hepatitis C virus stabilizes hypoxia-inducible factor 1alpha and stimulates the synthesis of vascular endothelial growth factor. J Virol **81:**10249-57.
281. **Navaratnarajah, C. K., S. Vongpunsawad, N. Oezguen, T. Stehle, W. Braun, T. Hashiguchi, K. Maenaka, Y. Yanagi, and R. Cattaneo.** 2008. Dynamic interaction of the measles virus hemagglutinin with its receptor signaling lymphocytic activation molecule (SLAM, CD150). J Biol Chem **283:**11763-71.
282. **Navas, S., J. Martin, J. A. Quiroga, I. Castillo, and V. Carreno.** 1998. Genetic diversity and tissue compartmentalization of the hepatitis C virus genome in blood mononuclear cells, liver, and serum from chronic hepatitis C patients. J Virol **72:**1640-6.
283. **Neil, D. A., and S. G. Hubscher.** 2001. Are parenchymal changes in early post-transplant biopsies related to preservation-reperfusion injury or rejection? Transplantation **71:**1566-72.
284. **Neumann, A. U., N. P. Lam, H. Dahari, D. R. Gretch, T. E. Wiley, T. J. Layden, and A. S. Perelson.** 1998. Hepatitis C viral dynamics in vivo and the antiviral efficacy of interferon-alpha therapy. Science **282:**103-107.
285. **Nielsen, S. U., M. F. Bassendine, A. D. Burt, C. Martin, W. Pumeechockchai, and G. L. Toms.** 2006. Association between hepatitis C virus and very-low-density lipoprotein (VLDL)/LDL analyzed in iodixanol density gradients. J Virol **80:**2418-28.
286. **Niessen, C. M.** 2007. Tight junctions/adherens junctions: basic structure and function. J Invest Dermatol **127:**2525-32.
287. **Nieto, M. A.** 2009. Epithelial-Mesenchymal Transitions in development and disease: old views and new perspectives. Int J Dev Biol **53:**1541-7.

288. **Nusrat, A., C. A. Parkos, P. Verkade, C. S. Foley, T. W. Liang, W. Innis-Whitehouse, K. K. Eastburn, and J. L. Madara.** 2000. Tight junctions are membrane microdomains. J Cell Sci **113 (Pt 10):**1771-81.
289. **Oft, M., J. Peli, C. Rudaz, H. Schwarz, H. Beug, and E. Reichmann.** 1996. TGF-beta1 and Ha-Ras collaborate in modulating the phenotypic plasticity and invasiveness of epithelial tumor cells. Genes Dev **10:**2462-77.
290. **Okano, J., G. Shiota, K. Matsumoto, S. Yasui, A. Kurimasa, I. Hisatome, P. Steinberg, and Y. Murawaki.** 2003. Hepatocyte growth factor exerts a proliferative effect on oval cells through the PI3K/AKT signaling pathway. Biochem Biophys Res Commun **309:**298-304.
291. **Okuda, M., K. Li, M. R. Beard, L. A. Showalter, F. Scholle, S. M. Lemon, and S. A. Weinman.** 2002. Mitochondrial injury, oxidative stress, and antioxidant gene expression are induced by hepatitis C virus core protein. Gastroenterology **122:**366-75.
292. **Omenetti, A., L. Yang, Y. X. Li, S. J. McCall, Y. Jung, J. K. Sicklick, J. Huang, S. Choi, A. Suzuki, and A. M. Diehl.** 2007. Hedgehog-mediated mesenchymal-epithelial interactions modulate hepatic response to bile duct ligation. Lab Invest **87:**499-514.
293. **Orban, E., E. Szabo, G. Lotz, P. Kupcsulik, C. Paska, Z. Schaff, and A. Kiss.** 2008. Different expression of occludin and ZO-1 in primary and metastatic liver tumors. Pathol Oncol Res **14:**299-306.
294. **Otto, G. A., and J. D. Puglisi.** 2004. The pathway of HCV IRES-mediated translation initiation. Cell **119:**369-80.
295. **Owen, D. M., H. Huang, J. Ye, and M. Gale, Jr.** 2009. Apolipoprotein E on hepatitis C virion facilitates infection through interaction with low-density lipoprotein receptor. Virology **394:**99-108.
296. **Owsianka, A. M., A. W. Tarr, Z. Y. Keck, T. K. Li, J. Witteveldt, R. Adair, S. K. Foung, J. K. Ball, and A. H. Patel.** 2008. Broadly neutralizing human monoclonal antibodies to the hepatitis C virus E2 glycoprotein. J Gen Virol **89:**653-9.
297. **Owsianka, A. M., J. M. Timms, A. W. Tarr, R. J. Brown, T. P. Hickling, A. Szwejk, K. Bienkowska-Szewczyk, B. J. Thomson, A. H. Patel, and J. K. Ball.** 2006. Identification of conserved residues in the E2 envelope glycoprotein of the hepatitis C virus that are critical for CD81 binding. J Virol **80:**8695-704.
298. **Parathath, S., M. A. Connelly, R. A. Rieger, S. M. Klein, N. A. Abumrad, M. De La Llera-Moya, C. R. Iden, G. H. Rothblat, and D. L. Williams.** 2004. Changes in plasma membrane properties and phosphatidylcholine subspecies of insect Sf9 cells due to expression of scavenger receptor class B, type I, and CD36. J Biol Chem **279:**41310-8.
299. **Paris, L., L. Tonutti, C. Vannini, and G. Bazzoni.** 2008. Structural organization of the tight junctions. Biochim Biophys Acta **1778:**646-59.
300. **Paul, J. H., W.P., A.Sabin.** 1945. Transmission experiments in serum jaundice and infectious hepatitis. Journal of the American Medical Association **128**.
301. **Pawlotsky, J. M.** 1999. Diagnostic tests for hepatitis C. J Hepatol **31 Suppl 1:**71-9.
302. **Peckett, A. J., D. C. Wright, and M. C. Riddell.** 2011. The effects of glucocorticoids on adipose tissue lipid metabolism. Metabolism.
303. **Peinado, H., and A. Cano.** 2008. A hypoxic twist in metastasis. Nat Cell Biol **10:**253-4.
304. **Pereira Tde, A., R. P. Witek, W. K. Syn, S. S. Choi, S. Bradrick, G. F. Karaca, K. M. Agboola, Y. Jung, A. Omenetti, C. A. Moylan, L. Yang, M. E. Fernandez-Zapico, R. Jhaveri, V. H. Shah, F. E. Pereira, and A. M. Diehl.** 2010. Viral factors induce Hedgehog pathway activation in humans with viral hepatitis, cirrhosis, and hepatocellular carcinoma. Lab Invest **90:**1690-703.
305. **Perrault, M., and E. I. Pecheur.** 2009. The hepatitis C virus and its hepatic environment: a toxic but finely tuned partnership. Biochem J **423:**303-14.

306. **Perz, J. F., and M. J. Alter.** 2006. The coming wave of HCV-related liver disease: dilemmas and challenges. J Hepatol **44:**441-3.
307. **Petit, J. M., A. Minello, L. Duvillard, V. Jooste, S. Monier, V. Texier, J. B. Bour, A. Poussier, P. Gambert, B. Verges, and P. Hillon.** 2007. Cell surface expression of LDL receptor in chronic hepatitis C: correlation with viral load. Am J Physiol Endocrinol Metab **293:**E416-20.
308. **Petracca, R., F. Falugi, G. Galli, N. Norais, D. Rosa, S. Campagnoli, V. Burgio, E. Di Stasio, B. Giardina, M. Houghton, S. Abrignani, and G. Grandi.** 2000. Structure-function analysis of hepatitis C virus envelope-CD81 binding. J Virol **74:**4824-30.
309. **Pfeffer, S., and T. F. Baumert.** 2009. Unravelling the importance of microRNAs during hepatitis C virus infection in the human liver. J Hepatol **51:**606-9.
310. **Pichard, L., E. Raulet, G. Fabre, J. B. Ferrini, J. C. Ourlin, and P. Maurel.** 2006. Human hepatocyte culture. Methods Mol Biol **320:**283-93.
311. **Pierce, L.** 1977. Anatomy and physiology of the liver in relation to clinical assessment. Nurs Clin North Am **12:**259-73.
312. **Pietschmann, T.** 2009. Virology: Final entry key for hepatitis C. Nature **457:**797-8.
313. **Pietschmann, T., V. Lohmann, A. Kaul, N. Krieger, G. Rinck, G. Rutter, D. Strand, and R. Bartenschlager.** 2002. Persistent and transient replication of full-length hepatitis C virus genomes in cell culture. J Virol **76:**4008-21.
314. **Pileri, P., Y. Uematsu, S. Campagnoli, G. Galli, F. Falugi, R. Petracca, A. J. Weiner, M. Houghton, D. Rosa, G. Grandi, and S. Abrignani.** 1998. Binding of hepatitis C virus to CD81. Science **282:**938-941.
315. **Pirenne, J., B. Gunson, H. Khaleef, S. Hubscher, S. Afford, P. McMaster, and D. Adams.** 1997. Influence of ischemia-reperfusion injury on rejection after liver transplantation. Transplant Proc **29:**366-7.
316. **Ploss, A., M. J. Evans, V. A. Gaysinskaya, M. Panis, H. You, Y. P. de Jong, and C. M. Rice.** 2009. Human occludin is a hepatitis C virus entry factor required for infection of mouse cells. Nature **457:**882-6.
317. **Ploss, A., M. J. Evans, V. A. Gaysinskaya, M. Panis, H. N. You, Y. P. de Jong, and C. M. Rice.** 2009. Human occludin is a hepatitis C virus entry factor required for infection of mouse cells. Nature **457:**882-886.
318. **Ploss, A., S. R. Khetani, C. T. Jones, A. J. Syder, K. Trehan, V. A. Gaysinskaya, K. Mu, K. Ritola, C. M. Rice, and S. N. Bhatia.** 2010. Persistent hepatitis C virus infection in microscale primary human hepatocyte cultures. Proceedings of the National Academy of Sciences **107:**3141-3145.
319. **Ploss, A., and C. M. Rice.** 2009. Towards a small animal model for hepatitis C. Embo Reports **10:**1220-1227.
320. **Podevin, P., A. Carpentier, V. Pène, L. Aoudjehane, M. Carrière, S. Zaïdi, C. Hernandez, V. Calle, J. F. Méritet, and O. Scatton.** 2010. Production of Infectious Hepatitis C Virus in Primary Cultures of Human Adult Hepatocytes. Gastroenterology **139:**1355-1364.e6.
321. **Pohlmann, S., J. Zhang, F. Baribaud, Z. Chen, G. J. Leslie, G. Lin, A. Granelli-Piperno, R. W. Doms, C. M. Rice, and J. A. McKeating.** 2003. Hepatitis C virus glycoproteins interact with DC-SIGN and DC-SIGNR. J Virol **77:**4070-80.
322. **Pohlmann, S., J. Zhang, F. Baribaud, Z. W. Chen, G. Leslie, G. Lin, A. Granelli-Piperno, R. W. Dom, C. M. Rice, and J. A. McsKeating.** 2003. Hepatitis C virus glycoproteins interact with DC-SIGN and DC-SIGNR. Journal of Virology **77:**4070-4080.
323. **Poordad, F., J. McCone, Jr., B. R. Bacon, S. Bruno, M. P. Manns, M. S. Sulkowski, I. M. Jacobson, K. R. Reddy, Z. D. Goodman, N. Boparai, M. J. DiNubile, V. Sniukiene, C. A. Brass, J. K. Albrecht, and J. P. Bronowicki.** 2011. Boceprevir for untreated chronic HCV genotype 1 infection. N Engl J Med **364:**1195-206.

324. **Popescu, C. I., and J. Dubuisson.** 2010. Role of lipid metabolism in hepatitis C virus assembly and entry. Biol Cell **102:**63-74.
325. **Powers, K. A., R. M. Ribeiro, K. Patel, S. Pianko, L. Nyberg, P. Pockros, A. J. Conrad, J. McHutchison, and A. S. Perelson.** 2006. Kinetics of hepatitis C virus reinfection after liver transplantation. Liver Transpl **12:**207-16.
326. **Presser, L. D., A. Haskett, and G. Waris.** 2011. Hepatitis C virus-induced furin and thrombospondin-1 activate TGF-beta1: role of TGF-beta1 in HCV replication. Virology **412:**284-96.
327. **Prince, A. M., Brotman B., Grady G. F., Kuhns W. J., Hazzi R., Levine W., and Millian S. J.** 1974. Long-incubation post-transfusion hepatitis without serological evidence of exposure to hepatitis-B virus. Lancet **2:**241-6.
328. **Quaglia, A., S. C. Lehec, R. D. Hughes, R. R. Mitry, A. S. Knisely, S. Devereaux, J. Richards, M. Rela, N. D. Heaton, B. C. Portmann, and A. Dhawan.** 2008. Liver after hepatocyte transplantation for liver-based metabolic disorders in children. Cell Transplant **17:**1403-14.
329. **Quintavalle, M., S. Sambucini, C. Di Pietro, R. De Francesco, and P. Neddermann.** 2006. The alpha isoform of protein kinase CKI is responsible for hepatitis C virus NS5A hyperphosphorylation. J Virol **80:**11305-12.
330. **Raine, A. E., R. Carter, J. I. Mann, and P. J. Morris.** 1988. Adverse effect of cyclosporin on plasma cholesterol in renal transplant recipients. Nephrol Dial Transplant **3:**458-63.
331. **Ramirez, S., S. Perez-Del-Pulgar, J. A. Carrion, J. Costa, P. Gonzalez, A. Massaguer, C. Fondevila, J. C. Garcia-Valdecasas, M. Navasa, and X. Forns.** 2009. Hepatitis C virus compartmentalization and infection recurrence after liver transplantation. Am J Transplant **9:**1591-601.
332. **Ramirez, S., S. Perez-Del-Pulgar, J. A. Carrion, J. Costa, P. Gonzalez, A. Massaguer, C. Fondevila, J. C. Garcia-Valdecasas, M. Navasa, and X. Forns.** 2009. Hepatitis C virus compartmentalization and infection recurrence after liver transplantation. American journal of transplantation : official journal of the American Society of Transplantation and the American Society of Transplant Surgeons **9:**1591-601.
333. **Ramirez, S., S. Perez-Del-Pulgar, J. A. Carrion, M. Coto-Llerena, L. Mensa, J. Dragun, J. C. Garcia-Valdecasas, M. Navasa, and X. Forns.** 2010. Hepatitis C virus superinfection of liver grafts: a detailed analysis of early exclusion of non-dominant virus strains. Journal of General Virology **91:**1183-1188.
334. **Randall, G., M. Panis, J. D. Cooper, T. L. Tellinghuisen, K. E. Sukhodolets, S. Pfeffer, M. Landthaler, P. Landgraf, S. Kan, B. D. Lindenbach, M. Chien, D. B. Weir, J. J. Russo, J. Ju, M. J. Brownstein, R. Sheridan, C. Sander, M. Zavolan, T. Tuschl, and C. M. Rice.** 2007. Cellular cofactors affecting hepatitis C virus infection and replication. Proc Natl Acad Sci U S A **104:**12884-9.
335. **Regan, A. D., and G. R. Whittaker.** 2008. Utilization of DC-SIGN for entry of feline coronaviruses into host cells. J Virol **82:**11992-6.
336. **Regeard, M., C. Lepere, M. Trotard, P. Gripon, and J. Le Seyec.** 2007. Recent contributions of in vitro models to our understanding of hepatitis C virus life cycle. FEBS J **274:**4705-18.
337. **Regeard, M., M. Trotard, C. Lepere, P. Gripon, and J. Le Seyec.** 2008. Entry of pseudotyped hepatitis C virus into primary human hepatocytes depends on the scavenger class B type I receptor. J Viral Hepat **15:**865-70.
338. **Resti, M., P. Jara, L. Hierro, C. Azzari, R. Giacchino, G. Zuin, L. Zancan, S. Pedditzi, and F. Bortolotti.** 2003. Clinical features and progression of perinatally acquired hepatitis C virus infection. J Med Virol **70:**373-7.

339. **Rexroad, J., T. T. Martin, D. McNeilly, S. Godwin, and C. R. Middaugh.** 2006. Thermal stability of adenovirus type 2 as a function of pH. J Pharm Sci **95:**1469-79.
340. **Rexroad, J., C. M. Wiethoff, A. P. Green, T. D. Kierstead, M. O. Scott, and C. R. Middaugh.** 2003. Structural stability of adenovirus type 5. J Pharm Sci **92:**665-78.
341. **Reynolds, G. M., H. J. Harris, A. Jennings, K. Hu, J. Grove, P. F. Lalor, D. H. Adams, P. Balfe, S. G. Hubscher, and J. A. McKeating.** 2008. Hepatitis C virus receptor expression in normal and diseased liver tissue. Hepatology **47:**418-27.
342. **Rhainds, D., P. Bourgeois, G. Bourret, K. Huard, L. Falstrault, and L. Brissette.** 2004. Localization and regulation of SR-BI in membrane rafts of HepG2 cells. J Cell Sci **117:**3095-105.
343. **Rice, C. M.** 2011. New insights into HCV replication: potential antiviral targets. Top Antivir Med **19:**117-20.
344. **Ripoli, M., A. D'Aprile, G. Quarato, M. Sarasin-Filipowicz, J. Gouttenoire, R. Scrima, O. Cela, D. Boffoli, M. H. Heim, D. Moradpour, N. Capitanio, and C. Piccoli.** 2010. Hepatitis C Virus-Linked Mitochondrial Dysfunction Promotes Hypoxia-Inducible Factor 1 alpha-Mediated Glycolytic Adaptation. Journal of Virology **84:**647-660.
345. **Roberts, A. B., and L. M. Wakefield.** 2003. The two faces of transforming growth factor beta in carcinogenesis. Proc Natl Acad Sci U S A **100:**8621-3.
346. **Rocha-Perugini, V., C. Montpellier, D. Delgrange, C. Wychowski, F. Helle, A. Pillez, H. Drobecq, F. Le Naour, S. Charrin, S. Levy, E. Rubinstein, J. Dubuisson, and L. Cocquerel.** 2008. The CD81 partner EWI-2wint inhibits hepatitis C virus entry. PLoS ONE **3:**e1866.
347. **Rosa, D., G. Saletti, E. De Gregorio, F. Zorat, C. Comar, U. D'Oro, S. Nuti, M. Houghton, V. Barnaba, G. Pozzato, and S. Abrignani.** 2005. Activation of naive B lymphocytes via CD81, a pathogenetic mechanism for hepatitis C virus-associated B lymphocyte disorders. Proc Natl Acad Sci U S A **102:**18544-9.
348. **Rosenstein, B. J.** 1967. Viral hepatitis in narcotics users. An outbreak in Rhode Island. JAMA **199:**698-700.
349. **Rothwangl, K. B., B. Manicassamy, S. L. Uprichard, and L. Rong.** 2008. Dissecting the role of putative CD81 binding regions of E2 in mediating HCV entry: putative CD81 binding region 1 is not involved in CD81 binding. Virol J **5:**46.
350. **Rowe, I. A., K. M. Barber, R. Birch, E. Curnow, and J. M. Neuberger.** 2010. Retransplantation for graft failure in chronic hepatitis C infection: a good use of a scarce resource? World journal of gastroenterology : WJG **16:**5070-6.
351. **Rubbia-Brandt, L., R. Quadri, K. Abid, E. Giostra, P. J. Male, G. Mentha,, and J. P. Z. L. Spahr, B. Borisch, A. Hadengue, and F. Negro.** 2002. Hepatocyte steatosis is a cytopathic effect of hepatitis C virus genotype 3. J Hepatol **33:**106-15.
352. **Rustgi, V. K.** 2007. The epidemiology of hepatitis C infection in the United States. Journal of Gastroenterology **42:**513-521.
353. **Saito, T., D. M. Owen, F. Jiang, J. Marcotrigiano, and M. Gale, Jr.** 2008. Innate immunity induced by composition-dependent RIG-I recognition of hepatitis C virus RNA. Nature **454:**523-7.
354. **Sala-Valdes, M., A. Ursa, S. Charrin, E. Rubinstein, M. E. Hemler, F. Sanchez-Madrid, and M. Yanez-Mo.** 2006. EWI-2 and EWI-F link the tetraspanin web to the actin cytoskeleton through their direct association with ezrin-radixin-moesin proteins. J Biol Chem **281:**19665-75.
355. **Samonakis, D. N., G. Germani, and A. K. Burroughs.** 2011. Immunosuppression and HCV Recurrence after Liver Transplantation. J Hepatol.
356. **Sangar, D. V., and A. R. Carroll.** 1998. A tale of two strands: reverse-transcriptase polymerase chain reaction detection of hepatitis C virus replication. Hepatology **28:**1173-6.

357. **Scarselli, E., H. Ansuini, R. Cerino, R. M. Roccasecca, S. Acali, G. Filocamo, C. Traboni, A. Nicosia, R. Cortese, and A. Vitelli.** 2002. The human scavenger receptor class B type I is a novel candidate receptor for the hepatitis C virus. Embo Journal **21:**5017-5025.
358. **Schalm, S. W., G. Fattovich, and J.T. Brouwer. .** 1997. Theraphy of hepatitis C: patients with cirrhosis Hepatology **26:**128S-132S.
359. **Scheel, C., T. Onder, A. Karnoub, and R. A. Weinberg.** 2007. Adaptation versus selection: the origins of metastatic behavior. Cancer Res **67:**11476-9; discussion 11479-80.
360. **Scheel, T. K., J. M. Gottwein, T. B. Jensen, J. C. Prentoe, A. M. Hoegh, H. J. Alter, J. Eugen-Olsen, and J. Bukh.** 2008. Development of JFH1-based cell culture systems for hepatitis C virus genotype 4a and evidence for cross-genotype neutralization. Proc Natl Acad Sci U S A **105:**997-1002.
361. **Schmidt-Mende, J., E. Bieck, T. Hugle, F. Penin, C. M. Rice, H. E. Blum, and D. Moradpour.** 2001. Determinants for membrane association of the hepatitis C virus RNA-dependent RNA polymerase. J Biol Chem **276:**44052-63.
362. **Schmitt, M., A. Horbach, R. Kubitz, A. Frilling, and D. Haussinger.** 2004. Disruption of hepatocellular tight junctions by vascular endothelial growth factor (VEGF): a novel mechanism for tumor invasion. Journal of Hepatology **41:**274-283.
363. **Schuster, C., and T. F. Baumert.** 2009. EWI-2wint--a host cell factor inhibiting hepatitis C virus entry. J Hepatol **50:**222-4.
364. **Schwarz, A. K., J. Grove, K. Hu, C. J. Mee, P. Balfe, and J. A. McKeating.** 2009. Hepatoma cell density promotes claudin-1 and scavenger receptor BI expression and hepatitis C virus internalization. J Virol **83:**12407-14.
365. **Seeff, L. B.** 2009. The history of the "natural history" of hepatitis C (1968-2009). Liver Int **29 Suppl 1:**89-99.
366. **Seeff, L. B.** 2002. Natural history of chronic hepatitis C. Hepatology **36:**S35-46.
367. **Seeff, L. B.** 2000. Why is there such difficulty in defining the natural history of hepatitis C? Transfusion **40:**1161-4.
368. **Selden, C., M. Khalil, and H. J. Hodgson.** 1999. What keeps hepatocytes on the straight and narrow? Maintaining differentiated function in the liver. Gut **44:**443-6.
369. **Semenza, G. L., L. A. Shimoda, and N. R. Prabhakar.** 2006. Regulation of gene expression by HIF-1. Novartis Found Symp **272:**2-8; discussion 8-14, 33-6.
370. **Shepard, C. W., L. Finelli, and M. J. Alter.** 2005. Global epidemiology of hepatitis C virus infection. Lancet Infect Dis **5:**558-67.
371. **Sherer, N. M., J. Jin, and W. Mothes.** Directional spread of surface-associated retroviruses regulated by differential virus-cell interactions. J Virol **84:**3248-58.
372. **Shields, P. L., C. M. Morland, M. Salmon, S. Qin, S. G. Hubscher, and D. H. Adams.** 1999. Chemokine and chemokine receptor interactions provide a mechanism for selective T cell recruitment to specific liver compartments within hepatitis C-infected liver. J Immunol **163:**6236-43.
373. **Shin, K., V. C. Fogg, and B. Margolis.** 2006. Tight junctions and cell polarity. Annu Rev Cell Dev Biol **22:**207-35.
374. **Shirota, Y., H. Luo, W. Qin, S. Kaneko, T. Yamashita, K. Kobayashi, and S. Murakami.** 2002. Hepatitis C virus (HCV) NS5A binds RNA-dependent RNA polymerase (RdRP) NS5B and modulates RNA-dependent RNA polymerase activity. J Biol Chem **277:**11149-55.
375. **Shoukry, N. H., A. Grakoui, M. Houghton, D.Y. Chien, J. Ghrayeb, K.A. Reimann, and C.M. Walker.** 2003. Memory CD8+ T cells are required for protection from persistent hepatitis c virus infection J Exp Med **197:**1645-55.

376. **Silvie, O., S. Charrin, M. Billard, J. F. Franetich, K. L. Clark, G. J. van Gemert, R. W. Sauerwein, F. Dautry, C. Boucheix, D. Mazier, and E. Rubinstein.** 2006. Cholesterol contributes to the organization of tetraspanin-enriched microdomains and to CD81-dependent infection by malaria sporozoites. J Cell Sci **119:**1992-2002.

377. **Simmonds, P., E. C. Holmes, T. A. Cha, S. W. Chan, F. Mcomish, B. Irvine, E. Beall, P. L. Yap, J. Kolberg, and M. S. Urdea.** 1993. Classification of Hepatitis-C Virus into 6 Major Genotypes and a Series of Subtypes by Phylogenetic Analysis of the Ns-5 Region. Journal of General Virology **74:**2391-2399.

378. **Smedsrod, B., P. J. De Bleser, F. Braet, P. Lovisetti, K. Vanderkerken, E. Wisse, and A. Geerts.** 1994. Cell biology of liver endothelial and Kupffer cells. Gut **35:**1509-16.

379. **Smith, A. E., and A. Helenius.** 2004. How viruses enter animal cells. Science **304:**237-42.

380. **Song, H., J. Li, S. Shi, L. Yan, H. Zhuang, and K. Li.** 2010. Thermal stability and inactivation of hepatitis C virus grown in cell culture. Virol J **7:**40.

381. **Spanakis, N. E., G. A. Garinis, E. C. Alexopoulos, G. P. Patrinos, P. G. Menounos, A. Sklavounou, E. N. Manolis, V. G. Gorgoulis, and D. Valis.** 2002. Cytokine serum levels in patients with chronic HCV infection. J Clin Lab Anal **16:**40-6.

382. **Strey, C. W., M. Markiewski, D. Mastellos, R. Tudoran, L. A. Spruce, L. E. Greenbaum, and J. D. Lambris.** 2003. The proinflammatory mediators C3a and C5a are essential for liver regeneration. J Exp Med **198:**913-23.

383. **Strickland, G. T., S. S. El-Kamary, P. Klenerman, and A. Nicosia.** 2008. Hepatitis C vaccine: supply and demand. Lancet Infect Dis **8:**379-86.

384. **Stumper, R., Y. M. Loo, E. Foy, K. Li, M. Yoneyama, T. Fujita, S. M. Lemon, and M. Gale.** 2005. Regulating intracellular antiviral defense and permissiveness to hepatitis C virus RNA replication through a cellular RNA helicase, RIG-I. Journal of Virology **79:**2689-2699.

385. **Su, A. I., J. P. Pezacki, L. Wodicka, A. D. Brideau, L. Supekova, R. Thimme, S. Wieland, J. Bukh, R. H. Purcell, P. G. Schultz, and F. V. Chisari.** 2002. Genomic analysis of the host response to hepatitis C virus infection. Proc Natl Acad Sci U S A **99:**15669-74.

386. **Sumpter, R., Jr., Y. M. Loo, E. Foy, K. Li, M. Yoneyama, T. Fujita, S. M. Lemon, and M. Gale, Jr.** 2005. Regulating intracellular antiviral defense and permissiveness to hepatitis C virus RNA replication through a cellular RNA helicase, RIG-I. J Virol **79:**2689-99.

387. **Sun, T., N. Zhao, X. L. Zhao, Q. Gu, S. W. Zhang, N. Che, X. H. Wang, J. Du, Y. X. Liu, and B. C. Sun.** 2010. Expression and functional significance of Twist1 in hepatocellular carcinoma: its role in vasculogenic mimicry. Hepatology **51:**545-56.

388. **Sun, Y. Y., C. Y. Wang, M. F. Hsu, S. H. Juan, C. Y. Chang, C. M. Chou, L. Y. Yang, K. S. Hung, J. Xu, Y. H. Lee, and C. Y. Hsu.** 2010. Glucocorticoid protection of oligodendrocytes against excitotoxin involving hypoxia-inducible factor-1alpha in a cell-type-specific manner. J Neurosci **30:**9621-30.

389. **Syder, A. J., H. Lee, M. B. Zeisel, J. Grove, E. Soulier, J. Macdonald, S. Chow, J. Chang, T. F. Baumert, J. A. McKeating, J. McKelvy, and F. Wong-Staal.** 2011. Small molecule scavenger receptor BI antagonists are potent HCV entry inhibitors. J Hepatol **54:**48-55.

390. **Tabor, E., R. J. Gerety, J. A. Drucker, L. B. Seeff, J. H. Hoofnagle, D. R. Jackson, M. April, L. F. Barker, and G. Pineda-Tamondong.** 1978. Transmission of non-A, non-B hepatitis from man to chimpanzee. Lancet **1:**463-6.

391. **Takyar, S. T., D. Li, Y. Wang, R. Trowbridge, and E. J. Gowans.** 2000. Specific detection of minus-strand hepatitis C virus RNA by reverse-transcription polymerase chain reaction on PolyA(+)-purified RNA. Hepatology **32:**382-7.

392. **Targett-Adams, P., S. Boulant, and J. McLauchlan.** 2008. Visualization of double-stranded RNA in cells supporting hepatitis C virus RNA replication. J Virol **82:**2182-95.
393. **Taub, R.** 2004. Liver regeneration: from myth to mechanism. Nat Rev Mol Cell Biol **5:**836-47.
394. **Tedbury, P., S. Welbourn, A. Pause, B. King, S. Griffin, and M. Harris.** 2011. The subcellular localization of the hepatitis C virus non-structural protein NS2 is regulated by an ion channel-independent function of the p7 protein. J Gen Virol **92:**819-30.
395. **Tellinghuisen, T. L., K. L. Foss, and J. Treadaway.** 2008. Regulation of hepatitis C virion production via phosphorylation of the NS5A protein. PLoS Pathog **4:**e1000032.
396. **Tellinghuisen, T. L., J. Marcotrigiano, A. E. Gorbalenya, and C. M. Rice.** 2004. The NS5A protein of hepatitis C virus is a zinc metalloprotein. J Biol Chem **279:**48576-87.
397. **Temel, R. E., B. Trigatti, R. B. DeMattos, S. Azhar, M. Krieger, and D. L. Williams.** 1997. Scavenger receptor class B, type I (SR-BI) is the major route for the delivery of high density lipoprotein cholesterol to the steroidogenic pathway in cultured mouse adrenocortical cells. Proc Natl Acad Sci U S A **94:**13600-5.
398. **Thiery, J. P., H. Acloque, R. Y. Huang, and M. A. Nieto.** 2009. Epithelial-mesenchymal transitions in development and disease. Cell **139:**871-90.
399. **Thimme, R., D.Oldach, K. M. Chang, C. Steiger, S. C. Ray, and F. V. Chisari.** 2001. Determinnts of viral clearance and persistence during acute hepatitis c virus infection. J Exp Med **194:**1395-406.
400. **Timpe, J. M., and J. A. McKeating.** 2008. Hepatitis C virus entry: possible targets for therapy. Gut **57:**1728-37.
401. **Timpe, J. M., Z. Stamataki, A. Jennings, K. Hu, M. J. Farquhar, H. J. Harris, A. Schwarz, I. Desombere, G. L. Roels, P. Balfe, and J. A. McKeating.** 2008. Hepatitis C virus cell-cell transmission in hepatoma cells in the presence of neutralizing antibodies. Hepatology **47:**17-24.
402. **Tscherne, D. M., C. T. Jones, M. J. Evans, B. D. Lindenbach, J. A. McKeating, and C. M. Rice.** 2006. Time- and temperature-dependent activation of hepatitis C virus for low-pH-triggered entry. J Virol **80:**1734-41.
403. **Tu, H., L. Gao, S. T. Shi, D. R. Taylor, T. Yang, A. K. Mircheff, Y. Wen, A. E. Gorbalenya, S. B. Hwang, and M. M. Lai.** 1999. Hepatitis C virus RNA polymerase and NS5A complex with a SNARE-like protein. Virology **263:**30-41.
404. **van Leeuwen, M. S., J. Noordzij, M. A. Fernandez, A. Hennipman, M. A. Feldberg, and E. H. Dillon.** 1994. Portal venous and segmental anatomy of the right hemiliver: observations based on three-dimensional spiral CT renderings. AJR Am J Roentgenol **163:**1395-404.
405. **van Zijl, F., G. Zulehner, M. Petz, D. Schneller, C. Kornauth, M. Hau, G. Machat, M. Grubinger, H. Huber, and W. Mikulits.** 2009. Epithelial-mesenchymal transition in hepatocellular carcinoma. Future Oncol **5:**1169-79.
406. **van Zijl, F., G. Zulehner, M. Petz, D. Schneller, C. Kornauth, M. Hau, G. Machat, M. Grubinger, H. Huber, and W. Mikulits.** 2009. Epithelial-mesenchymal transition in hepatocellular carcinoma. Future oncology **5:**1169-79.
407. **Vanwolleghem, T., J. Bukh, P. Meuleman, I. Desombere, J. C. Meunier, H. Alter, R. H. Purcell, and G. Leroux-Roels.** 2008. Polyclonal immunoglobulins from a chronic hepatitis C virus patient protect human liver-chimeric mice from infection with a homologous hepatitis C virus strain. Hepatology **47:**1846-55.
408. **Vegiopoulos, A., and S. Herzig.** 2007. Glucocorticoids, metabolism and metabolic diseases. Mol Cell Endocrinol **275:**43-61.
409. **Voisset, C., N. Callens, E. Blanchard, J. Dubuisson, and N. Vu-Dac.** 2005. High density lipoproteins facilitate hepatitis C virus entry through the scavenger receptor class B type I. Journal of Biological Chemistry **280:**7793-7799.

410. **Voisset, C., A. O. de Beeck, P. Horellou, M. Dreux, T. Gustot, G. Duverlie, F. L. Cosset, N. Vu-Dac, and J. Dubuisson.** 2006. High-density lipoproteins reduce the neutralizing effect of hepatitis C virus (HCV)-infected patient antibodies by promoting HCV entry. Journal of General Virology **87:**2577-2581.
411. **Voisset, C., and J. Dubuisson.** 2004. Functional hepatitis C virus envelope glycoproteins. Biol Cell **96:**413-20.
412. **von Hahn, T., B. D. Lindenbach, A. Boullier, O. Quehenberger, M. Paulson, C. M. Rice, and J. A. McKeating.** 2006. Oxidized low-density lipoprotein inhibits hepatitis C virus cell entry in human hepatoma cells. Hepatology **43:**932-942.
413. **von Hahn, T., B. D. Lindenbach, A. Boullier, O. Quehenberger, M. Paulson, C. M. Rice, and J. A. McKeating.** 2006. Oxidized low-density lipoprotein inhibits hepatitis C virus cell entry in human hepatoma cells. Hepatology **43:**932-42.
414. **von Hahn, T., and C. M. Rice.** 2008. Hepatitis C virus entry. Journal of Biological Chemistry **283:**3689-3693.
415. **Wakita, T., T. Pietschmann, T. Kato, T. Date, M. Miyamoto, Z. Zhao, K. Murthy, A. Habermann, H. G. Krausslich, M. Mizokami, R. Bartenschlager, and T. J. Liang.** 2005. Production of infectious hepatitis C virus in tissue culture from a cloned viral genome. Nat Med **11:**791-6.
416. **Wali, M. H., M. Heydtmann, R. F. Harrison, B. K. Gunson, and D. J. Mutimer.** 2003. Outcome of liver transplantation for patients infected by hepatitis C, including those infected by genotype 4. Liver Transpl **9:**796-804.
417. **Wang, H., C. Wang, T. Feng, H. Zhou, L. Li, F. Wang, G. Zhao, T. Zhu, and B. Zhou.** 2008. [DC-SIGNR polymorphisms and its association with HIV-1 infection]. Zhonghua Yi Xue Yi Chuan Xue Za Zhi **25:**542-5.
418. **Wang, L., and J. L. Boyer.** 2004. The maintenance and generation of membrane polarity in hepatocytes. Hepatology **39:**892-9.
419. **Wang, N., Y. Liang, S. Devaraj, J. Wang, S. M. Lemon, and K. Li.** 2009. Toll-like receptor 3 mediates establishment of an antiviral state against hepatitis C virus in hepatoma cells. J Virol **83:**9824-34.
420. **Waris, G., K. D. Tardif, and A. Siddiqui.** 2002. Endoplasmic reticulum (ER) stress: hepatitis C virus induces an ER-nucleus signal transduction pathway and activates NF-kappaB and STAT-3. Biochem Pharmacol **64:**1425-30.
421. **Wiggins, D., and G. F. Gibbons.** 1996. Origin of hepatic very-low-density lipoprotein triacylglycerol: the contribution of cellular phospholipid. Biochem J **320 (Pt 2):**673-9.
422. **Witteveldt, J., M. J. Evans, J. Bitzegeio, G. Koutsoudakis, A. M. Owsianka, A. G. Angus, Z. Y. Keck, S. K. Foung, T. Pietschmann, C. M. Rice, and A. H. Patel.** 2009. CD81 is dispensable for hepatitis C virus cell-to-cell transmission in hepatoma cells. J Gen Virol **90:**48-58.
423. **Wolk, B., D. Sansonno, H. G. Krausslich, F. Dammacco, C. M. Rice, H. E. Blum, and D. Moradpour.** 2000. Subcellular localization, stability, and trans-cleavage competence of the hepatitis C virus NS3-NS4A complex expressed in tetracycline-regulated cell lines. J Virol **74:**2293-304.
424. **Wong-Staal, F., A. J. Syder, and J. McKelvy.** 2010. Targeting HCV Entry For Development of Therapeutics. Viruses **2:**1718-1733.
425. **Woodhouse, S. D., R. Narayan, S. Latham, S. Lee, R. Antrobus, B. Gangadharan, S. Luo, G. P. Schroth, P. Klenerman, and N. Zitzmann.** 2010. Transcriptome sequencing, microarray, and proteomic analyses reveal cellular and metabolic impact of hepatitis C virus infection in vitro. Hepatology **52:**443-53.
426. **Wozniak, A. L., S. Griffin, D. Rowlands, M. Harris, M. Yi, S. M. Lemon, and S. A. Weinman.** 2010. Intracellular proton conductance of the hepatitis C virus p7 protein and its contribution to infectious virus production. PLoS Pathog **6:**e1001087.

427. **Wunschmann, S., J. D. Medh, D. Klinzmann, W. N. Schmidt, and J. T. Stapleton.** 2000. Characterization of hepatitis C virus (HCV) and HCV E2 interactions with CD81 and the low-density lipoprotein receptor. J Virol **74:**10055-62.

428. **Wunschmann, S., H. M. Muller, C. S. Stipp, M. E. Hemler, and J. T. Stapleton.** 2006. In vitro interaction between hepatitis C virus (HCV) envelope glycoprotein E2 and serum lipoproteins (LPs) results in enhanced cellular binding of both HCV E2 and LPs. Journal of Infectious Diseases **194:**1058-1067.

429. **Wustner, D., M. Mondal, A. Huang, and F. R. Maxfield.** 2004. Different transport routes for high density lipoprotein and its associated free sterol in polarized hepatic cells. J Lipid Res **45:**427-37.

430. **Yamashita, T., S. Kaneko, Y. Shirota, W. Qin, T. Nomura, K. Kobayashi, and S. Murakami.** 1998. RNA-dependent RNA polymerase activity of the soluble recombinant hepatitis C virus NS5B protein truncated at the C-terminal region. J Biol Chem **273:**15479-86.

431. **Yan, W., Y. Fu, D. Tian, J. Liao, M. Liu, B. Wang, L. Xia, Q. Zhu, and M. Luo.** 2009. PI3 kinase/Akt signaling mediates epithelial-mesenchymal transition in hypoxic hepatocellular carcinoma cells. Biochem Biophys Res Commun **382:**631-6.

432. **Yang, M. H., C. L. Chen, G. Y. Chau, S. H. Chiou, C. W. Su, T. Y. Chou, W. L. Peng, and J. C. Wu.** 2009. Comprehensive analysis of the independent effect of twist and snail in promoting metastasis of hepatocellular carcinoma. Hepatology **50:**1464-74.

433. **Yang, M. H., and K. J. Wu.** 2008. TWIST activation by hypoxia inducible factor-1 (HIF-1): implications in metastasis and development. Cell Cycle **7:**2090-6.

434. **Yang, W., C. Qiu, N. Biswas, J. Jin, S. C. Watkins, R. C. Montelaro, C. B. Coyne, and T. Wang.** 2008. Correlation of the tight junction-like distribution of Claudin-1 to the cellular tropism of hepatitis C virus. J Biol Chem **283:**8643-53.

435. **Ye, J., C. Wang, R. Sumpter, Jr., M. S. Brown, J. L. Goldstein, and M. Gale, Jr.** 2003. Disruption of hepatitis C virus RNA replication through inhibition of host protein geranylgeranylation. Proc Natl Acad Sci U S A **100:**15865-70.

436. **Yokoo, H., T. Kondo, K. Fujii, T. Yamada, S. Todo, and S. Hirohashi.** 2004. Proteomic signature corresponding to alpha fetoprotein expression in liver cancer cells. Hepatology **40:**609-17.

437. **Zahn, A., and J. P. Allain.** 2005. Hepatitis C virus and hepatitis B virus bind to heparin: purification of largely IgG-free virions from infected plasma by heparin chromatography. J Gen Virol **86:**677-85.

438. **Zeisberg, M., C. Yang, M. Martino, M. B. Duncan, F. Rieder, H. Tanjore, and R. Kalluri.** 2007. Fibroblasts derive from hepatocytes in liver fibrosis via epithelial to mesenchymal transition. J Biol Chem **282:**23337-47.

439. **Zeisel, M. B., I. Fofana, S. Fafi-Kremer, and T. F. Baumert.** 2011. Hepatitis C virus entry into hepatocytes: molecular mechanisms and targets for antiviral therapies. J Hepatol **54:**566-76.

440. **Zeisel, M. B., G. Koutsoudakis, E. K. Schnober, A. Haberstroh, H. E. Blum, F. L. Cosset, T. Wakita, D. Jaeck, M. Doffoel, C. Royer, E. Soulier, E. Schvoerer, C. Schuster, F. Stoll-Keller, R. Bartenschlager, T. Pietschmann, H. Barth, and T. F. Baumert.** 2007. Scavenger receptor class B type I is a key host factor for hepatitis C virus infection required for an entry step closely linked to CD81. Hepatology **46:**1722-31.

441. **Zennou, V., C. Serguera, C. Sarkis, P. Colin, E. Perret, J. Mallet, and P. Charneau.** 2001. The HIV-1 DNA flap stimulates HIV vector-mediated cell transduction in the brain. Nat Biotechnol **19:**446-50.

442. **Zeuzem, S.** 2004. Heterogeneous virologic response rates to interferon-based therapy in patients with chronic hepatitis C: who responds less well? Ann Intern Med **140:**370-81.

443. **Zhang, J., G. Randall, A. Higginbottom, P. Monk, C. M. Rice, and J. A. McKeating.** 2004. CD81 is required for hepatitis C virus glycoprotein-mediated viral infection. Journal of Virology **78:**1448-1455.

444. **Zhang, X. A., W. S. Lane, S. Charrin, E. Rubinstein, and L. Liu.** 2003. EWI2/PGRL associates with the metastasis suppressor KAI1/CD82 and inhibits the migration of prostate cancer cells. Cancer Res **63:**2665-74.

445. **Zhang, Y. Y., B. H. Zhang, K. Ishii, and T. J. Liang.** A Novel Function of CD81 in Controlling Hepatitis C Virus Replication. J Virol.

446. **Zheng, A. H., F. Yuan, Y. Q. Li, F. F. Zhu, P. P. Hou, J. Q. Li, X. J. Song, M. X. Ding, and H. K. Deng.** 2007. Claudin-6 and claudin-9 function as additional coreceptors for hepatitis C virus. Journal of Virology **81:**12465-12471.

447. **Zhong, J., P. Gastaminza, G. Cheng, S. Kapadia, T. Kato, D. R. Burton, S. F. Wieland, S. L. Uprichard, T. Wakita, and F. V. Chisari.** 2005. Robust hepatitis C virus infection in vitro. Proc Natl Acad Sci U S A **102:**9294-9.

448. **Zhu, W., L. Wang, Y. Yang, J. Jia, S. Fu, Y. Feng, Y. He, J. P. Li, and G. Liang.** 2010. Interaction of E2 glycoprotein with heparan sulfate is crucial for cellular infection of Sindbis virus. PLoS One **5:**e9656.

449. **Zylberberg, H., A. C. Rimaniol, S. Pol, A. Masson, D. De Groote, P. Berthelot, J. F. Bach, C. Brechot, and F. Zavala.** 1999. Soluble tumor necrosis factor receptors in chronic hepatitis C: a correlation with histological fibrosis and activity. J Hepatol **30:**185-91.